Óbuda University

PhD Thesis

Closed-Loop Controller Design Possibilities for Nonlinear Physiological Systems

by

György Eigner

Supervisor:

Prof. Dr. habil Levente Kovács

Applied Informatics and Applied Mathematics Doctoral School

Budapest, 2017

Final Examination Committee:

Chair:
Prof. Dr. habil Aurél Galántai, DSc
Members:
Dr. Márta Takács, PhD
Prof. Dr. habil Péter Baranyi, DSc

Public Defense Committee:

Opponents:
Prof. Dr. Clara M. Ionescu, PhD (Ghent University, Belgium)
Dr. Chee-Kong Chui, PhD (National University of Singapore, Singapore)

Chair:
Prof. Dr. Sándor Kristály, DSc

Replacement Chair:
Prof. Dr. habil Aurél Galántai, DSc

Secretary:
Dr. Péter Galambos, PhD

Replacement Secretary / Member:
Dr. habil Gyula Hermann, CSc

Members:
Dr. habil Szilveszter Kovács, PhD (University of Miskolc)
Dr. Szilveszter Pletl, PhD (University of Szeged)
Dr. Márta Takács, PhD

Replacement Member:
Dr. habil László Horváth, CSc

Date of Public Defense:

Declaration of Authorship

I, György Eigner, declare that this thesis titled, 'Closed-Loop Controller Design Possibilities for Nonlinear Physiological Systems' and the work presented in it are my own. I confirm that:

- This work was done while in candidature for a research degree at this University.
- Where I have consulted the published work of others, this is always clearly attributed.
- Where I have quoted from the work of others, the source is always given. With the exception of such quotations, this thesis is entirely my own work.
- I have acknowledged all main sources of help.

_____

PhD Candidate

_____

Date

"If we knew what we were doing, it wouldn't be called research."

Albert Einstein

Contents

Acknowledgments

First of all, I would like to thank my doctoral supervisor, *Prof. Levente Kovács* – without his guidance and support from the beginning of my master studies this dissertation would not have been written. He believed in me when I was not and sometimes only his faith has been keeping my spirit up.

Next, I would like to special thank *Prof. József K. Tar*, from whom I have learnt a lot not just professionally but also humanly – his help was eternally in order to finish this work.

After, I would also like to say thank *Prof. Imre Rudas* – who has gave me extraordinary possibilities and embraced me.

I would like highlight my colleague *Dr. Tamás Ferenci*, who provided me practical advices while I was writing the dissertation.

Special thanks behoove the leaders of the Doctoral School *Prof. Aurél Galántai* and *Prof. László Horváth* for their support.

I want to say thanks to my family without they help this work would have been impossible – to my Mother-in-Law *Kati* and brother-in-law *Benji*; to *Dr. Bernadett Eigner and Aunt Mary* for their humanly and financial support; to my *Sis* for her kindness; to my *Grandma* who always supported me; to my *Dad* for his encouragement; to my *Mom* for her continuous love and support.

I would like to also thank to all of those who are not personally listed here – many of my colleagues and friends from whom I learned a lot.

Finally, I would like to say special thanks to my beloved fiancée *Barbi* for her endless patience and love – as she always says this work would have been shorter but more boring without her.

List of Figures

List of Tables

Abstract

The usage of modeling and control on the field of biomedical engineering has essential importance in these days. The phenomena dates back to the occurrence of first high capacity computers with which the online monitoring, modeling and control became possible. Currently, several physiological processes can be handled by internal (eg. pacemakers and other implants, etc.) and external (eg. heart-lung monitors, insulin pumps, etc.) controllers which provide accurate control signals with good quality – it can be stated that the modern medicine is unimaginable without these improvements.

One of the most widespread disease the diabetes mellitus and accompanying diseases, which mostly the side-effects of the main problem. Due to unknown autoimmune processes, civilizational reasons and most common genetic failures the diabetes mellitus threads significant part of the global population. The last decades have presented that via the biomedical engineering approaches and developments the diabetes mellitus can be sufficiently handled and the occurrence of side-effects can be decreased – thankfully the achievements on the field of physiological related modeling and control.

This dissertation presented modeling and control solutions which can be applied in case of physiological processes including diabetes mellitus.

The first thesis group investigated the usability of RFPT theorems in conjunction with T1DM control. I have examined three cases, which were different from the applied T1DM model, absorption submodel point of view, however, I used almost the same control strategies in each cases, namely, PID-kind control laws in the control block. I followed the general RFPT controller design steps, what I summarized at the beginning of the given chapter. The results showed that the RFPT-based controllers can be used in case of T1DM models with low and high complexity beside unfavorable disturbances (glucose loads). The developed controller were able to keep the BG level in the normal glycemic range; totally avoid hypoglycemia; however, short hyperglycemic periods occurred during the simulations. With this research I can be proven that the RFPT-based controller design method can be used for controller design in case of T1DM models with high nonlinearities.

The second thesis group introduce a two novel achievements on the field of LPV-based control. I have developed a norm based tool in which the norm (2-norm) is defined on the abstract parameter space of LPV systems and can be used as a metric between LTI systems. This tool can be used as error or difference metric and via quality requirements can be defined with it. The second achievement can be divided into two parts: I have

developed a novel LPV completed controller scheme which can be used for control of LPV (and trough nonlinear) systems with given properties; moreover, I have developed a completed LPV controller-observer scheme in order to control given LPV systems. The novel controller design tools are a mixture of linear state-feedback theorem and matrix similarity theorems and exploiting the properties of the LPV parameter space. I have proven the usability of the methods via nonlinear physiological examples including DM control. I provided deep analysis of the methods.

The third thesis group investigates the TP modeling possibilities of different DM models – due to I want to use the developed TP models as subjects for TP-based controller design in the future. The first step of this direction was made during my research, namely, I have introduced control oriented LPV models via mathematical transformation from the existing DM models and I successfully developed the TP model form of them. I showed three possible direction during this part: it is possible to use TP model transformation and realize TP model in case of simple ICU kind DM model with high nonlinearities; it is possible to use TP model transformation and realize TP model in case of highly complex T1DM model with high nonlinearities and coupling; and I showed that how is it possible to increase the robustness of the TP model (from parameter point of view).

Absztrakt

A modellezés és szabályozás használata az egészségügyi mérnöki területen alapvető fontossággal bír napjainkban. A jelenség visszadatálható az első nagy teljesitmenyű szamitógépek megjelenésére, amelyekkel az online monitorozás, modellezés és szabályozás tervezés megvalósíthatóvá vált. Manapság számos élettani folyamat szabályozható belső (pl. pacemaker és egyéb implantátumok, stb.) vagy külső (pl. szív-tüdő monitor, inzulin pumpa, stb.) szabályozókkal, amelyek pontos és jó minőségű szabályozást tesznek lehetővé – kijenelthetjük, hogy a modern medicína elképzelhetetlen lenne ezen fejlesztések nelkül.

Az egyik legelterjedtebb kór a cukorbetegség és ennek mellékhatásaként kialakuló társult betegségek. Az ismeretlen autoimmun folyamatok, civilizációs hatások és genetikai betegségek következtében kialakuló cukorbetegség a globális populáció jelentős részét fenyegeti. Az elmúlt évtizedekben bebizonyosodott, hogy az egészségügyi mérnöki megoldásokkal a cukorbetegség hatékonyan kezelhető és a társult betegségek előfordulásának gyakorisága is redukálható – köszönhetően a számos új eredménynek a fiziológiai rendszerek modellezésével és szabályozásával kapcsolatban.

Ez a disszertáció olyan modellezési és szabályozási megoldásokat mutat be, amelyek használhatóak az élattani folyamatokkal kapcsolatosan, beleértve a cukorbetegséget is.

Az első tézis csoportban megvizsgáltam a Robusztus Fix-Pont Transzformáció (RFPT)-alapú szabályozás tervezési lehetőségeket egyes típusú DM (T1DM) szabályozásával kapcsolatban. Három esetet vettem vizsgálat alá, amelyek az alkalmazott T1DM modell és felszívódási modell tekintetében különbözők voltak, azonban a használt szabályozasi stratégia, vagyis a Proporcionális-Integráló-Deriváló (PID)-alapú szabályozási törvény a szabályozó blokkban ugyanazon elven alapult. Az általános RFPT tervezési lépéseket követtem, amelyeket összefoglalóan megadtam fiziológiai rendszerek esetére a fejezet elején. Az eredmények memutatták, hogy az RFPT-alapú szabályozók használhátóak alacsony és magasrendű T1DM modellek szabályozásához nagymertekű zavarás (nagymértekű szénhidrát (CHO) terhelés) mellett. A kifejlesztett szabályozások a szimulációs idő alatt képesek voltak a vércukor szintet normál glikémiás tartományban tartani; teljesen elkerülni a hypoglikémiás epizódokat; habár rövid idejű hyperglikémiás epizódók előfordultak. Ezzel a kutatással sikerült bizonyítanom, hogy az RFPT-alapú szabályozó tervezési eljárások használhatóak szabályozók tervezésére nagymertekű nemlinearitásokkal rendelkező T1DM modellekhez.

A második téziscsoportban két új, eredeti eredményemet mutatom be a lineáris parameterváltozós rendszer (LPV)-alapú szabalyozások területéről. Kifejlesztettem egy

norma alapú eszközt, ahol a norma (2-es norma) az LPV rendszerek absztrakt paraméter terén értelmezve metrikaként hasznalható LTI rendszerek között. Ez az eszköz alkalmas hiba- vagy különbség-metrikaként való használatra is és általa minőségi követelmények is megfogalmazhatóak. A második fejlesztés két részre osztható: kifejlesztettem egy új LPV kiegeszített szabályozó sémát, amely LPV rendszerek szabályozásához használható fel; továbbá, egy új, kiegészített LPV szabályozó-megfigyelő struktúrát is fejlesztettem LPV rendszerek szabályozásához. Az új eszközök egy keverékét alkotják a lineáris állapot-visszacsatolás alapú szabályozásnak és a mátrix hasonlósági tételeknek és kihasználják az LPV paraméter tér tulajdonságait. Bebizonyítottam a használhatóságukat nemlineáris fiziológiai példákon keresztül, beleértve a diabetes mellitusz (DM) szabályozást is. Elvégeztem az eszközök teljeskörű analízisét is.

A harmadik téziscsoportban a tenzor szorzat (TP)-alapú modellezési lehetőségeket vizsgáltam meg különböző DM modellek esetén – mivel ezeket a realizált TP modelleket akarom felhasználni a további TP-alapú szabályozástervezési kutatásokhoz. Ennek az első lépése került kidolgozásra a kutatásomban, azaz bevezettem letező DM modellek kontroll-orientált LPV változatait matematikai transzformációkon keresztül, majd ezeken sikeresen alkalmaztam a TP model transzformaciót előállítva TP-alapú modelljeiket. Három lehetséges irányt vázoltam fel: bemutattam, hogy lehetséges a TP-model transzformáció használata TP modellek realizálásához egyszerű, intenzív őrzőkre szabott (ICU) DM modell esetén, amely nagymértékű nemlinearitásokkal rendelkezik; lehetséges a TP-model transzformáció használata TP modellek realizálásához komplex T1DM modell esetén, amely nagymértékű nemlinearitásokkal es csatolásokkal rendelkezik; és megmutattam, hogy lehetséges a TP modell robusztizálása modell paraméterek szempontjából.

List of abbreviations

Abbreviation	Meaning
LTI	Linear Time Invariant
LTV	Linear Time Variant
NLTV	Nonlinear LTV
LPV	Linear Parameter Varying
qLPV	quasi LPV
TP model	Tensor Product model
SS	State Space
PS	Parameter Space
PB	Parameter Box
DM	Diabetes Mellitus
CHO	Carbohydrate
LMI	Linear Matrix Inequality
LQR	Linear Quadratic Regulation
MVS	Minimal Volume Simplex
SVD	Singular Value Decomposition
HOSVD	Higher-Order SVD
AP	Artificial Pancreas
T1DM	Type 1 DM
T2DM	Type 2 DM

List of mathematical notations

Notation	Meaning
$a, b, ...$	scalars
$\mathbf{a}, \mathbf{b}, ...$	vector
$\mathbf{A}, \mathbf{B}, ...$	matrices
$\mathbf{a}_i, \mathbf{b}_i, ...$	ith row vector of $\mathbf{A}, \mathbf{B}, ...$ matrices
$a_{i,j}, b_{i,j}, ...$	jth elements of the $\mathbf{a}_i, _i, ...$ row vectors
$\mathbb{R}, \mathbb{C}$	sets
$\mathcal{A}, \mathcal{B}, ...$	tensors
$\mathcal{S} \overset{\mathrm{N}}{\underset{\mathrm{n=1}}{\boxtimes}} \mathbf{w}_n$	multiple tensor products,
	e.g. $\mathcal{S} \times_1 \mathbf{w}_1 ... \times_N \mathbf{w}_N$

1. Introduction

1.1. Research focus

The aim of this theses is to introduce such kind of modeling and controller design solutions which can be used in case of nonlinear biological systems. Each proposed methods are universal ones and can be used in case of arbitrary nonlinear processes, however, the application of them is unique in the current research field.

My main motivating goal was the use of the developments and applications in the research of DM from engineering point of view - in this spirit I always kept in the focus how the reached results will be useful to reach this goal. Namely, how can the proposed techniques be applied in case of DM.

Modeling and control is extremely important in the artificial regulation of physiological processes, especially where the good quality of external control is a must [1]. However, the given field is loaded by several challenges. Most of them are highly nonlinear, poorly described in full aspects due to the multiple and diverse connections between the physiological systems, deep investigations and measurements cannot be done or possible but with hard constraints, etc. [2]. Although these facts, the evolution and process of different types of DM became well described in the recent decades [3].

DM is a serious, chronic disease connected to the metabolic system of the human body. The disease occurs either when the amount of insulin produced by the pancreas is insufficient or when the body cannot effectively use the insulin it produces [4].

Insulin is the key hormone of the blood glucose regulation produced by the β-cells in the Langerhans-islets in the pancreas [5]. It makes possible the entering of the glucose into the glucose consuming body cells. Most of the cells feast glucose which is the major energy source in living organisms [6].

DM researches are hot topics on the biomedical engineering field due to the dramatically increasing number of diabetic patients. According to the newest estimations of the International Diabetes Federation (IDF) for the number of people who live with such form of diagnosed and undiagnosed DM is about 415 million worldwide in 2015 [3]. Furthermore, the short term prospects suggest that this number can be reached the 642

million, around 6.8% of the expected global population by 2040 [3, 4]. Figure 1.1. shows the estimated distribution of diabetic population worldwide.

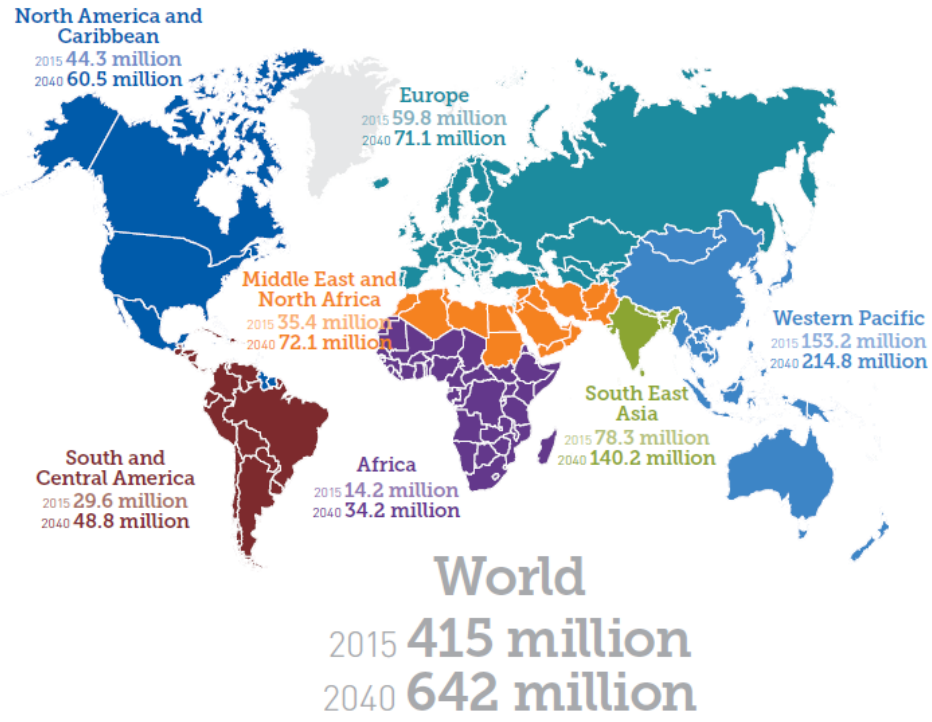

Figure 1.1.: Estimated number of people with diabetes worldwide and per region in 2015 and 2040 (20-79 years) [3]

DM is classified into Type 1 DM (T1DM), Type 2 DM (T2DM), Gestational DM, Double DM, Genetic DM, Secondary DM, etc. [3, 7]. Despite the several different types of DM, the T1DM and T2DM are the most widespread.

The T1DM is related to the insulin hormone, since during the emergence of the disorder, the insulin producer β-cells are burned out due to intense autoimmune reaction in which the patient's own immune cells destroy them. The occurrence of T1DM is around 10% in the diabetic population [7].

The most common type of DM is T2DM [3]. The incidence of it is around 90% in the diabetic population. The disease evolves over longer period in the patients body. However, the body is able to produce insulin internally, the body cells become resistant to the hormone and the effect of it becomes insufficient. Over long period persistent hyperglycemia and increasing insulin resistance can be observed [5, 8].

A frequently occurred DM type is the Gestational DM, which appears in women during pregnancy. Most of the time it disappear after childbirth, however, the state can become permanent in case of genetic flair for DM [4].

The other types are rarely occurred in the population [3].

Important that the DM state can leads to several secondary disease in the absence of appropriate therapy, which means not just proper medication, but the change of lifestyle, as well.

The required therapies to handle the diabetic state are different in accordance the given type of DM. In case of T1DM the patients need exogenous administered insulin due to the lack of internally produced insulin. In case of T2DM, the regular therapy starts with drug administration. These can be gluconeogenesis inhibitors which obstruct the daily glucose production of the liver and decrease the insulin resistance [6]. Although, over time externally administered insulin can be required in order to keep the blood glucose level in a healthy range.

The common therapy - beside prescription about the lifestyle (physical activities and diet) - is the external insulin administration. Insulin is delivered via subcutaneous injections. There are different devices with which the diabetic patients can manage the insulin delivery. Usually, it is done by insulin pen which is a small pen shape mechanical device which consists of dispenser, insulin reservoir, injection mechanics and thin needle parts. In this way with this device the patients are able to manage their blood glucose level. The dosage is manual and leaves the insulin delivery to the patients based on preliminary rules laid down, the feed intake, physical activities and the prescription of the clinicians. During the self-administered therapy, the patients can use rapid acting insulin (bolus insulin to handle the feed intake) and slowly acting insulin (for keep the basal insulin rate), as well [7, 9].

An other solution for insulin administration is the semi-automatic or automatic insulin pump or Continuous Subcutaneous Insulin Infusion (CSII) devices, which can be used both DM cases as well, however, the indications of usage are different [10–14]. The pump or injection system contains insulin reservoir which connects to the subcutaneous regions via thin catheter. This electromechanical devices are able to delivery insulin boluses automatically based on predefined rules. The pumps using rapid acting insulin and the delivery protocols are varying as demands the patients need.

The long term goal of the research of DM from engineering point of view is to develop the so-called Artificial Pancreas (AP) concept (Fig. 1.2). This development consist of three major part [15–21]:

1. An insulin pump or insulin pump completed with external insulin injection system,

which stores and injects the rapid acting insulin;

2. A Continuous Glucose Monitoring System (CGMS) for continuous blood sugar level measurement and transmit;

3. Appropriate software components including control algorithms, user interfaces, drivers.

The CGMS system is used in parallel with the insulin pump. The operation of CGMS are based on various principles. In practice, the most widely used systems are external devices fixed on the abdominal skin surface and connected to the subcutaneous level through a thin catheter. The most frequent measuring principle are enzymatic based (Glucose Oxidase (GOx)). Beside its several benefits CGMS has also some disadvantages mostly from control engineering point of view: sensors measurements are done only every 5 minutes. Implantable CGMS have been also appeared, but these are not available on the market, yet [22].

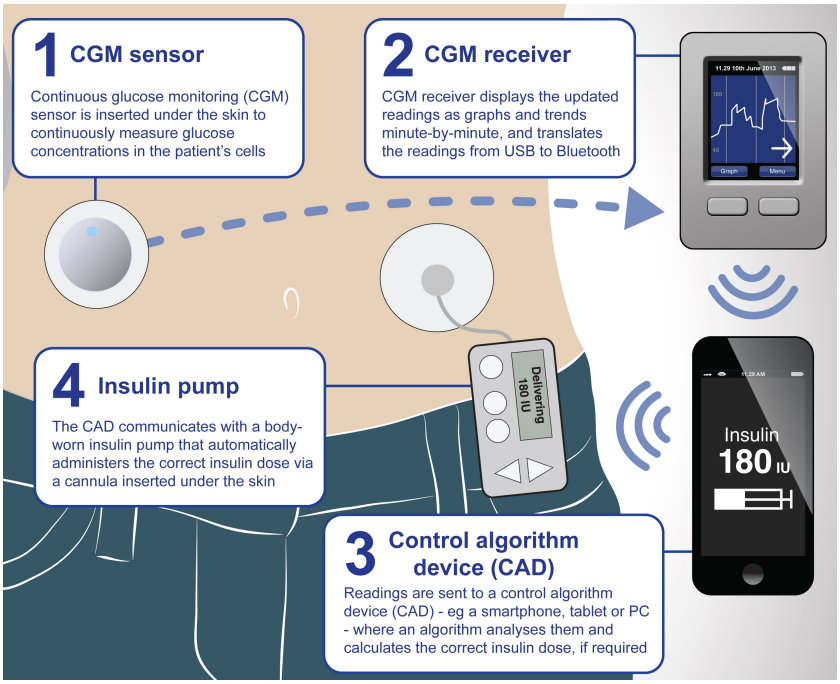

Figure 1.2.: The AP concept [23]

The newest concepts calculate with the benefits of the available smart devices, like smartphones [18]. In this way the control algorithms which may need high computational

capacity can be exported to the smart device instead of the compact insulin pumps. Figure 1.2. shows the schematic representation of the latest AP concept.

As mentioned above, the third necessary component to realize the AP is the appropriate software elements, including the control algorithms, the ”soul” of this approach.

Due to the fact that insulin pump therapies are used mostly in case of T1DM, the advanced control algorithms developed inside AP researches focus on this DM form. The main expectation from an AP control algorithm is the automatic glucose regulation in order to keep the blood glucose concentration in the normal glycemic range, i.e. 70-110 mg/dL (3.9-6 mmol/L) and relying if possible on the compliance of the patient. The ultimate goal is to avoid the dangerously low blood glucose levels (massive hypoglycemia) that could directly endanger the patients' life.

1.2. Relevant control engineering methods from this theses point of view

In this section I introduce the most important control design techniques from the DM and more specifically from the AP concept point of view – correspondingly to the aforementioned aims of the theses.

The soul of the AP concept is the usage of appropriate control algorithms. Over the last decades, most of the available control concepts have tested on this field. Figure 1.3 shows the AP concept completed with the most frequently used control algorithms.

The most important directions focus on model predictive control (MPC), fuzzy rule-based and other soft computing techniques, classical, robust and fractional PID control techniques; however, without having yet a general solution on the problem [15–17, 20, 21, 24].

Simplistically, every control algorithm considers similar principles; namely, the fulfillment of prescribed quality and quantity properties. The first attempts on this area were related to ”Proportional-Integral-Derivative (PID)” control being still the most widely used classical control technique in the industry. Although the basic concept of PID control is not too sophisticated, highly advanced solutions like robust PID [20, 25] or switching PID [26, 27] have been applied for the AP concept. Fractional PID control is in the mainframe of the physiological related control tasks [28]. There is example regarding to the application of fractional PID in the research field, like [29], but the usage as a common technique is not usual in the research field, however.

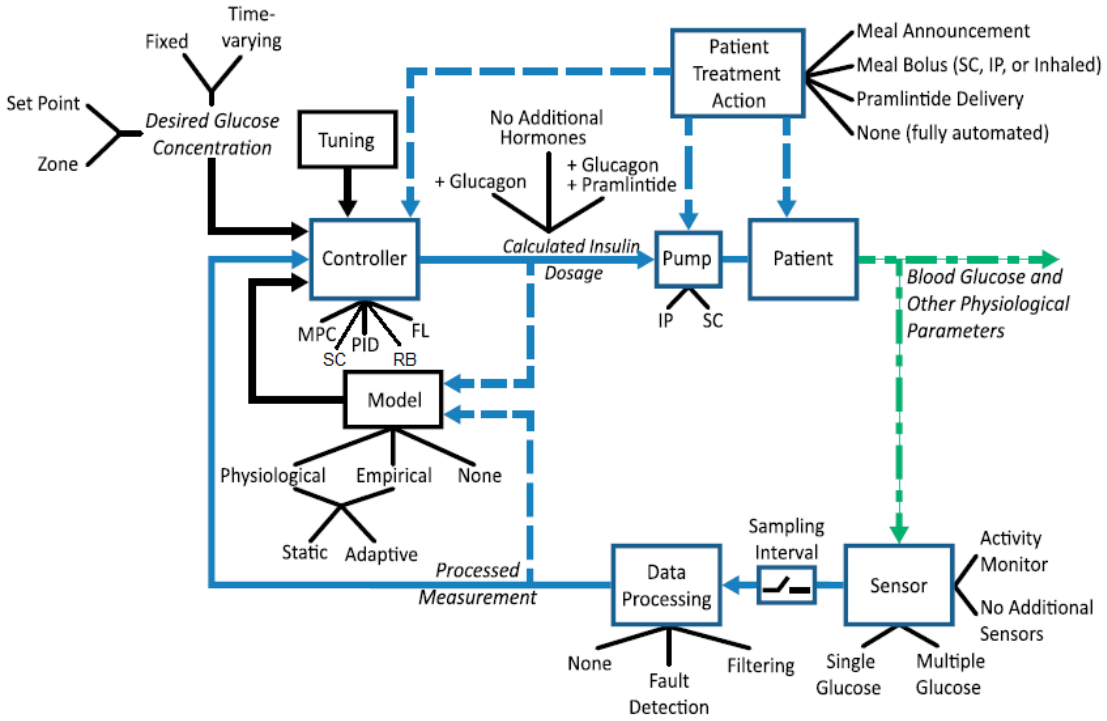

Figure 1.3.: AP taxonomy - *"Solid lines demonstrate connections that are always present and dashed lines represent connections that may only be present in some configurations. The tuning, model, and desired glucose concentration are all part of the controller, as signified by the black arrows. Green color distinguishes physiological states or properties from measured or digital signals. Black lines are used to indicate predetermined features of a block, and blue lines indicate signals or actions conducted during closed-loop operation"* [20] ; Controller: MPC - Model Predictive Control, SC - Soft-Computing, PID - Proportional-Integral-Derivative Control, RB - Robust Control, FL - Fuzzy-rule based Control

The MPC based solutions are widely used successfully since almost thirty years ago in the control engineering [30–33] and in physiological related context as well [34–36]. MPC techniques represent probably the mostly used advanced control method in the AP concept, but they suffers from intra- and inter-patient variabilities and external noises. MPC is a model based solution meaning that the controller tuning is based on the properties of a mathematical model (called nominal model). Nonetheless, MPC algorithms produce the best results in individual therapy with considering closely ideal conditions. Several, highly developed MPC based control solutions appeared in the recent years like Robust MPC (RMPC), Nonlinear MPC (NMPC), Robust, Nonlinear MPC (RNMPC), MPC with moving horizon [37–40]. One of the most straightforward

direction is the MPC design by using soft computing tuning tools [41]. The latter technique was successfully implemented on embedded systems which is a part of an artificial implementable AP [42].

Soft computing methodologies have been applied also several times in the AP concept, but only in the recent years have been investigated in clinical trials [43–45].

Modern robust control methods like $\mathcal{L}_2$- or $\mathcal{H}_\infty$-based ones were introduced in the AP researches in order to stave off the determinative uncertainties coming from inter- and intra-patient variability. Supplemented by LPV methodology (providing the opportunity to handle the original nonlinear system/model as a linear one; hence, to give access using the original nonlinear model for linear control methods enumerated above), modern robust control successfully deals with the quality and quantity requirements [46–49]. Another useful direction in this domain proved to be the combination of LPV methodologies with LMI-based one [49–51].

Dual hormone controllers consider beside the insulin the glucagon hormone as well; hence, it represents another conceptual control approach in AP researches [52]. Clinical trials also stared in this direction with encouraging results [53].

1.3. Outline of this theses

In Chapter 2., I introduce the latest results on the field of adaptive robust control of T1DM via RFPT framework. Beside the introduction, I demonstrate the developments applying on sophisticated T1DM models.

Chapter 3. presents the development of a new quality marker ("metric") for LPV modeling and control based on a given norm interpreted on the LPV parameter space. Further, a novel completed LPV controller and observer scheme for nonlinear systems is proposed, which can be used in control of biomedical systems. The applicability of them are demonstrated on nonlinear compartmental and different DM models. Most of the widely used DM models are based on compartmental modeling due to an applied nonlinear physiological compartmental model is used for demonstration.

Chapter 4 details the TP modeling possibilities regarding to DM in order to realize control oriented LPV-TP models, which will be the subjects of the controller design later.

In Chapter 5., I conclude my presented results.

Four Appendix encloses the theses. Appendix A. is a summary of the thesis points; Appendix B. summarizes the description and parameters of the DM model which were used; Appendix C. summarizes of the DM and the current state-of-the art of the research of it; and Appendix D. introduces the types of the LPV systems which were applied in

the thesis.

The simplified structure and the interconnections between the Chapters and Appendices are presented by Fig. 1.4.

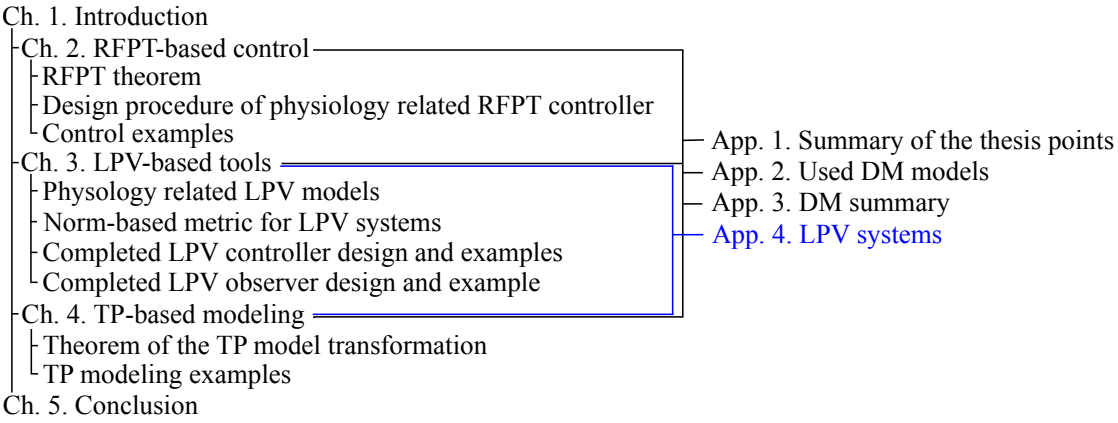

Figure 1.4.: Structure of the thesis

2. Opportunities of using Robust Fixed Point Transformation-based controller design in control of Diabetes Mellitus

In this Chapter, I have detailed my results concerning the application possibilities of the RFPT-based control theorem for control of T1DM.

First, I present the main ideas behind the RFPT-based control theorem.

Second, I describe the general method which can be used to realize the RFPT-based controllers which are able to deal with control of physiological models.

After, I have presented three case studies regarding the control of T1DM for models that are diverse from complexity, nonlinearity, structure and other points of view.

Finally, it should be noted that I have used Excel^{TM} for some calculations and SCILAB^{TM} for the simulation part, however, the figures were made by MATLAB^{TM}.

2.1. Ideas which brought the RFPT-based control into life

In control engineering the use of high complexity models have significant practical disadvantages. Typical problem is the reliability of the model parameters for the particular person under control. Furthermore, such models are difficult to handle. The traditional design methodologies formulate the feedback by the use of the actual system state in the given moment. In practice it is often impossible to obtain satisfactory information on the system's actual state variable as a whole, only its certain components can be measured, either directly or indirectly. In the latter case, complicated model-based state estimation processes should be applied for the computation of the control signal. However, we are often lacking the necessary sensors.

A possible choice to handle these circumstances is the usage of Lyapunov's methods. Before the famous work of Lyapunov in the end of the 19th century, the scientist who was investigating the stability of nonlinear systems had to face with many challenges. Lyapunov's work provided a universal mathematical tool which let the researchers to decide whether a nonlinear system is stable or not [54, 55]. Lyapunov's second or direct

method provides a way to determine the stability of a nonlinear system without solving the equations of motion. Due to the fact that most of the real life problems do not have analytical solutions in closed form and the validity of numerical solutions is limited, Lyapunov's method is extremely useful and most of the controller design methods are based on that even today.

The heart of the method is the evolution of the properties of the so-called Lyapunov function $V(t,x)$ over time. Consider a general nonlinear dynamic system, where $\xi = 0$ is an equilibrium point:

$$\dot{x}(t) = f(t,x) \qquad f(t,0) = 0 \qquad f(t,x) \in C_{t,x}^{(0,1)} \ . \tag{2.1}$$

If, $\exists V(t,x) \in C_{t,x}^{(1,1)}([a,\infty) \times D_x)$ positive definite Lyapunov function that alongside $\forall x(t)$ trajectories

$$\dot{V}(t,x) = \frac{\mathrm{d}V(t,x)}{\mathrm{d}t} < 0 \qquad (\dot{V} \ \text{negative definite}) \tag{2.2}$$

then $\xi = 0$ solution (equilibrium) is asymptotically stable in Lyapunov sense [56].

Nevertheless, the use of this method has several drawbacks. Although Lyapunov's method makes it possible to guarantee the asymptotic stability of various nonlinear systems, it does not provide information on the subtle details of the stabilization process. The transients in the motion of the controlled systems normally remain obscure and may contain practically intolerable sessions. Mathematically it is hard to handle, and it has strict limitations. There are only a few rules of thumb and examples, therefore its application or adaptation to a given problem requires the highly creative thinking of an expert designer. Each nonlinear problem needs unique approach. Moreover, often direct measurements or state estimations are needed for the feedback which is not possible in the given circumstances.

In classical control theorems, for example PID or state feedback based controls, the control rule and action is based on the expected-observed control scheme. That means, we have a predefined or "desired" system behavior r^d and the purpose of the control action via the control signal u is to enforce the system φ to reach the desired behavior. If the observed behavior differs from the desired one, error signals emerge in the trajectory tracking. The classical Model Predictive Controllers try to compensate them by error feedback terms on the basis of the assumption that they are in the possession of "exact system models". In other words, instead of directly concentrating on the response error, they rather observe only their consequences, and try to eliminate them on the basis of a not completely correct hypotheses. However, real physiological and physical systems can

be modeled only approximately [57]. In classical control theorems, the control goal can be formulated as:

$$r^r = \varphi(u) \ , \tag{2.3}$$

where r^r is the actual (realized) system response after u affected on it. In this case, the control signal calculation via exact inverse model can be described as:

$$u^d = \varphi^{-1}(r^r) \ , \tag{2.4}$$

where u^d is the desired control signal to be applied in order to reach the r^r system response.

In contrast to the Lyapunov method or classical control, the RFPT-based controller design has many advantages. It focuses on the kinematics of the motion which may have more importance than the global asymptotic stability; it does not require precise model of the controlled process, just an approximate one may do well (may be as highly approximate that the state feedback may become unimportant); the parameter uncertainties are well tolerated; and finally, the realization of the method is easier alongside certain given steps.

The main importance is that the RFPT theorem calculates with the high approximation of the given process and turns this property to a benefit. In the absence of exact models, approximate model can be used to describe the approximate control signal:

$$u^d_{appr} = \varphi^{-1}_{appr}(r^d) \ , \tag{2.5}$$

where u^d_{appr} is the approximate control signal which is necessary to reach the r^d desired system response.

Hence, the connection between the realized response r^r and the desired response r^d of the system can be described as:

$$r^r \equiv \varphi(\varphi^{-1}_{appr}(r^d)) \equiv f(r^d) \neq r^d \ . \tag{2.6}$$

The RFPT-based adaptive control is just a possible alternative to the traditional approaches. This approach sharply distinguishes between the "kinematic" and the "dynamic" aspects.

It starts with a purely kinematically formulated trajectory tracking error relaxation strategy. This results a given order time-derivative of certain variables as desired system response r^d that instantaneously can be realized by the available control signal. This control signal is estimated by the use of the available approximate system model φ^{-1}_{appr}

and it is exerted on the controlled system φ. The realized response r^r of the controlled system that is obtained for a kinematic prescription r can be considered as a response function as $f(r,\ldots)$ in which the symbol "..." refers to the parameters of the exact and the approximate system models. Evidently r and $f(r)$ have the same dimensions and they need not comprise all the components of the state variable. In practical cases the complexity of the approximate model may be much lower than the exact model.

The basic idea is that instead of tuning the parameters of the approximate model, the kinematically prescribed r^d value is adaptively deformed to $r_\star$ so that $r^d = f(r_\star)$. The necessary deformation is constructed in the following manner: in the first step the control problem is transformed into a fixed point problem so that the solution of the control task is its fixed point. After that, an iterative sequence of control signals is generated by the digital controller as $\{r_0 \stackrel{def}{=} r^d, r_1 = G(r_0)\ldots, r_{n+1} = G(r_n), \ldots\}$. If the parameters of the transformation function G are well set then this sequence converges to the solution of the control task, i.e. $r_n \to r_\star$. Normally r^d depends only on the lower order time-derivatives of the considered state variables while r can be abruptly modified. Therefore, although during one digital cycle only one step of iteration can be done, in the practice acceptable convergence can be achieved.

The idea of transforming various problems into fixed point problems is not a novel one. It goes back to the 17th century e.g. in the Newton-Raphson method [58–60]. Such kind of methods often occur in adaptive control as well [61, 62]. In 1922 Stefan Banach generalized the method for linear, normed, complete metric spaces [63] via the application of contractive maps. In this case, in which the response function is a single-variable real function, the transformation is made by the function [64]:

$$r_{n+1} = G(r_n; r^d) \stackrel{def}{=} (r_n + K_c) \times \left\{1 + B_c \left[\tanh(A_c(f(r_n) - r^d))\right]\right\} - K_c \ , \qquad (2.7)$$

where K_c, A_c, and B_c ($B_c = \pm 1$) are the *adaptive control parameters*. Clearly we have two fixed points as $r = -K_c$ (that is trivial and useless for the controller), and $r_\star$ for which $f(r_\star) = r^d$, that is the solution of the control task. If $\left|\dfrac{\mathrm{d}G}{\mathrm{d}r}\right| < 1$ during the iteration then the appropriate sequence converges to the solution of the control task. In general it is not difficult to satisfy this condition within a bounded region of the response values by manipulating the two parameters K_c and A_c. (Further details regarding the appropriate setting of the control parameters was given in [64, 65]).

The general RFPT controller structure can be seen on Fig. 2.1.

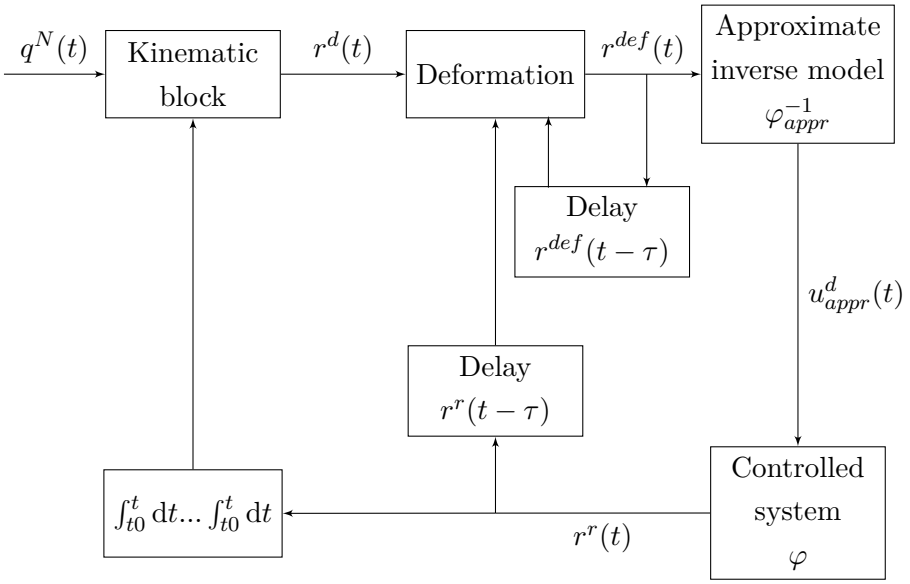

Figure 2.1.: General RFPT controller scheme: the controller learns from the recent model inputs and observed responses [$q^N(t)$ – Nominal trajectory; $r^d(t)$ – Desired system response; $r^{def}(t)$ – Deformed system response; $r^r(t)$ – Realized system response; τ – Time shift]

2.2. RFPT-based controller design in case of physiological processes

In this Section, I analyze the main steps of the controller design procedure starting with the general properties of the mathematical model of the phenomenon that I wish to use in the control. By revealing the more specific model properties an effect chain can be deduced that determines the relative order of the control tasks. By the use of a simple approximate model, the need for the information on the components of certain state variables can be evaded. The adaptivity of the designed controller can compensate the consequences of this modeling imprecision.

2.2.1. Considered modeling difficulties in general

In diabetes research, mathematical modeling of the physiological processes and the in-vitro investigations have absolute relevance due to the fact that the in-vivo experimenting possibility is limited since the subjects of the examinations are human beings. In such investigations, the real patients are substituted with models of various complexity called "patient models". These can be completed with other sub-models (e.g.: absorption

model, sensor model, noise model, etc.) in order to simulate the behavior of the human metabolic system regarding the glucose-insulin household. However, when the available mathematical models are used during the controller design, several unfavorable model properties come to light such as strong non-linearities and time delay effects that are essential parts of the reality [1]. Efficient handling of the intra- and inter-patient variabilities is also challenging, since a virtual patient can be described with a given parameter set of the mathematical model. Identification of the models is also crucial. Because of the inputs have impulse nature (food boluses, insulin injections), the aforementioned variabilities cannot be determined *a priori*. The output values are provided by real physiological measurements, therefore they are available only in given time moments. Furthermore, an identified individualized virtual patient model belongs only to a given real patient. That means that the model-based controller design solutions based on a virtual patient model as "exact model" may be seriously affected by these problems: they can handle only a particular group of patients who have the same metabolic attitudes. Further limitation is that these attitudes are assumed to be permanent in time, that does not seem to be a realistic hypothesis. However, in spite of these unfavorable circumstances, maintaining the generality of the controller and in the same time providing "personalized" control would be most beneficial. In general, adaptive controllers can provide such solutions. Specifically the RFPT-based adaptive controller design methodology can be a possible solution due to that fact that it requires only a roughly approximate mathematical model of the controlled phenomenon. The realization of such approximate models is detailed in the next section. Beside the approximate model, the appropriate control task will be provided by the prescribed control law (type of control).

2.2.2. Investigation of the effect chain of the control action

In order to realize the RFPT-based controller, an approximate inverse model is needed which effectively captures the approximate dynamics of the connection between the control signal (the injected insulin) and the controlled variable (the BG level). The most simple way is using a virtual patient model at this point instead of a real patient, however, models can be created based on measurements, as well. Three possible cases can arise:

- Real patient data is used: a model can be created that describes the relationship between the insulin signal and the BG level;
- Simple virtual patient model is used: usually, the insulin affects higher derivatives of the BG level via simple interconnections that determine the necessary order

of the control law; the model structure can be considered and transformed to an approximate model to capture this dynamics;

- Complex virtual patient model is used: insulin affects higher derivatives of the BG level via complex interconnections; the model structure cannot be used during the approximate model design.

2.2.3. Designing the approximate model

If a real patient's BG measurements and insulin injection data are available, a general mathematical model can be created and the well known identification procedures can also be used at this point. The main restrictions are that the CHO intake can be considered only with a random disturbance input and, while the insulin injections are known, still same as the CHO intake these have impulse attitude. Moreover, the sensor noise influences the BG measurements. Beside these unfavorable circumstances, the goal is to create such a mathematical model, which can approximately catch the dynamics of the process. For example, a nonlinear discrete autoregressive-type NARMAX model can be a reasonable choice because its simplicity and general usability [8].

The rough approximation model can be also generated from the given patient model if its structure is simple, namely, in case of a few state variables. This does not correspond to "model-based" process in the classical meaning of the expression, although the model structure is utilized during the procedure. The parameters of the model can be arbitrarily determined or randomized within reasonable limits. For instance, assume that the original first order non-linear system is described as

$$\dot{G}(t) = f(t, G(t), u(t), d(t)) \ , \tag{2.8}$$

where variable $G(t)$ denotes the BG level. Via restructuring the equation, the dynamic connection among the insulin input and the first derivative of the BG level will be:

$$u(t) = h(t, \dot{G}(t), G(t), u(t), d(t)) \ . \tag{2.9}$$

In the case of more complex models it can happen that the insulin input influences directly the higher order derivatives of the BG level. If the insulin input affects directly only a very high order derivative of $G(t)$ the use of this model in its original form is not reasonable. Although certain parts of the original models can be considered during the approximate model design (e.g. the connections between the subsystems), the complex model can be handled as a virtual patient and similar techniques can be used as in the

first case when the patient measurements are available. That means that measurements can be generated based on in-silico trials and identification can be applied. However, another opportunity also exists. Since the macro-scaled physiological processes are slowly varying, the Quasi Stationary Theorem (QST) from Classical Thermodynamics ([66]) can be used in approximate model design. In this approach, if the solution of the equations of motion is stable stationary, little modification of the stationary outputs generated by that of the inputs can be mapped for stationary inputs.

2.2.4. Selection of the control law

Since the design of the RFPT-based adaptive controller is commenced with determining a purely kinematic prescription of the tracking error, various possibilities can be chosen for this purpose. For instance, if it is known that the 3rd derivative of $G(t)$ can be instantaneously controlled with a $\Lambda > 0$ time-constant PID-type tracking that can be prescribed as

$$\left(\frac{\mathrm{d}}{\mathrm{d}t} + \Lambda\right)^4 \int_{t_0}^{t} \left(G^N(\xi) - G(\xi)\right) \, \mathrm{d}\xi = 0, \tag{2.10}$$

where $G^N(t)$ is the "nominal' BG concentration to be tracked, $G(t)$ is the realized BG concentration, and the error signal is the $e(t) = G^N(t) - G(t)$ ought to exponentially converge to zero in infinity, namely $e \to 0$ as $t \to \infty$. Evidently, due to the integration of the tracking error in (2.10) $\dddot{G}(t)$ has to appear. This value can be considered as the desired response (in this case 3rd derivative) $\dddot{G}^{Des}(t)$. However, other control laws can be used, too. Depending on the given application, P-, PD- and PID-kind control laws also can be used.

2.2.5. Finalization of the control environment

Using the aforementioned considerations, a general RFPT-based physiological related control environment can be finalized as it is shown in Fig. 2.2. It also depends on the approximate model applied.

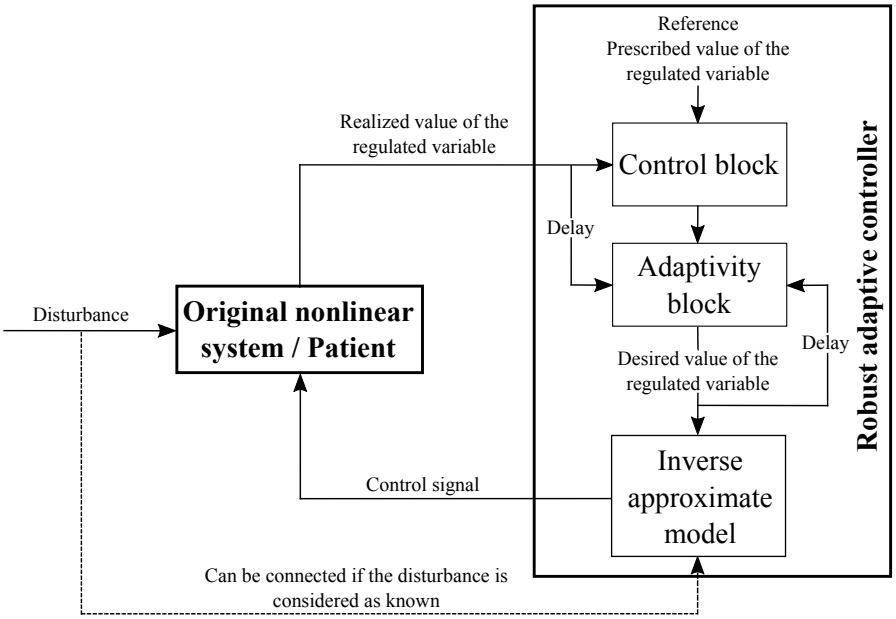

Figure 2.2.: The scheme of the RFPT-based controller: the two delay blocks correspond to the cycle time of the digital controller.

2.2.6. Considerations and restrictions regarding the controller design in case of T1DM

Modeling and control of T1DM is affected by several unfavorable practical and physiological constraints. These include the lack of information on the internal state variables of the patient model (as it is in the case of a real patient), the inputs having impulse nature, the output (the BG level) being quantized and not available in every time instant, the controller unable to administer arbitrarily big insulin ingress, etc. Every mentioned impact can be handled with sub-models or restrictions that increase the complexity of the model. Naturally, simplifications can be done in order to reduce the complexity. During my investigations I applied simplifications in modeling the feed intake. Since the absorption sub-models well characterize the rate of appearance of glucose in blood in a general way (they provide satisfying approximations), I assumed that the outputs of the applied absorption models are known. Furthermore, the total amount of insulin consumed up in the control of glycemia is also important: practically this value is limited. I have experimented with such kind of ”strong” restrictions as well, where the maximum amount of injectable insulin was limited.

2.3. Control of T1DM via RFPT-based control framework

In order to demonstrate and prove the usability of the RFPT-based design methodology, I show realized control strategies on different T1DM models later on which are frequently used in the scientific research [15, 17, 67]. However, I did not apply parameter identification: I used the models with the given parameters. Since my goal was the introduction of a new physiological related controller design method, and as I did not wish to develop an industrial application, this was a reasonable choice.

During my investigations I mostly applied unfavorable circumstances, namely, high glucose amounts and long simulation times in order to prove the long term usability of the developed controllers. The direct comparison between the obtained results is not possible because of the differences in the used models. However, the indirect comparison of the used control laws, and parameters of controllers can be done, as it was demonstrated during the design procedures in the different cases.

In general, I applied PID-kind control laws in every case, the outputs of the absorption models were considered as known, however, the details of controller design methodologies were different.

2.3.1. Control of the Minimal model

The first selected model was the so-called Minimal model in its form that occurred in [15]. It consists of only three state variables as (B.1a),(B.1b) and (B.1d) show. The Minimal model does not have embedded absorption submodel. Thus, to reach realistic simulation environment, instead of the peak-kind feed intake, a smoother glucose rate of appearance can be achieved, if the Minimal model is complemented with an external absorption submodel. For the sake of comparability, I have used the absorption submodel of the Hovorka model, which are given in (B.3a) and (B.3b). The complete model equations and their descriptions can be found in the Appendix B.

The effect chain

In order to develop an approximate model which describes the connection between the control signal $u(t)$ (injected insulin) and the controlled variable $G(t)$ (BG level), the effect chain of the control action (through the state variables) should be mapped. In this case, the original model was used to generate the approximate model. Thus, the effect chain could be derived by using the equations of the original model. In the followings this route was mapped. The word *Desired* represents the control action (via the input and the states) which is necessary to reach the desired control goal.

The injected insulin $u(t)$, which appears in the third equation of (B.1d) directly affects the insulin level in the plasma $I(t)$. The plasma insulin level is connected to the BG level ($G(t)$) via a coupling variable, $X(t)$. That means that the insulin input directly reaches the third derivative of $G(t)$. The thread is straightforward from this point, namely, this direct route have to be created. The quantity $\dot{I}(t)$ occurs in $\ddot{X}(t)$ as

$$\ddot{X}(t) = -p_2\dot{X}(t) + p_3\dot{I}(t) \ . \tag{2.11}$$

$\ddot{X}(t)$ occurs in the third derivative of $G(t)$:

$$\dddot{G}(t) = -(p_2 + X(t))\ddot{G}(t) - \ddot{X}(t)G(t) - 2\dot{X}(t)\dot{G}(t) + \ddot{p}(t) \ . \tag{2.12}$$

Equation (2.12) determines the relative order of the effect chain: $u(t)$ affects only $\dddot{G}(t)$. This fact should be considered during the control law selection. Trough step-by-step substitutions this relation can be expressed as

$$\ddot{X}^{Desired}(t) = -\frac{\dddot{G}(t)}{G(t)} - \frac{(p_2 + X(t))\ddot{G}(t) - 2\dot{X}(t)\dot{G}(t) + \ddot{p}(t)}{G(t)} \ , \tag{2.13}$$

$$A = -\frac{(p_2 + X(t))\ddot{G}(t) - 2\dot{X}(t)\dot{G}(t) + \ddot{p}(t)}{G(t)} \ , \tag{2.14}$$

$$\ddot{X}^{Desired}(t) = -\frac{\dddot{G}(t)}{G(t)} + A \ , \tag{2.15}$$

$$\dot{I}^{Desired}(t) = \frac{\ddot{X}^{Desired}(t) + p_2\dot{X}(t)}{p_3} \ , \tag{2.16}$$

$$\dot{I}^{Desired}(t) = \frac{-\dfrac{\dddot{G}(t)}{G(t)} + A + p_2\dot{X}(t)}{p_3} \ , \tag{2.17}$$

$$B = \frac{A + p_2\dot{X}(t)}{p_3} \ , \tag{2.18}$$

$$\dot{I}^{Desired}(t) = -\frac{\dddot{G}(t)}{p_3 G(t)} + B \ , \tag{2.19}$$

$$u^{Desired}(t) = \dot{I}^{Desired}(t) + n(I(t) - I_B) \ , \tag{2.20}$$

$$u^{Desired}(t) = -\frac{\dddot{G}(t)}{p_3 G(t)} + B + n(I(t) - I_B) \ , \tag{2.21}$$

$$Additive \ \ term = B + n(I(t) - I_B) \ , \tag{2.22}$$

$$u^{Desired}(t) = -\frac{\dddot{G}(t)}{p_3 G(t)} + Additive \ \ term \ . \tag{2.23}$$

Equation (2.23) shows the direct connection between $u(t)$ and $\dddot{G}(t)$.

Design of approximate model

Equation (2.23) can be directly used in the approximate model design. The appropriate control signal will be provided by the adaptivity block. Thus, more simplification is possible as the big advantage of the RFPT-based controller is that it can tolerate highly imprecise approximations. The equation has an A*dditive term* part as well, but the effects of this term are insignificant from the RFPT-based control law viewpoint, therefore it can be selected as constant. Furthermore, in the present case, $G(t)$ can be substituted with a constant value in the denominator of (2.23) as follows:

$$u^{Desired}(t) = -\frac{\dddot{G}^{Desired}(t)}{p_3 G_b} + Additive \ \ term \ . \tag{2.24}$$

The control action in this given case depends on only the realized $\dddot{G}(t)$. However, this simplification requires the estimation of the $\dddot{G}(t)$, that is a constraint of usability.

Control block

As previously mentioned, PID-kind control law was used in the control block. This can be formalized with kinematic requirements. Moreover, a third order law has to be used since the control signal $u(t)$ affects the third derivative of the $G(t)$ BG level in plasma. The applied form was the same as that in (2.10). Transforming this specific case, the short form of the control law is given as follows:

$$\dddot{G}^{Desired}(t) = \dddot{G}^{N}(t) + \sum_{s=0}^{3} \binom{4}{s} \Lambda^{4-s} \left(\frac{\mathrm{d}}{\mathrm{d}t}\right)^{s} \int_{t_0}^{t} \left(G^{N}(\xi) - G(\xi)\right) \, \mathrm{d}\xi \ . \tag{2.25}$$

A significant difficulty should be mentioned regarding the use of PID-type laws. Since

the controller can only decrease the BG level with the control signal and the feed intake is a disturbance from this point of view, dead periods may occur in the control after the insulin injections. If too much insulin is injected, and it causes dangerous decrease in the BG level, the controller has to wait for the depletion of the insulin via the natural channels, because there is no practical means to extract insulin from the human body. (The desired control action in this case should cause instant decrease in the insulin level that is impossible. The best realizable control signal in this case is the zero insulin ingress rate.) Furthermore, the integrated error can considerably increase during the "dead" periods. There are several solutions to handle this problem, namely the use of a "forgetting integrator", or the application of other (e.g. PD-type) control laws, or cutting the error signal at zero if the prescribed nominal BG level G^N is higher than the actual $G(t)$. In this case the PID-kind control law was appropriate without modification.

Simulation results - Minimal model

I tried to simulate as realistic circumstances as possible. For this purpose, I used realistic feed intake protocol based on the recommendations of the World Health Organization (WHO) [68]. In order to apply this protocol, I have considered the treatment for a 27 years old female patient of 70 kg weight with "little" physical activity. Based on the WHO recommendations, the required calorie intake for a day is described by Eq. (2.26) [68]:

$$CHO_{req/day} = 15.3BW + 679 = 1750\frac{\text{kcal}}{\text{day}} \ . \tag{2.26}$$

Since the applied absorption model allows the CHO as the only input parameter, I assumed that the total calorie intake was made up only from CHO, namely glucose. Generally, the carbohydrates and complex meals have lower glycemic index and needs longer absorption, therefore this simplification can be considered as a "worst case scenario", because of the fast increment of the glucose concentration in the blood. Because the exactly accurate coordination of the feed intakes cannot be provided (it depends on the lifestyle), I designed a randomization in the amounts and time frames of the glucose intakes. Further, since 1 g CHO is equivalent with 4.2 kcal [5], the total calculated CHO intake should be equal with 416.667 g. I divided this amount into 5 parts, 3 bigger meals (breakfast, lunch, dinner) and 2 smaller meals (snacks). Randomization were made in the amounts and time frames of different intakes, as follows:

Table 2.1.: The randomized feed intake protocol

Notation	Amount $[g]$	Duration $[min]$	Time frame of intake $[min]$
$CHO_{breakfast}$	$20 - 25\%$ of $CHO_{req/day}$	$15 \pm 5\%$	$210 \pm 5\%$
CHO_{snack1}	$10 - 15\%$ of $CHO_{req/day}$	$10 \pm 5\%$	$390 \pm 5\%$
CHO_{lunch}	$25 - 30\%$ of $CHO_{req/day}$	$20 \pm 5\%$	$510 \pm 5\%$
CHO_{snack2}	$10 - 15\%$ of $CHO_{req/day}$	$10 \pm 5\%$	$780 \pm 5\%$
CHO_{dinner}	$20 - 25\%$ of $CHO_{req/day}$	$20 \pm 5\%$	$900 \pm 5\%$

Furthermore, I have applied a strict constraint on the total calorie intake, namely:

$$\begin{aligned} CHO_{breakfast} + CHO_{lunch} + CHO_{dinner} &= 75\% \text{ of } CHO_{req/day} \\ CHO_{snack1} + CHO_{snack2} &= 25\% \text{ of } CHO_{req/day} \ . \end{aligned} \tag{2.27}$$

PID-based control law was used during the simulations. I transformed the units of the output in order to unify them.

The simulations were made in SCILAB$^{\text{TM}}$ and the figure plots were created with MATLAB$^{\text{TM}}$.

Figure 2.3. shows a representative 48 hours long simulation of the Minimal model, with the designed controller's insulin injections and the glucose rate of appearance. It can be seen that the absorbed glucose appeared around at 210 min. Before this time-instant the model did not get any input, since the controller was activated only when the model "behavior" required the control action. The simulation started with the reduction of the initial glucose contents (the initial states were $x(0) = [G_B, 0, I_B]^\top$). After that, the model's BG level reached the equilibrium (85 mg/dL in this case) (that is a model specificity). Without external inputs, the model holds this BG level. It is clearly visible that after the appearence of the absorbed glucose, the controller reacted by changing the BG level with external insulin injections and reached good performance, since it was able to hold the BG level inside a tight range. After the glucose rate of appearance achieved zero, the controller did not need to act, since the model was in its equilibrum. Consequently, the controller was able to deal with the unfavorable external glucose disturbances.

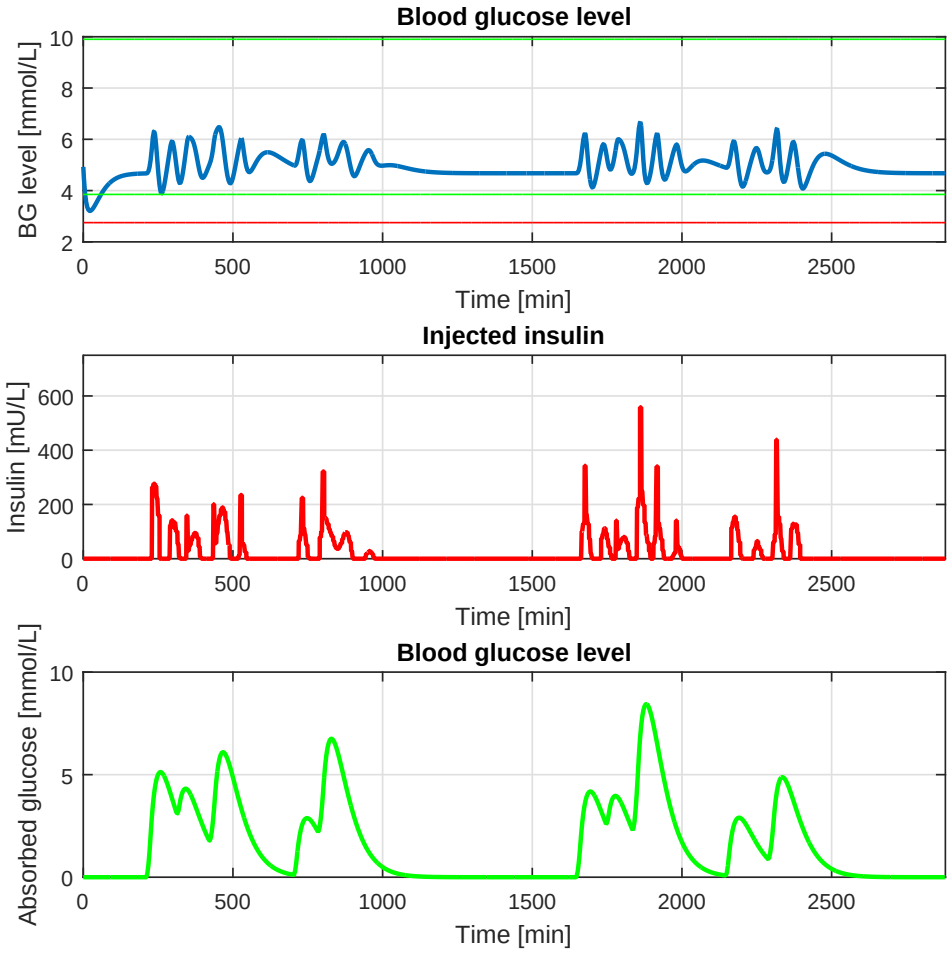

Figure 2.3.: Results of the 48 hours long simulation with the Minimal model [$G_N = 85$ mg/dL (4.675 mmol/L), $\Lambda = 0.08$, $A_c = 1/10|K_c|$, $K_c = -200$ and $B_c = 1$]

Figure 2.4. shows a Control Variability Grid Analysis (CVGA) plot [69] that was developed for the analysis of the performances of different control algorithms. The CVGA plot contains red dots, which belong to a one week long simulations with the Minimal model. Each dot represents a 24 hours time frame from the simulations. The position of a dot is determined by the minimum and maximum BG levels of the given time frame. The settings of the controller values were exactly the same as previously.

It can be concluded that the controller performed well, since none of the red dots was

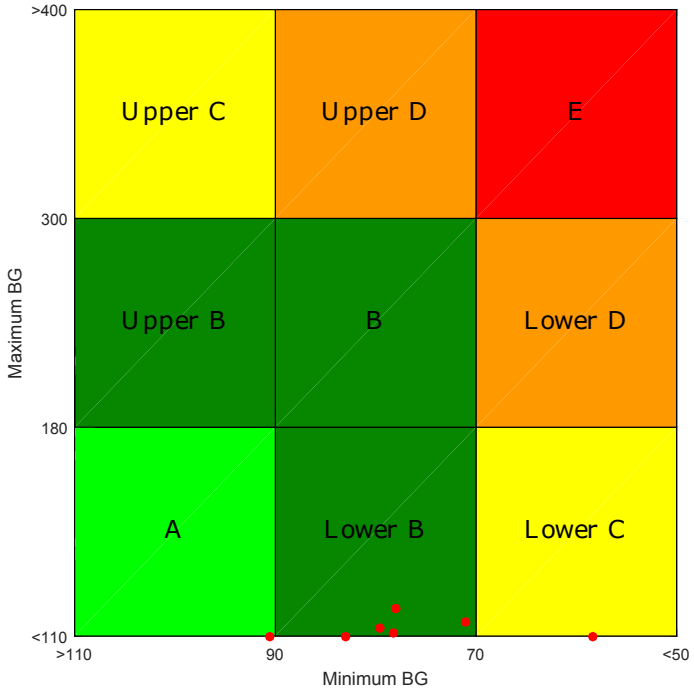

Figure 2.4.: Results of the one week long simulations

situated in the critical D or E regions. Five of the red dots are situated in the Lower B region and one in the A region. The red dots did not change their position drastically alongside of the Maximum BG axis (the daily maximum BG values are low) which is a straightforward consequence that the control target was chosen to be equal to the model equilibrium, namely $G_N = 85$ mg/dL (4.675 mmol/L). Because the controller produced efficient and fast reaction to the changes of the BG level and kept it in a narrow range, the maximum values of the BG level were close (or under) to the 110 mg/dL (6.05 mmol/L). However, the daily minimum values (vertical positions of the red dots) show a wider deviation. One red dot was in region C, however this belonged to the first day, which started with the natural reduction of the initial trajectories. Without external inputs, due to the applied initial conditions, the BG level reached a low value, however, this is a model specificity. This effect can be seen on Fig. 2.3. from $0 - 100$ min and this causes that this red dot in the C region.

Summary

It can be concluded that the designed controller can handle the nonlinear Minimal model. Moreover, it is able to deal with the unfavorable varying and unfavorable disturbance (CHO intake) and it can keep the BG level in a narrow range. The CVGA-plot shows that the controller keeps tight the BG variability as well and it does not let high variabilities.

2.3.2. Control of the Cambridge (Hovorka) model

The next discussed complex T1DM model, namely, the *Hovorka model* is determined by (B.3a)-(B.3j). It originally occurred in [70]. In this Theses, I used this model in its form that was presented in [71]. The model has ten state variables that describe not just the glucose-insulin dynamics as the Minimal model does, but also capture the externally injected insulin's absorption and distribution, the insulin effects, the insulin independent BG changes, and the internal glucose production too. Furthermore, it also contains an embedded glucose absorption model. The model equations and the descriptions of the parameters can be found in the Appendix B.

The effect chain and the approximate model

The relative order of possible kinematic type control is five, since the "pure" control signal reflects in the 5th derivative of the controlled state $Q_1(t)$. That means that high order derivative will appear from (B.3e) in the approximate model. This circumstance entails that high abandonment is necessary against the elements of the exact model. Thus, the relative order of the control is 5th, the 5th derivative of the state $Q_1(t)$ to be controlled should be determined. Two kind of approximation can be used: parameter approximation instead of exact parameters and neglecting of model elements. I applied both of these here.

First, I investigated the 5th derivative of the $Q_1(t)$ state, which can be derived from (B.3e):

$$\begin{aligned} Q_1^{(5)}(t) = \frac{D_2^{(4)}(t)}{V_G \tau_D} - F_{01,c}^{(4)}(t) - F_R^{(4)}(t) - x_1^{(4)}(t) Q_1(t) - 4x_1^{(3)}(t)\dot{Q}_1(t) - \\ -5\ddot{x}_1(t)\ddot{Q}_1(t) - 4\dot{x}_1(t) Q_1^{(3)}(t) x_1(t) Q_1^{(4)}(t) + k_{12} Q_2^{(4)}(t) - EGP_0 x_3^{(4)}(t) \end{aligned} . \tag{2.28}$$

The (2.28) can be rearranged and completed with a new term, the $Affine\ term$, which represents each neglected elements. Thus, the control signal directly appears in

$x_1^{(4)}(t)$ and $x_3^{(4)}(t)$ states derivatives, the approximate model is:

$$Q_1^{(5)}(t) = -x_1^{(4)}(t)Q_1(t) - EGP_0x_3^{(4)}(t) + Affine\ term\ . \tag{2.29}$$

The 4th derivative of $x_1^{(4)}(t)$ and $x_3^{(4)}(t)$ can be derived from the model equation (B.3e). However, first the route of the control signal has to be explored. Through the following equations, this can be done.

$$\dot{S}_1(t) = u(t) - \frac{S_1(t)}{\tau_S}\ . \tag{2.30}$$

$$\ddot{S}_2(t) = \frac{\dot{S}_1(t)}{\tau_S} - \frac{\dot{S}_2(t)}{\tau_S} = \frac{u(t)}{\tau_S} - \frac{S_1(t)}{\tau_S^2} - \frac{\dot{S}_2(t)}{\tau_S}\ . \tag{2.31}$$

$$I^{(3)}(t) = \frac{\ddot{S}_2(t)}{V_I\tau_S} - k_e\ddot{I}(t) = \frac{u(t)}{V_I\tau_S^2} - \frac{S_1(t)}{V_I\tau_S^3} - \frac{\dot{S}_2(t)}{V_I\tau_S^2} - k_e\ddot{I}(t)\ . \tag{2.32}$$

$$\begin{aligned} &x_1^{(4)}(t) = -k_{a1}x_1^{(3)}(t) + k_{b1}I^{(3)}(t) = \\ &= -k_{a1}x_1^{(3)}(t) + k_{b1}\left(\frac{u(t)}{V_I\tau_S^2} - \frac{S_1(t)}{V_I\tau_S^3} - \frac{\dot{S}_2(t)}{V_I\tau_S^2} - k_e\ddot{I}(t)\right)\ . \end{aligned} \tag{2.33}$$

$$\begin{aligned} &x_3^{(4)}(t) = -k_{a3}x_1^{(3)}(t) + k_{b3}I^{(3)}(t) = \\ &= -k_{a3}x_3^{(3)}(t) + k_{b3}\left(\frac{u(t)}{V_I\tau_S^2} - \frac{S_1(t)}{V_I\tau_S^3} - \frac{\dot{S}_2(t)}{V_I\tau_S^2} - k_e\ddot{I}(t)\right)\ . \end{aligned} \tag{2.34}$$

Equations (2.33) and (2.34) can be substituted to (2.29). Further, the neglected subparts can be incorporated to the $Affine\ term$, as follows:

$$Q_1^{(5)}(t) = -k_{b1}\frac{u(t)}{V_I\tau_S^2}Q_1(t) - EGP_0k_{b3}\frac{u(t)}{V_I\tau_S^2} + Affine\ term\ . \tag{2.35}$$

From (2.35) via rearranging the equation the connection between the control signal and the 5th derivative of $Q_1(t)$:

$$u(t) = \frac{Q_1^{(5)}(t) - Affine\ term}{-k_{b1}Q_1(t) - EGP_0k_{b3}}V_I\tau_S^2 = \frac{-Q_1^{(5)}(t) + Affine\ term}{k_{b1}Q_1(t) + EGP_0k_{b3}}V_I\tau_S^2\ . \tag{2.36}$$

The (2.36) is eligible to use as approximate model. I applied further approximation, since the exact model parameters are not available in every cases. The finalized and used

approximate model, what I applied in this study was the following:

$$u(t) \approx \frac{-Q_1^{(5)}(t) + Affine\ term_{const}}{k_{b1_{app}} Q_1(t) + EGP_{0_{app}} k_{b3_{app}}} V_{I_{app}} \tau_{S_{app}}^2 \ , \tag{2.37}$$

where I used 10% random deviation in the approximated parameters, moreover, I replaced the $Affine\ term$ with a constant, $Affine\ term_{const}$.

Control block

I assumed that the glucose distribution volume is known at this point as well which means I could write the kinematic type PID control law to $Q_1(t)$, which was the following:

$$Q_1^{(5),Des}(t) = Q_1^{(5),N} + \sum_{s=0}^{5} \binom{6}{s} \Lambda^{6-s} \left(\frac{\mathrm{d}}{\mathrm{d}t}\right)^s \int_{t_0}^{t} \left(Q_1^N(\xi) - Q_1(\xi)\right) \mathrm{d}\xi \tag{2.38}$$

Simulation results – Hovorka model

The Hovorka model is much more complex than the Minimal model which requires not just different controller design approach, but also the evaluation of the results is different. The Hovorka-model has several nonlinearities, attenuations and cross actions between the states.

It should be noted that I applied exactly the same feed intake during the present investigations that I used in the case of the Minimal model in 2.3.1 in Table 2.1. Thus the glucose rate of appearance in blood were the same in both cases beside this randomized glucose load.

I have used PID-based control law.

The simulations were made in Scilab$^{\mathrm{TM}}$ and the figure plots were created with MATLAB$^{\mathrm{TM}}$.

The initial states of the 48 hours long simulation were $x_{ini} = [D_{1,ini}, D_{2,ini}, S_{1,ini}, S_{2,ini}, I_{ini}, x_{1,ini}, x_{2,ini}, x_{3,ini}, Q_{1,ini}, Q_{2,ini}]^\top = [0, 0, 687.5, 687.5, 10.783, 5.521e-2, 8.842e-3, 0.5607e-1, 86.3, 63.66]^\top$.

The Hovorka model behaves differently than the Minimal model as it can be seen on Fig. 2.5. Without external glucose intake, the BG level is increasing due to the glucose secretion of the liver, which is an embedded part of the model. The applied controller starts the insulin injection when the BG level is increasing, however, it turns off, when the BG level is decreasing. This switching attitude can be derived from the applied control strategy and this is a consequence that the controller cannot affect with "negative"

control input. It can be seen that despite the continuously absorbing external glucose, the controller can manage the glycemia, namely, it is able to avoid the hypoglycemia beside minimizing hyperglycemia. The latter cannot be totally avoided because of the high and random glucose intakes.

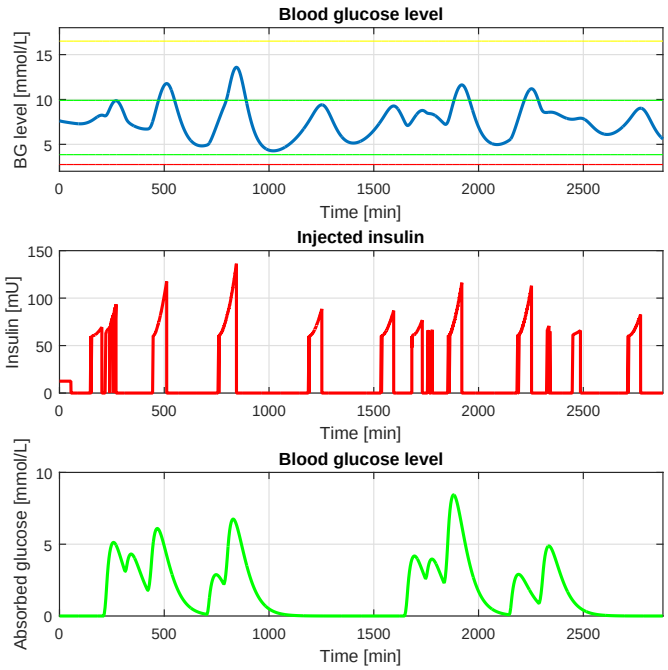

Figure 2.5.: Results of the 48 hours long simulation of the Hovorka model [$Q_1^N = 90$ mmol/L ($G^N = Q_1^N/V_G \approx 8.036$ mmol/L), $\Lambda = 1e-4$, $A_c = 1/10|K_c|$, $K_c = 5e-1$ and $B_c = -1$]

On the CVGA plot (Fig. 2.6.), each of the white dots represent a 24 hours long simulation period of the Hovorka model.

The vertical movement alongside with the maximum BG axis comes from that the minimum BG levels of this 24 hours periods were higher than 110 mg/dL (6.05 mmol/L). However, three points are in the B regions, which assumes a higher BG level variability – moreover, one point belongs to day 6 is totally overlapped with the point belongs to day 1. Nevertheless, the results showed that this controller configuration successfully deals with the randomized, unfavorable feed intakes and can keep the BG level among an appropriate range.

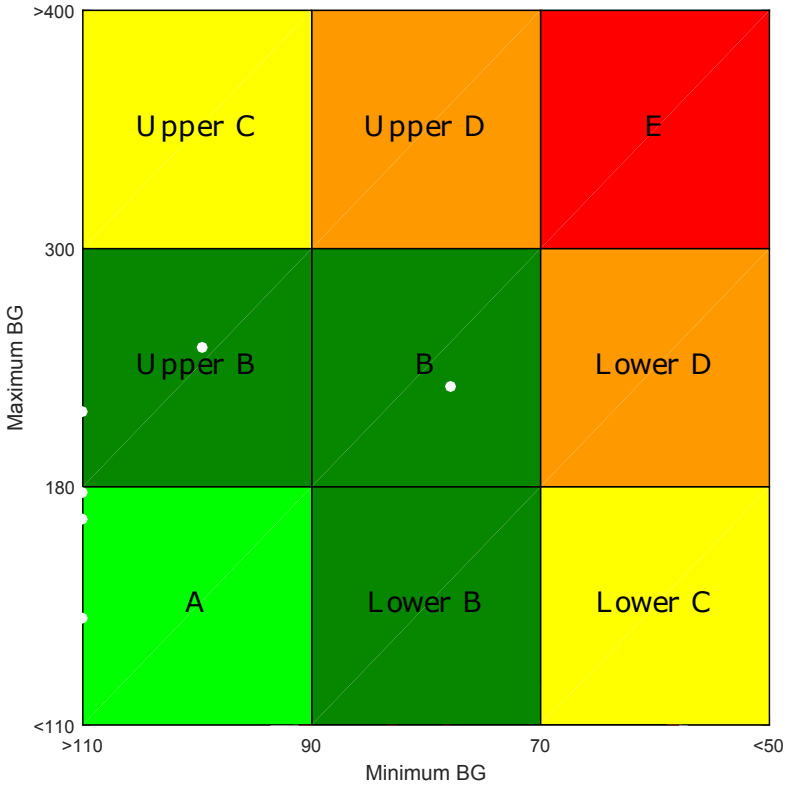

Figure 2.6.: Results of the one week long simulations

Summary

In this Section, I have successfully demonstrated the usability of RFPT-based controller design method in case of highly complex T1DM model step-by-step. The controller was capable to avoid hypoglycemic periods, however, soft hyperglycemia occurred due to the internal attenuations and highlighted liver effects (high internal glucose load) of the model. As the text reflects, it is possible to follow the demonstrated straightforward path to use in order to realize RFPT-based controllers in complex cases as well.

2.3.3. Control of the UVA-Padova (Magni) model

Specifics of the Model

During the development, quite a few general control, physiological and phenomenological constraints have to be considered, as listed below:

- As each of the state variables denotes the concentration of certain chemical component, they must have either positive value, or – after the depletion of the appropiate component – it must remain zero. These "truncation-type" nonlinearities make the application of any *"linearization"* dubious, whenever a given component is depleted. This fact seriously affects any considerations related to the frequency domain analysis that is widely used in the case of linear more or less linearizable systems. In the sequel, a qualitative analysis of present model is given.
- Each time-constant model parameter should be positive.
- Each state variable has its own exponential decay constant.
- Any coupling between the coupled pairs of state variables is of exponential nature: the decrease in the concentration of given state variable generates increase in that of the coupled one and vice-versa.
- Without finite input or extraction terms all the state variables should converge to zero.
- The state propagation quantities as $\dot{X}, \dot{I}_d, \dot{I}_1, \dot{I}_p, \dot{I}_L, \dot{S}_2$ and $\dot{S}_1$ are completely independent of the state variables G_M, G_p and G_t.
- Each element of the state propagation group $\dot{G}_M, \dot{G}_p$ and $\dot{G}_t$ directly is concerned by the input $\dot{R}_a$ and the state variables $\dot{X}$ and $\dot{I}_d$ belonging to the other group.
- To sum up, $u > 0$ makes X increase. Increasing X decrease $\dot{G}_t$ and G_t. Decreasing G_t decreases $\dot{G}_p$ due to which (B.6) gives possibility for decreasing G_M by properly big insulin input u. It is important to note that depletion of X – since $\dot{X} = 0$ if $X = 0$ – makes any possibility for controlling G_M via u cease. This introduces a strong nonlinear asymmetry into the system: drastic glucose R_a drastically increase G_M, via drastic insulin input u its effect can be contained.
- u is directly related to a high order time-derivative of the directly measureable state variable G_M.

The effect chain of control action

In order to design the approximate model, which provides the control signal, the effect chain of injected insulin (which is the control signal) needs to be mapped.

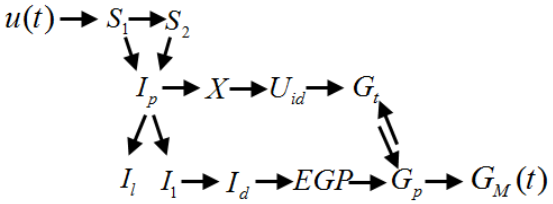

Figure 2.7.: Effect chain of insulin

Fig. 2.7. shows the particular effect chain of injected insulin $u(t)$. The physiological model specialties determine how the injected insulin affects on the $G_M(t)$, namely, through the insulin-dependent glucose utilization (U_{id}), which is the glucose uptake by insulin-dependent tissues and the endogenous glucose production of the liver (EGP), thus, the inhibition of gluconeogenesis.

Design of approximate model

It can be concluded based on the Sec. 2.3.3 that a kinematic prescription (which is used by the RFPT-method) are not expedient in this case, since the relative order of the control chain is at least 8. That means, the kinematic prescription should contain the 8th time derivative of the G_M. At the same time, the required order of the control law should be 8 as well, in order to handle this high derivative. To avoid this unpleasant effect, other approaches should be used. A possible solution, if the exact model is *hided* as a black box, and only the input and output are investigated. Naturally, this step is reducing the accuracy of the control, nevertheless, it can be used because of the adaptivity of the method. If the steady state of the system can be approached over one cycle and the G_M is available at the end of this cycle, the necessary insulin input which is need to be injected at the next cycle can be calculated by the controller. However, this condition is not usable itself, because of the glucose input dynamics is faster then the system's settling characteristics. Therefore, a simple dynamic scheme has to be developed, which can describe not only the $\Delta\tilde{u}$ determined by the actual glucose input, but also takes the affect of the past control actions on the actual condition into account, beside the appropriate time delays, determined by the system's dynamics. During the approximate

model design, I supposed that the R_a is known, since the glucose input is can be settled. In this way, based on the model equations the $\tilde{G}_M(\tilde{u}, \tilde{R}_a)$ can be calculated. The selected equation to describe the connection between the insulin input $u(t)$ and regulated output $G_M(t)$ is a quite simple one:

$$G_M(t) \approx au(t) + b \ . \tag{2.39}$$

Let $\tilde{u} \in [250, 600]$ and $\tilde{G}_M$ be calculated, where $\tilde{R}_a = 60n$, where $n \in \{0 \dots 15\}$ integer. Based on (2.39), with numerical approximation, the a and b are calculable. To reduce complexity, a second order polynomials can be fitted on the $a(R_a)$ and $b(R_a)$ which occurred with the calculation of a and b.

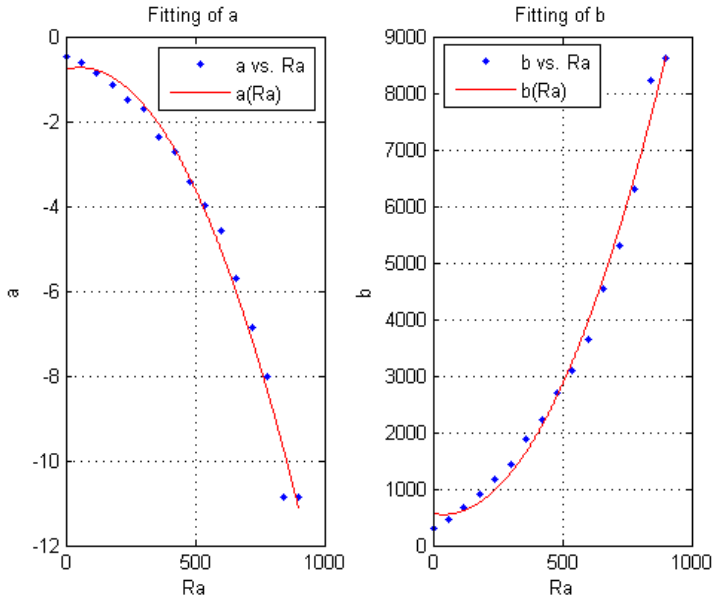

Figure 2.8.: Results of curve fittings based on (2.39) (for example, beside $n = 0$, $\tilde{R}_a = 0$, $\tilde{u}_{min} = 250$ and $\tilde{u}_{max} = 600$), then $\tilde{G}_{M,stac}(u_{min}) \approx 200$ and $\tilde{G}_{M,stac}(u_{max}) \approx 40$, the numerical calculation gives $a_{est} = -0.46$ and $b_{est} = 314.29$).

Due to the fact that the polynomials are known, $\Delta\tilde{u}$ can be estimated by:

$$\Delta G_M^{Desired}(t) \approx \frac{\mathrm{d}a(R_a)}{\mathrm{d}R_a}\Delta R_a\tilde{u} + a(R_a)\Delta\tilde{u} + \frac{\mathrm{d}b(R_a)}{\mathrm{d}R_a}\Delta R_a, \tag{2.40}$$

where $\Delta\tilde{G}_M^{Desired}(t)$ denotes the changing of the desired subcutaneous glucose level

determined by the measurements. The prescribed approximation for $\Delta\tilde{G}_M^{Desired}(t)$ is *"purely"* kinematic and contains several simplification from the control point of view. These simplifications are occurring as strong constraints during the control and the inaccuracies should be controlled by the adaptivity law.

The rough approximate model can be constructed by using the second order polynomials and combine with (B.6), (2.38) and (2.40):

$$\dot{u}^{Desired} = \frac{G_M + \dot{G}_M^{Desired} - a(R_a)u - b(R_a)}{a(R_a)} - \frac{\frac{\mathrm{d}a(R_a)}{\mathrm{d}R_a}u - \frac{\mathrm{d}b(R_a)}{\mathrm{d}R_a}}{a(R_a)} \tag{2.41}$$

The rough approximate model, according to the (2.41) gives an estimation about the G_M and u and provides the control signal as well. The tuning parameters are the specifics of the polynomials, $a(R_a)$ and $b(R_a)$. These approximations include the physical constraint at the same time that the control signal, namely, the injected insulin cannot be negative. It can be seen, that finally, the changing of the desired insulin level is determined by the followings:

- Actual BG measurements (G_M), which are available at every 5 *min* (accordingly the available CGMS systems).
- The changing of the desired BG level ($\dot{G}_M$), affected by the control law.
- The used polynomials and the changing of them, affected by the u. Furthermore, the polynomials are determined by the glucose input, which is a good approximation of the reality, where the insulin dosing is determined by the ingested food, namely, the glucose input.

Control law

The control law can be formalized with the kinematic requirements. Due to the approximate model (2.41) is a second order model, the control law should be a second order one as well. From simplicity reasons I have implemented a *"Fixed Set-Point type of Control"* with G^N as set-point parameter. The tracking error is taken as a prescription and such a PID kind feedback with a proportional term $\Lambda > 0$ could be suitable:

$$(\frac{\mathrm{d}}{\mathrm{d}t} + \Lambda)^3 \int_{t_0}^{t_1} \Big(G^N(\xi) - G(\xi)\Big)\ \mathrm{d}\xi = 0 \tag{2.42}$$

where $G^N(t)$ is the nominal blood glucose concentration of the nominal model, $G(t)$ is the realized blood glucose concentration and the exact requirement is that the error signal, $G^N(t) - G(t)$, should converge to zero as $t \to \infty$. Naturally, the fixed-set point control determines that the derivatives of G^N will be zero. With mathematical transformations of (2.42), the desired G_M derivate is equal to

$$\ddot{G}_M^{Desired}(t) = \left(\frac{\mathrm{d}}{\mathrm{d}t}\right)^2 G^N(t) + \sum_{s=0}^{2} \binom{3}{s} \Lambda^{3-s} \left(\frac{\mathrm{d}}{\mathrm{d}t}\right)^s \int_{t_0}^{t_1} \Big(G^N(\xi) - G(\xi)\Big)\mathrm{d}\xi \ . \tag{2.43}$$

where $G^N(t)$ is the BG concentration of the nominal model, $G(t)$ is the realized blood glucose concentration and the exact requirement is that the error signal, $G^N(t) - G(t)$, should converge to zero as $t \to \infty$. Naturally, the fixed-set point control determines that the derivatives of G^N will be zero. I have implemented a forgetting integral also, because the former tracking errors were considered with lower weight to dismiss the overload of the integrated error. The changing of $\dot{G}_M^{Desired}$ is reflecting in the rough approximate model and affects the injected insulin level at every cycle.

Adaptivity law

In order to increase the speed of the adaptivity other adaptivity laws can be selected instead of (2.7), which also satisfies the mathematical requirements of the RFPT-based method. In this case I selected the following adaptivity law [64, 65]:

$$r_{n+1} = G(r_n; r^d) \stackrel{def}{=} (r_n + K_c) \times \left\{1 + B_c \left[\Psi(A_c(f(r_n) - r^d))\right]\right\} - K_c \ , \tag{2.44}$$

where, beside the K_c, A_c, and B ($B_c = \pm 1$) adaptive control parameters instead of the *tanh* function and other Ψ sigmoid function was used (similar properties as the hyperbolic tangent), namely $\Psi(x) = \dfrac{x}{1 + |x|}$.

Results – Magni model

I have tested this solution with two glucose intake protocols – different than the previously detailed one – in the developed in-silico simulation environment with different length. The first glucose intake protocol was the following: 8 am, 50 g; 13 pm, 70 g; 20 pm, 70 g. This sequence is repeating over a week, the total simulation time was 168 hours. The result can be seen on Fig. 2.9.

Fig. 2.9. shows that the controller can handle the appearing glucose ($R_a(t)$) and

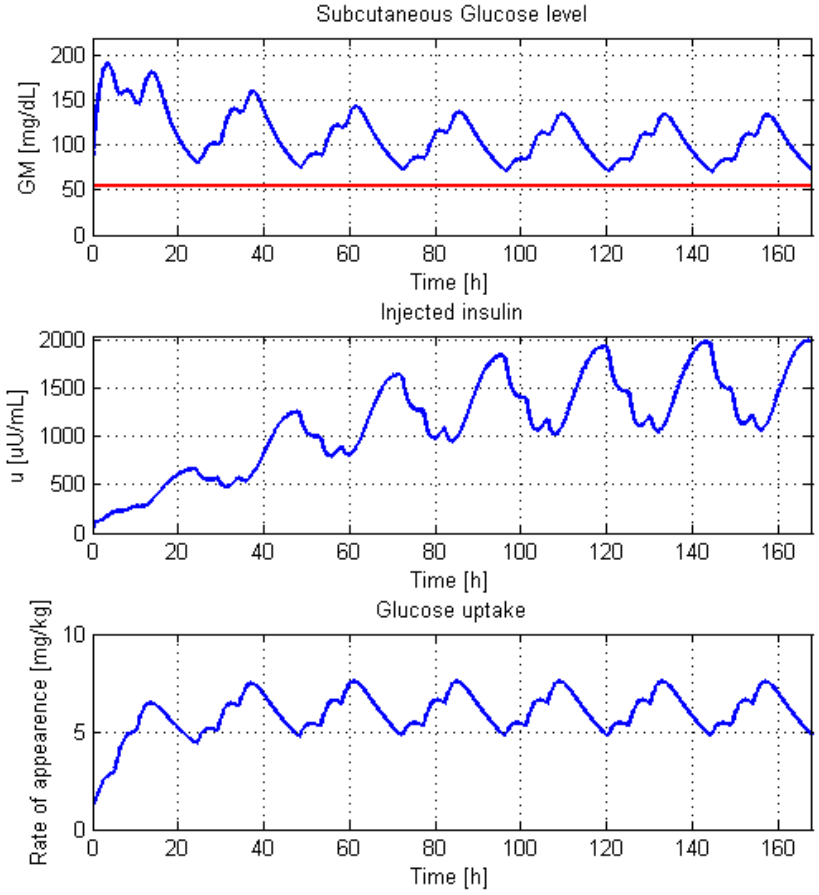

Figure 2.9.: Result of a one week simulation with first feeding protocol [Control parameters: $\Lambda = 0.015$, $A_c = 110^{-4}$, $K_c = -1000$, $B_c = 1$, Set-point (G_N)=100 mg/dL]

adapted to the requirements of the system with injecting insulin to reach the prescribed set-point value. The variables started from the steady-state condition and after the initial transient relaxation, because of the recurring input the system showed the expected recurring, oscillating behavior.

The second glucose intake protocol was a randomized one with various intake amounts and time-points. On Fig. 2.10. it can be seen that after the initial transients, the controller adapting to the systems needs, however, because of the randomized intake, this adoption is changing all the time, as expected. The initial values of the simulation were calculated based on B.6, beside 36 μU/mL ($\approx$ 250 pmol/L).

It is clearly visible, that the controller can handle the uncertainties like this.

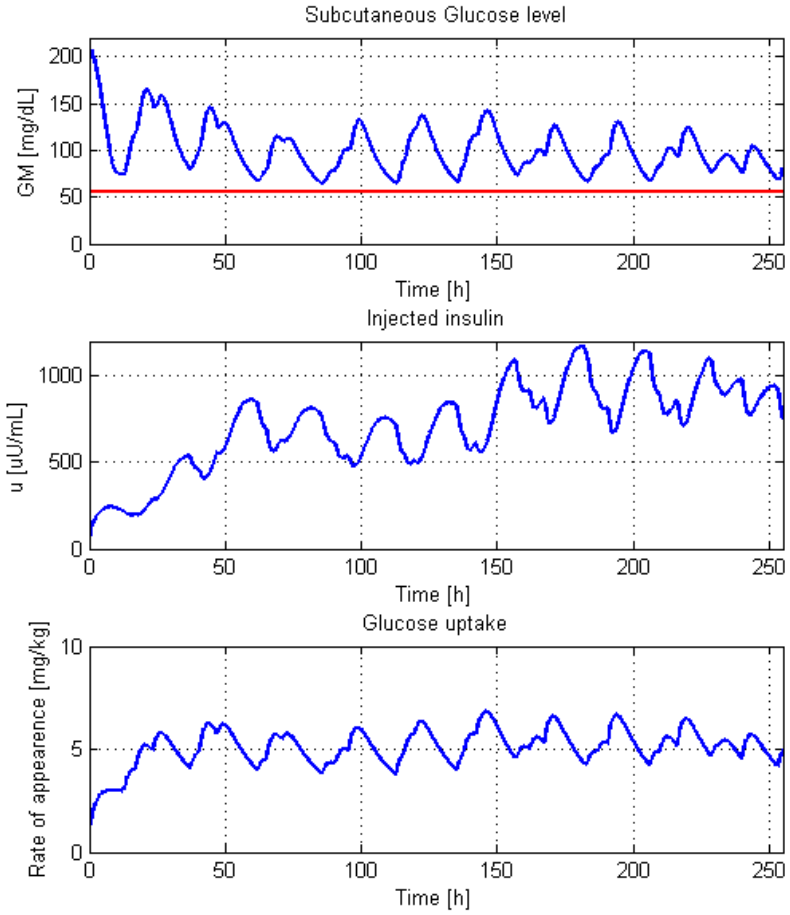

Figure 2.10.: Result of a 255 hours simulation with second feeding protocol [Control parameters: $\Lambda = 0.0125$, $A_c = 110^{-3}$, $K_c = -1000$, $B_c = -1$, Set-point (G_N)=95 mg/dL]

The last figure shows a CVGA result of a 53 days long simulation with the following control parameters: $\Lambda = 0.0125$, $A_c = 110^{-3}$, $K_c = -1000$, $B_c = -1$. The randomized intake parameters were: 3 glucose intake at every 24 hours with taking into account that the virtual patient feeding happens during the first 16 hours with minimum 4 hours between the each intakes; the amounts are changing between 40 g and 70 g, randomly. The results is shown by Fig. 2.11.

The Fig. 2.11. shows that the controller can handle this varying variable, however, the unfavorable randomized intakes degrade the adaptivity and produce higher deviation in

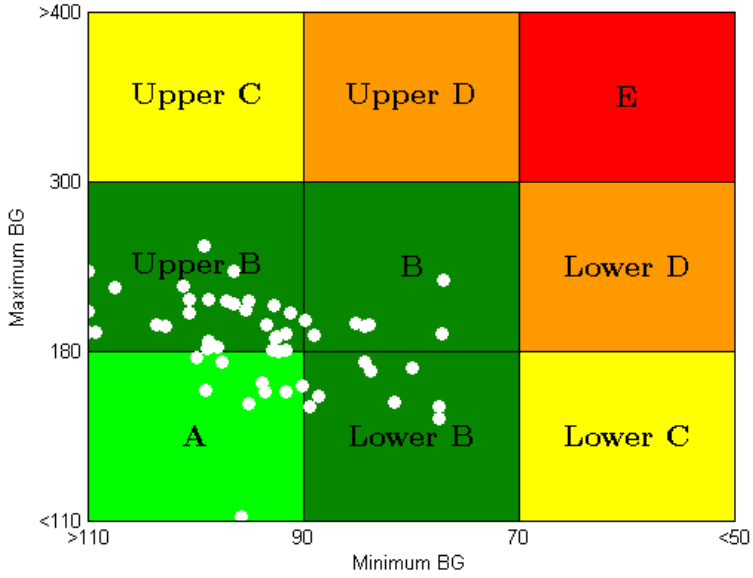

Figure 2.11.: Result of a 255 hours simulation with second feeding protocol [Control parameters: $\Lambda = 0.0125$, $A_c = 110^{-3}$, $K_c = -1000$, $B_c = -1$, Set-point (G_N)=95 mg/dL]

the daily maximum and minimum of BG levels.

Summary

In this Section, my goal was to proove the usability of the RFPT-based control design method in case of highly complex T1DM model. I have investigated several situations and the simulations demonstrated the the developed RFPT-based controller can deal with managing the blood glucose level of the T1DM model. Moreover, I have used different adaptivity law than the control of Hovorka-model in order to increase the speed of the adaptivity. The controller successfully kept the blood glucose level in the selected ranges without any hypoglycemic effect, beside soft hyperglycemia in a few cases.

Thesis Group 1

Thesis group 1: T1DM control via RFPT framework

Thesis 1

I have developed an RFPT-based controller design framework for physiological systems. The provided solutions allows the using of highly approximating (rough) model of the physiological system to be controlled.

Thesis 1.1

I have proven the usability of the developed framework in case of the low complexity T1DM model, the Minimal Model. The designed controller keeps the BG level in a narrow range and it is able to suppress high glucose variability as well.

Thesis 1.2

I have proven the usability of the RFPT-based controller design framework in case of highly complex T1DM models: the Cambridge model (so called Hovorva-model) and the Pavia-Padova model (so called Magni-model). The developed RFPT-based controllers provide fast adaptivity and they are able to keep the blood glucose level of the complex T1DM models inside a given selected range even under unfavorable glucose loads or soft blood sugar variability.

Relevant own publications pertaining to this thesis group: [22, 72, 73, 74, 75].

3. Novel perspective in the Control of Nonlinear Systems via a Linear Parameter Varying method

This Chapter covers three major topics: short summary about the investigated LPV system class; presentation of the developed LPV based tool which aims to compare and qualify different systems and control approaches; and a novel control and observer scheme developed during the research, which is appropriate to handle nonlinear systems that belong to the investigated LPV system class.

In detail, I first present a summary about those LPV system classes in which the developed tools can be used in a nutshell.

Thereafter, I introduce the novel approach on how can we use the regular $\mathcal{L}_2$ norm defined in the parameter space of the LPV system in order to realize a quality marker tool for modeling and control purposes.

Afterwards, I present the novel completed controller and observer scheme, which is a general controller design method for particular class of nonlinear system via LPV theorem, but also can be used in control of DM. Moreover, I demonstrate the applicability of these tools in concrete examples.

The theoretical background regard to the LPV modeling can be found in Appendix D.

Finally, it should be noted that I have used MATLAB$^{\mathrm{TM}}$ in order to realize the theoretical achievements.

3.1. Specificities of physiological LPV models

Most of the mathematical models which describe physiological processes have nonlinear attitude, where the nonlinearity comes from several sources (e.g. type of connections, communication between parts, enzyme kinetics, etc.) [1]. These models can be described with the LPV theorem without exception. It is generally true that in most of the cases, the nonlinearities are connected to the central model structure, which means that these nonlinearities occur in the state matrix $\mathbf{A}$ and the inputs and outputs of the models are

not affected by them [76, 77]. Therefore, when the LPV form of them are constructed, only the state matrix will be parameter dependent: $\mathbf{A}(\mathbf{p}(t))$. However, there are models, where nonlinearities occur in connection with the input or output. A typical example when enzyme of drug kinetics are considered during the input construction [78].

In the followings I detail the main considerations according to the complex physiological models investigated in the thesis:

- Inputs are not affected by nonlinearities; they have impulse attitude (injections); do not directly affect the outputs (in state space representation this means that the $\mathbf{D}$ matrix contains only zero elements and it does not depend on the parameter vector $\mathbf{p}$);
- Output(s) are connected a few states which can be directly or indirectly measured; not affected by nonlinearities;
- Since the nonlinearities do not affect the inputs and the outputs, it is not necessary to select their elements as scheduling parameters, which means that $\mathbf{B}$ and $\mathbf{C}$ are independent from the parameter vector $\mathbf{p}$; moreover, these usually do not depend on time;
- The nonlinearities occur in the state matrix ($\mathbf{A}$) regarding to nonlinear dynamic connection between parts of the system, drug absorption and/or kinetics; the intra- and inter-patient variabilities are represented in the elements of $\mathbf{A}$ and usually these are time dependent; scheduling variables should be selected from the elements of $\mathbf{A}$ in order to hide the nonlinearities and make the handling of $\mathbf{A}$ convenient from control point of view.

The aforementioned properties are true in case of DM as well:

- Inputs have impulse nature (insulin injection, nutrient bolus), however, they do have linear attitude; $\mathbf{D}$ is zero (no direct input-output connection);
- Output(s) are connected to the blood glucose level (or the blood glucose level is the output itself); not affected by nonlinearities;
- $\mathbf{B}$ and $\mathbf{C}$ are independent from the parameter vector $\mathbf{p}$; these do not depend on time;
- The nonlinearities occur in the state matrix ($\mathbf{A}$) regarding to glucose-insulin dynamics, glucose and/or insulin absorption, effect and dynamics of insulin; the

intra- and inter-patient variabilities are represented in the elements of $\mathbf{A}$ and usually these are time dependent; scheduling variables should be selected from the elements of $\mathbf{A}$.

From the aforementioned consideration it can be derived that the LPV-type diabetes models have the following form which can be observed in several studies [49, 50, 79]:

$$\begin{aligned} \dot{\mathbf{x}}(t) &= \mathbf{A}(\mathbf{p}(t))\mathbf{x}(t) + \mathbf{B}\mathbf{u}(t) \\ \mathbf{y}(t) &= \mathbf{C}\mathbf{x}(t) + \mathbf{D}\mathbf{u}(t) \end{aligned} \tag{3.1}$$

where the system matrix $\mathbf{S}$ is the following:

$$\mathbf{S}(\mathbf{p}(t)) = \begin{pmatrix} \mathbf{A}(\mathbf{p}(t)) & \mathbf{B} \\ \mathbf{C} & \mathbf{D} \end{pmatrix} \tag{3.2}$$

and the state space representation in compact form is:

$$\begin{pmatrix} \dot{\mathbf{x}}(t) \\ \mathbf{y}(t) \end{pmatrix} = \mathbf{S}(\mathbf{p}(t)) \begin{pmatrix} \mathbf{x}(t) \\ \mathbf{u}(t) \end{pmatrix} . \tag{3.3}$$

Equation (3.1) shows that in this form the LPV-type diabetes models only contain dependency from the parameter vector $\mathbf{p}$ in the state matrix $\mathbf{A}$ and all time dependent components are selected as scheduling variable.

It has to be noted that the aforementioned system class is the typical in most nonlinear biomedical model cases [76, 77].

In this Chapter, I focus not only on DM models, but on other simple models too, given that they have these properties (only the $\mathbf{A}(\mathbf{p}(t))$ is parameter dependent).

3.2. Different interpretations of quality based on LPV configurations

In this Section, I introduce a unique norm interpretation regarding the PS of the LPV systems. I used the well-known matrix $\mathcal{L}_2$ norm, since the properties of the PS allow us to declare such constructs.

3.2.1. Norm-based "difference" definition in the parameter space

Each dimension of the PS correspond to an element of the parameter vector ($\mathbf{p} \in \mathbb{R}^q$). Inside this abstract space each point can be determined by the corresponding parameter vector $\mathbf{p}(t)$. Furthermore, this abstract PS can be handled as an Euclidean vector space and vector $\mathcal{L}_p$ norms can be interpreted inside the PS. Assume two parameter vectors $\mathbf{p}_a, \mathbf{p}_b \in \mathbb{R}^q$ in the PS. The $\mathcal{L}_2$ norm based distance between the vectors can be described as follows:

$$\|\mathbf{p}_a - \mathbf{p}_b\|_2 = e. \tag{3.4}$$

Naturally, the $e(t)$ of (3.4) becomes time dependent if one of the parameter vectors are varying in time ($\mathbf{p}_a(t)$ or $\mathbf{p}_b(t)$). The defined $e(t)$ can be used in various ways depending on the interpretation of the PS which are presented in the next section.

3.2.2. Possible interpretations of the defined norm-based difference in the Parameter Space

The points of the PS which are determined by the parameter vector can be interpreted on their own as vectors, whose elements consist of the parts of the system. However, the parameter vectors can unequivocally determine an underlying LTI system in the affine LPV case and a well-characterized LTI system in the polytopic case. The following statements are general LPV model properties regardless of whether it is the affine or polytopic type LPV model.

When the goal is to emphasize particular properties of a system, each of the parts representing these properties have to be selected as scheduling variables. For example, investigate the nonlinear system from (D.12) and complete it with another term:

$$\begin{aligned} \dot{x_1}(t) &= \sqrt{x_1(t)}x_2(t) + u(t) \\ \dot{x_2}(t) &= -k_1 x_2(t) + k_2 \frac{x_1(t)}{x_2(t)} \\ y(t) &= x_1(t) \end{aligned} \quad . \tag{3.5}$$

Assume another scheduling variable $p_2(t) = \dfrac{1}{x_2(t)}$ and $\{p_2(t) \in \mathbf{p}(t) : p_2(t) = [p_{2,min}, \dots, p_{2,max} : x_2(t) \neq 0]\}$.

Hence, according to (D.13):

$$\begin{pmatrix} \dot{\mathbf{x}}(t) \\ \mathbf{y}(t) \end{pmatrix} = \begin{bmatrix} 0 & p_1(t) & 1 \\ k_2 p_2(t) & -k_1 & 0 \\ 1 & 0 & 0 \end{bmatrix} \begin{pmatrix} \mathbf{x}(t) \\ \mathbf{u}(t) \end{pmatrix}, \tag{3.6}$$

where $\mathbf{p}(t) = [p_1(t), p_2(t)]^\top$ and the PS is 2 dimensional. Assume a permanent and a time varying vector in the PS, where the fixed vector $\mathbf{p}_A(t_a)$ belongs to a given time moment t_a, i.e. $\mathbf{p}_A(t_a) = [p_{1,a}, p_{2,a}]^\top$ and $\mathbf{p}_B(t)$ is time varying. In this case, the introduced $e(t)$ is appropriate to define a "difference" between the $\mathbf{p}_A(t_a)$ and $\mathbf{p}_B(t)$. Consider a case where $\mathbf{p}_A(t_a)$ is determined as permanent reference vector and $\mathbf{p}_{ref} = \mathbf{p}_A(t_a)$ and $\mathbf{p}_B(t)$ is the actual parameter vector varying over time ($\mathbf{p}_{actual}(t) = \mathbf{p}_B(t)$). In this case $e(t) = \|\mathbf{p}_{ref} - \mathbf{p}_{actual}(t)\|_2$ determines the 2-norm based difference of them and this can be interpreted as an "error" or "quality" signal, if $\mathbf{p}_{ref}$ and $\mathbf{p}_{actual}(t)$ are different during operation. Generally, this interpretation can be extended for any q dimensional $\mathbf{p}(t)$ parameter vector.

If the question is to design a controller, the key point is what the selected scheduling variables are. At this point several approaches and interpretations can be distinguished. The main ones are the following:

1. The selected scheduling variables are those properties which have to be monitored during the operation. In this case, the 2-norm based difference can be used as "quality" signal and the performance of different controllers can be compared with this quality signal in the PS.

2. The selected scheduling variables are those properties which have to be controlled and monitored during operation. In this case, we can interpret the 2-norm based signal as "error" signal. This type of error can be used during the controller design and the control signal will be depend on it.

3. The selected scheduling variables are those components which are time dependent in LTV case. The parameter vector unequivocally determines the underlying LTI systems which can occur from the general LTV system during operation at given time moments. In this case, the defined 2-norm difference can be used as "metric" in order to compare LTI systems in the PS.

4. The selected scheduling variables are those components which are causing nonlinearities in NLTV case. The general purpose of this approach is that the linear

controller design techniques become usable. If all nonlinearity causing and time dependent parameters are selected as scheduling variables, the parameter vector unequivocally (general and affine LPV case) or satisfactorily (polytopic LPV case) determines an LTI system during operation at given time moments. In this case the defined 2-norm difference can be used as metric in order to compare LTI systems in the PS.

In the following sections, I detailed the key aspects from the above mentioned points.

The 2-norm based difference as quality and error signal

The most important issue in these cases is the way how the parameters are selected from the original model and the interpretation of them.

If the scheduling parameters are selected one-by-one and are not grouped, then each dimension of the PS will be an individual variable with physical or physiological meaning (e.g. the $p_1(t) = \sqrt{x_1(t)}$ and $p_2(t) = \dfrac{1}{x_2(t)}$ parameter from (3.5)).

However, the scheduling variables can be grouped as well. For example, one can imagine a situation, where $p_2(t) = \dfrac{k_2}{x_2(t)}$ from (3.5). In this case the $p_2(t)$ scheduling variable can loose its original meaning and cannot be interpreted individually, if the k_2 is not a unitless scalar but rather a meaningful scalar, which describes a property of the system.

Nevertheless, the grouped scheduling parameters allow to interpret the 2-norm based difference in a more sophisticated manner.

If the goal is to monitor how the specific properties of the system vary over time and compare this variation with predefined requirements, the 2-norm based difference can be interpreted as quality signal. This approach can be important in such applications where the different parts of the system cannot change too drastically relative to each other. Naturally, in this case, these specific parts have to be selected as scheduling variables.

It has to be noted that the observability should be considered in this case, since the selected parts have to be observable or estimable. Fig. 3.1(a). shows a 2 dimensional parameter space. For example, a possible goal (beside other goals) of the applied controller can be to hold permanently two system properties during operation. If these properties (which are represented with different parts of the system) are selected as scheduling variables, the performance of the controller can be assessed based on the $e(t)$ signal.

During controller design the 2-norm based difference can be used as an ”error” signal in the classical meaning. The appropriate selection and interpretation of the scheduling

variables are necessary. The observability and controllability of the scheduling variables are important issues as well.

The first step is the selection of parts of the models as scheduling variables which have to be controlled. However, in case of grouped factor out (e.g. $p_2(t) = \frac{k_2}{x_2(t)}$) should be reasonable. The error signal ought to be known at every time moment as the basis of control.

If the elements of the parameter vector are not observable, they have to be estimated or approximated. The control signal affects the scheduling variables directly or through coupling. Without connection, the scheduling variables cannot be influenced by the control signal.

In general, the recently developed Robust Fixed Point Transformation (RFPT)-based controller design methodology can be used [65] as well. The first stage is the investigation of the effect chain of the control action, namely, how the control signal affects the controlled variables which are here the scheduling variables $\mathbf{p}(t) = f(\mathbf{p}(t)^-, \mathbf{u}(t))$, where $\mathbf{p}(t)^-$ is the a-priori knowledge about the $\mathbf{p}(t)$ and $\mathbf{u}(t)$ is the control signal. With approximate inverse kinematic description ($\tilde{\mathbf{u}}(t) = f(\mathbf{p}(t), \mathbf{p}(t)^-)$) and appropriate control laws, an RFPT-based controller can be designed. In this case the error signal can be the developed by 2-norm based difference ($e(t)$), which arises when the nominal prescriptions of the controlled variables (the scheduling variables) are not equal with the actual values of them. Geometrically, the nominal prescriptions of the controlled variables can be a permanent point of the PS ($\mathbf{p}_{ref}$) and the actual values $\mathbf{p}_{act}(t)$ are varying in time during operation. Based on the arised error signal $e(t)$ an RFPT-based controller can be designed [65].

In Fig. 3.1(a). a $2D$ example can be seen, where $e(t)$ can be interpreted as the mentioned error signal. The comparability of the order of magnitudes of the scheduling variables represents a significant point. The nature of the Euclidean norms determine that particular difference signals affect the 2-norm based difference the most which have the highest magnitudes (e.g. the $p_{reference,1} - p_{actual,1} \gg p_{reference,k} - p_{actual,k}$, $p \in \mathbb{R}^k$, $k \neq 1$ determines that the 2-norm based difference will have strong connection with the variation of $p_{reference,1} - p_{actual,1}$). If the scheduling variables have to be considered with the same "weight" (they have the same importance), different normalization and weighting techniques can be used [80].

The 2-norm based difference as comparison of systems

Generally, LPV techniques are used in order to embed the uncertainties into a system model or hide the system model nonlinearities by making the application of linear

controller design techniques possible. Classical control design solutions can be used regard to LPV models, however, the use of such models according to LMI based controller design methodologies are possible as well.

Almost each control design method can be formulated as an LMI problem and can be solved via iterative numerical processes [81]. In recent years, parallel with numerical computational evolution, a wide range of LMI applications were discovered and used in control engineering [82–84].

However, the basic concept behind the LPV-LMI based modeling and control approaches consist in guaranteeing and exploiting the convexity properties. Basically, this means that it is enough to design such sub-controllers which can deal with the LTI systems in the vertices of the convex polytope, and the convex combination of such controllers can handle each occurring LTI system during operation, if the basic LPV model was appropriate.

In order to use the developed 2-norm based difference as a "metric" on the underlying systems which are determined by parameter vectors inside the PS, several control and mathematical constraints have to be considered. Particular parameter vectors belong to each of the points inside the PS. Since the parameter vector $\mathbf{p}(t)$ consists of elements which were multiplied out from the SS model, a parameter vector can determine an underlying system. The key questions are the type of the underlying systems with respect to the parameter vector and how the parameter vector can be used to describe differences among the underlying systems. A few scenarios can be considered depending on the type of the original and the describing LPV systems.

The reasonable original system can be NLTV, LTV and LTI beside the describing LPV system (affine or polytopic).

- In LTI-LPV case, each of the points inside the PS is an LTI system and is fully determined by the parameter vector;
- In LTV case, a parameter vector determines the underlying system only if each time-dependent element is selected as scheduling variable;
- In NLTV case, if each time-dependent and nonlinearity causing element is selected as scheduling variable, the parameter vector determines the underlying system.

In all three cases, the parameter vectors $\mathbf{p}(t)$ determine an underlying LTI system. In NLTV-LTV-LPV case, the original models become simpler. Furthermore, during operation these get around a path inside the PS. The most typical application is when the nonlinearity causing elements are selected as scheduling variables from the NLTV

system and the obtained LPV model is used in a LPV-LMI control application. However, in this case, a parameter vector does not determine equivocally the underlying system, since the time-dependent components can cause hidden differences, which cannot be seen through the parameter vector.

Assume that the selection of the scheduling variables was appropriate and each parameter vector determines an underlying LTI system equivocally. That means the parameter vector-based differences can be interpreted as a "metric' on the occurring LTI systems to which these vectors belong. Namely, instead of the Frobenius-norm based difference in the systems' space, the Euclidean-norm based difference in the PS can be used to determine the "difference" between the occurring LTI systems.

$$\|\mathbf{S}(\mathbf{p}_a) - \mathbf{S}(\mathbf{p}_b)\|_F \rightarrow \|\mathbf{p}_a - \mathbf{p}_b\|_2 = e. \tag{3.7}$$

In the convex polytope, every LTI system is uniquely specified with their parameter vectors as a consequence of the aforementioned statements. However, the LTI systems in the convex polytope can be calculated as the convex combination of the vertices of the convex polytope. The key question then is the determination of barycentric coordinates ($\alpha_j \in \mathbb{R}^j$) via the uniqueness of the vertices of the given polytope.

Inside the convex polytope each occurring LTI system is overdefined, since in a q dimensional parameter space j coordinates are used to define them, where $j > q$. That means, if the barycentric coordinates are arbitrarily defined, the occurring LTI system description will not be unequivocal, since with the same set of coordinates describes more than one system. In other words, because of the null space problem (differences could occur in the null spaces of the given LTI system) the parameter vector based metric cannot be used as a classic "metric" and cannot be unequivocally interpreted on the LTI systems behind.

Nevertheless, the calculation of the barycentric coordinates ($S = \sum_{i=1}^{j} \alpha_i S_i$) is connected to the selected vertices of the convex polytope and equivocally defined by (D.20-D.23). With this condition, the defined metrics can be valid on the occurring LTI systems in case of polytopic LPV systems as well.

The developed parameter vector based metric can be used in modeling and control as a "quality marker". For example, if a given LPV model is used during identification, the identified model $\mathbf{S}(\mathbf{p}_{ident})$ can be compared to a reference model $\mathbf{S}(\mathbf{p}_{ref})$ in order to estimate the efficiency of the identification procedure. Furthermore, this can be an on-line estimation as well, when the system under identification is described with $\mathbf{S}(\mathbf{p}_{actual}(t_p))$. This procedure can be characterized by the developed $e(t)$ instead of the Frobenius-norm

based difference. If the goal is to monitor the variation of the system during operation compared to a reference system, the previous solution can be used here as well.

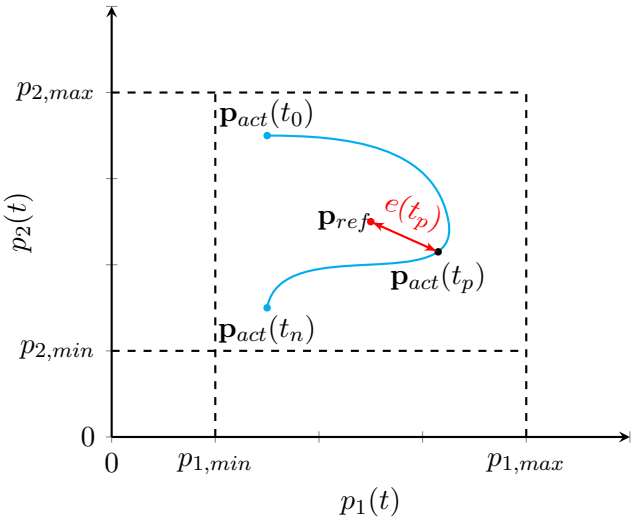

(a)

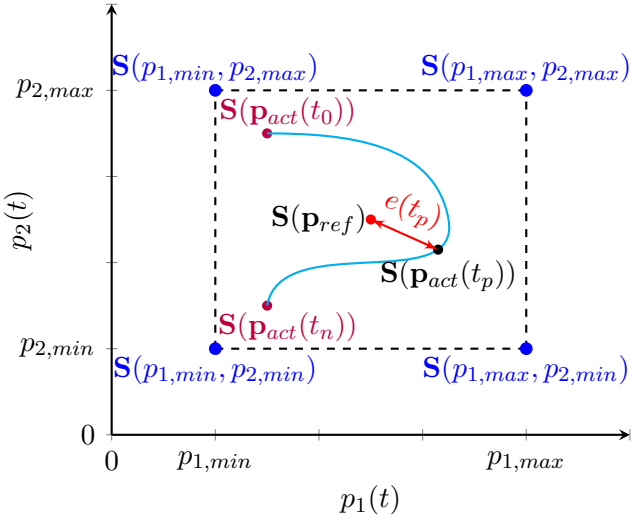

(b)

Figure 3.1.: Examples of the possible interpretations of the 2-norm based difference

Fig. 3.1(b). shows a $2D$ example for the aforementioned interpretations. The PB is the rectangle which is determined by the $p_{min,1,2}$ and $p_{max,1,2}$ in the PS. Furthermore, this is the validity border of the affine LPV model. At the same time, the rectangle forms a convex polytope. Inside the polytope each occurring LTI system can be calculated as

the convex combination of the vertices of the convex polytope.

In the light of the detailed description from above the consequences regard to Fig. 3.1. can be summed-up as follows: Fig. 3.1(a). presents how the parameter vector $\mathbf{p}(t)$ varies over time. In this case, the $\mathbf{p}_{ref}$ is the selected reference parameter vector, $\mathbf{p}_{act}(t_0)$, $\mathbf{p}_{act}(t_n)$ and $\mathbf{p}_{act}(t_p)$ are the initial-, final- and actual-values of the varying parameter vectors, respectively. The 2-norm based difference is interpreted as $e(t_p) := \|\mathbf{p}_{ref} - \mathbf{p}_{act}(t_p)\|_2$. At the same time Fig. 3.1(b). demonstrates how the underlying LTI system $(\mathbf{S}(\mathbf{p}(t_{act})))$ varies over time accordingly the belonging $\mathbf{p}_{act}(t_p)$.

Each aforementioned interpretations and issues are demonstrated on biomedical engineering examples concerning diabetes in Sec. 3.2.3.

3.2.3. Usability of the development approach

Selected diabetes model and LPV form of it

I have selected a simple DM patient model developed by Wong et al. in [85, 86] for the Intensive Care Unit (ICU) treatment. The selection was plausible, since it has several benefits to use as a test model. It is a 3rd order model and contains saturation type nonlinearities. The model is described by (B.2). The model equations can be handled as in (3.1)-(3.2), which means only the state matrix depends on the parameter vector $(\mathbf{A}(\mathbf{p}(t)))$.

The main goal of the model is to describe the glucose-insulin dynamics of an inpatient who suffers from T1DM and is nurtured on the ICU [85, 86]. It is expected that this simple model – after preliminary identification – can provide the current and the future blood glucose level of the patient with a precision that is good enough for the realization of the tight glycemic control (TGC). Detailed description and used parameters of the model can be found in Subsection B.2.1.

qLPV model of the original Wong model

I have selected the following scheduling parameters as the elements of the parameter vector based on [87]:

$$\mathbf{p}(t) = \begin{bmatrix} p_1(t) \\ p_2(t) \\ p_3(t) \end{bmatrix} = \begin{bmatrix} \dfrac{S_I Q(t)}{1+\alpha_G Q(t)} \\ \dfrac{S_I G_E}{1+\alpha_G Q(t)} \\ \dfrac{1}{1+\alpha_I I(t)} \end{bmatrix} . \tag{3.8}$$

These selection reduces the model complexity, however, the $\mathbf{p}(t)$ contains grouped variables. $p_1(t)$ and $p_2(t)$ have Michaelis-Menten attitude and they keep their original physiological meaning, namely, the nonlinear kinetic effect of the appearing insulin on the blood glucose level. Each nonlinearity causing element was selected as scheduling variable.

Based on (B.2) and (D.16), the affine qLPV model of the matrix terms of the system matrix of the original Wong model can be described as follows:

$$\mathbf{A}(\mathbf{p}(t)) = \mathbf{A}_0 + \mathbf{A}_1 p_1(t) + \mathbf{A}_2 p_2(t) + \mathbf{A}_3 p_3(t) =$$

$$\begin{bmatrix} -p_G & 0 & 0 \\ 0 & -k & k \\ 0 & 0 & 0 \end{bmatrix} + \begin{bmatrix} 0 & -1 & 0 \\ 0 & 0 & 0 \\ 0 & 0 & 0 \end{bmatrix} p_1(t) + \begin{bmatrix} 0 & -1 & 0 \\ 0 & 0 & 0 \\ 0 & 0 & 0 \end{bmatrix} p_2(t) + \begin{bmatrix} 0 & 0 & 0 \\ 0 & 0 & 0 \\ 0 & 0 & -n \end{bmatrix} p_3(t) \quad . \tag{3.9}$$

$$\mathbf{B} = \begin{bmatrix} 1 & 0 & 0 \\ 0 & 0 & 0 \\ 0 & \dfrac{1}{V_L} & -p_4 I_b \end{bmatrix} \quad \mathbf{C} = \begin{bmatrix} 1 & 0 & 0 \end{bmatrix} \quad \mathbf{D} = \begin{bmatrix} 0 & 0 & 0 \end{bmatrix}$$

After defining the border of the parameter box, i.e. the vertices of the convex polytopic space, the polytopic model form of the qLPV model can be easily obtained based on the affine qLPV form of (3.9). I have selected tight ranges in every dimension in order to

catch the dynamics as precisely as possible:

$$p(t) = \begin{pmatrix} p_1(t) \\ p_2(t) \\ p_3(t) \end{pmatrix} = \begin{pmatrix} [p_1^- \dots p_1^+] \\ [p_2^- \dots p_2^+] \\ [p_3^- \dots p_3^+] \end{pmatrix} = \begin{pmatrix} [0 \dots 0.3] \\ [0.0095 \dots 0.0106] \\ [0.9 \dots 1.1] \end{pmatrix} . \tag{3.10}$$

Results

The main goal was to test the usability of the developed "metric" without physiological constraints. In this demonstration, I did not seek the physiological validity, just to introduce the developed approach. Therefore, I have used randomized input signals and not physiologically valid ones. However, the physiologically valid input signals are much favorable (less time period, less amplitude) then the used ones. In the given circumstances, the output of the nonlinear original system and the LPV version of it can be found on Fig. 3.2. below, where it can be seen that the nonlinear original model provides the same output as the LPV version.

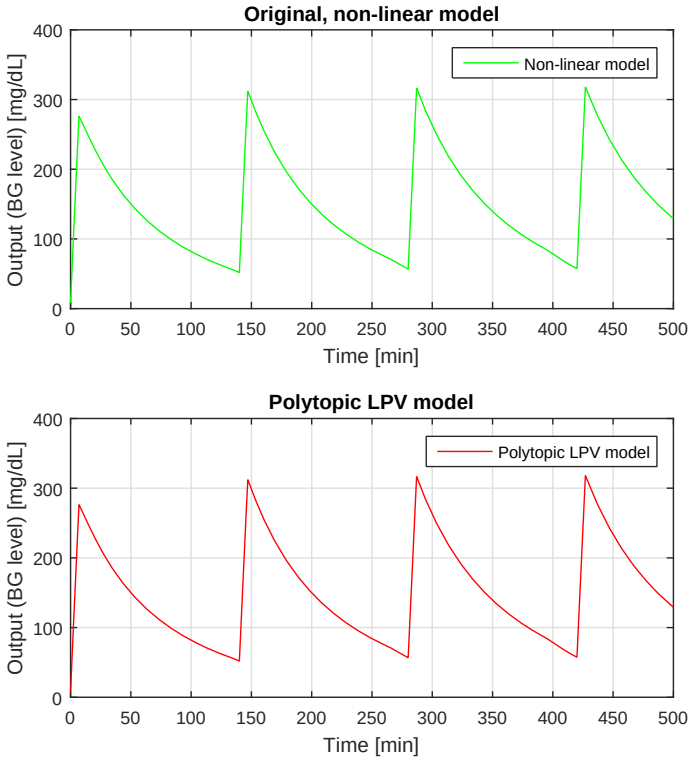

Figure 3.2.: The outputs of the models

Figure 3.3. shows the varying of the elements of the parameter vector $\mathbf{p}(t)$ and the developed 2-norm based difference. On every diagram, the dashed line represents the fixed value, which belongs to the $p_{ref} = [0.2,\ \ 0.01025,\ \ 0.98]^T$. The input is selected to be a symmetrical repeating impulse ($P(t) = 40$ at every 140 min for 7 min long and $u_{ex}(t) = 100$ at every 130 min for 6.5 min long) and it can be seen that after the first period's decay, the parameter vector have taken the same values in each cycle, which means the same LTI systems occurs over time in each cycle.

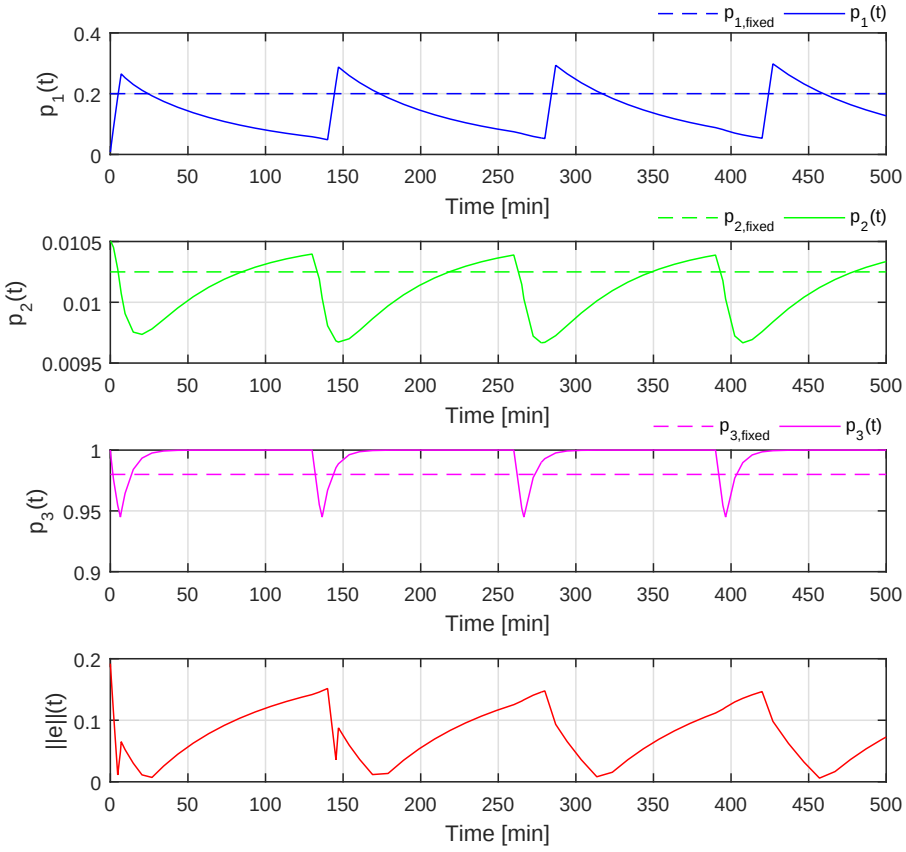

Figure 3.3.: Varying of the scheduling variables and the norm-based error signal

Fig. 3.4. shows the same signals as Fig. 3.3. on one diagram in order to compare the orders of magnitudes. It can be seen that those signals that reflect mostly in the $\|e(t)\|_2$ have the highest amplitude. Since in this case the $p_1(t)$ has the highest amplitude, the $\|e(t)\|_2$ correlated mostly with $p_1(t)$. If each scheduling variables have to be considered

with the same weight, normalization procedures can be done [80]. However, I did not apply such methods as the goal was only demonstration.

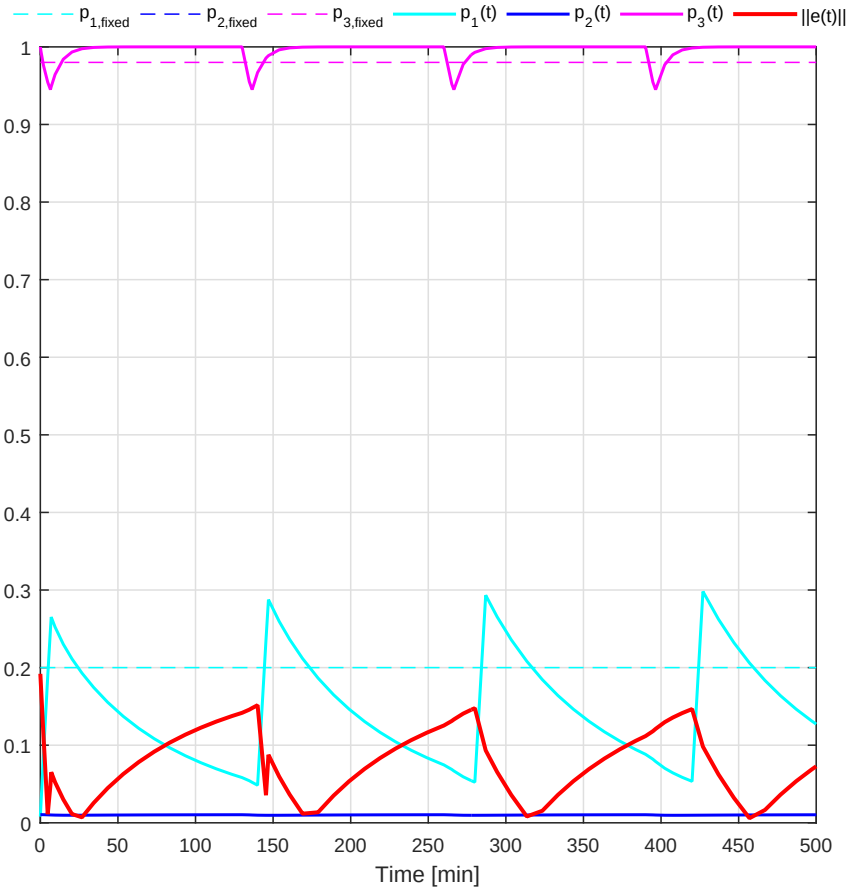

Figure 3.4.: Comparison of the magnitudes of the scheduling variables and the norm-based error signal

In order to make this demonstration complete, Fig. 3.5. shows the scheduling parameters and the $3D$ parameter space too. It can be seen that the parameter vector starts from a given point and ends at another. During the simulation time the parameter vector runs through a trajectory in the PS. Naturally, that means that the system matrices belonging to the different parameter vectors are varying in time, as well.

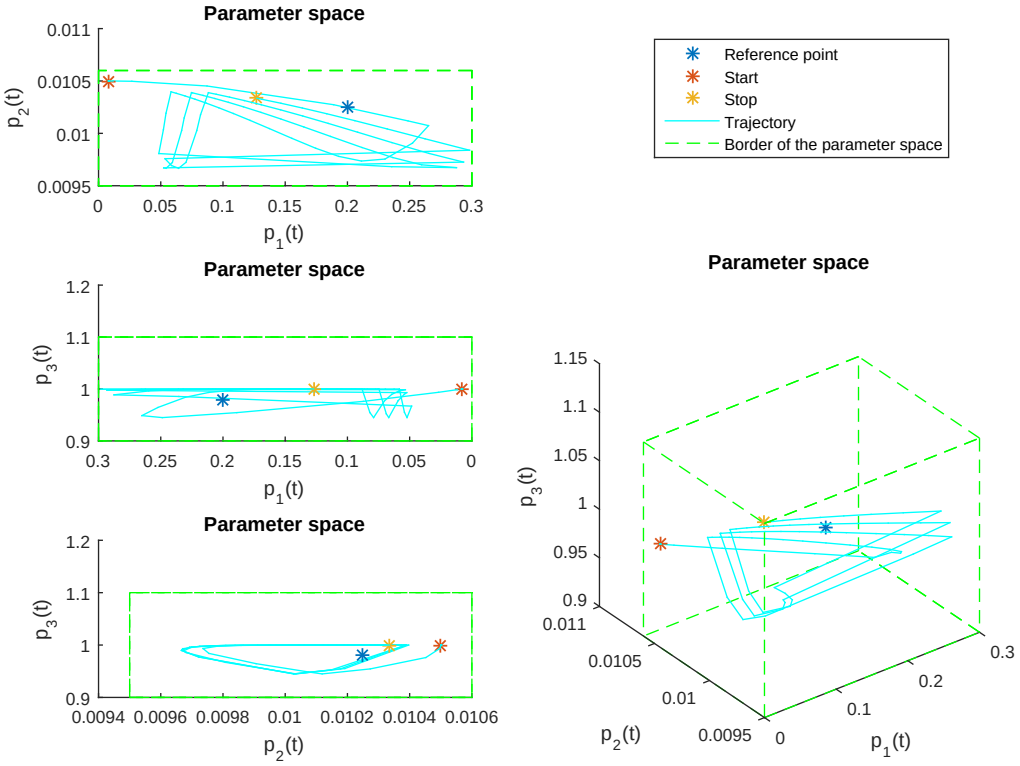

Figure 3.5.: Evolution of the scheduling variables in the parameter space during operation

If the parameter vectors fully determine the underlying LTI systems during operation, the parameter vector based metric can be used to compare the ”difference” between these systems. Figure 3.6. shows this issue in case of the selected model and parameter vector, namely, instead of the Frobenius-norm based ”difference” the developed metric can approximately provide similar results. Naturally, the signals are not the same, since the numerical computations are different. The upper diagram presents that the signals are covering each other. The lower diagram shows the difference between these – furthermore, the generated maximum root mean square error (RMSE) of the was $5.8352\ \ 10^{-4}$ based on the difference between the given signals.

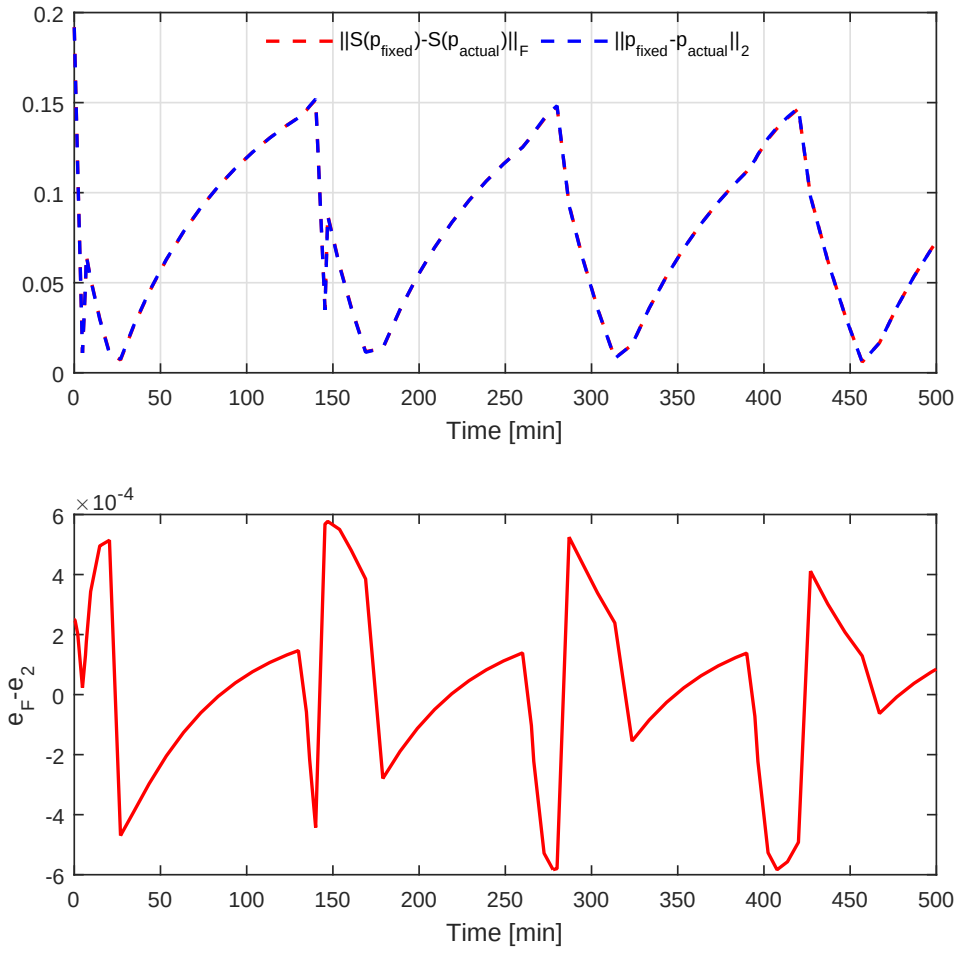

Figure 3.6.: Different norm-based differences

Summary

In this section, I have introduced a norm based ”difference” interpretation that can be applied to LPV systems, based on the properties of the LPV parameter space. I have defined how to use these interpretations as error and quality criteria during modeling and control and demonstrated my theoretical findings by a particular example in diabetes modeling and control of ICU patients.

3.3. Novel completed controller scheme for LPV systems

In this Section, I introduce the developed completed controller and observer scheme for a particular class of LPV systems. This approach is based on the classical linear state feedback theorems and the matrix similarity theorems.

I will demonstrate the developed tools in case of nonlinear systems, including DM as well.

3.3.1. State feedback and gain-scheduling control

The idea of optimal state feedback control for LTI systems originates from the sixties of 20th century, when the cost function based optimization first appeared in modern control engineering. Over decades, different cost functions and feedback gain calculation techniques appeared customized to the specifics of the control problem, like quadratic regulation, energy minimization, time minimization or tracking error minimization, etc. [88]. As far as LPV systems are concerned, the first generation of gain scheduling control techniques were developed in the late nineties of the previous century [89, 90].

In case of state feedback control, the control signal occurs in the following form:

$$\mathbf{u}(t) = -\mathbf{K}\mathbf{x}(t) \ , \tag{3.11}$$

where the control input $\mathbf{u}(t)$ is the linear combination of the feedback gain matrix $\mathbf{K} \in \mathbb{R}^{m \times n}$ and the state vector $\mathbf{x}(t)$. The $\mathbf{K}$ can be designed via different iteration-based methods. For example, in case of Linear-Quadratic (LQ) control, the control input of (3.11) is minimizing the following cost function [80]:

$$J(\mathbf{u}) = \int_0^\infty \Big(\mathbf{x}^\top \mathbf{Q}\mathbf{x} + \mathbf{u}^\top \mathbf{R}\mathbf{u} + 2\mathbf{x}^\top \mathbf{N}\mathbf{u}\Big)\mathrm{d}t \ , \tag{3.12}$$

and the optimal gain $\mathbf{K}$ can be designed by solving the following control Ricatti equation [80]:

$$\begin{aligned} &\mathbf{A}^\top \mathbf{X} + \mathbf{X}\mathbf{A} - (\mathbf{X}\mathbf{B} + \mathbf{N})\mathbf{R}^{-1}(\mathbf{B}^\top \mathbf{X} + \mathbf{N}^\top) + \mathbf{Q} = 0 \\ &\mathbf{K} = \mathbf{R}^{-1}(\mathbf{B}^\top \mathbf{S} + \mathbf{N}^\top) \end{aligned} \ . \tag{3.13}$$

The optimal $\mathbf{K}$ gain ensures that LTI systems which are non-stable or stable but do not have eligible properties become stable, with better control performances through pole-placement. In general, this configuration modifies the open-loop $\mathbf{A}_{open}$ state matrix into $\mathbf{A}_{closed} = \mathbf{A}_{open} - \mathbf{B}\mathbf{K}$. The poles of the characteristic equation can be calculated

as follows:

$$\lambda(\mathbf{A}+\mathbf{BK}) =\mid \mathbf{I}\lambda-\mathbf{A}+\mathbf{BK} \mid= 0 \ . \tag{3.14}$$

In gain-scheduling control, which is a natural choice for an affine LPV system, the optimal gain becomes parameter dependent [89]:

$$\mathbf{u}(t) = -\mathbf{K}(\mathbf{p}(t))\mathbf{x}(t) \ . \tag{3.15}$$

The class of $\mathbf{p}(t)$ dependent controller of (3.15) is able to deal with the class of $\mathbf{p}(t)$ dependent system of (3.3). Since, the continuous controller design is impossible, the reasonable choice is to divide the q dimensional parameter space into different slices. Then, different controllers have to be designed for each slice and these controllers can handle the occurring LTI systems inside these slices. The drawback is high computational capacity, complex switching schedule (regarding to the variation of $\mathbf{p}(t)$ over time) and the necessary advanced methods, which provides global stability.

Instead of this natural, however sometimes unmanageable configuration, the polytopic model configuration and polytopic controller design spread out in control engineering [81, 82, 91].

In polytopic case, the number of necessary controllers are reduced. If, the parameter space is handled as a vector space and the occurring LTI systems ("system trajectory") are inside a given region of the vector space, a convex hull can be design, which wraps the system trajectory. Finally, it is enough to design specified number of controllers to the determining point of the **p**-space. Thus, if the convexity properties are fulfilled, the resulting controller, as the convex combination of the designed controllers can handle each occurring LTI systems inside the polytope [91, 92]. The benefits of the methods are the drawbacks at the same time: the necessary deep mathematical knowledge and understanding, high computational capacity and the global stability is only particularly true, if the system trajectory does not exit from the convex hull (the value of $\mathbf{p}(t)$ exits from among the predefined limits) [93].

3.3.2. Important properties of the investigated LPV system class

In the previous Section, I investigated the opportunities of using the mathematical properties of the parameter space in order to define norm-based performance markers for LPV systems. Moreover, I examined the general properties of such models, which are usually used in physiological and in particular, DM researches.

Hence, these observations are strongly presumed in the following, so I shortly sum-up

these again below:

- Input(s) are not affected by nonlinearities and do not have direct connection between the inputs and outputs (the consequence being that $\mathbf{D}$ is persistent in time and is zero matrix);
- Output(s) are not affected by nonlinearities;
- Since the nonlinearities do not affect the inputs and the outputs, it is not necessary to select their elements as scheduling parameters, which means that $\mathbf{B}$ and $\mathbf{C}$ are independent from the parameter vector $\mathbf{p}$; moreover, these usually do not depend on time;
- The nonlinearities only appear in the state matrix $\mathbf{A}(\mathbf{p}(t))$ regarding to the nonlinear system dynamics, nonlinear cross effects and nonlinear coupling; the patient variabilities are mostly occur in the elements of $\mathbf{A}$.

If the parameter vector is persistent in time, the belonging parameter dependent LPV system simplifies to an LTI system. Moreover, the variation of $\mathbf{p}(t)$ realizes the system trajectory, which consists of infinite number of LTI systems. In this case, each points in the parameter space equivocally determines an underlying LTI system. (This property allows us to define different norms in the parameter space on the parameter vectors, however, most of them can be interpreted on the underlying LTI system.)

Preliminarily, I showed that every parameter dependent LPV system is equivocally determined by the belonging parameter vector, if the conditions above are fulfilled. In other words, each $\mathbf{p}$ parameter vector (a point in the parameter space) belongs to an underlying LTI system $\mathbf{S}(\mathbf{p})$, furthermore, each $\mathbf{S}(\mathbf{p})$ is equivocally determined by its corresponding $\mathbf{p}$ parameter vector.

The necessity, which originally brought the LPV methods and theories to life was to handle the nonlinear systems as linear ones with each benefits of this fact. Thus, each elements of $\mathbf{A}$, which are time dependent or causing nonlinearities should be selected as scheduling variables.

3.3.3. Differences between the investigated LPV systems

The previously developed 2-norm based tool ($e(t)$) can be used for various reasons as it was discussed in the previous sections. Although, it should be highlighted that the "pure" deviation between the LPV systems, more specifically, between the parameter dependent parts ($\mathbf{A}(\mathbf{p})_i - \mathbf{A}(\mathbf{p})_j$) of the LPV systems also can be used.

By using the $e(t)$ as quality marker we can get sophisticated information about the quality and goodness of the used controllers. However, from the controller and observer design point of view – where the aim is to realize specific matrix structures in order to complete a given reference controller and observer as it can be seen later – it is enough to use the $(\mathbf{A}(\mathbf{p})_i - \mathbf{A}(\mathbf{p})_j)$ difference.

What is important to see that the $e(t) = \|\mathbf{p}_i - \mathbf{p}_j\|_2$ quality marker (or error signal), the $\mathbf{p}_i - \mathbf{p}_j$, the $\mathbf{S}(\mathbf{p})_i - \mathbf{S}(\mathbf{p})_j$ and the $\mathbf{A}(\mathbf{p})_i - \mathbf{A}(\mathbf{p})_j$ structures carry the same information, namely, the dissimilarity of LPV systems based on their parameter vectors. The discrepancy among these structures occur in the interpretation and the mathematical description. $e(t)$ is a real time function, $\mathbf{p}_i - \mathbf{p}_j$ is a real vector function, $\mathbf{S}(\mathbf{p})_i - \mathbf{S}(\mathbf{p})_j$ and $\mathbf{A}(\mathbf{p})_i - \mathbf{A}(\mathbf{p})_j$ are real matrix functions.

As it can be seen later, from the practical usage point of view the $e(t)$ is the most convenient to measure the quality of the control action, but use of $\mathbf{A}(\mathbf{p})_i - \mathbf{A}(\mathbf{p})_j$ is the easiest to design completed controller and observer structures – which are the basis for the novel controller and observer schemes.

3.3.4. Mathematical background

Here, I define the necessary mathematical tools, which will be used during this section later.

Consider that the $\mathbf{A}, \mathbf{B}$ and $\mathbf{C}$ matrices used now to define the mathematical tools are not the same as previously used ones in control theory, rather, I keep the original notations from the cited literature.

The first and most important property is the matrix similarity [94]:

Definition 3.3.1. Similarity of matrices: A quadratic, $n \times n$ matrix $\mathbf{A}$ is similar to a matrix $\mathbf{B}$, if it is exist an invertible $\mathbf{C}$ matrix that is $\mathbf{A} = \mathbf{C}^{-1}\mathbf{B}\mathbf{C}$. Notation: $\mathbf{A} \sim \mathbf{B}$. ■

This definition has wide ranging applications. Two of them are the following theorems, whose proof can be found in various sources, among others, in [94, 95]:

Theorem 3.3.1. *Similarity invariance of the determinants of matrices: If* $\mathbf{A} \sim \mathbf{B}$*, then* $|\mathbf{A}| = |\mathbf{B}|$.

Proof 3.3.1.1. *Let* $\mathbf{A} \sim \mathbf{B}$*, namely,* $\mathbf{A} = \mathbf{C}^{-1}\mathbf{B}\mathbf{C}$*. Then* $|\mathbf{A}| = |\mathbf{C}^{-1}\mathbf{B}\mathbf{C}| = |\mathbf{C}^{-1}||\mathbf{B}||\mathbf{C}| = |\mathbf{B}|$*, since* $|\mathbf{C}||\mathbf{C}^{-1}| = 1$ *[94].*

Theorem 3.3.2. *If* $\mathbf{A} \sim \mathbf{B}$*, then the characteristic polynomials of the matrices and thus, the eigenvalues and the geometric and algebraic multiplicities of the eigenvalues of the matrices are the same.*

Proof 3.3.2.1. *Let* $\mathbf{A} \sim \mathbf{B}$*, namely,* $\mathbf{A} = \mathbf{C}^{-1}\mathbf{B}\mathbf{C}$*. Then* $\mathbf{A}-\lambda\mathbf{I} = \mathbf{C}^{-1}\mathbf{B}\mathbf{C}-\lambda\mathbf{C}^{-1}\mathbf{I}\mathbf{C} = \mathbf{C}^{-1}(\mathbf{B}\mathbf{C} - \lambda\mathbf{I}\mathbf{C}) = \mathbf{C}^{-1}(\mathbf{B} - \lambda\mathbf{I})\mathbf{C}$*, namely,* $\mathbf{A} - \lambda\mathbf{I} \sim \mathbf{B} - \lambda\mathbf{I}$ *[94].*

These mathematical tools can be used to define eigenvalues equality rules for state feedback systems and allow us to complete the state feedback structures.

3.3.5. The completed feedback gain matrix

Consider the LPV system descriptions of (3.1-3.2). For convenience, I provide here the equations from above:

$$\begin{pmatrix} \dot{\mathbf{x}}(t) \\ \mathbf{y}(t) \end{pmatrix} = \begin{pmatrix} \mathbf{A}(\mathbf{p}(t)) & \mathbf{B} & \mathbf{E} \\ \mathbf{C} & \mathbf{D} & \mathbf{D}_2 \end{pmatrix} \begin{pmatrix} \mathbf{x}(t) \\ \mathbf{u}(t) \\ \mathbf{d}(t) \end{pmatrix} = \mathbf{S}(\mathbf{p}(t)) \begin{pmatrix} \mathbf{x}(t) \\ \mathbf{u}(t) \\ \mathbf{d}(t) \end{pmatrix} , \tag{3.16}$$

where $\mathbf{S}(\mathbf{p}(t)) \in \mathbb{R}^{(n+p)\times(n+m+l)}$.

When $\mathbf{p}$ is persistent in time, (3.16) simplifies to a LTI system, which is represented by $\mathbf{S}$ of (3.17):

$$\begin{pmatrix} \dot{\mathbf{x}}(t) \\ \mathbf{y}(t) \end{pmatrix} = \mathbf{S} \begin{pmatrix} \mathbf{x}(t) \\ \mathbf{u}(t) \\ \mathbf{d}(t) \end{pmatrix} . \tag{3.17}$$

Each LPV system is dependent from the parameter vector $\mathbf{p}(t)$, which may vary in time. As I mentioned earlier, this variation realizes a system trajectory $\mathbf{S}(\mathbf{p}(t))$ in the parameter space, which consist of an infinite number of LTI system. These LTI systems appear over time, during the variation of $\mathbf{p}(t)$. The only difference between the occurring LTI system are the different parameter vectors that belong to them, if the aforementioned requirements – each nonlinearity causing and time variant terms and variables have to be selected as scheduling parameter in order to avoid underlying differences, nullspace problem, etc. [91] – are fulfilled.

From the state feedback design point of view, without gain scheduling or other advanced techniques that would mean that we need infinite number of optimal gains to handle the occurring LTI systems (in continuous time), which is obviously impossible. However, if we want to apply the linear state feedback controller design techniques to the given LPV system, we can utilize this favorable property, namely, that the difference between the occurring LTI systems only appear in the values of the defined $\mathbf{p}(t)$. In the followings

I investigate how can be this favorable property exploited via the introduced matrix similarity theorems.

Define a reference point in the parameter space $\mathbf{p}_{ref}$, which serves as the reference parameter vector. The associated underlying LTI system would call as reference system $\mathbf{S}(\mathbf{p}_{ref})$.

For the sake of simplicity, hereinafter I use the $\mathbf{S}_{ref}$ or $\mathbf{S}(\mathbf{p}_{ref})$ to indicate the reference LTI system and $\mathbf{K}_{ref}$ or $\mathbf{K}(\mathbf{p}_{ref})$ to indicate the reference optimal feedback gain.

Since $\mathbf{S}_{ref}$ is a LTI system, classical state feedback design can be applied to it. Generally, the goal of the controller design in such methodologies is to provide optimal feedback gains as a result of an integral optimization process. The appearing optimal feedback gain has to stabilize the system, if it is unstable and/or reach better properties for the system to be controlled in a particular environment of the system. From the characteristic equation of the closed-loop system point of view that means the new poles – which are determined by the feedback – have to provide the stability of the LTI system.

Consider that $\mathbf{K}_{ref}$ is an eligible and optimal gain for the $\mathbf{S}_{ref}$ LTI system. In this case, the modified state matrix of the state-feedback reference system is $\mathbf{A}(\mathbf{p}_{ref}) - \mathbf{B}\mathbf{K}_{ref}$ and the eigenvalues λ_{ref} can be calculated via solving the characteristic equation:

$$\mid \mathbf{I}\lambda_{ref} - (\mathbf{A}_{ref} - \mathbf{B}\mathbf{K}_{ref}) \mid = \mid \mathbf{I}\lambda_{ref} - \mathbf{A}_{ref} + \mathbf{B}\mathbf{K}_{ref} \mid = 0 \ . \tag{3.18}$$

In the parameter space, each underlying parameter dependent LTI system $\mathbf{S}(\mathbf{p})$ is unequivocally determined by its belonging parameter vector $\mathbf{p}$. Since the dissimilarity between the parameter dependent LTI systems can be described by the parameter vectors, it is possible to use this connection to define a unique, completed state feedback controller $\mathbf{K}(t)$, which is designed for a reference LTI system $\mathbf{S}(\mathbf{p}_{ref})$, but also dealing with each occurring LTI system $\mathbf{S}(\mathbf{p}(t))$ during operation. Moreover, if this completed controller can provide the stability and good performance criteria for the reference system $\mathbf{S}(\mathbf{p}_{ref})$, it can provide the same properties for each occurring $\mathbf{S}(\mathbf{p})$ (and the LPV system $\mathbf{S}(\mathbf{p}(t))$).

On the other hand, this also means that if we have a nonlinear system, we can transform it to an LPV system and with this approach, we can design a controller, which is able to handle this LPV and, ultimately, the nonlinear system itself.

First, I consider that the LPV system is in the form of (3.1). Thus, only the state matrix $\mathbf{A}(\mathbf{p}(t))$ is parameter dependent. In order to solve the problem, I proposed here a novel, parameter dependent state feedback control scheme.

Let the closed-loop system matrix be the following:

$$\mathbf{A}(\mathbf{p}(t)) - \mathbf{B}(\mathbf{K}_{ref} + \mathbf{K}(t)) \ , \tag{3.19}$$

$\mathbf{K}_{m\times n}$ is a continuously calculable gain.

At this point, two main consideration is needed:

- First, this configuration has to provide the stability, namely, the state matrix of the newly defined closed-loop system does have eigenvalues with negative real parts, which are appropriate from the control loop point of view.
- Second, this criteria can be satisfied if we apply a specific form of the above mentioned Theorems (3.3.1)-(3.3.2).

Let $\mathbf{A}_{ref} - \mathbf{B}\mathbf{K}_{ref} \sim \mathbf{A}(\mathbf{p}(t)) - \mathbf{B}(\mathbf{K}_{ref} + \mathbf{K}(t))$, which means that the eigenvalues of the closed loop reference matrix $\lambda(\mathbf{p}_{ref})$ and the closed loop varying parameter dependent matrix $\lambda(\mathbf{p}(t))$ become equal during operation. Namely, $\lambda(\mathbf{p}_{ref}) = \lambda(\mathbf{p}(t))$ for $\forall\mathbf{p}(t)$, if $\lambda(\mathbf{p}(t))$ means the eigenvalues of $(\mathbf{A}(\mathbf{p}(t)) - \mathbf{B}(\mathbf{K}_{ref} + \mathbf{K}(t)))$. This is only possible if the similarity transformation matrix is the $\mathbf{I}_{n\times n}$ unity matrix. Namely, $\mathbf{A}_{ref} - \mathbf{B}\mathbf{K}_{ref} = \mathbf{I}^{-1}(\mathbf{A}(\mathbf{p}(t)) - \mathbf{B}(\mathbf{K}_{ref} + \mathbf{K}(t)))\mathbf{I}$, i.e. the introduced completed gain has to provide the "smoother" similarity, but also the "strict" equality criteria as well. Shortly, the proposed completed feedback gain $\mathbf{K}_{ref} + \mathbf{K}(t)$ has to provide the equality of not just the eigenvalues $\lambda(\mathbf{p}_{ref}) = \lambda(\mathbf{p}(t))$, but also the equality of the matrices as well:

$$\mathbf{A}_{ref} - \mathbf{B}\mathbf{K}_{ref} = \mathbf{A}(\mathbf{p}(t)) - \mathbf{B}(\mathbf{K}_{ref} + \mathbf{K}(t)) \ . \tag{3.20}$$

3.3.6. Controller design, consequences and limitations

Controller design

Let me now assume that $\mathbf{p}(t)$ can be measured or estimated. In this case, the only unknown in (3.20) is $\mathbf{K}(t)$. By rearranging (3.20), the $\mathbf{K}(t)$ can be calculated at every $\mathbf{p}(t)$:

$$\mathbf{K}(t) = -\mathbf{B}^{-1}(\mathbf{A}_{ref} - \mathbf{B}\mathbf{K}_{ref} - \mathbf{A}(\mathbf{p}(t)) + \mathbf{B}\mathbf{K}_{ref}) = -\mathbf{B}^{-1}(\mathbf{A}_{ref} - \mathbf{A}(\mathbf{p}(t))) \tag{3.21}$$

In this way by substituting (3.21) into (3.22):

$$\begin{aligned} &\mathbf{A}(\mathbf{p}(t)) - \mathbf{B}(\mathbf{K}_{ref} + \mathbf{K}(t)) = \\ &\mathbf{A}(\mathbf{p}(t)) - \mathbf{B}\Big(\mathbf{K}_{ref} - \mathbf{B}^{-1}(\mathbf{A}_{ref} - \mathbf{A}(\mathbf{p}(t)))\Big) = \ , \\ &\mathbf{A}_{ref} - \mathbf{B}\mathbf{K}_{ref} \end{aligned} \tag{3.22}$$

such controller structure appears which can ensure that the LPV system $\mathbf{S}(\mathbf{p}(t))$ is going to behave as the feedback controlled LTI reference system $\mathbf{S}(\mathbf{p}_{ref})$ itself, regardless of the actual value of $\mathbf{p}(t)$. In short, the LPV system and via the original nonlinear system will mimics the feedback controlled reference LTI system.

Figure 3.7. demonstrates the general completed control loop in compact form.

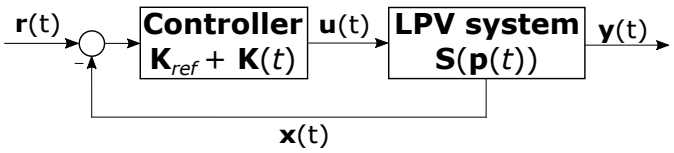

Figure 3.7.: General feedback control loop with completed gain

The basic property of classical state feedback control is to enforce the states to reach zero over time. Therefore, in practical applications the state feedback control in the detailed form can be only used if the states have to reach zero over time. Nevertheless, in most of the physiological related applications the aim of the control is different. In this manner the developed controller scheme should be completed with the so-called feed forward compensator or control oriented ("transformed") model form also can be a solution. These are detailed in the followings.

Parameter dependent feed forward compensator

The practical application requires an other configuration than Fig. 3.7. Based on [56, 80, 88], the rearrangement of the completed controller structure is needed – as it can be seen on Fig. 3.8. The general structure has to be completed with a parameter dependent reference compensator term $\mathbf{N}(\mathbf{p}(t))$, which becomes also a parameter dependent part of the control structure.

Because of the $\mathbf{A}(\mathbf{p}(t))$ is parameter dependent and varies in time, the necessary compensator has to follow this changes and it should be parameter dependent, as well (through the $\mathbf{A}(\mathbf{p}(t))$). The parameter dependent compensator matrices can be calculated

as follows [56, 80]:

$$\begin{bmatrix} \mathbf{A}(\mathbf{p}(t)) & \mathbf{B} \\ \mathbf{I}_n & \mathbf{0}_{n\times m} \end{bmatrix} \begin{bmatrix} \mathbf{N}_x \\ \mathbf{N}_u \end{bmatrix} = \begin{bmatrix} \mathbf{0}_{n\times m} \\ \mathbf{I}_m \end{bmatrix}$$

$$\begin{bmatrix} \mathbf{N}_x \\ \mathbf{N}_u \end{bmatrix} = \begin{bmatrix} \mathbf{A}(\mathbf{p}(t)) & \mathbf{B} \\ \mathbf{I}_n & \mathbf{0}_{n\times m} \end{bmatrix}^{-1} \begin{bmatrix} \mathbf{0}_{n\times m} \\ \mathbf{I}_m \end{bmatrix} , \tag{3.23}$$

$$\mathbf{N}(\mathbf{p}(\mathbf{t})) = \begin{bmatrix} \mathbf{N}_x \\ \mathbf{N}_u \end{bmatrix}$$

where $\mathbf{I}_n$ is the feedback "selector" matrix (here is a unity matrix), $\mathbf{O}_{n\times m}$ is zero matrix and $\mathbf{I}_m$ is unity matrix.

By using the $\mathbf{N}(\mathbf{p}(t))$ compensator, the reference signal and control signal will be compensated and through the states approach given predefined values and not the zero over time.

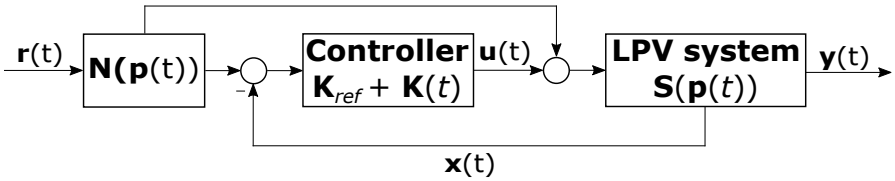

Figure 3.8.: General feedback control loop with completed gain with feed forward compensator

Control oriented model form

In control engineering, the control oriented model form a popular tool which is widely used regarding the different versions of state feedback based control [80]. The main advantage that it models the error dynamics, namely, the deviation of the controlled parameters or states from prescribed values or equilibrium. The method requires the redefinition of the state variables. The new state variables will be the difference state variables which should be equal to zero over time. That means, that the goal of the control is to make these states equal to zero via the control. During operation, each load or disturbance are dodging the difference based states from the equilibrium (or from zero) and the controller enforces the reduction and finally elimination of this effect. Usage

of these modified models can be seen in classical state feedback control, fuzzy control and gain scheduling methods too [96]. This tool is a convenient method in case of TP transformation based modeling and control as well.

Consider the $\mathbf{x}(t) \in \mathbb{R}^n$ state vector. We can find a model equilibrium (a permanent value of each states), which is beneficial from the given application point of view. Assume that this equilibrium is described by the permanent $\mathbf{x}_d \in \mathbb{R}^n$. In this case, the difference based state variables become:

$$\Delta\mathbf{x}(t) = \mathbf{x}(t) - \mathbf{x}_d \ , \tag{3.24}$$

where $\Delta\mathbf{x}(t) \in \mathbb{R}^n$ and the goal of the control becomes $\Delta\mathbf{x}(t) \to 0$.

Figure 3.9. shows the finalized completed control environment in control oriented model form.

In this case, reference compensation is not needed, although, the reference signal is also transformed: $\mathbf{r}(t)$ is the time dependent reference signal and $\mathbf{r}_d$ is the applied "shift" which belongs to the given equilibrium. Therefore, $\Delta\mathbf{r}(t) = \mathbf{r}(t) - \mathbf{r}_d$. In most of the cases we apply constant shifted reference, namely $\Delta\mathbf{r} = \mathbf{0}$. This means that the control goal becomes to eliminate the deviation of the value of the states from a given reference determined by $\mathbf{r}_d$.

The completed controller design has to be done on that SS matrices which belong to the $\Delta\mathbf{x}(t)$ states ($\Delta\mathbf{A}(\mathbf{p}_{ref})$). Consequently, the control signal provided by the controller will be a shifted control signal $\Delta\mathbf{u}(t)$ and ensures that $\Delta\mathbf{x}(t) \to 0$, namely, the $\mathbf{r}(t) - \mathbf{x}(t) = 0$, $t \to \infty$. In order to apply the generated shifted control signal $\Delta\mathbf{u}(t)$ on the given LPV system (or on the original nonlinear system) a transformation is needed: $\mathbf{u}(t) = \Delta\mathbf{u}(t) + \mathbf{u}_d$, where $\mathbf{u}_d$ belongs to the given equilibrium.

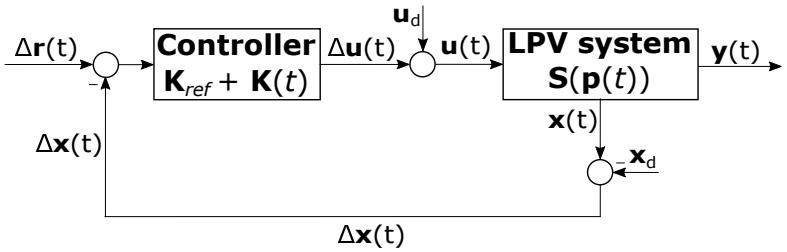

Figure 3.9.: General feedback control loop with completed gain in control oriented form

Consequences and limitations

At this point, the main steps which are needed in order to realize the proposed scheduling parameter selection and controller design method can be summarized as follows:

1. If the nonlinear model contains input and/or output nonlinearities transform the model in order to embed these into the state matrix. (Eg. add extra dynamics or handle the input and/or output as a state variable). If the nonlinearities only occurs in the state matrix, jump to step two;

2. Select the nonlinearity causing terms as scheduling variables ($p_i(t)$) and add to the parameter vector ($\mathbf{p}(t)$). Determine the reasonable limits of the $\mathbf{p}(t)$ based on the requirements of the physical/physiological applications.

3. Realization and validation of LPV models in appropriate form as in (3.16) (from the original nonlinear model);

4. Selection the reference point in the parameter space, namely the reference parameter vector $\mathbf{p}_{ref}$, which determines $\mathbf{S}(\mathbf{p}_{ref})$ reference LTI system in accordance with the needs of reality. The selection of such a reference LTI $\mathbf{S}(\mathbf{p}_{ref})$ system is needed, which can provide the best operating results from the given application point of view;

5. State feedback controller design via linear controller design methods in order to realize the optimal reference feedback gain $\mathbf{K}_{ref}$ for the reference LTI system $\mathbf{S}(\mathbf{p}_{ref})$;

6. Design of the eligible controller scheme, including the appropriate form of (3.21)-(3.22);

7. Realization of the control environment;

8. Validation.

Through the above mentioned points, the controller design is possible and easy to handle.

This novel method may provide an alternative controller design possibility beside the gain scheduling, or LPV-LMI based ideas, or else, although has its own limitations. I collected the main limitations and their possible solutions in the following:

1. First, I summarize the considerations so far, which are needed in order to use this controller design approach. The LPV system should be given in form of (3.16) or has to be transformed to this term; only the $\mathbf{A}(\mathbf{p}(t))$ can be parameter dependent in (3.16); $\mathbf{p}(t)$ should be measurable or estimable; the reference LTI system ($\mathbf{S}(\mathbf{p}_{ref})$) should be a well selected from the given application point of view. Each nonlinear system which is state space represented, can be transformed to the form of ($\mathbf{S}(\mathbf{p}_{ref})$), if the nonlinearities are connected to the selected state variables – or each nonlinear term can be linked to a selected state variable via mathematical transformations (e.g. multiplication with 1, or addition of 0, where the 1 consists of the division of given reasonable state variable (e.g. $\cdot x_i(t)/x_i(t) = 1$) and the 0 is consist of addition and subtraction of given state variable ($+x_i - x_i = 0$); in this way non-connected state can be involved to different permanent terms and these can be dependent from the given states. Through this method, almost every nonlinear systems can be transformed in a way of (3.16)).

2. The invertibility of the input matrix $\mathbf{B}$ is a key point (later during the observer design, this point is complemented with the invertibility of $\mathbf{C}$, as well). Generally, $\mathbf{B}_{n\times m}$ is not a square matrix and occasionally contains linearly dependent columns as well.

   I have investigated three cases here: $\mathbf{B}$ is square matrix and invertible; $\mathbf{B}$ is not a square matrix, but does not contain linearly dependent columns; $\mathbf{B}$ is not square matrix and does contain linearly dependent columns.

   In the first case, $\mathbf{B}$ is invertible and (3.21) can be used to calculate $\mathbf{K}(t)$.

   In the second case, if $\mathbf{B}$ is not a square matrix, but its columns are linearly independent, pre-multiplying $\mathbf{B}$ with $\mathbf{B}^\top$ can be a solution. In this manner, the extension of (3.21)-(3.22) is necessary, as follows:

$$\begin{aligned}
&\mathbf{A}_{ref} - \mathbf{B}\mathbf{K}_{ref} = \mathbf{A}(\mathbf{p}(t)) - \mathbf{B}(\mathbf{K}_{ref} + \mathbf{K}(t)) \\
&(\mathbf{A}_{ref} - \mathbf{B}\mathbf{K}_{ref} - \mathbf{A}(\mathbf{p}(t)) + \mathbf{B}\mathbf{K}_{ref}) = -\mathbf{B}\mathbf{K} \\
&(\mathbf{A}_{ref} - \mathbf{A}(\mathbf{p}(t))) = -\mathbf{B}\mathbf{K}(t) \qquad , \\
&\mathbf{B}^\top(\mathbf{A}_{ref} - \mathbf{A}(p(t))) = -\mathbf{B}^\top\mathbf{B}\mathbf{K}(t) \\
&\mathbf{K}(t) = -(\mathbf{B}^\top\mathbf{B})^{-1}\mathbf{B}^\top(\mathbf{A}_{ref} - \mathbf{A}(\mathbf{p}(t))
\end{aligned} \tag{3.25}$$

   where the $\mathbf{B}^\top\mathbf{B}$ term is now a square matrix and without linear dependency among the columns of $\mathbf{B}$, it is invertible.

In the most unfavorable case, $\mathbf{B}$ is not a square matrix and does have linear dependency. In this case, $\mathbf{B}^\top\mathbf{B}$ may singular. However, with other techniques, for example via singular value decomposition [95] $\mathbf{B}^\top\mathbf{B}$ can be approximated or through Gram-Schmidt orthogonalization method [97] the $\mathbf{B}^\top\mathbf{B}$ can be transformed in such a way that the linear dependency can be eliminated. However, if these techniques are not usable, only the joint term $\mathbf{BK}(t)$ can be calculated, the $\mathbf{K}(t)$ in form of (3.21) not.

Furthermore, if, $\mathbf{B}$ is not a square matrix and $\mathbf{B}^\top\mathbf{B}$ is singular, the input virtualization can be the solution. This is an algebraic equivalent transformation of the model of the system by adding zero to the equations, where zero consists of the addition and subtraction of the same input signal and makes $\mathbf{B}$ invertible. With this technique, the input signals will be involved into each equations, however, it does not change the model behavior. I will introduce this latter technique later in 3.4.2.

In the following section, I demonstrate how this new controller design methodology can be used in case of different nonlinear models between various circumstances.

3.4. Control of nonlinear physiological systems via competed LPV controller

In this chapter I introduce two different control examples, where the subjects were nonlinear systems. I made the examinations alongside the aforementioned main steps in each cases:

1. Realization of valid LPV models in appropriate form
2. Design of the eligible controller scheme
3. Realization of the control environment
4. Assessment of the performance of the developed controllers

It should be noted that I have used the general considerations and assumptions of the state feedback theorem. My focus was the introduction of the developed control structure and not the completely precise presentation of the state feedback design or other used complementer technique. In that spirit, I mostly used arbitrary selections of the reference LTI systems and rules of thumb during the reference controller design.

For example, my main goal was to design a reference controller, which provides stability, low transients and appropriate eigenvalues for the closed system – however, I did not analyzed what can be the best eigenvalues for the given system.

3.4.1. Control of nonlinear compartment model

In this example, I demonstrate the developed controller solution in case of a physiological compartmental model with high nonlinearities. Compartmental modeling is extremely useful and widely used in modeling of physiological systems [1]. Moreover, it is generally used in modeling of DM [98]. Since this example system can be handled as a physiological system, I tried the operation of the controller beside saturations, as well.

Let an arbitrary compartmental model given by the following equations:

$$\begin{aligned} \dot{x_1}(t) &= -k\frac{x_1(t)}{1+ax_1(t)} + bx_2(t) - c(x_2(t)+z)x_1(t) + \frac{u_1(t)}{V_1} \\ \dot{x_2}(t) &= -k\frac{x_2(t)}{(1+dx_2(t))} - bx_2(t) + \frac{u_2(t)}{V_2} \\ y(t) &= x_1(t) + x_2(t) \end{aligned} \quad , \tag{3.26}$$

where $a = 0.4$ L/mmol, $b = 0.1$ 1/min, $c = 0.5$ 1/min, $d = 0.005$ L/mmol, $k = 0.8$ 1/min, $z = 0.1$ mmol/L, V_1=2 L and V_2=1 L. The $x_1(t)$ and $x_2(t)$ are the states and u_1 and u_2 mmol/min are the inputs. The model has three nonlinearities: the natural degradations of the compartments are loaded with Michaelis-Menten-type saturations and x_2 has a coupling to an output of x_1. Figure 3.10. shows the graphical representation of the model.

The selected scheduling variables were $\mathbf{p}(t) = \left[\frac{k}{1+ax_1(t)}, x_2(t)+z, \frac{k}{1+dx_2(t)}\right]^\top$, which means we have a $3D$ parameter space.

Assume that the model is valid, the states ($x_1(t)$ and $x_2(t)$) and through the $\mathbf{p}(t)$ can be measured (if the states are measurable and the model is valid then we can calculate the $\mathbf{p}(t)$ directly from the states).

The state space representation and the state matrices of the LPV system can be written

as follows:

$$\begin{pmatrix}\dot{x}_1(t)\\ \dot{x}_2(t)\end{pmatrix} = \mathbf{A}(\mathbf{p}(t))\begin{pmatrix}x_1(t)\\ x_2(t)\end{pmatrix} + \mathbf{B}\begin{pmatrix}u_1(t)\\ u_2(t)\end{pmatrix}$$

$$\mathbf{A}(\mathbf{p}(t)) = \begin{bmatrix}0 & b\\ 0 & -b\end{bmatrix} + \begin{bmatrix}-1 & 0\\ 0 & 0\end{bmatrix} p_1(t) + \begin{bmatrix}0 & 0\\ -c & 0\end{bmatrix} p_2(t) + \begin{bmatrix}0 & 0\\ 0 & -1\end{bmatrix} p_3(t)\ . \tag{3.27}$$

$$\mathbf{B} = \begin{bmatrix}1/V_1 & 0\\ 0 & 1/V_2\end{bmatrix}\quad \mathbf{C} = \begin{bmatrix}1 & 1\end{bmatrix}\quad \mathbf{D} = \begin{bmatrix}0 & 0\end{bmatrix}$$

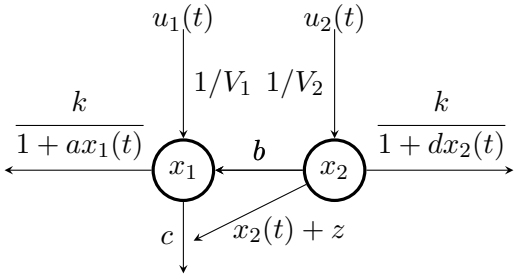

Figure 3.10.: Nonlinear compartmental model

Let me assume that the reference parameter vector is $\mathbf{p}_{ref} = [0.6667, 0.6, 0.64]^\top$ (where $[x_{1,d}, x_{2,d}]^\top = [0.5, 0.5]^\top$). At the reference point, the $\mathbf{A}(\mathbf{p}_{ref})$ is equal to:

$$\mathbf{A}(\mathbf{p}_{ref}) = \begin{bmatrix}-0.6697 & 0.1\\ 0 & -0.74\end{bmatrix}\ . \tag{3.28}$$

and the eigenvalues of the $\mathbf{A}(\mathbf{p}_{ref})$ are $\lambda = [-0.6697, -0.74]^\top$, i.e. the reference LTI system is stable, however, the poles are close to zero.

The next step was the design of the reference controller $\mathbf{K}_{ref}$. The rank of the controllability matrix was equal to 2, i.e. the reference LTI system is controllable ($n = 2$).

In this case, I decided to use the MATLAB$^{\text{TM}}$ *care* order to design the $\mathbf{K}_{ref}$ gain beside $\mathbf{Q} = \mathbf{I}_2$ (unity matrix) and $\mathbf{R} = 0.01\mathbf{I}_2$.

The embedded *care* order calculates the unique solution for $\mathbf{X}$ in continuous-time

control algebraic Ricatti equation [99]:

$$\mathbf{A}^\top\mathbf{X}\mathbf{E}+\mathbf{E}^\top\mathbf{X}\mathbf{A}-(\mathbf{E}^\top\mathbf{X}\mathbf{B}+\mathbf{S})\mathbf{R}^{-1}(\mathbf{B}^\top\mathbf{X}\mathbf{E}+\mathbf{S}^\top)+\mathbf{Q}=\mathbf{O} \tag{3.29}$$

and returns with an optimal gain $\mathbf{G}=\mathbf{R}^{-1}(\mathbf{B}^\top\mathbf{X}\mathbf{E}+\mathbf{S}^\top)$. I have applied the following parameters: $\mathbf{Q}=\mathbf{I}_2$, $\mathbf{R}=0.01\mathbf{I}_2$, $\mathbf{S}=\mathbf{0}$ and $\mathbf{E}=\mathbf{I}$.

As a result, the optimal gain turned out to be

$$\mathbf{K}_{ref}=\begin{bmatrix}8.7493 & 0.058\\ 0.1161 & 9.2883\end{bmatrix}. \tag{3.30}$$

This $\mathbf{K}_{ref}$ means that the eigenvalues of the closed-loop reference state matrix $\mathbf{A}(\mathbf{p}_{ref})-\mathbf{B}\mathbf{K}_{ref}$ are $\lambda_{ref,closed}=[-5.046,-10.0267]^\top$ – which is a substantial improvement since the eigenvalues are much farther from zero without any imaginary component.

The completed controller structure will ensure that the parameter dependent LPV system's closed-loop state matrix will be equal to $\lambda_{ref,closed}$ regardless of the actual value of $\mathbf{p}(t)$. From here, $\mathbf{K}(t)$ can be calculated at each iterations by using (3.21).

Since the control goal was different than ensuring zero states, the use of reference compensation was needed. In order to realize this, I have used (3.23) to calculate the compensator matrices at each iteration during operation. The selected reference levels were $\mathbf{r}=[8,7]^\top$, the initial states $\mathbf{x}_0=[20,10]^\top$.

The achieved results can be seen on Fig. 3.11. The upper left diagram shows the changing of the state variables of the reference LTI system $\mathbf{S}(\mathbf{p}_{ref})$ in time, while the upper right diagram is the changing of the state variables of the parameter dependent LPV system $\mathbf{S}(\mathbf{p}(t))$ over time. The difference (error) between them is represented by the lower left diagram. However, the $\mathbf{p}(t)$ varies over time (as the lower right diagram shows), there is only numerical difference between the states of $\mathbf{S}(p_{ref})$ and $\mathbf{S}(\mathbf{p}(t))$. That means, the LPV system and indirectly the original nonlinear system precisely mimics the behavior of the reference LTI system over time.

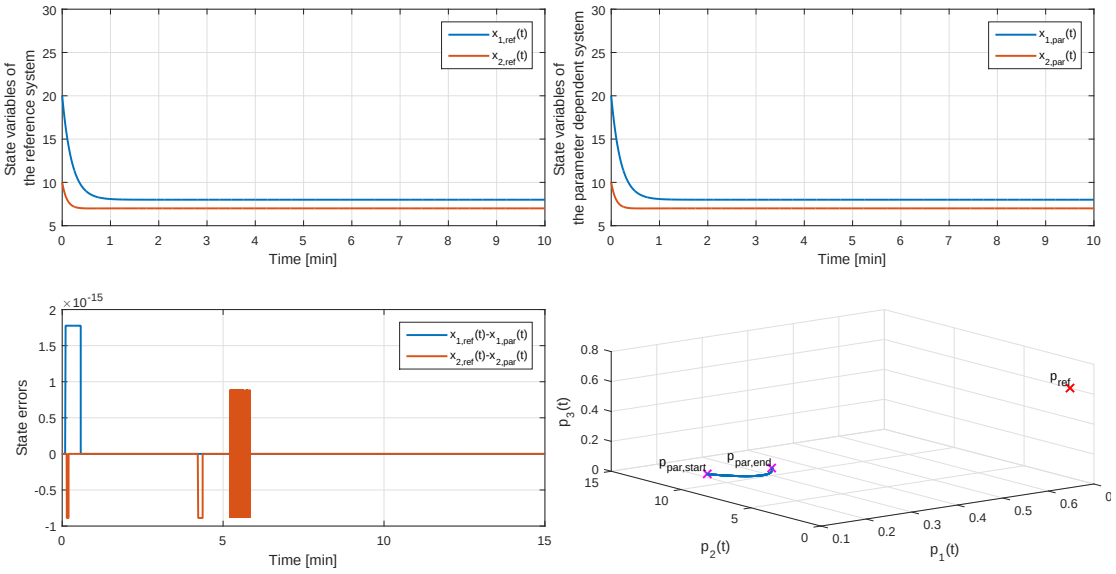

Figure 3.11.: Results of the simulation without control input saturations

Since the given example is a physiological one, I investigated the accuracy of the proposed controller structure if there is saturation on the control input, which does not allow the occurrence of physiologically irrelevant control inputs. Control inputs only can be positive. I found that the results are different than the previous case, which mostly comes from that fact that the selected scheduling variables are dependent from the actual values of the states. Namely, the state variables are coupled to the $\mathbf{S}(\mathbf{p}(t))$ through the $\mathbf{p}(t)$. However, I did not use any saturation on the values of the state variables, which could compensate for the effect of the control input saturation.

Figure 3.12. represents this latter scenario when saturation is applied. Each parameter were the same during the simulation, except that I consider that the input signal cannot be negative at all. The results show that there is a difference between the states of $\mathbf{S}(\mathbf{p}_{ref})$ and $\mathbf{S}(\mathbf{p}(t))$ over time. However, the controller can handle this situation and can provide stable control for $\mathbf{S}(\mathbf{p}(t))$. Finally, the difference is slowly decreasing and the state variables reached the predefined reference levels.

In both cases (saturation free and loaded) the varying system did not get close to the reference system, namely, the trajectory of the $\mathbf{p}(t)$ was not closing $\mathbf{p}_{ref}$ and the $\|\mathbf{p}_{ref} - \mathbf{p}(t)\| = 0$ did not appear during operation.

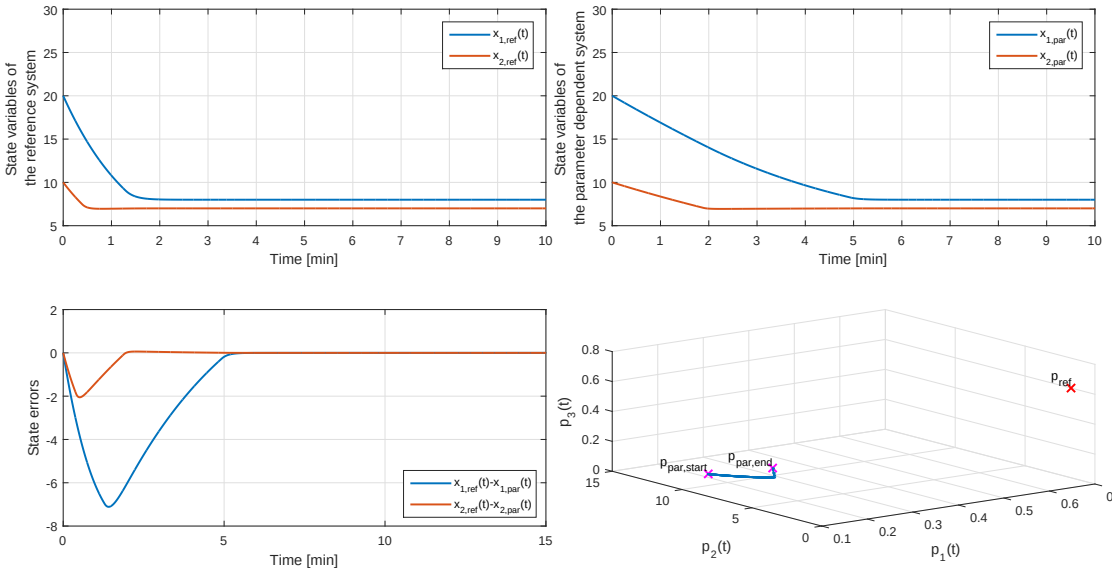

Figure 3.12.: Results of the simulation with control input saturations

3.4.2. Control of T1DM

In this Subsection, I provide an example which demonstrates the application of the developed control design method for DM. In this case, several challenging issues occur which have to be solved during the controller design. The main issues are summarized in the followings:

1. Nonlinearity of the model: the applied model contains nonlinear part;
2. Disturbance input: the feed intake should be handled as disturbance and not as control input. From this reason such controller has to be designed which can compensate the effect of the disturbance beside it provides stability;
3. Control input: we have only one control input, the insulin intake. Thus, the controller can effect only via this control input. Moreover, this means that the **B** is not directly invertible.
4. Reachability: only the BG level is measurable, but the other states are not available. Thus, the states have to be observed or estimated.
5. Reference compensation: the feed forward compensation is not available, because the disturbance is unknown. Therefore, we cannot prepare our controller to compensate it. Consequently, we have to apply other complementer solution regard to the state feedback based controller.

In the light of the aforesaid issues the application of the control oriented model form and control (Sec. 3.3.6) and the input virtualization (Sec. 3.3.6) can be used to bypass these problems.

The general control oriented model form with disturbance input is represented by Fig. 3.13). This realization will be used in this case as well. Nevertheless, to solve the reachability of the states the closed loop should be completed by an observer or estimator.

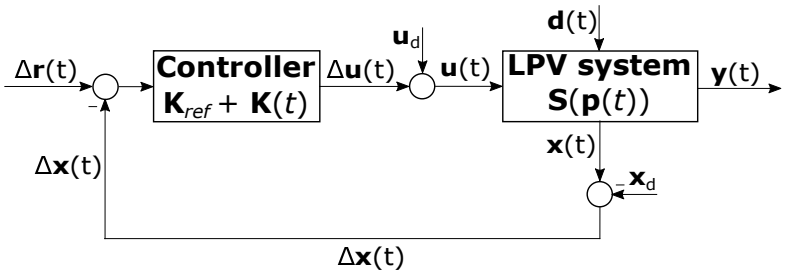

Figure 3.13.: General difference based completed controller structure with external disturbance

In this example, I used the same Minimal Model as in Chapter 2. The model is described by (B.1a)-(B.1d). I considered a T1DM patient in this Subsection, which means, the (B.1a)-(B.1b) and (B.1d) were used here. The description of the model and the used parameters are available in the Appendix B.1.

The first step was the transformation of the system equation to realize the control oriented model form in an LPV sense. The $\Delta G(t)$ can be reached via rearrangement of (B.1a), where the model equilibria concerning to $\dot{G}_d \equiv 0$:

$$\begin{aligned}
\dot{G}(t) - 0 &= -(p_1 + X(t))G(t) + p_1 G_B + d(t) - (-(p_1 + X_d)G_d + p_1 G_B + d_d) = \\
\Delta\dot{G}(t) &= -p_1 G(t) - X(t)G(t) + p_1 G_B + d(t) + p_1 G_d + X_d G_d - p_1 G_B - d_d = \\
\Delta\dot{G}(t) &= -p_1 (G(t) - G_d) - X(t)G(t) + (d(t) - d_d) + X_d G_d + 0 = \\
\Delta\dot{G}(t) &= -p_1 \Delta G(t) - X(t)G(t) + X_d G_d + \Delta d(t) + G(t)X_d - G(t)X_d = \\
\Delta\dot{G}(t) &= -p_1 \Delta G(t) - G(t)\Delta X(t) - X_d \Delta G(t) + \Delta d(t) = \\
\Delta\dot{G}(t) &= -(p_1 + X_d)\Delta G(t) - G(t)\Delta X(t) + \Delta d(t)
\end{aligned} \tag{3.31}$$

The $\Delta X(t)$ and $\Delta I(t)$ states can be calculated similar to (3.31) from (B.1b) and (B.1d)

by using the $\dot{X}_d \equiv 0$ and $\dot{I}_d \equiv 0$ equilibriums:

$$\begin{aligned}
&\dot{X}(t) - 0 = -p_2 X(t) + p_3(I(t) - I_B) - (-p_2 X_d + p_3(I_d - I_B)) = \\
&\Delta\dot{X}(t) = -p_2(X(t) - X_d) + p_3(I(t) - I_d) - p_3 I_B + p_3 I_B = \\
&\Delta\dot{X}(t) = -p_2 \Delta X(t) + p_3 \Delta I(t)
\end{aligned} \tag{3.32}$$

and

$$\begin{aligned}
&\dot{I}(t) - 0 = -n(I(t) - I_B) + u(t) - (-n(I_d - I_B) + u_d) = \\
&\Delta\dot{I}(t) = -n\Delta I(t) + \Delta u(t)
\end{aligned} . \tag{3.33}$$

From (3.31) - (3.33) it is clear that the $G(t)$ has to be selected as scheduling variable in order to realize the difference based control oriented model form in LPV sense, namely $\mathbf{p}(t) = p(t) = G(t)$. The SS representation based on (3.31)-(3.33) can be written as:

$$\begin{pmatrix} \Delta\dot{G}(t) \\ \Delta\dot{X}(t) \\ \Delta\dot{I}(t) \end{pmatrix} = \mathbf{A}(\mathbf{p}(t)) \begin{pmatrix} \Delta G(t) \\ \Delta X(t) \\ \Delta I(t) \end{pmatrix} + \mathbf{B}\Delta u(t) + \mathbf{E}\Delta d(t)$$

$$\mathbf{A}(\mathbf{p}(t)) = \begin{bmatrix} -(p_1 + X_d) & 0 & 0 \\ 0 & -p_2 & p_3 \\ 0 & 0 & -n \end{bmatrix} + \begin{bmatrix} 0 & -1 & 0 \\ 0 & 0 & 0 \\ 0 & 0 & 0 \end{bmatrix} p_1(t) \ . \tag{3.34}$$

$$\mathbf{B} = \begin{bmatrix} 0 \\ 0 \\ 1 \end{bmatrix} \quad \mathbf{E} = \begin{bmatrix} 1 \\ 0 \\ 0 \end{bmatrix} \quad \mathbf{C} = \begin{bmatrix} 1 & 0 & 0 \end{bmatrix} \quad \mathbf{D} = \begin{bmatrix} 0 & 0 & 0 & 0 \end{bmatrix}$$

The key point is the invertibility of $\mathbf{B}$. However, in this case this criteria is not satisfied, since $\mathbf{B}$ is a rectangular matrix and not invertible. To bridge this problem, I have applied another tool, the input virtualization. That means, I have added zero to the (3.31) and (3.32) equations, which consists of the addition and subtraction of the control signal: $+\Delta u(t) - \Delta u(t) = 0$. In this way, the dimension of the $\mathbf{B}$ matrix can be arbitrarily extended to $\mathbf{B}_{extended}$. In order to avoid the unit incompatibility problem, the extended $\mathbf{B}_{extended}$ has to contain "unit compensator" scalars, but the value of these can be 1.

To realize the input virtualization the following modifications were applied on (3.31)

and (3.32):

$$\Delta\dot{G}(t) = -(p_1 + X_d)\Delta G(t) - G(t)\Delta X(t) + \Delta d(t) + \phi_1\Delta u(t) - \phi_1\Delta u(t) \ , \tag{3.35}$$

where ϕ_1 unit compensator is $\phi_1 = 1\dfrac{mg\,mL}{\mu U dL}$, namely $\phi_1\Delta u(t) = [mg/dL/min])$.

$$\Delta\dot{X}(t) = -p_2\Delta X(t) + p_3\Delta I(t) + \phi_2\Delta u(t) - \phi_2\Delta u(t) \ , \tag{3.36}$$

where ϕ_2 unit compensator is $\phi_2 = 1\dfrac{mL}{\mu U}$, namely $\phi_2\Delta u(t) = [min^{-1}])$.

These modifications reflects in the extended input matrix:

$$\mathbf{B}_{extended} = \begin{bmatrix} \phi_1 & 0 & -\phi_1 \\ 0 & \phi_2 & -\phi_2 \\ 1 & 0 & 0 \end{bmatrix} = \begin{bmatrix} 1 & 0 & -1 \\ 0 & 1 & -1 \\ 1 & 0 & 0 \end{bmatrix} \ , \tag{3.37}$$

where $\mathbf{B}_{extended}$ now is invertible.

From control engineering point of view, that means we apply the same $\Delta\mathbf{u}(t)$ control signal on each state. Namely the new input vector becomes $\Delta\mathbf{u}(t) = [\Delta u(t), \Delta u(t), \Delta u(t)]^\top$. Nevertheless, the control signal did not affect the $G(t)$ and $X(t)$ states directly, because of the special form of $\mathbf{B}_{extended}$. From mathematical point of view, the realization of this structure is only possible if the $\mathbf{K}_{ref} + \mathbf{K}(t)$ completed controller gain has exactly the same rows. This requirement is a direct consequence of the definition of the control signal.

To provide the full picture about this property, let me now assume $\mathbf{A}(p(t))$ from (3.34) and $\mathbf{B}_{extended}$ from the (3.37) and realize the closed completed control equation based on (3.21) and (3.22):

$$\begin{aligned} \Delta\dot{\mathbf{x}}(t) &= \mathbf{A}(\mathbf{p}(t))\Delta\mathbf{x}(t) + \mathbf{B}_{extended}\Delta\mathbf{u}(t) + \mathbf{E}\Delta d(t) = \\ \Delta\dot{\mathbf{x}}(t) &= \Big(\mathbf{A}(\mathbf{p}(t)) - \mathbf{B}_{extended}(\mathbf{K}_{ref} + \mathbf{K}(t))\Big)\Delta\mathbf{x}(t) + \mathbf{E}\Delta d(t) \end{aligned} \tag{3.38}$$

and

$$\mathbf{B}_{extended}(\mathbf{K}_{ref}+\mathbf{K}(t)) = \\ \begin{bmatrix} 1 & 0 & -1 \\ 0 & 1 & -1 \\ 1 & 0 & 0 \end{bmatrix} \begin{bmatrix} k_{r,1}+k(t)_1 & k_{r,2}+k(t)_2 & k_{r,3}+k(t)_3 \\ k_{r,1}+k(t)_1 & k_{r,2}+k(t)_2 & k_{r,3}+k(t)_3 \\ k_{r,1}+k(t)_1 & k_{r,2}+k(t)_2 & k_{r,3}+k(t)_3 \end{bmatrix} = \\ \begin{bmatrix} 0 & 0 & 0 \\ 0 & 0 & 0 \\ k_{r,1}+k(t)_1 & k_{r,2}+k(t)_2 & k_{r,3}+k(t)_3 \end{bmatrix} . \tag{3.39}$$

What is important to notice is that the rows of the $\mathbf{K}_{ref}+\mathbf{K}(t)$ complex have to be the same to fulfill the requirement of realizability. That means that individually both the $\mathbf{K}_{ref}$ and the $\mathbf{K}(t)$ can have different rows. This property becomes very useful in the followings. The structure of $\mathbf{K}_{ref}$ and $\mathbf{K}(t)$ is known, thus we can manipulate them – in this way the realizability can be reached.

The state feedback can be applied only if we have information about the states via measurement, observation or estimation. The output of the system is the $G(t)$ BG level which is the only measurable state. In this case, the presence of disturbance and the incomplete observability criteria make the observation (observer design) insufficient. Therefore, the solution can be to estimate the $X(t)$ and $I(t)$ states. Although, estimation is possible, but challenging because the nonlinearity and the mixed effects: the disturbance has to be handled as non-additive effect and an organic part of the model; the sensor noise is an additive effect coming from external source. I have taken into account these requirements and decided to apply a discrete mixed non-additive/additive Extended Kalman Filter (EKF) to estimate the states.

In the followings I present the design of the used EKF based on [100, 101] and by using the experiences from [102]. The formulation of the mixed non-additive/additive EKF can be described as follows.

Consider the general system model (non-additive disturbance) and observation model (additive noise):

$$\begin{aligned} \mathbf{x}_{k+1} &= f(\mathbf{x}_k, \mathbf{u}_k, \mathbf{w}_k) \\ \mathbf{z}_k &= h(\mathbf{x}) + \mathbf{v}_k \end{aligned} , \tag{3.40}$$

where $\mathbf{x}_{k+1}$ is the output of f system model (represents the next state), $\mathbf{x}_k$ is the actual state, $\mathbf{u}_k$ is the actual control signal, $\mathbf{w}_k$ is the actual disturbance. $\mathbf{x}$, $\mathbf{u}$ and $\mathbf{w}$ is

non-additive parts of f. $\mathbf{v}_k$ is the actual noise. $\mathbf{x}$ is the non-additive and $\mathbf{v}_k$ is additive part of the h observation model which has $\mathbf{z}$ output (estimation).

In this given case the $\mathbf{v}_k$ is additive white noise with zero mean and 5 mg/dL variance, thus $\mathbf{v}_k \sim \mathcal{N}(0, \mathbf{R}_k)$ with $\mathbf{R}_k$ covariance matrix. $\mathbf{w}_k \sim \mathcal{N}(0, \mathbf{Q}_k)$ is non-additive disturbance affecting the states with assumingly zero mean Gaussian distribution and $n_w \times n_w$ real positive semidefinite $\mathbf{Q}_k$ covariance matrix. Naturally, because of the dimension of disturbance $n_w = 1 \rightarrow \mathbf{Q}_{k,1\times 1}$.

In the light of the afore mentioned considerations, the prediction and update algorithm of the EKF can be described as follows.

Predict

$$\text{Predicted state estimate}: \ \hat{\mathbf{x}}_{k+1|k} = f(\hat{\mathbf{x}}_{k|k}, \mathbf{u}_k, \mathbf{w}_k)$$
$$\text{Predicted covariance estimate}: \ \mathbf{P}_{k+1|k} = \mathbf{F}_k \mathbf{P}_{k|k} \mathbf{F}_k^\top + \mathbf{L}_k \mathbf{Q}_k \mathbf{L}_k^\top$$

Udpate

$$\text{Innovation residual}: \ \tilde{\mathbf{y}}_{k+1} = \mathbf{z}_{k+1} - h(\hat{\mathbf{x}}_{k+1|k})$$
$$\text{Innovation covariance}: \ \mathbf{S}_{k+1} = \mathbf{H}_{k+1} \mathbf{P}_{k+1|k} \mathbf{H}_{k+1}^\top + \mathbf{R}_{k+1}$$
$$\text{Kalman gain}: \ \mathbf{K}_{k+1} = \mathbf{P}_{k+1|k} \mathbf{H}_{k+1}^\top \mathbf{S}_{k+1}^{-1}$$
$$\text{Updated state estimate}: \ \hat{\mathbf{x}}_{k+1|k+1} = \hat{\mathbf{x}}_{k+1|k} + \mathbf{K}_{k+1} \tilde{\mathbf{y}}_{k+1}$$
$$\text{Updated covariance estimate}: \ \mathbf{P}_{k+1|k+1} = (\mathbf{I} - \mathbf{K}_{k+1} \mathbf{H}_{k+1}) \mathbf{P}_{k+1|k} \quad , \tag{3.41}$$

where $\mathbf{I}$ is the unit matrix, $\mathbf{F}_k = \left.\dfrac{\partial f}{\partial \mathbf{x}}\right|_{\hat{\mathbf{x}}_{k|k}, \mathbf{u}_k}$ and $\mathbf{H}_{k+1} = \left.\dfrac{\partial h}{\partial \mathbf{x}}\right|_{\hat{\mathbf{x}}_{k+1|k}}$ are the state transition and observation matrices defined by their Jacobians, respectively [100, 101].

It should be stated that my primary goal was to demonstrate the usability of the developed completed LPV based controller design method. Hence, I have considered simplifications regard to the realization of the system, controller and EKF which were the following: *(i)* I decided to use the continuous original nonlinear system; *(ii)* I applied the developed continuous completed LPV controller; *(iii)* I applied the introduced mixed non-additive/additive EKF. Consequently, I had to apply a small sampling time (in the given case 0.1 min) at the EKF to preserve the convergence of the filter. In real life applications all sub-parts have to be discrete and the sampling time of the system and controller has to be comparable magnitude with the EKF's sampling time. For example, $T_s = 1$ min for the system and controller and $T_s = 5$ min for the EKF (5 min is a usual

value coming from the limitations of continuous glucose measurement systems).

The final control environment can be seen on Fig. 3.14.

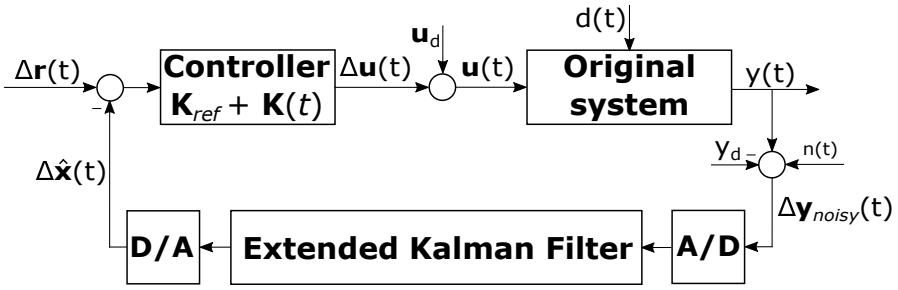

Figure 3.14.: Finalized control environment with the original system, differnce based completed LPV controller with input virtualization and the mixed non-additive/additive EKF

From this point the design procedure is straightforward. By calculating the G_d, X_d, I_d, d_d and u_d values the (3.31) - (3.33) equations can be finalized and the SS structure from (3.34) appears. I used the model equilibrium which means (B.1a)-(B.1d) can be used to calculate them. I applied the model own equilibrium determined by G_B and I_B, which means $G_d = G_B$ and $I_d = I_B$. In order to reach this the X_d, d_d and u_d have to be equal to zero according to the model equations.

$$\begin{aligned} 0 &= -(p_1 + X_d)G_d + p_1 G_B + d_d \rightarrow d_d = 0 \rightarrow G_d = G_B \\ 0 &= -p_2 X_d + p_3(I_d - I_B) \rightarrow I_d = I_B \rightarrow X_d = 0 \\ 0 &= -n(I_d - I_B) + u_d \rightarrow u_d = 0 \rightarrow I_d = I_B \end{aligned} \quad . \tag{3.42}$$

The next step is the design of the completed LPV controller structure.

I selected the reference parameter vector as $\mathbf{p}_{ref} = 85$ mg/dL which is the – as aforesaid – model equilibria. The eigenvalues of the difference based reference LTI system are $\lambda = [-0.0280, -0.0250, -0.2300]^\top$, which means that the selected LTI system is stable.

The rank of the controllability matrix of the reference state matrix $\mathbf{A}(\mathbf{p}_{ref})$ (concerning to the difference based states) was equal to 3, the system is controllable.

In this case, the glucose intake has to be handled as an external disturbance and the previous state feedback design proceedings cannot be used. In order to bridge this problem, I have selected the MATLAB$^{\text{TM}}$ *care* order to design a $\mathcal{H}_\infty$ type controller. In this case, the *care* order provides stabilizing robust feedback gain $\mathbf{K}_{ref}$ via the solution

of the following $\mathcal{H}_\infty$ like Ricatti equation [99]:

$$\mathbf{A}^\top\mathbf{K}+\mathbf{K}\mathbf{A}-\begin{bmatrix}\mathbf{B} & \mathbf{E}\end{bmatrix}\mathbf{R}^{-1}\begin{bmatrix}\mathbf{B}^\top \\ \mathbf{E}^\top\end{bmatrix}\mathbf{K}+\mathbf{C}^\top\mathbf{C}=0\ , \tag{3.43}$$

where $\mathbf{R}=\begin{bmatrix}-\gamma^2\mathbf{I} & 0 \\ 0 & \mathbf{I}\end{bmatrix}^{-1}$, beside $\gamma=5$ and $\mathbf{Q}=\mathbf{C}^\top\mathbf{C}$.

It is important to notice that the reference controller design has to be done by using the original $\mathbf{B}$ and from the two calculated gain what are provided by the *care* command only that can be used which belongs to the insulin input. The obtained robust stabilizing gain was:

$$\mathbf{K}_{ref}=\begin{bmatrix}0.9724 & -80.6320 & -0.0085\end{bmatrix}\ . \tag{3.44}$$

The closed loop eigenvalues $\lambda_{ref,closed}=[-1.0004,-0.2302,-0.0231]^\top$ are provided by the designed $\mathbf{K}_{ref}$ – which means a smaller improvement, however, the closed system will be able to deal with the disturbances in $\mathcal{H}_\infty$ sense.

Now by applying the (3.21), (3.22), (3.38), (3.39) and (3.40) the completed controller structure can be realized. First, the investigation of the $\mathbf{K}(t)$ is necessary. By using the $\mathbf{B}_{extended}$ in (3.21) we get:

$$\mathbf{K}(t)=\begin{bmatrix}0 & 0 & -1\\ 1 & -1 & -1\\ 1 & 0 & -1\end{bmatrix}\begin{bmatrix}0 & \Delta p(t) & 0\\ 0 & 0 & 0\\ 0 & 0 & 0\end{bmatrix}=\begin{bmatrix}0 & 0 & 0\\ 0 & \Delta p(t) & 0\\ 0 & \Delta p(t) & 0\end{bmatrix}\ , \tag{3.45}$$

which means that the structure of the $\mathbf{K}_{ref,extended}$ should be created to compensate the $\mathbf{K}_{ref,extended}+\mathbf{K}(t)$ complex. The rows of the $\mathbf{K}_{ref,extended}+\mathbf{K}(t)$ will be equal in that case if $\mathbf{K}_{ref,extended}$ is set as:

$$\mathbf{K}_{ref,extended}=\begin{bmatrix}0.9724 & -80.6320+\Delta p(t) & -0.0085\\ 0.9724 & -80.6320 & -0.0085\\ 0.9724 & -80.6320 & -0.0085\end{bmatrix}\ , \tag{3.46}$$

which is possible because all information are available. Now, the rows of the $\mathbf{K}_{ref,extended}+\mathbf{K}(t)$ complex become equal and the realization of the control environment is possible. By replacing the $\mathbf{B}$ with $\mathbf{B}_{extended}$ and using the (3.39) for the feedback, the virtual inputs do not affect at all to the $\Delta G(t)$ and $\Delta X(t)$.

Now I introduce the initial conditions were applied during the simulations. The initial values of the states of the original nonlinear system were $\mathbf{x}(0) = [100, 0, 0]^\top$. We assumed T1DM, thus the $X(0)$ and $I(0)$ can be considered as 0, which is equivalent with the zero insulin intake – which is a known information. Therefore, the initial values of the states of the EKF were $\mathbf{x}(0)_{EKF} = [90, 0, 0]^\top$, represents an estimation error at the first state (BG level). The initial covariance matrix was set to zero, namely $\mathbf{P}_{k|k} = \mathbf{0}$ in the first predict step. The applied difference based reference signal was selected as constant, namely $\Delta\mathbf{r} = [0, 0, 0]^\top$. The latter means that the states should reach the equilibrium over time, ie. the G_d, X_d and I_d levels.

Control input saturation has been applied as well to avoid the physiologically irrelevant input signals: the injected insulin cannot be lower than zero (lower limit). Upper limit was not used.

I used an extreme external glucose load during the simulations. In order to make the in silico tests more realistic, the absorption sub-model from the Hovorka model (B.3a)-(B.3b) was used – since the applied Minimal-model does not have embedded absorption sub-model. I assumed 100 g CHO at every 180 min. The doses were 20 g over 5 min. The simulation time was 720 min – a half day.

It has to be mentioned that the BG levels are transformed from mg/dL to mmol/L – in this way the comparison to the other results becomes easier.

The achieved results can be seen on Fig. 3.15. and Fig. 3.16. The signals on the figures are not the difference based signals, but the original ones in order to make the understanding easier.

On Fig. 3.15, the upper diagram represents the noisy output of the system which is measured (blue line). The EKF provided a filtered signal which is smoother than the measurable one (red line). The "true" $G(t)$, namely the BG level belongs to the original model can be seen with yellow. The lower left diagram shows the estimated $X(t)$ provided by the EKF (red) and the original $X(t)$. The lower right diagram represents the estimated $I(t)$ provided by the EKF (red) and the $I(t)$ belongs to the original model. The results agrees with the preliminary expectations. Both of the non-additive and additive disturbances are directly affect to the BG level. The non-additive disturbance affects to the $G(t)$ accordingly (B.1a). The additive noise affects to the output of the model, namely the $G(t)$. The disturbance effect reaches the $X(t)$ and $I(t)$ via coupling. This attenuates the effect of the disturbance in the remaining states. Consequently, the estimation and the original states are almost overlapping (in case of $X(t)$ and $I(t)$). The EKF works well, namely, it provides a smoother $G(t)$; and $X(t)$ and $I(t)$ with high accuracy.

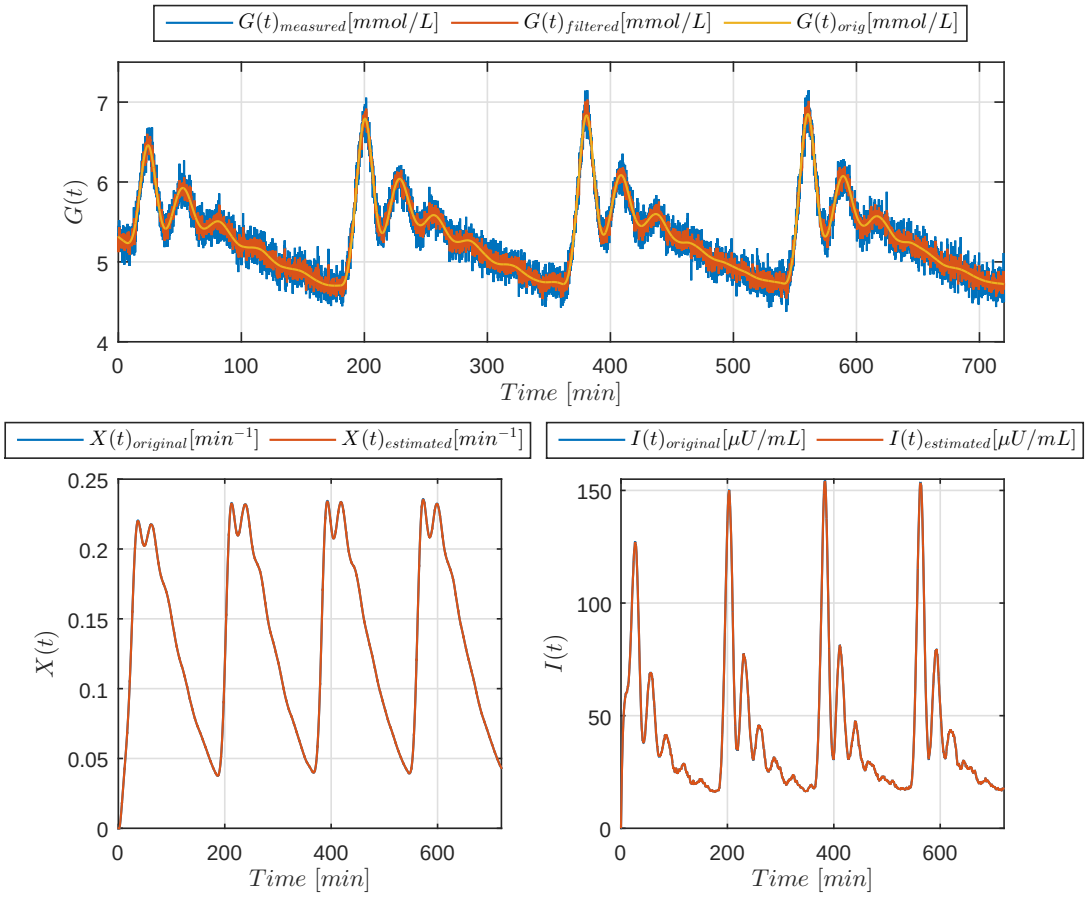

Figure 3.15.: Comparison of the original system's states and the estimated states (provided by the EKF)

Figure 3.16. shows the vary of the states of the original model (upper diagram), the insulin intake (middle diagram) and the glucose rate of appearance (lower diagram). The controller was able to keep the BG level in a tight and healthy range: the BG level varied between 4.7022 and 6.85 mmol/L. It is visible that after the first cycle the signals are repeating, which behavior is coming from the applied, symmetric pulse kind disturbance input. In order to present the signals on the same diagram, I modified their order of magnitude: $10 \cdot X(t)$ and $I(t)/100$ appear on the diagram as it was noted in the caption. From the middle diagram can be seen that the control signal is affected by the filtered sensor noise through the EKF. This property can be avoided if we apply additional

smoothers. Because the aim was here only the demonstration of the LPV based controller design method, I did not apply any smoothers.

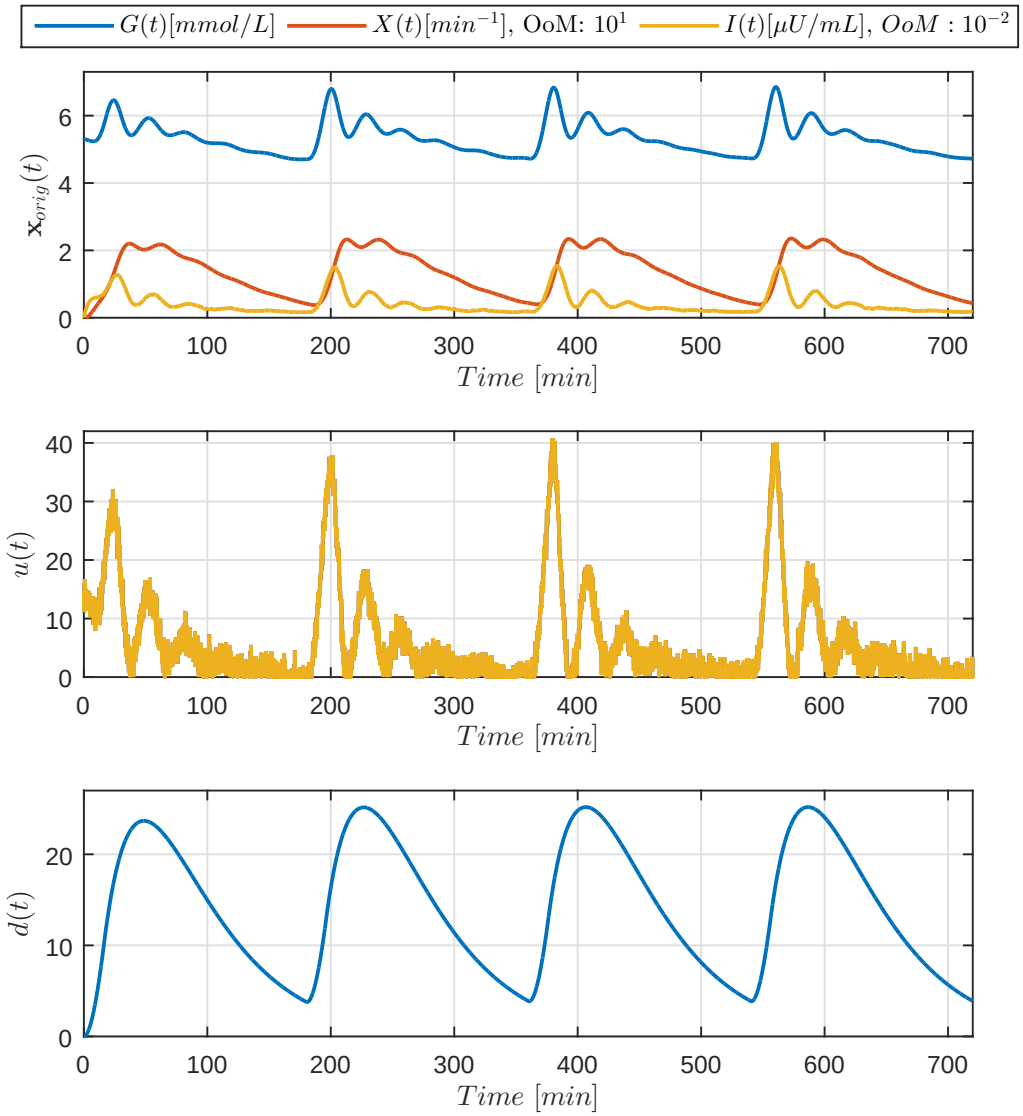

Figure 3.16.: Results of the simulation of T1DM control, OoM: Order of Magnitude

Although, it is not visible on the figures (because of the repeating disturbance input), but the control goal was reached by the controller's structure. I made other examination, when I applied only one bigger impulse as disturbance. After the decay, the states approached the prescribed G_d, X_d and I_d values. However, they did not reach perfectly -

which is caused by the additional noise through the EKF. The deviation was small with 10^{-1} magnitude in all states, which is acceptable considering the high additional noise.

It should be noted, that the states of the reference original system and the LPV system are varying fast. The explanation of this phenomenon is that glucose and insulin absorption sub-model is not included in this simple Minimal Model. Probably, the dynamics of the systems would be slower in case of an embedded glucose and insulin absorption sub-model – however, the investigation of this possibility is beyond this theses and will be a part of my future work.

3.4.3. Summary

In this Section, I have introduced a novel, LPV-based controller design approach. This method provides a mixture of classical optimal state-feedback control and a kind of supplementary control which is based on the parameter vectors of the LPV parameter space. The main advantage of the proposed controller structure is the fact that it is enough to design a reference controller for a reference LTI system and the actual, necessary control action over time will be determined by comparison to this reference controller through algebraic manipulations.

I presented the properties, key points and usability of the developed completed controller scheme.

I have investigated different scenarios in order to exemplify the usability of the developed tools: two nonlinear sample systems with and without saturations and disturbance.

Without disturbance and saturations, the LPV system perfectly mimics the behavior of the reference system over time.

In case of saturation, the dynamics of the reference LTI and the LPV systems will be different, however, the completed controller structure provides stability and good reference tracking.

In the case when disturbance occurs, the completed controller structure provide stability and good control action.

To sum up, in both cases, the developed completed controller structure works finely and provides the expected results. The completed controller can guarantee the stability of the LPV system. Moreover, it is enough to determine performance specifications only to the reference LTI system – because the completed controller forces the LPV system to reach these specifications as well.

3.5. Observer based control for LPV systems

In this section, I will investigate a completed observer structure, which is based on the same consideration as the previous Sections. This method uses the classical state observer theorem, however, the completed observers are parameter dependent and fit to the developed completed controller structure.

I demonstrate the usability of the completed observer structure on the model of Sections 3.4.1.

3.5.1. Classical linear observer design

It may happen that the states of a given system are directly not available. In such situations, a state observer or state estimator can be used. Although other possibilities are available, e.g. family of Kalman filters, I only focused on the classical observer design.

A linear observer can be designed, if the main criteria, the observability is satisfied. That means, that the rank of the observability matrix has to be equal to n, the number of the states. This property refers to the structure of the $\mathbf{A}$ and $\mathbf{C}$ matrices. If observability is satisfied, linear observer design is possible.

In case of full order linear observer, the linear observer is a dynamic system whose output is the $\hat{\mathbf{x}}(t)$ estimated state vector. In case of asymptotic observer, the estimation error, namely $\tilde{\mathbf{x}}(t) := \mathbf{x}(t) - \hat{\mathbf{x}}(t)$ has to converge to zero over time [56].

The general form of the full order linear observer can be described as follows:

$$\dot{\hat{\mathbf{x}}}(t) = \mathbf{F}\hat{\mathbf{x}}(t) + \mathbf{G}\mathbf{y}(t) + \mathbf{H}\mathbf{u}(t) \ , \tag{3.47}$$

where $\mathbf{F} \in \mathbb{R}^{n \times n}$ is the observer state matrix, $\mathbf{G} \in \mathbb{R}^{k \times n}$ is the observer gain matrix and $\mathbf{H} \in \mathbb{R}^{n \times m}$ is the observer input matrix.

The velocity of the disappearance of the observation error can be prescribed by the eigenvalues of the $\mathbf{F}$, which is traceable to the determination of the characteristic polynomial of $\mathbf{F}$ [56, 88]:

$$|s\mathbf{I} - \mathbf{F}| = |s\mathbf{I} - \mathbf{A} - \mathbf{G}\mathbf{C}| = |s\mathbf{I} - \mathbf{A}^\top - \mathbf{C}^\top\mathbf{G}^\top| \ . \tag{3.48}$$

In this way an asymptotic state observer design leads to a state feedback design task, where the $\mathbf{G}$ observer gain provide that the closed loop poles of the observer become equal to the predefined observer poles.

In order to design a full order observer, the following criteria have to be satisfied by

which the observer's parameter can be calculated at the same time [56, 88]:

$$\begin{aligned} &\mathbf{F} = \mathbf{A} - \mathbf{GC}, \\ &\mathbf{H} = \mathbf{B}, \\ &\dot{\tilde{\mathbf{x}}}(t) = \mathbf{F}\tilde{\mathbf{x}} \text{ stable and fast} \end{aligned} \quad . \tag{3.49}$$

The selected observer poles have to be higher negative values than the LTI system has in order to provide fast operation, namely, fast error disappearance.

3.5.2. Completed parameter dependent observer design

In this case, I demonstrate that Theorems 3.3.1 and 3.3.2 can be used in the same way as in (3.19) and (3.20) to design state observer, based on similar principles.

Let $\mathbf{F}_{ref} = \mathbf{A}_{ref} - \mathbf{G}_{ref}\mathbf{C} \sim \mathbf{F}(t) = \mathbf{A}(\mathbf{p}(t)) - (\mathbf{G}_{ref} + \mathbf{G}(t))\mathbf{C}$, which means that the eigenvalues of $\mathbf{F}_{ref}$, the $\lambda(\mathbf{F}_{ref})$ and $\lambda(\mathbf{F}(t))$ become equal during operation. So, $\lambda(\mathbf{F}_{ref}) = \lambda(\mathbf{F}(t))$ at $\forall\mathbf{p}(t)$, if $\lambda(\mathbf{F}(t))$ are the eigenvalues of $\mathbf{F}(t) = \mathbf{A}(\mathbf{p}(t)) - (\mathbf{G}_{ref} + \mathbf{G}(t))\mathbf{C}$. This is only possible if the similarity transformation matrix is the $\mathbf{I}_{n\times n}$ unity matrix, namely, $\mathbf{F}_{ref} = \mathbf{I}^{-1}\mathbf{F}(t)\mathbf{I}$. As previously, that means that the introduced observer gain has to provide the "smoother" similarity, but also the "strict" equality criteria as well. Shortly, the proposed completed observer gain $\mathbf{G}_{ref} + \mathbf{G}(t)$ has to provide the equality of not just the eigenvalues $\lambda(\mathbf{F}_{ref}) = \lambda(\mathbf{F}(t))$, but also the equality of the matrices, as well:

$$\begin{aligned} &\mathbf{F}_{ref} = \mathbf{F}(t) \\ &\mathbf{A}_{ref} - \mathbf{G}_{ref}\mathbf{C} = \mathbf{A}(\mathbf{p}(t)) - (\mathbf{G}_{ref} + \mathbf{G}(t))\mathbf{C} \end{aligned} \quad . \tag{3.50}$$

3.5.3. Consequences, observer design and limitations

Consider the case when $\mathbf{p}(t)$ can be measured or estimated. In this case, $\mathbf{G}(t)$ can be calculated via rearranging the (3.50) at every $\mathbf{p}(t)$:

$$\begin{aligned} &\mathbf{A}_{ref} - \mathbf{G}_{ref}\mathbf{C} = \mathbf{A}(\mathbf{p}(t)) - \mathbf{G}_{ref}\mathbf{C} - \mathbf{G}(t)\mathbf{C} \\ &(\mathbf{A}_{ref} - \mathbf{G}_{ref}\mathbf{C} - \mathbf{A}(\mathbf{p}(t)) + \mathbf{G}_{ref}\mathbf{C})\mathbf{C}^{-1} = -\mathbf{G}(t)\mathbf{C}\mathbf{C}^{-1} \\ &\mathbf{G}(t) = -(\mathbf{A}_{ref} - \mathbf{G}_{ref}\mathbf{C} - \mathbf{A}(\mathbf{p}(t)) + \mathbf{G}_{ref}\mathbf{C})\mathbf{C}^{-1} \\ &\mathbf{G}(t) = -(\mathbf{A}_{ref} - \mathbf{A}(\mathbf{p}(t)))\mathbf{C}^{-1} \end{aligned} \tag{3.51}$$

By rearranging (3.51):

$$\begin{aligned}&\mathbf{A}(\mathbf{p}(t)) - (\mathbf{G}_{ref} + \mathbf{G}(t))\mathbf{C} = \\ &\mathbf{A}(\mathbf{p}(t)) - \Big(\mathbf{G}_{ref} - (\mathbf{A}_{ref} - \mathbf{A}(\mathbf{p}(t)))\mathbf{C}^{-1}\Big)\mathbf{C} = \ , \\ &\mathbf{A}_{ref} - \mathbf{G}_{ref}\mathbf{C}\end{aligned} \tag{3.52}$$

an observer structure appears, which can ensure that the parameter dependent observer is going to behave as the reference observer itself, regardless of the actual value of $\mathbf{p}(t)$.

Similar to the previous Section, I have assumed that the parameter vector $\mathbf{p}(t)$ can be measured or estimated, which is an important limitation. However, most of the cases if the parts of $\mathbf{p}(t)$ cannot be measured, it can be estimated by the observer itself, or external estimator also can be used.

The control structure with the completed observer can be seen on Fig. 3.17.

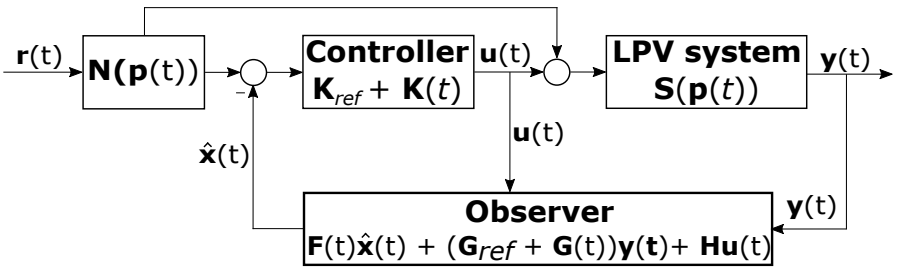

Figure 3.17.: General feedback control loop with completed observer and gain

The key points which are needed in order to realize the proposed completed observer design method can be summarized as follows – which should follow the afore mentioned realization steps of the completed controller:

1. Realization of the completed LPV controller structure;
2. State observer design via linear controller design methods in order to realize the observer gain $\mathbf{G}_{ref}$ for the reference LTI system $\mathbf{S}(\mathbf{p}_{ref})$;
3. Design of the eligible observer scheme, including the appropriate form of (3.51);
4. Realization of the control environment.

I present the main limitations and their possible solutions below.

1. The first step is the same as the completed controller design.

2. The invertibility of the output matix $\mathbf{C}$ is the key point. The structure of a system's output and the output equation is structurally different than the input. That means, we have to face strict limitations. Two bottleneck has to be investigated, the mathematical and the control one. Mathematically, the $\mathbf{C}$ matrix has to be a square matrix and has to be invertible. The control interpretation of this restriction is that the number of the output (and thus the number of the output equations) has to be equal to the number of the states, namely, each state has to be an output, or should has direct affect on the output. This prescription makes the columns of the $\mathbf{C}$ matrix linearly independent and thus invertible.

   There is a chance that this property can be handled through mathematical transformations, which transforms the completed equation of (3.51) into an other abstract space (by using basis transformations), however, I did not investigated this possibility yet.

In the following section, I demonstrate how the completed controller and observer design works in practice on given nonlinear physiological system.

3.6. Illustrative example for the completed observer structure

In this Section, I demonstrate the usability of the developed completed observer structure in practice.

Two remarkable considerations has to be emphasized:

1. I only investigated such kind of structure where the prescribed requirements against the model structure were satisfied, namely, each states are outputs and $\mathbf{C}$ is invertible.

2. I have used a modified model of Subsection 3.4.1; the considerations, circumstances, completed controller design were exactly the same and these processes were not affected by the modification of the system equations. The same controller structure were used, however, completed with an observer.

3.6.1. Control of nonlinear compartmental model beside observer

In this example I demonstrate the developed completed observer solution on the same system as Subsection 3.4.2. The only difference is the modification of the outputs in order to satisfy the requirement against the invertibility of $\mathbf{C}$.

Consider the compartmental system of (3.26) with modified $y_{1,2}(t)$ outputs:

$$\begin{aligned}
\dot{x_1}(t) &= -k\frac{x_1(t)}{1+ax_1(t)} + bx_2(t) - c(x_2(t)+z)x_1(t) + \frac{u_1(t)}{V_1} \\
\dot{x_2}(t) &= -k\frac{x_2(t)}{(1+dx_2(t))} - bx_2(t) + \frac{u_2(t)}{V_2} \\
y_1(t) &= x_1(t) \\
y_2(t) &= x_2(t)
\end{aligned} \quad . \tag{3.53}$$

The modified output matrix $\mathbf{C}$ becomes different than (3.27):

$$\mathbf{C} = \begin{bmatrix} 1 & 0 \\ 0 & 1 \end{bmatrix} . \tag{3.54}$$

The selected scheduling variables were $\mathbf{p}(t) = \left[\frac{k}{1+ax_1(t)}, x_2(t)+z, \frac{k}{1+dx_2(t)}\right]^\top$, which means we have a $3D$ parameter space. As previously, these "state based" scheduling variables are not directly measurable and in the given case they will provided by the observer.

Assume that the reference parameter vector is $\mathbf{p}_{ref} = [0.6667, 0.6, 0.64]^\top$.

I have applied the same reference controller $\mathbf{K}_{ref}$ for the same reference LTI system $\mathbf{S}(\mathbf{p}_{ref})$ as in Subsection 3.4.1.

The next step was the inspection of observability. The rank of the observability matrix was 2, meaning that the reference LTI system was observable.

I have designed the reference observer gain $\mathbf{G}_{ref}$ by using the MATLAB$^{\text{TM}}$ *place* command [99]. The obtained $\mathbf{G}_{ref}$ was the following:

$$\mathbf{G}_{ref} = \begin{bmatrix} 110.47 & -0.3041 \\ -1.3758 & 207.3741 \end{bmatrix} . \tag{3.55}$$

Afterwards, the realization of the completed observer structure is possible (as in Fig. 3.17).

I have used the same protocol during my investigations: I compared the controlled LPV system (without observer) to the controlled and observed LPV system.

In this case, I applied a lower bound saturation on the control input signal, namely, the control signal cannot be lower than zero in both cases.

The results can be seen on Fig. 3.18. The upper left figure shows the varying of the state variables of the controlled LPV system, while the top right figure shows the changing of the estimated state variables provided by the completed observer. The lower left diagram shows the outputs of the controlled LPV system, while the lower right diagram represents the output of the controlled and observed LPV system. It can be seen that both systems reach their desired steady state values without static error and there is no difference between the outputs and states of the given LPV systems. However, as Fig. 3.19. shows, a small, oscillating error occurred between the states and outputs of the systems. The order of the error is around 10^{-3} – 10^{-4}.

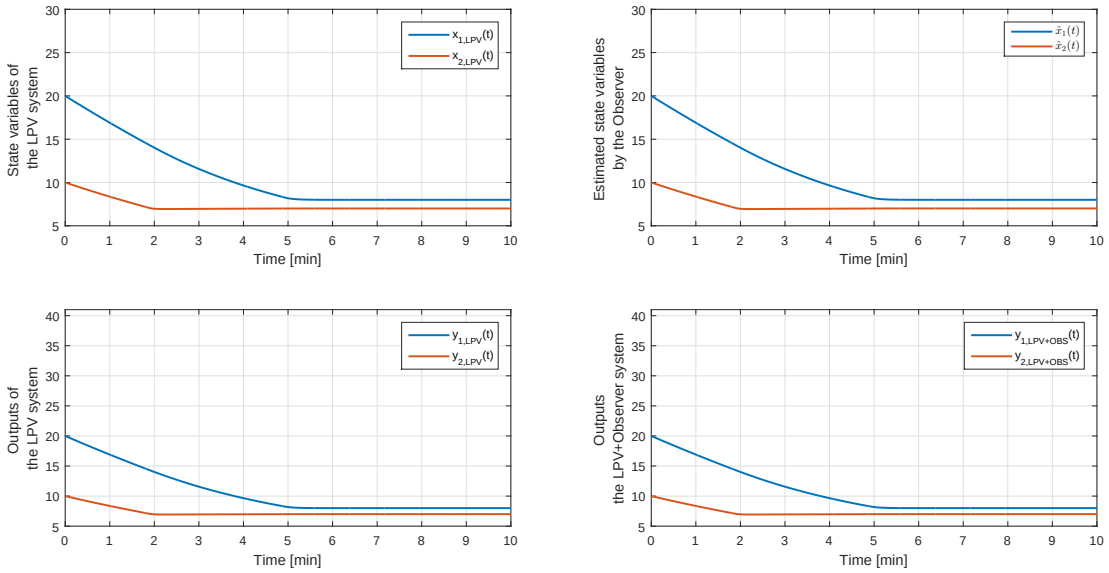

Figure 3.18.: States and outputs of the controlled LPV and controlled and observed LPV system

Figure 3.20. shows the PS of the simple LPV system and the PS, which is realized by the observer. The order of the error between the scheduling variables are very low: 10^{-2}, which means the completed observer approximates the scheduling variables, however, with high accuracy.

3.6.2. Summary

In the Section above, I have introduced an LPV-based completed observer design approach. This method provides a mixture of classical state observer design and a kind of supplementary observer which is based on the parameter vectors (and belonging parameter dependent LTI systems) of the LPV parameter space.

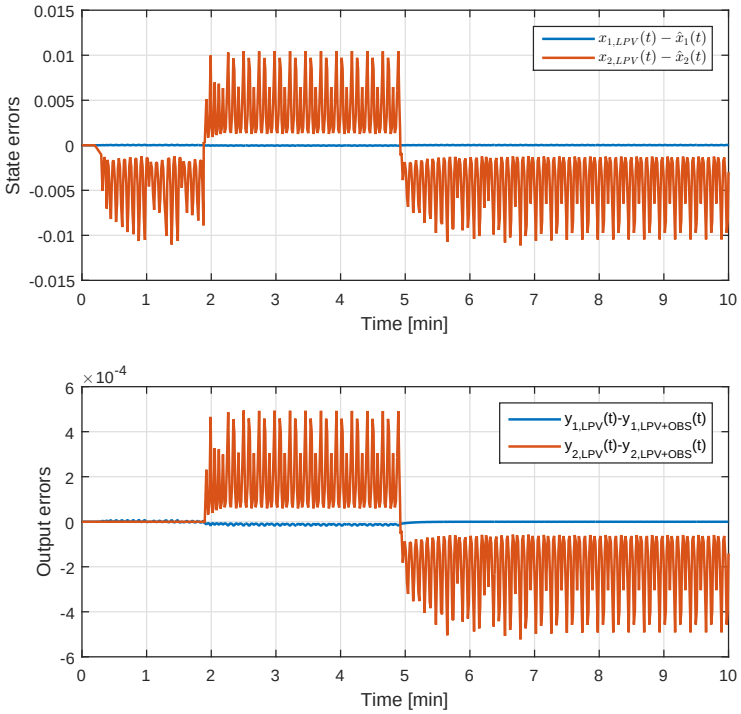

Figure 3.19.: Result of the simulations

I presented the properties, key points and usability of the developed completed observer scheme.

The developed LPV based completed observer structure is able to estimate the actual values of the states in case the states are directly not measurable. I presented the usability of the developed tools in case of nonlinear physiological system.

I found that the completed observer can accurately estimate the states of the given specific LPV system.

Finally, a crucial point should be noted at this point: the key issue in this Subsection is the invertibility of $\mathbf{C}$. I demonstrated the usability of the completed observer method in a favorable case. However, the method is able to deal with such situations, when $\mathbf{C}$ is invertible, but not a diagonal matrix. That means, the states do not occur by their own on the output, or the order of the output equations are different. In that situations, when there is a coupling, eg. $y_1(t) = x_1(t) + x_3(t)$, $y_2(t) = x_3(t)$ and $y_3(t) = x_2(t)$ the

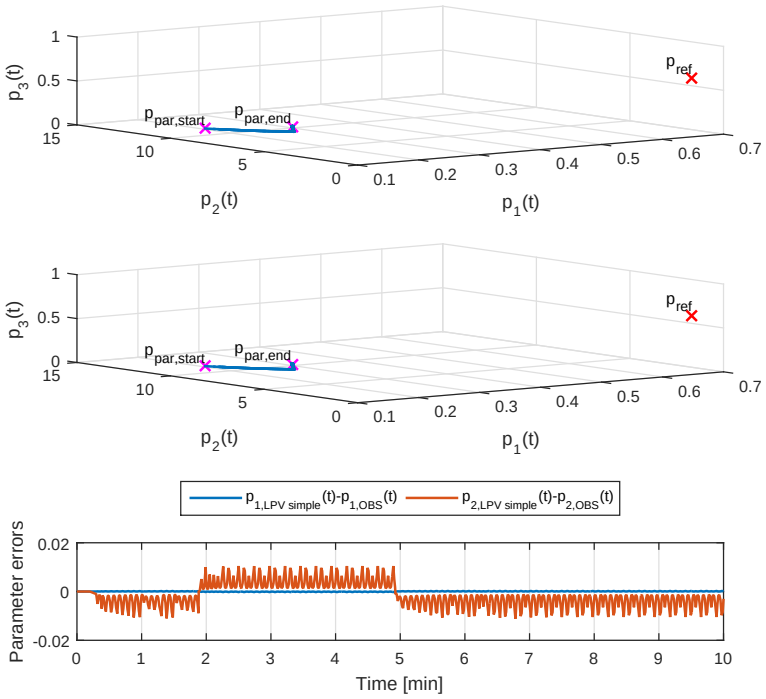

Figure 3.20.: Parameter space and parameter errors. Upper row: PS of LPV system; middle row: PS of the observer; lower row: parameter error

$\mathbf{C} = \begin{bmatrix} 1 & 0 & 1 \\ 0 & 0 & 1 \\ 0 & 1 & 0 \end{bmatrix}$ and the inverse is $\mathbf{C} = \begin{bmatrix} 1 & -1 & 0 \\ 0 & 0 & 1 \\ 0 & 1 & 0 \end{bmatrix}$. The completed observer structure can deal with such situations – however, the complex investigation of these circumstances will be a part of my future work.

Thesis Group 2

Thesis group 2: Completed LPV controller and observer scheme for LPV systems.

Thesis 2

I have introduced mathematical tools for LPV related control tasks which successfully exploit the possibilities lied in the specific properties of the parameter space of LPV systems. By using these tools different quality markers can be defined and specific complementary LPV controller and observer structures can be designed.

Thesis 2.1

I have introduced a norm based "difference" interpretation regarding the LPV systems, based on the properties of the LPV parameter space. I have defined how to use these interpretations as error and quality criteria during modeling and control and demonstrated my theoretical findings on a concrete example in diabetes modeling.

Thesis 2.2

I have developed an LPV based complementary controller structure in order to control nonlinear systems. The developed method requires the knowledge of classical state feedback theorems and less complex than the LMI-based methods, moreover it requires less computational capacity than the LMI-based techniques. I have demonstrated the usability of the developed tool in case of different nonlinear systems, with unfavorable circumstances demonstrating that the developed method provides stability and appropriate control action.

Thesis 2.3

I have developed an LPV based complementary observer structure which can estimate the actual values of the states in case of directly not measurable ones. I demonstrated the usability of the developed tools in case of a nonlinear system. I have proven that the complementary observer can accurately estimate the states of the given specific LPV systems.

Relevant own publications pertaining to this thesis group: [91, 103, 104, 105].

4. Tensor-Product model transformation based modeling

This Chapter consists of three main parts: motivation of using TP related tools, theoretical background, and different case studies, where I used the TP model transformation in order to realize TP models. The Chapter is organized as follows.

First, I collected the main motivation of using the TP related framework.

Secondly, I present the theoretical material including the mathematics of TP model transformation and the control oriented modeling technique.

Thereafter, an investigation of the TP-based modeling possibilities for known ICU DM model follows.

After it, I present the results of the robustization possibilities with TP-modeling in case of a Minimal DM model.

Afterwards, I demonstrate the investigation of a complex T1DM model via TP model transformation.

It should be noted that I have used MATLAB$^{\text{TM}}$ in order to realize the theoretical achievements.

Finally, in the practical example I used the control oriented model form from Sec. 3.3.6 when I realized the qLPV models.

4.1. Motivation behind the usage of TP model transformation

In nonlinear physiological systems one crucial point is the effective handling of the nonlinearity. This is challenging even now, when several methods are available, because all of the processes and systems require unique approach. There is no general solution, yet. Although, the recently appeared TP transformation based modeling and controller design provide a general way regard to the issues concerning the control of such systems. The TP model transformation can be effectively combined with LPV techniques and LMI or Bilinear Matrix Inequality (BMI) based design methods.

The basis is a well defined qLPV model as in Chapter D. However, in contrast to the previous chapter our aim is not to use the whole parameter space and exploit its

properties concerning to the $\mathbf{p}(t)$ parameter vector. Now, our goal is to determine the most tight bounding simplex ($\mathbf{\Omega}$) in the parameter space which contains the all possibly occurring LTI systems depends on the actual value of the $\mathbf{p}(t)$. By realizing a dense sampling on the parameter space and mapping the possible values of $\mathbf{p}(t)$, a minimal volume simplex ($\mathbf{\Omega}$) can be realized (Fig. 4.1).

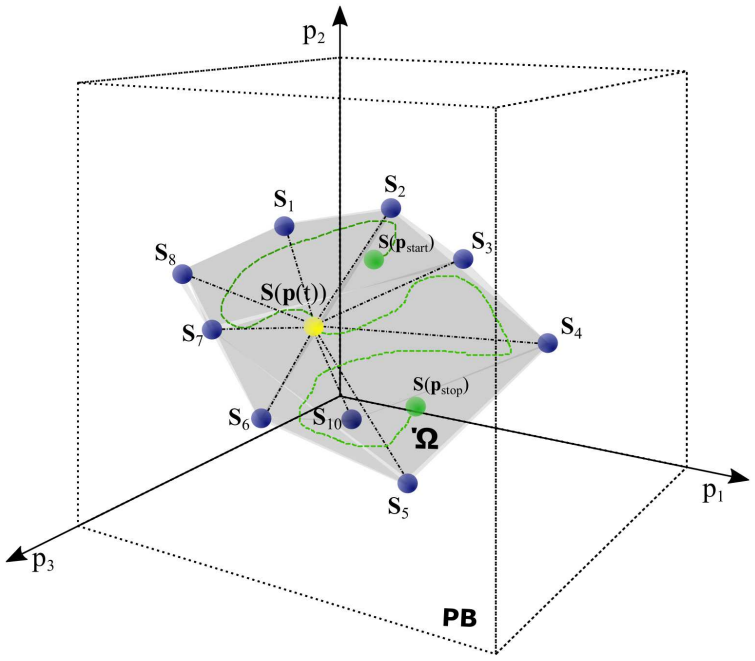

Figure 4.1.: Parameter space of a LPV system with defined parameter box (cube) and $\mathbf{\Omega}$ bounding simplex

Since, we know the vertices of this simplex (consist of $\mathbf{S}_i$ LTI systems), we are able to use different LMIs (or BMIs) to design $\mathbf{K}_i$ controllers which fulfill the prescribed requirements defined in the LMIs. The final system and controller (and observer) can be described as a convex combination of the $\mathbf{K}_i$ controller ($\mathbf{G}_i$ observers) as I present later. The main benefits compared to other LMI based methods is the less computational capacity, deeper understanding of the processes behind, more sophisticated or strict requirements can be embedded into the LMIs – moreover, the occurred core tensor structure via the TP model transformation can be used in the controller as well and other manipulations are not needed. The appropriate control action will be guaranteed

via this method.

The first step of this path is to realize appropriate TP models through the TP model transformation which can be used later for controller design purposes. In this Chapter I present this "first step" and realize the TP models which will be the part of my later research in this regard.

4.2. Theoretical background

4.2.1. TP related mathematical tools

The TP model transformation based approaches originate from the parameter dependent fuzzy system techniques [96]. The TP method was originally described in [106, 107]. The approach was summarized in [92] in case of qLPV based systems and controller design. Concisely summarized, the TP model transformation is able to transforms a given function into a determined TP function form regardless of the type of the original function, if the exact transformation is possible; otherwise, the TP model transformation provides a TP function form approximation with given accuracy.

The TP form complexity can be settled by sampling frequency on the given parameter domain which allows to determine the approximation accuracy of the original function by the TP function. Since most of the qLPV models can be described by qLPV functions, TP model based transformation can be used on them. Through this process, a TP transformation based TP model can be created which can approximate the original qLPV model. In other words, the resulting TP model can approximate the original qLPV model. This approximation can be a "close-to-original" approximation (lower accuracy) or maybe a "mimicry" (high accuracy) of the original model depending on the used simplifications (regarding to HOSVD and convex hull) during the transformation. TP transformation is an effective way for convex hull manipulation of polytopic structures and can be well combined with LMI-based techniques. These properties allow to reach less conservative, more optimal LMI-based controller design possibilities than the usual LMI-methods [92].

For reasons of convenience, I repeat here the SS form of a qLPV model from (D.9), (D.10) and (D.14), since this will be the base whereon we build the further definitions:

$$\begin{aligned}\dot{\mathbf{x}}(t) &= \mathbf{A}(\mathbf{p}(t))\mathbf{x}(t) + \mathbf{B}(\mathbf{p}(t))\mathbf{u}(t) + \mathbf{E}(\mathbf{p}(t))\mathbf{r}(t)\\ \mathbf{y}(t) &= \mathbf{C}(\mathbf{p}(t))\mathbf{x}(t) + \mathbf{D}(\mathbf{p}(t))\mathbf{u}(t) + \mathbf{D_2}(\mathbf{p}(t))\mathbf{u}(t)\end{aligned} \tag{4.1}$$

$$\mathbf{S}(\mathbf{p}(t)) = \begin{pmatrix} \mathbf{A}(\mathbf{p}(t)) & \mathbf{B}(\mathbf{p}(t)) & \mathbf{E}(\mathbf{p}(t)) \\ \mathbf{C}(\mathbf{p}(t)) & \mathbf{D}(\mathbf{p}(t)) & \mathbf{D}_2(\mathbf{p}(t)) \end{pmatrix} . \tag{4.2}$$

At this point, I have to repeat the definition of the PB from the TP point of view, because their interpretation is different, although they are basically equivalent. In this Chapter, the notations of the dimensions will be different than the previous Chapter due to I strove to use the TP related nomenclature.

Let the $\mathbf{p}(t) \in \mathbf{\Omega} \in \mathbb{R}^H$ be the time dependent parameter vector.

Definition 4.2.1. Transformational Space (TS) $\mathbf{\Omega}$: the bounded (closed) H dimensional hyperspace (hypercube), which is determined by the minimum and maximum values of the scheduling parameters, as the elements of the parameter vector $p(t)$: $\mathbf{\Omega} = [p_{1,min}, p_{1,max}] \times [p_{2,min}, p_{2,max}] \times \ldots \times [p_{H,min}, p_{H,max}] \in \mathbb{R}^H$. ■

Remark 4.2.1.1. *The TS practically equivalent to the PB.*

Definition 4.2.2. Finite element convex polytopic model [108]: it describes the actual model $\mathbf{S}(t)$ as the convex combination of the $\mathbf{S}_r \in \mathbb{R}^{(n+k)\times(n+m+p)}$ LTI vertex systems and the $w_r(\mathbf{p}(t))$ weighting function inside the TS $\mathbf{\Omega}$ ($\mathbf{p}(t) \in \mathbf{\Omega}$):

$$\mathbf{S}(\mathbf{p}(t)) = \sum_{r=1}^{R} w_r(\mathbf{p}(t)) \mathbf{S}_r \ . \tag{4.3}$$

The convexity conditions requires that

$\forall r, \mathbf{p}(t) : w_r(\mathbf{p}(t)) \in [0,1]$ and $\forall \mathbf{p}(t) : \sum_{r=1}^{R} w_r(\mathbf{p}(t)) = 1.$ ■

Definition 4.2.3. Finite element TP-type convex polytopic model [109]: in case $\mathbf{S}(\mathbf{p}(t))$ is given by (4.3) for any $\mathbf{p}(t)$ as the parameter varying combination of the LTI vertex system $\mathbf{S}_r \in \mathbb{R}^{(n+k)\times(n+m+p)}$

$$\mathbf{S}(\mathbf{p}(t)) = \sum_{i_1=1}^{I_1} \sum_{i_2=1}^{I_2} \ldots \sum_{i_H=1}^{I_H} \prod_{h=1}^{H} w_{h,i_h}(\mathbf{p}_h(t)) \mathbf{S}_{i_1,i_2,\ldots,i_H} \tag{4.4}$$

and the compact notation of (4.4) based on [92]:

$$\mathbf{S}(\mathbf{p}(t)) = \mathcal{S} \bigotimes_{\mathrm{h}=1}^{\mathrm{H}} w_h(\mathbf{p}_h(t)) \ , \tag{4.5}$$

where the coefficient tensor $\mathcal{S} \in \mathbb{R}^{I_1 \times I_2 \times \ldots \times I_H \times (n+k) \times (n+m+p)}$ is derived from the $\mathbf{S}_{i_1,i_2,\ldots,i_H}$

LTI vertex system and the row vector $w_h(\mathbf{p}_h(t))$ consists of $w_{h,i_h}(\mathbf{p}_h(t))$ $(i_h = 1, \ldots, I_H)$ univariate continuous weighting functions. ■

Remark 4.2.3.1. *The TP models according to (4.5) belong to a particular, special class of the polytopic models as (4.3). In this case, the weighting functions are decomposed to a tensor product of univariate functions [110].*

Definition 4.2.4. TP model transformation: the TP model transformation provides an effective numerical method that transforms a given qLPV model of (4.1) into the TP model form of (4.5). In this way, several LMI based controller design methodology can be applied directly to the provided TP model. The TP model transformation does allow the utilization of convex hull manipulation during the transformation. The accuracy of the resulting TP model depends on the number of used LTI vertices, the properties of the applied HOSVD process and the used TP function. Detailed description with examples can be found in [92]. ■

Definition 4.2.5. Canonical form of qLPV models based on HOSVD method: without complexity reduction and convex hull manipulation, the result of the TP model transformation is the numerical reconstruction of the HOSVD of the given qLPV model. Here, because of the HOSVD is used on qLPV models (matrix functions), the resulting HOSVD canonical form consists of a singular function in orthonormal structure and a core tensor, which contains system vertices assigned to the higher order singular values. For further details see [92]. ■

Definition 4.2.6. Convex TP model: a resulting TP model is convex if the following criteria about the weighting functions are satisfied:

$$\begin{aligned} &\forall h, i, \mathbf{p}_h(t) : w_{h,i_h}(\mathbf{p}_h(t)) \in [0,1] \\ &\forall h, \mathbf{p}_h(t) : \sum_{i=1}^{I_h} w_{h,i_h}(\mathbf{p}_h(t)) = 1 \end{aligned} \quad . \tag{4.6}$$

Several convex hulls can be applied in the parameter space depending on the type of application (qLPV model) and the required properties [92]. A tight convex hull is the MVS type hull, which is applied in this Theses. ■

Definition 4.2.7. MVS-type convex TP model: the following TP model

$$\mathbf{S}(\mathbf{p}) = \mathcal{S} \overset{\mathrm{H}}{\underset{\mathrm{h=1}}{\boxtimes}} \mathbf{w}^{(h)}(\mathbf{p}_h) \ , \tag{4.7}$$

is an MVS-type convex model if the $(\mathcal{S})_{j_h=j}$ h-mode sub-tensors evolve a minimal volume bounding simplex for $\mathcal{S} \times_h \mathbf{w}_{jh}^{(h)}(p_h)$ trajectory over $h = 1..H$ for the $\mathcal{S} \in \mathbb{S}^{J_1 \times \cdots \times J_H}$ core tensor, which is realized from the $\mathbf{S}_{j_1,\ldots,j_H}$ matrices.

■

Further derivations, explanations and case studies can be found in [92, 93, 108, 109, 111, 112]. I have utilized the TP Toolbox$^{\text{TM}}$ in this study. The toolbox is a MATLAB$^{\text{TM}}$ based tool and means a convenient and effective possibility to realize the TP based approached. The TP toolbox is available under [113].

It should be noted that the TP model transformation requires the LPV model in general form as Sec. D.1.2.

4.3. Investigation of the TP-based modeling possibility of a nonlinear ICU diabetes model

In this Subsection, I have used the same ICU model with same model parameters as in Sec. 3.2.3. from Wong et al. [85, 86]. The model is an appropriate sample model, because it unifies each drawbacks of the DM models: high nonlinearities, impulse kind inputs and internal coupling between the states.

4.3.1. Derivation of the LPV and TP models

Steady state analysis

The steady state of the model can be calculated in different ways. One of these is when the steady G_d state and p_d input are given. Q_d, I_d and $u_{ex,d}$ can be calculated by using the (B.2) equations. An important question is the relation of G_d to G_E. The qLPV model should approximate the system dynamics around the equilibrium points; hence, G_d can be a "desired" equilibria and can be different from G_E. The equality of G_d and G_E becomes important during a TP based controller design, because the G_d will that desired blood glucose level, what the controller has to provide.

In the first case, I assumed that $G_d = G_E$. As a result, the dynamics of the plasma glucose concentration at the equilibrium point becomes:

$$\dot{G}(t) = 0 = -p_G G_d - S_I 2 G_d \frac{Q_d}{1 + \alpha_G Q_d} + p_d \ . \tag{4.8}$$

With reformulation of (4.8), Q_d can be calculated, as follows:

$$Q_d = \frac{-p_G G_d + p_d}{S_I 2 G_d}(1 + \alpha_G Q_d) = A(1 + \alpha_G Q_d) \tag{4.9}$$

$$Q_d = \frac{A}{1 - \alpha_G A} \ . \tag{4.10}$$

I_d appears by using the rearranged (4.11) equation, if $Q(t)$ state is at the equilibrium point:

$$\dot{Q}(t) = 0 = -kQ_d + kI_d \tag{4.11}$$

$$I_d = Q_d \ . \tag{4.12}$$

As a result, the dynamics of $I(t)$ at the equilibria can be described as follows:

$$\dot{I}(t) = 0 = -\frac{nI_d}{1 + \alpha_I I_d} + \frac{u_{ex,d}}{V} \ , \tag{4.13}$$

from which the necessary $u_{ex,d}$ can be calculated to hold the equilibrium of the states beside the predefined G_d and p_d:

$$u_{ex,d} = \frac{nI_d}{1 + \alpha_I I_d} V \ . \tag{4.14}$$

The other investigated case is when $G_d \neq G_E$. Only the (4.8), (4.11) and (4.12) equations will be different in this case. Naturally, the numerical values of I_d, Q_d and $u_{ex,d}$ will change accordingly:

$$\dot{G}(t) = 0 = -p_G G_d - S_I(G_d + G_E)\frac{Q_d}{1 + \alpha_G Q_d} + p_d \ . \tag{4.15}$$

By rearranging (4.8), Q_d can be calculated as follows:

$$Q_d = \frac{-p_G G_d + p_d}{S_I(G_d + G_E)}(1 + \alpha_G Q_d) = B(1 + \alpha_G Q_d) \tag{4.16a}$$

$$Q_d = \frac{B}{1 - \alpha_G B} \ . \tag{4.16b}$$

Investigated qLPV models

In this Subsection I investigated different approaches as more than one realizable control oriented qLPV form can be derived.

Consider the two above-mentioned cases: $G_d = G_E$ and $G_d \neq G_E$. Many options can be selected as aim of TP-based control. One of them is when the aim of the controller is to prevent the system's deviation from the selected equilibrium point; or if the deviation leads to provide fast action leading the system back to the equilibrium. A natural way to describe this evasive error dynamics is to take the difference of the actual states and the steady states.

First, I consider the $G_d = G_E$ case. The error dynamics becomes as follows (subtracting $S_I G(t)\frac{Q_d}{1+\alpha_G Q_d}$ from the last two parts of (4.17)):

$$\begin{aligned}
&\Delta\dot{G}(t) = \dot{G}(t) - 0 = -p_G G(t) - S_I(G(t)+G_d)\frac{Q(t)}{1+\alpha_G Q(t)} + p(t) \\
&-\left[- p_G G_d - S_I 2 G_d \frac{Q_d}{1+\alpha_G Q_d} + p_d \right] = -p_G G(t) + p_G G_d + p(t) - p_d - \\
&S_I G(t)\frac{Q(t)}{1+\alpha_G Q(t)} - S_I G_d \frac{Q(t)}{1+\alpha_G Q(t)} + S_I G_d \frac{Q_d}{1+\alpha_G Q_d} + S_I G_d \frac{Q_d}{1+\alpha_G Q_d} = \\
&-p_G(G(t)-G_d) + (p(t)-p_d) - S_I G_d \left(\frac{Q(t)}{1+\alpha_G Q(t)} - \frac{Q_d}{1+\alpha_G Q_d)} \right) - \\
&S_I G(t)\frac{Q(t)}{1+\alpha_G Q(t)} + S_I G_d \frac{Q_d}{1+\alpha_G Q_d} = \\
&-p_G \Delta G(t) + \Delta p(t) - S_I G_d \frac{1}{(1+\alpha_G Q(t))(1+\alpha_G Q_d)} \Delta Q(t) \\
&-S_I G(t)\frac{Q(t)}{1+\alpha_G Q(t)} + S_I G_d \frac{Q_d}{1+\alpha_G Q_d}
\end{aligned} \quad , \tag{4.17}$$

$$\begin{aligned}
&-S_I G(t)\frac{Q(t)}{1+\alpha_G Q(t)} + S_I G_d \frac{Q_d}{1+\alpha_G Q_d} + S_I G(t)\frac{Q_d}{1+\alpha_G Q_d} - S_I G(t)\frac{Q_d}{1+\alpha_G Q_d} = \\
&-S_I G(t)\left(\frac{Q(t)}{1+\alpha_G Q(t)} - \frac{Q_d}{1+\alpha_G Q_d)} \right) - -S_I \frac{Q_d}{1+\alpha_G Q_d}(G(t)-G_d) = \\
&-S_I G(t)\frac{1}{(1+\alpha_G Q(t))(1+\alpha_G Q_d)}\Delta Q(t) - -S_I \frac{Q_d}{1+\alpha_G Q_d}\Delta G(t)
\end{aligned} \quad . \tag{4.18}$$

From here, the error dynamics of G state at the equilibrium point can be described as:

$$\Delta\dot{G}(t) = -(p_G + S_I\frac{Q_d}{1+\alpha_G Q_d})\Delta G(t) - \\ S_I(G(t)+G_d)\frac{1}{(1+\alpha_G Q(t))(1+\alpha_G Q_d)}\Delta Q(t) + \Delta p(t) \tag{4.19}$$

The second case is when $G_d \neq G_E$. In this case, the error dynamics $\Delta G(t)$ becomes as follows:

$$\Delta\dot{G}(t) = -(p_G + S_I\frac{Q_d}{1+\alpha_G Q_d})\Delta G(t) - \\ S_I(G(t)+G_E)\frac{1}{(1+\alpha_G Q(t))(1+\alpha_G Q_d)}\Delta Q(t) + \Delta p(t) \tag{4.20}$$

As a result, the error dynamics of the $Q(t)$ and $I(t)$ can be easily derived as in (4.21):

$$\Delta\dot{Q}(t) = \dot{Q}(t) - 0 - kQ(t) + kI(t) - [-kQ_d + kI_d] = \\ -k(Q(t)-Q_d) + k(I(t)-I_d) = \Delta\dot{Q}(t) = -k\Delta Q(t) + k\Delta I(t) \tag{4.21}$$

$$\Delta\dot{I}(t) = \dot{I}(t) - 0 = -n\frac{I(t)}{1+\alpha_I I(t)} + \frac{u_{ex}}{V} - \left[-n\frac{I_d}{1+\alpha_I I_d} + \frac{u_{ex,d}}{V}\right] = \\ -n\left(\frac{I(t)}{1+\alpha_I I(t)} - \frac{I_d}{1+\alpha_I I_d)}\right) + \frac{1}{V}(u_{ex} - u_{ex,d}) = \\ \Delta\dot{I}(t) = -n\frac{1}{(1+\alpha_I I(t))(1+\alpha_I I_d)}\Delta I(t) + \frac{1}{V}\Delta u_{ex}(t) \tag{4.22}$$

A convenient way is to represent the error dynamics-based qLPV models with their SS form. In this way the inputs can be separated: the control input becomes the external insulin intake $u_{ex}(t)$, while the disturbance is the $p(t)$ external CHO intake. I have switched the order of the inputs for the sake of clarity, namely, the first input in the state-space representation is the insulin intake $u_{ex}(t)$, while the second is the CHO disturbance $p(t)$. As the goal is to describe the error dynamics, the difference between the actual input and steady inputs should be considered. In this way, the inputs are: $\Delta\mathbf{u}(t) = [\Delta u_{ex}(t), \Delta p(t)]^\top$. The states of the qLPV models are based on the error dynamics, namely $\Delta\mathbf{x}(t) = [\Delta G(t), \Delta Q(t), \Delta I(t)]^\top$. From these considerations and the (4.19)-(4.22) equations, the SS representations of the derived qLPV models are

represented by (4.23) considering $G_d = G_E$ and (4.24) considering $G_d \neq G_E$.

$$\Delta\dot{\mathbf{x}}(t) = \begin{bmatrix} -(p_G + \frac{S_I Q_d}{1+\alpha_G Q_d}) & \frac{-S_I(G(t)+G_d)}{(1+\alpha_G Q(t))(1+\alpha_G Q_d)} & 0 \\ 0 & -k & k \\ 0 & 0 & \frac{-n}{(1+\alpha_I I(t))(1+\alpha_I I_d)} \end{bmatrix} \Delta\mathbf{x}(t) + \begin{bmatrix} 0 & 1 \\ 0 & 0 \\ \frac{1}{V} & 0 \end{bmatrix} \Delta\mathbf{u}(t) \tag{4.23}$$

$$\Delta\dot{\mathbf{x}}(t) = \begin{bmatrix} -(p_G + \frac{S_I Q_d}{1+\alpha_G Q_d}) & \frac{-S_I(G(t)+G_E)}{(1+\alpha_G Q(t))(1+\alpha_G Q_d)} & 0 \\ 0 & -k & k \\ 0 & 0 & \frac{-n}{(1+\alpha_I I(t))(1+\alpha_I I_d)} \end{bmatrix} \Delta\mathbf{x}(t) + \begin{bmatrix} 0 & 1 \\ 0 & 0 \\ \frac{1}{V} & 0 \end{bmatrix} \Delta\mathbf{u}(t) \tag{4.24}$$

4.3.2. TP models

The TP model transformation can be applied on the $\mathbf{S}\{(G(t), Q(t), I(t))|_{G_d=G_E}\}$ of (4.23) and $\mathbf{S}\{(G(t), Q(t), I(t))|_{G_d\neq G_E}\}$ of (4.24) qLPV system matrices, respectively. The transformation provides the following TP model structure:

$$\begin{aligned} &\mathbf{S}\{(G(t), Q(t), I(t))|_{G_d=G_E}\} = S \overset{3}{\underset{\mathrm{h}=1}{\boxtimes}} \mathbf{w}_h(\mathbf{p}_h(t)) = \\ &S \times_1 \mathbf{w}_1(G(t)) \times_2 \mathbf{w}_2(Q(t)) \times_3 \mathbf{w}_3(I(t)) \end{aligned} \tag{4.25}$$

$$\mathbf{S}\{(G(t),Q(t),I(t))|_{G_d\neq G_E}\} = S \overset{3}{\underset{\mathrm{h=1}}{\boxtimes}} \mathbf{w}_h(\mathbf{p}_h(t)) = \\ S \times_1 \mathbf{w}_1(G(t)) \times_2 \mathbf{w}_2(Q(t)) \times_3 \mathbf{w}_3(I(t)) \quad . \tag{4.26}$$

Figure 4.2 shows the MVS-type weighting functions with dense sampling (left column belongs to (4.23) and the right column belongs to (4.24)). There are no evaluable difference between the given weighting functions; however, small numerical differences appeared.

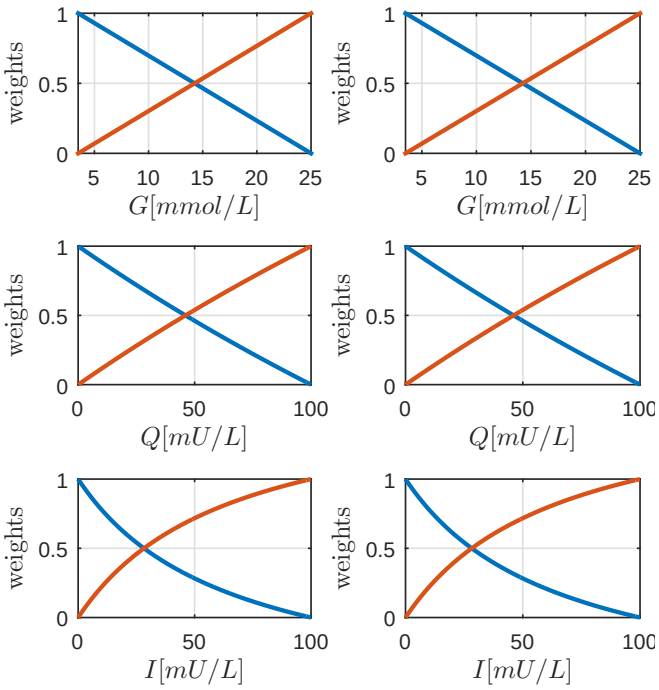

Figure 4.2.: Weighting functions of the TP polytopic model. Left column: $\mathbf{w}_n(p(t))_{G_d=G_E}$, right column: $\mathbf{w}_n(p(t))_{G_d\neq G_E}$.

4.3.3. Validation of the generated models

To validate the generated models, I have built a validation environment in MATLAB which is able to make the comparisons between the original and realized qLPV and TP models automatically.

The main considerations during the validation were the following:

1. Investigated parameter domain: $G = 3.5 \ldots 25$, $Q = 0 \ldots 100$ and $I = 0 \ldots 100$;

2. Comparison was done between every state of every model;

3. Dense (considered number of samples (NoS): $NoS_G = 31$, $NoS_Q = 101$, $NoS_I = 101$) and less dense ($NoS_G = 17$, $NoS_Q = 81$, $NoS_I = 81$) parameter sampling in the parameter domain;

4. Comparison only in case of initial state decay and in case of given inputs;

5. Usage of Root-Mean Square Error (RMSE) as basis of comparison.

The results of the validation are summarized in Table 4.1-4.2. In every subtable, the upper triangular partition belongs to the dense sampling, namely, the number of samples (NoS) was higher on the investigated parameter domain. The model notation is the following:

- original nonlinear model: *Original* (B.2);
- qLPV model of (4.23): $qLPV_1$;
- qLPV model of (4.24): $qLPV_2$;
- TP model of (4.25): TP_1;
- TP model of (4.26): TP_2.

For Table 4.1a., a less than 100 minutes decay was investigated for the initial values of the state variables. The difference between dense and less dense sampling is negligible. However, both TP models had small RMSE under the given circumstances, but the TP_1 model where $G_d = G_E$ had the best performance.

Table 4.2b. shows a scenario where external CHO and insulin inputs were impulse functions (similar to reality), as follows:

- CHO intake: Height: 4 g, Width: 5 min, Period: 50 min
- Insulin intake: Height: 1 U, Width: 2 min, Period: 50 min

I transformed the inputs from g to mmol/L (CHO) and U to mU/L (insulin) based on the model parameters in Table B.3. The density of sampling did not cause evaluable difference in the resulting RMSE of the states based on the data. In this case, TP_2 model produced the smallest RMSE under 300 minutes.

During the investigations, the following parameter set was used: $G_E = 10.5$ mmol/L, $p_G = 0.01$ 1/min, $S_I = 0.001$ L/mU/min, $V = 12$ L, $k = 0.0198$ 1/min, $n = 0.16$ 1/min, $\alpha_I = 0.0017$ L/mU and $\alpha_G = 0.0154$ L/mU.

Table 4.1.: Results of the RMSE-based investigations: RMSE-based comparison of the states of the realized models on the given parameter domain under 100 minutes. Initial conditions: $G_0 = 15$, $Q_0 = 3$ and $I_0 = 5$.

G [mmol/L]

		NoS=31				
		Original	$qLPV_1$	$qLPV_2$	TP_1	TP_2
NoS=17	*Original*	-	1.4295	0.0982	0.0469	0.1273
	$qLPV_1$	1.4295	-	1.3278	1.3826	1.5568
	$qLPV_2$	0.0982	1.5278	-	0.1452	0.0290
	TP_1	0.0469	1.3826	0.1452	-	0.1743
	TP_2	0.1273	1.5569	0.0291	0.1742	-

Q [mU/L]

		NoS=101				
		Original	$qLPV_1$	$qLPV_2$	TP_1	TP_2
NoS=81	*Original*	-	0.0051	0.0051	0.0022	0.0051
	$qLPV_1$	0.0051	-	0	0.0073	0
	$qLPV_2$	0.0051	0	-	0.0073	0
	TP_1	0.0022	0.0073	0.0073	-	0.0073
	TP_2	0.0051	0	0	0.0073	-

I [mU/L]

		NoS=101				
		Original	$qLPV_1$	$qLPV_2$	TP_1	TP_2
NoS=81	*Original*	-	0.0031	0.0031	0.0052	0.0030
	$qLPV_1$	0.0031	-	0	0.0083	0
	$qLPV_2$	0.0031	0	-	0.0083	0
	TP_1	0.0052	0.0083	0.0083	-	0.0083
	TP_2	0.0030	0	0	0.0083	-

Table 4.2.: Results of the RMSE-based investigations: RMSE-based comparison of the states of the realized models on the given parameter domain under 300 minutes beside given impulse-kind inputs. Initial conditions: $G_0 = 15$, $Q_0 = 3$ and $I_0 = 5$

G [mmol/L]

		NoS=31				
		Original	$qLPV_1$	$qLPV_2$	TP_1	TP_2
NoS=17	*Original*	-	2.3666	0.0339	1.3614	0.0244
	$qLPV_1$	2.3666	-	2.4005	1.0052	2.391
	$qLPV_2$	0.0339	2.4005	-	1.3953	0.0095
	TP_1	1.3611	1.0055	1.3950	-	1.3858
	TP_2	0.0246	1.0055	0.0093	1.3857	-

Q [mU/L]

		NoS=101				
		Original	$qLPV_1$	$qLPV_2$	TP_1	TP_2
NoS=81	*Original*	-	0.0127	0.0127	0.0254	0.0125
	$qLPV_1$	0.0127	-	0	0.0127	0.0002
	$qLPV_2$	0.0127	0	-	0.0127	0.0002
	TP_1	0.0254	0.0127	0.0127	-	0.0129
	TP_2	0.0125	0.0002	0.0002	0.0129	-

I [mU/L]

		NoS=101				
		Original	$qLPV_1$	$qLPV_2$	TP_1	TP_2
NoS=81	*Original*	-	0.0088	0.0088	0.0005	0.0089
	$qLPV_1$	0.0088	-	0	0.0083	0.0001
	$qLPV_2$	0.0088	0	-	0.0083	0.0001
	TP_1	0.0005	0.0083	0.0083	-	0.0084
	TP_2	0.0089	0.0001	0.001	0.0084	-

Figure 4.3. shows the results of the second investigation (as in Table 4.2b). in case of dense sampling. It can be seen that the variation of $Q(t)$ and $I(t)$ are almost the same. However, the TP_2 model proved to be much more accurate than the TP_1 in the $G(t)$ state, as the $G_{Orig}(t)$ and $G_{TP_2}(t)$ states overlap each other.

On Figure 4.4 the error of the states was highlighted in such a way that the state variation of the realized TP models were subtracted from the original states. The results confirmed the numerical RMSE-based evaluation in Table 4.2b. and one can see that TP_1 is more suitable to substitute the original nonlinear model.

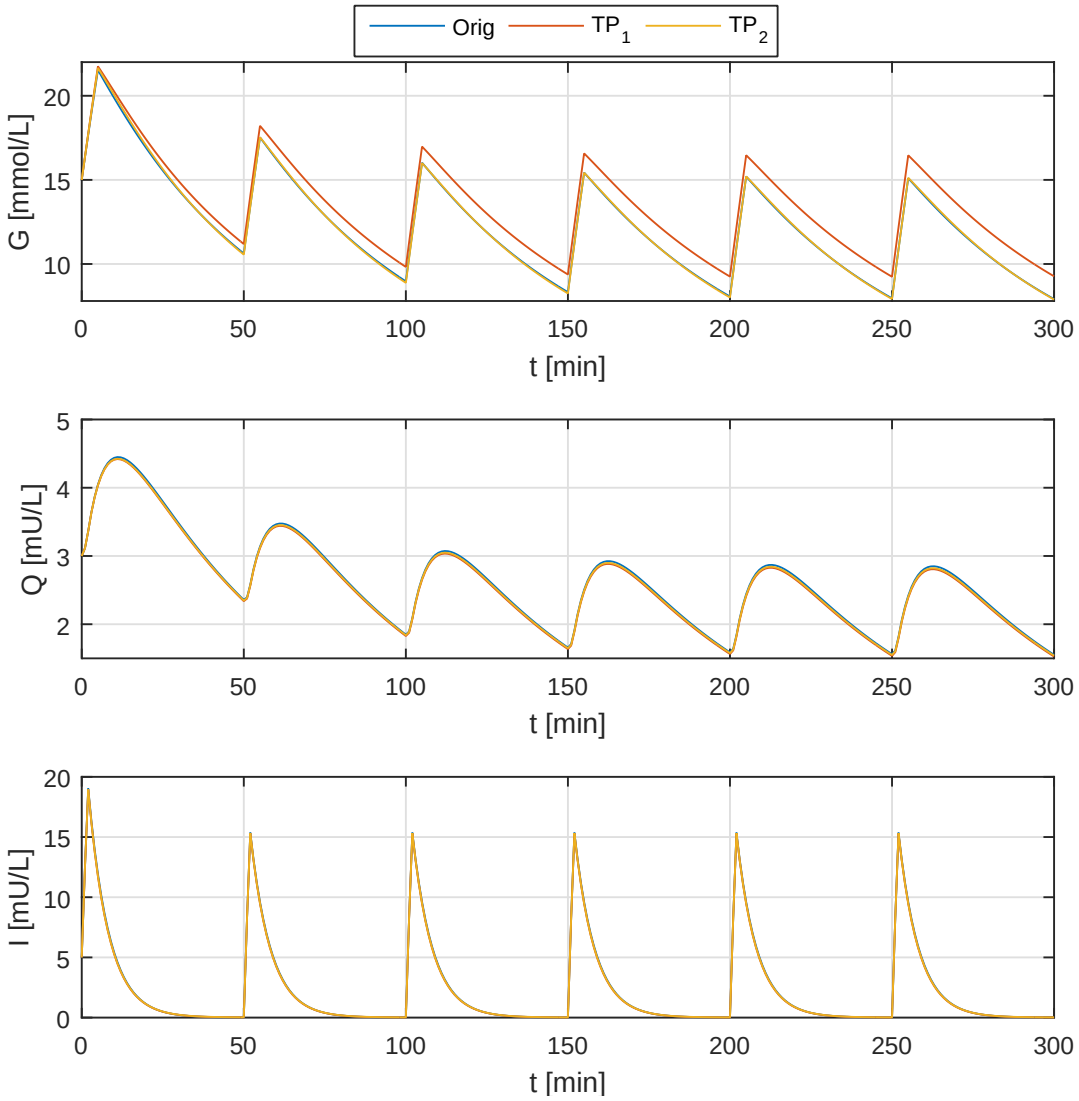

Figure 4.3.: 300 minutes long simulation in case of realistic inputs.

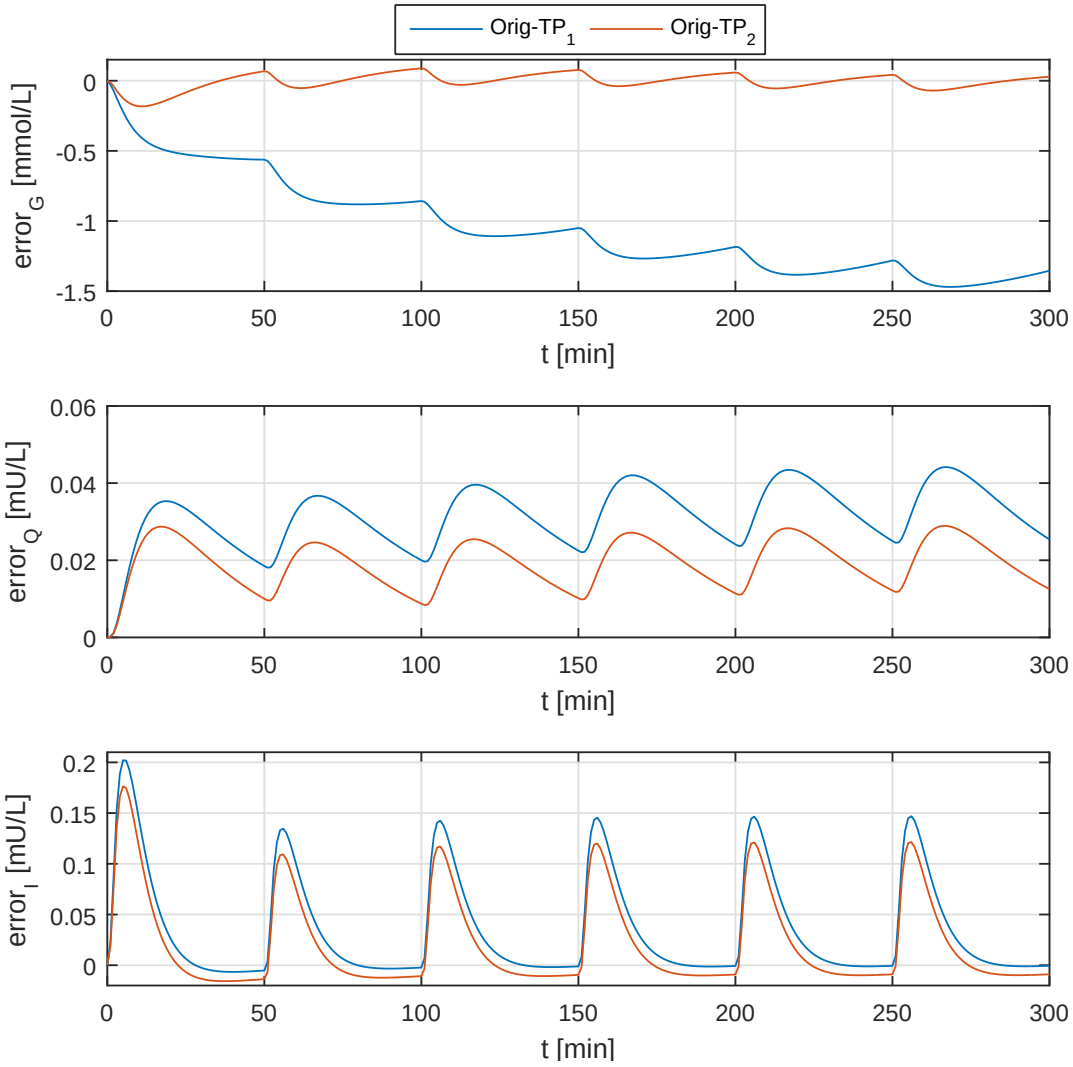

Figure 4.4.: State error evolution over 300 minutes long simulation in case of realistic inputs.

4.3.4. Summary

In this Section, I investigated the applicability of TP model transformation in case of a well-known ICU diabetes model in order to realize different TP models. I have examined two cases: the TP model, when the "operating equilibrium of glycemia (G_d)" of the model was considered equal to the model equilibrium of glycemia (G_E) and were it was not. Based on numerical validation I found that in case of realistic simulations I can reach better performance, namely, smaller difference between the realized TP model and the original model, when the operating equilibrium is not equal to the model equilibrium.

4.4. Robustization possibilities via TP model framework

I used a modified version of the Minimal Model in this Section, which is appropriate to describe the T1DM and T2DM cases, respectively [15]. The model equations (B.1a)-(B.1d) and the parameter descriptions can be found in the Appendix B.

The T1DM version of this model in control oriented form was been used in Sec. 3.4.2. Nevertheless, to provide the full picture I presented here the transformation again. In this way the difference between the T1DM and T2DM is more understandable.

In this study, I have used the following parameter set: $G_b = 110$ mg/dL, $I_b = 1.5$ μU/mL, $p_1 = 0.028$ 1/min, $p_2 = 0.025$ 1/min, $p_3 = 0.00013$ min^{-2}/(μU/mL), $n = 0.23$ 1/min, $h = 130$ mg/dL, $\gamma = 0.01$ (μU/mL)/(mg/dL)/min. These parameters belong to a real patient based on [15]. As the goal is to demonstrate the applicability of TP-model approach I did not distinguish the different cases on the parameter level; hence, the method works regardless of the used parameter sets.

4.4.1. Possible deviation-based qLPV and TP models

First, I investigated the steady-state conditions in a possible equilibrium. I have selected $G_d = 90$ and $u_d = 0$ as steady-state values (the blood glucose concentration is 90 mg/dL and there is no external insulin intake). Moreover, I assumed that $G_d \neq G_B$. From here, the other necessary steady-state values can be calculated by rearranging (B.1a)-(B.1d). It should be noted that $h > G_d$, so (B.1c) and (B.1d) has the same I_d:

$$I_d = \frac{nI_b + u_d}{n} \ . \tag{4.27}$$

$$X_d = \frac{p_3}{p_2} I_d \ . \tag{4.28}$$

$$d_d = (p_1 + X_d)G_d - p_1 G_B \ . \tag{4.29}$$

With the calculated steady-state values, the deviation based model can be derived from the model equations, as follows. First, the $\Delta G(t)$ has been determined. Note that since the $G(t)$ is measurable in real life, I tried to realize a form where only $G(t)$ appears

in the state matrix of the deviation based model:

$$\begin{aligned}
&\Delta\dot{G}(t) = \dot{G}(t) - 0 = -(p_1 + X(t))G(t) + p_1 G_B + d(t) - \\
&\qquad \Big[-(p_1 + X_d)G_d + p_1 G_B + d_d \Big] = \\
&-p_1(G(t) - G_d) + (d(t) - d_d) - X(t)G(t) + X_d G_d = \\
&-p_1 \Delta G(t) + \Delta d(t) - X(t)G(t) + X_d G_d + X_d G(t) - X_d G(t) \ | \\
&\Delta\dot{G}(t) = -(p_1 + X_d)\Delta G(t) + \Delta d(t) - G(t)\Delta X(t)
\end{aligned} \quad . \tag{4.30}$$

The same tools as in case of (4.30) resulting for ΔX as follows:

$$\Delta\dot{X}(t) = -p_2 \Delta X(t) + p_3 \Delta I(t) \ . \tag{4.31}$$

In case of ΔI, I had to separate the deviation based forms for T1DM (I_{T1DM}) and T2DM (I_{T2DM}):

$$\Delta\dot{I}_{T1DM}(t) = -n\Delta I(t) + \Delta u(t) \tag{4.32}$$

and

$$\Delta\dot{I}_{T2DM}(t) = \begin{cases} \gamma \dfrac{(G(t) - h)}{\Delta G(t)} \Delta G(t) - n\Delta I(t) + \Delta u(t) \\ \qquad\qquad \text{for } \ G(t) > h \\ -n\Delta I(t) + \Delta u(t) \\ \qquad\qquad \text{for } \ G(t) \leq h \end{cases} \quad . \tag{4.33}$$

A convenient solution results if we use the derived deviation based model in state-space form. In this case, the states should be $\Delta x(t) = [\Delta G(t), \Delta X(t), \Delta I(t)]^\top$. Thus, the investigated qLPV models become as described in (4.34)-(4.35):

$$\Delta\dot{\mathbf{x}}_{T1DM}(t) = \begin{bmatrix} -(p_1 + X_d) & -G(t) & 0 \\ 0 & -p_2 & p_3 \\ 0 & 0 & -n \end{bmatrix} \Delta\mathbf{x}(t) + \begin{bmatrix} 0 \\ 0 \\ 1 \end{bmatrix} \Delta u(t) + \begin{bmatrix} 1 \\ 0 \\ 0 \end{bmatrix} \Delta d(t) \ . \tag{4.34}$$

$$\Delta\dot{\mathbf{x}}_{T2DM}(t) = \begin{bmatrix} -(p_1 + X_d) & -G(t) & 0 \\ 0 & -p_2 & p_3 \\ \gamma\dfrac{(G(t)-h)}{\Delta G(t)}t & 0 & -n \end{bmatrix} \Delta\mathbf{x}(t) + \begin{bmatrix} 0 \\ 0 \\ 1 \end{bmatrix} \Delta u(t) + \begin{bmatrix} 1 \\ 0 \\ 0 \end{bmatrix} \Delta d(t) \ . \quad (4.35)$$

Applying the TP model transformation on these (having only one parameter), the general TP model structure becomes $\mathbf{S}(G(t)) = S \times \mathbf{w}(G(t))$.

As a result, the variation of the obtained MVS type weighting functions are presented on Fig. 4.5. In case of T1DM, the weighting function is linear, however, in T2DM case the weighting function is nonlinear because of the fraction in (4.34).

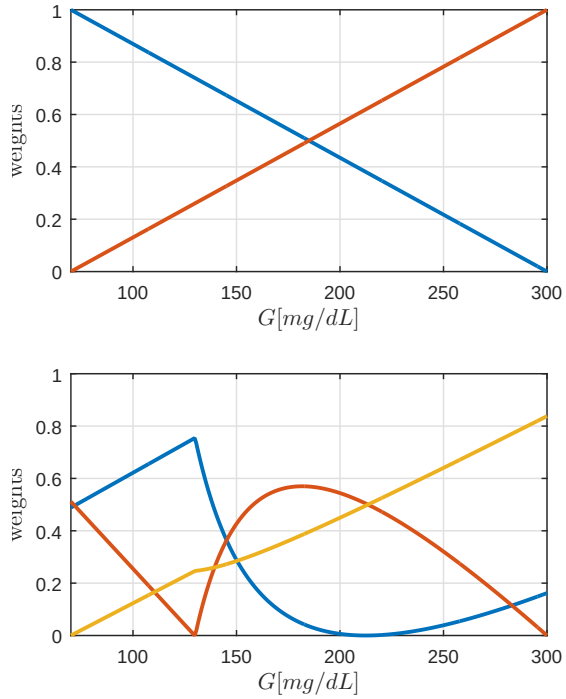

Figure 4.5.: Weighting functions of the TP polytopic model; simple model case. Upper diagram: T1DM case; Lower diagram: T2DM case.

It should be noted that, $\Delta G(t)$ cannot be zero until the G_d is lower than h.

4.4.2. Robustness of the models

In order to increase the robustness of the model (and the realizable controller based on the TP models) the most determinant model parameters should be investigated from the model output point of view. Special property of the TP transformation based modeling and control is that the modeling and controller design can be coupled directly to LMI-based controller design methods. This coupling provides a unique way to increase the robustness through the elements of the parameter vector increasing the control performance. If the parameter vector contains several parameters and the borders of them are given then the controller will be prepared for the variation of these parameters between the given limits.

The output of the model is the blood glucose level $G(t)$, the only measurable variable in real life circumstances. Thus, it is reasonable to investigate how model parameter variation affects $G(t)$. I applied simple perturbation analysis based investigation to identify the most determining model parameter. I used the non-normalized Root Mean Square Error (RMSE) to evaluate the results.

The same investigation process was used both for T1DM and T2DM cases:

- Compare the output of the nominal model $G_{orig}(t_i)$ to the output of the perturbed model $G_{pert}(t_i)$, $RMSE_{param} = \sum_{t_i=0}^{T} \sqrt{G_{orig}(t_i) - G_{pert}(t_i)}$.
- Use a $\pm 35\%$ perturbation for each parameter.
- Apply impulse input signals both for CHO and insulin inputs (Parameters: CHO: $d(t) = 10$ mg/dL over 6 minutes; insulin: $u(t) = 20$ uU/mL over 6 minutes ; injection time: beginning of simulation (minute 0)). The simulation length was set to be $T = 100$ min.

Table 4.3. summarizes the results.

Through this investigation it turned out that the most determining parameters to $G(t)$ are the p_1, p_2 and n. As the model is quite simple, each parameter variation may induce high perturbations that should be handled separately (our goal was finding a method appropriately providing the most important parameters).

Hence, we have selected p_1, p_2 and n as time varying parameters (beside $G(t)$) resulting a $4D$ parameter space determined by the parameter vector $p_4(t) = [G(t), p_1(t), p_2(t), n(t)]^\top$. The new elements are slowly changing in time, which allows handling them as constants. Naturally, the accurate values of them have to be updated after the identifications (done automatically).

Table 4.3.: Results of the RMSE-based investigations.

		Type	
Parameter	Perturbation	RMSE_{T1DM}	RMSE_{T2DM}
p_1	-35%	8.2385	9.2256
	$+35\%$	5.5199	6.0665
p_2	-35%	11.0671	11.3595
	$+35\%$	7.5582	7.842
p_3	-35%	7.6965	7.5272
	$+35\%$	6.0048	5.8129
n	-35%	9.832	9.8148
	$+35\%$	5.832	5.834
h	-35%	-	3.0358
	$+35\%$	-	1.4574
γ	-35%	-	0.5817
	$+35\%$	-	0.5605

The biggest advantage of this scenario lies in increasing the robustness of the controller in a special way. The S core tensor provided by the TP model transformation can be used directly in LMI-based controller design. If the model parameters are handled as scheduling parameters, the controller will be prepared for the changing of these. In other words, as the core tensor is used during controller design and the core tensor contains the parameter dependencies, the controller could be even a simple state feedback one being handled inside the complex polytope.

Naturally, the TP model form is different in this case (having four scheduling parameters):

$$\begin{aligned}&\mathbf{S}(G(t), p_1, p_2, n) = S \underset{\text{n=1}}{\overset{4}{\boxtimes}} \mathbf{w}_n(\mathbf{p}_n(t)) = \\ &S \times_1 \mathbf{w}_1(G(t)) \times_2 \mathbf{w}_2(p_1) \times_3 \mathbf{w}_3(p_2) \times_4 \mathbf{w}_4(n)\end{aligned} . \tag{4.36}$$

The MVS type weighting functions of the robustified TP models can be seen on Fig. 4.6. The main difference occurred again in the upper row: in case of T1DM, the weighting function is linear, however, in T2DM case the weighting function is nonlinear because of the fraction in (4.34). The weighting functions belong to other parameters are linear in both models.

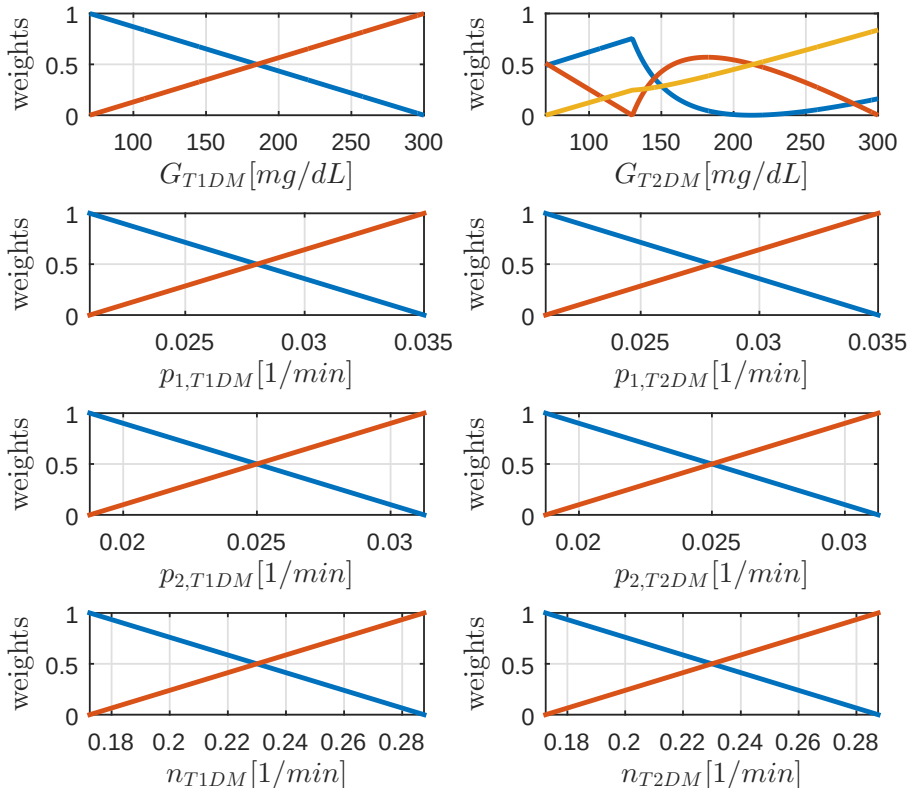

Figure 4.6.: Weighting functions of the TP polytopic model; robust model case.

4.4.3. Validation

During the validation, we investigated the discrepancy between the original nonlinear models and their TP versions via the changing of their state variable over time during simulations. For evaluation we have used again the RMSE-based method.

We have applied symmetric impulse functions during the simulations both for the CHO and insulin inputs using the following protocol:

- CHO (d) 4g over 5 min at every 50 min with $V_g = 11.2$ dL distribution volume, $Ag = 0.8$ utilization and molar weight $Mw = 180.12$ g/mol (CHO=$d \cdot Ag \cdot 1000/Mw/V_g$; here: 28.2326 mg/dL over 5 min at every 50 min);
- insulin (u) 0.5 U over 2 min at every 50 min with $V_i = 8.4$ dL distribution volume (insulin=$u \cdot 1000/V_i$; here 59.5238 $\mu U/mL$ over 2 min at every 50 min).

Conforming to the reality, the input functions have impulse nature. However, they are

unfavorable because of the higher amplitude and shorter time period occurring through real input signals. This is the reason why the above mentioned protocol was used ensuring that the TP model works under all circumstances.

Table 4.4. shows the results of the RMSE-based comparison between the state variables of the original nonlinear model and the realized TP models in the simple model case where only the $G(t)$ was the scheduling parameter. The first row describes the comparison between the original T1DM model and the TP version of it, while the second row presents the comparison between the original T2DM model and the TP version of the given model. We used high sampling density in the parameter domain. The borders of the domain were $70 - 300$ mg/dL (as it can see on the horizontal axis of Fig. 4.6).

In both cases, beside the given inputs and initial values the TP models "mimic" the original nonlinear models with high precision (only numerical errors occurred, i.e. magnitude lower than 10^{-8}). Fig. 4.7. illustrates the obtained results. Negligible difference can be observed between the original model and the TP ones.

Table 4.4.: Results of the RMSE-based investigations; simple model case. Initial values: $G_0 = 100$, $X_0 = 0$, $I_0 = 11.5$; simulation length: 150 min; Sampling density in the parameter domain: 301.

	Original model		
	G	**X**	**I**
TP_{T1DM}	2.984e-13	7.372e-17	2.22e-16
TP_{T2DM}	1.477e-8	8.566e-12	3.329e-12

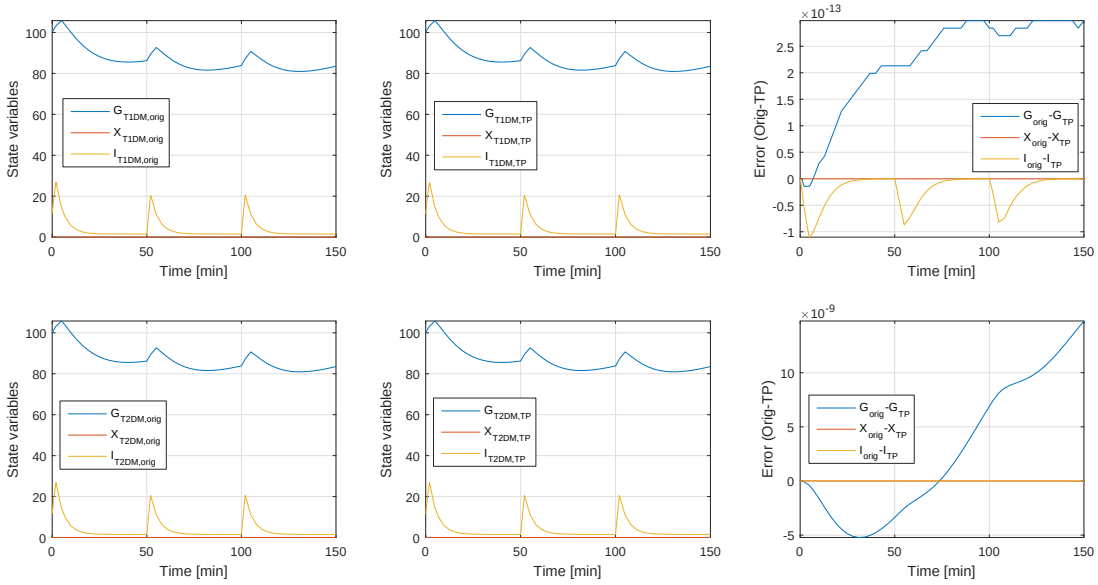

Figure 4.7.: Comparison of the original nonlinear models and the TP versions of them; simple model case. Upper row: T1DM models; Lower row: T2DM models.

Table 4.5. shows the results of the RMSE-based comparison between the state variables of the original nonlinear model and the realized TP models in robust model case (the parameter vector contains four scheduling variables $\mathbf{p}(t) = [G(t), p_1, p_2, n]^\top$). I applied again a high sampling density in the parameter domain (301 for G and 11 for p_1, p_2 and n). The borders of the domains were set again $70 - 300$ mg/dL for G, and $\pm 25\%$ of the nominal p_1,p_2 and n values (Fig. 4.6.). Similar to the previously presented case, the same inputs have been used for initial values.

With simple randomization, I investigated several parameter configurations for p_1, p_2 and n inside the parameter ranges. Three specific cases (where I have found the highest errors) are highlighted here. The given p_1, p_2 and n parameters and the belonging data can be found in Table 4.5. The comparisons have similar meanings as previously: the first row describes the RMSE between the original nonlinear T1DM model and the TP models, while the second row represents the RMSE between the original nonlinear T2DM model and the TP models. The highest errors in each case occur in the G state as a natural consequence of the nonlinear attitude of the given weighting function (see the second column in the first row on Fig. 4.6). However, we found that the error can be tolerated being lower than 1 over the $300min$ long simulation. The results in Table 4.5. are connected to the simulations of Fig. 4.8. One can see that the small deviation that

occurred did not cause significant error in the dynamics of the models. The upper row describes the state variable of the T1DM models (original nonlinear and TP version) with the occurring error in time. The lower row presents the same comparison, however, for the T2DM models. It can be seen that the error has a "saturation" and the dynamics follow the dynamics of the state variables.

Table 4.5.: Results of the RMSE-based investigations; robust model case. Initial values: $G_0 = 100$, $X_0 = 0$, $I_0 = 11.5$; simulation length: 300 min; Sampling density in the parameter domain: $G - 301$, $p_1 - 11$,$p_2 - 11$ and $p_3 - 11$.

Original model

	$p_1 = 0.0266$, $p_2 = 0.0258$, $n = 0.2231$		
	G	**X**	**I**
TP_{T1DM}	0.877	5.898e-16	0
TP_{T2DM}	0.877	1.9646e-16	2.442e-15
	$p_1 = 0.0280$, $p_2 = 0.025$, $n = 0.23$		
	G	**X**	**I**
TP_{T1DM}	1.165e-12	5.8417e-16	0
TP_{T2DM}	7.1e-13	2.688e-16	2.44e-15
	$p_1 = 0.0293$, $p_2 = 0.0248$, $n = 0.2266$		
	G	**X**	**I**
TP_{T1DM}	0.728	6.059e-16	0
TP_{T2DM}	0.728	2.923e-16	1.776e-15

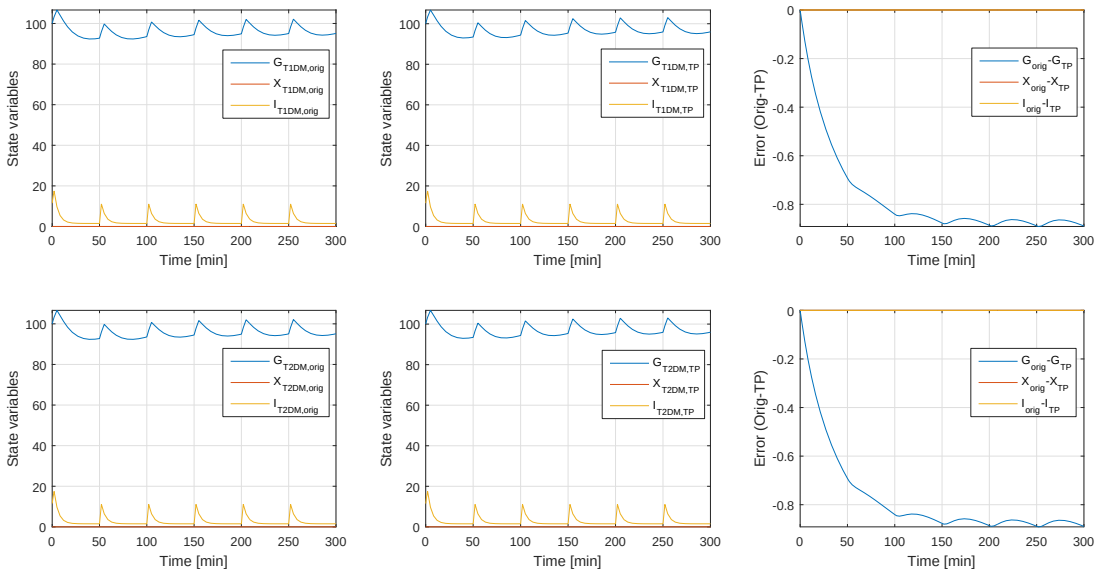

Figure 4.8.: Comparison of the original nonlinear models and the TP versions of them; robust model case. Upper row: T1DM models; Lower row: T2DM models. Parameters: $p_1 = 0.0266$, $p_2 = 0.0258$, $n = 0.2231$.

4.4.4. Summary

The Section examined the utilization of the TP model transformation for T1DM and T2DM models. I demonstrated that TP models can perfectly mimic the original nonlinear systems behavior over time beside given initial values and inputs. Moreover, I investigated the robustness of the realized TP models from parameter variation point of view. Since the TP model transformation can be easily used for LMI-based controller design, this property can be useful in guaranteeing the controller's robustness by the created robust TP model.

4.5. TP-modeling possibility for a complex T1DM model

In this Section I have used a modified version of the Hovorka-model, which is a well known and widely used higher order T1DM model originally developed by Hovorka et al in [70] and modified by Naerum in [71]. The model equations (B.3a)-(B.3j) and parameters can be found in the Appendix B.

I derived each of the possible qLPV models from the original Hovorka model, which

can serve as basis for the later investigations regarding to controller design. Since there are several possible model equilibria and the mathematical tools allow several algebraic transformations, more than one possible qLPV model exists. It should be noted that only the nonlinearity containing state equations (B.3e)-(B.3f) have more than one possible transformed form and each of the other equations has only one possible transformation.

According to the previous general considerations, the investigation of possible steady states is required first.

4.5.1. Steady state calculations

I started from this consideration: if the $Q_{1,d}$ and u_d are considered as known, each steady state value of the states can be determined by the rearrangement of the model equations. In practice, if Q_{1d} and u_d are given, the steady states (equilibria) are:

$$\begin{aligned} S_{1d} &= u_d \tau_S \\ S_{2d} &= S_{1d} \end{aligned} \quad , \tag{4.37a}$$

$$I_d = \frac{1}{\tau_S V_I k_e} S_{2d} \ , \tag{4.37b}$$

$$x_{1d} = k_{b1}/k_{a1} I_d \ , \tag{4.37c}$$

$$x_{2d} = k_{b2}/k_{a2} I_d \ , \tag{4.37d}$$

$$x_{3d} = k_{b3}/k_{a3} I_d \ , \tag{4.37e}$$

$$Q_{2d} = x_{1d} Q_{1d}/(k_{12} + x_{2d}) \ , \tag{4.37f}$$

$$\begin{aligned} D_{2d} &= (F_{01,c,d} + FR_d + x_{1d} Q_{1d} - k_{12} Q_{2d} - EGP_0(1 + x_{3d})) \\ D_{1d} &= D_{2d} \end{aligned} \quad , \tag{4.37g}$$

$$d_d = D_{1d} M_{wG}/(1000 A_G \tau_D) \ . \tag{4.37h}$$

4.5.2. qLPV Model derivation

In the following, I follow these steps: *i* – demonstration of the transformation on one state; *ii* – description of each transformed state, which only have one possible transformed form; *iii* – investigation of the "critical states".

For the algebraic transformation of (B.3a), I used the direct substitution of (B.4a) as well:

$$\begin{aligned}
&\Delta\dot{D}_1(t) = \dot{D}_1(t) - 0 = \\
&= \frac{1000A_G}{MwG}d(t) - \frac{1}{\tau_D}D_1(t) - \left[\frac{1000A_G}{MwG}\Delta d_d - \frac{1}{\tau_D}D_{1d}\right] = \\
&\frac{1000A_G}{MwG}(d(t) - d_d) - \frac{1}{\tau_D}(D_1(t) - D_{1d}) = \\
&\frac{1000A_G}{MwG}\Delta d(t) - \frac{1}{\tau_D}\Delta D_1(t)
\end{aligned} \quad . \tag{4.38}$$

I derived the resulting state variables, except Q_1 and Q_2:

$$\Delta\dot{D}_2(t) = \frac{1}{\tau_D}\Delta D_1(t) - \frac{1}{\tau_D}\Delta D_2(t) \ . \tag{4.39}$$

$$\Delta\dot{S}_1(t) = \Delta u(t) - \frac{1}{\tau_S}\Delta S_1(t) \ . \tag{4.40}$$

$$\Delta\dot{S}_2(t) = \frac{1}{\tau_S}\Delta S_1(t) - \frac{1}{\tau_S}\Delta S_2(t) \ . \tag{4.41}$$

$$\Delta\dot{I}(t) = \frac{1}{\tau_S V_I}\Delta S_2(t) - k_e\Delta I(t) \ . \tag{4.42}$$

$$\Delta\dot{x}_1(t) = -k_{a1}\Delta x_1(t) + k_{b1}\Delta I(t) \ . \tag{4.43}$$

$$\Delta\dot{x}_2(t) = -k_{a2}\Delta x_2(t) + k_{b2}\Delta I(t) \ . \tag{4.44}$$

$$\Delta\dot{x}_3(t) = -k_{a3}\Delta x_3(t) + k_{b3}\Delta I(t) \ . \tag{4.45}$$

In case of Q_1 and Q_2, more than one nonlinearity causing effects have to be considered: the multiplications of time functions and the ramp type saturations belong to $F_{01,c}$ and F_R. The two saturations can be merged into one term, if we use directly the term

$G(t) = Q_1(t)/V_G$ from (B.4b), as follows:

$$\Delta F(Q_1) = F(Q_1) - F(Q_{1,d}) = \begin{cases} 0.003\left(\dfrac{Q_1}{V_G} - 9\right)V_G & \text{if} \quad 9 \leq \dfrac{Q_1(t)}{V_G} \\ 0 & \text{if} \quad 4.5 \leq \dfrac{Q_1(t)}{V_G} < 9 \\ F_{01}\left(\dfrac{Q_1}{4.5V_G} - 1\right) & \text{if} \quad \dfrac{Q_1(t)}{V_G} < 4.5 \end{cases} . \tag{4.46}$$

Practically, $\Delta Q_1(t)$ will not be zero at any time. Hence, the limits of the saturation guarantees that the involvement of $\Delta Q_1(t)$ term into the (4.45) as a multiplication by 1 cannot causes critical singularity at any time, so:

$$\frac{\Delta F(Q_1)}{\Delta Q_1(t)}\Delta Q_1(t) = \begin{cases} \dfrac{0.003\left(\dfrac{Q_1}{V_G} - 9\right)V_G}{\Delta Q_1(t)}\Delta Q_1(t) & \text{if} \quad 9 \leq \dfrac{Q_1(t)}{V_G} \\ \dfrac{0}{\Delta Q_1(t)}\Delta Q_1(t) & \text{if} \quad 4.5 \leq \dfrac{Q_1(t)}{V_G} < 9 \\ \dfrac{F_{01}\left(\dfrac{Q_1}{4.5V_G} - 1\right)}{\Delta Q_1(t)}\Delta Q_1(t) & \text{if} \quad \dfrac{Q_1(t)}{V_G} < 4.5 \end{cases} , \tag{4.47}$$

term can be used in order to connect the saturation to the $\Delta Q_1(t)$ state, which makes the accurate mathematical transformation possible.

It should be noted that more than one possible transformed form can be derived from (B.3e) and (B.3f). However, that one is the most useful, where the parameter vector is $p = [Q_1(t), Q_2(t)]^\top$, which means that only the $Q_1(t)$ and $Q_2(t)$ states are the scheduling variables. In practice, only the blood glucose related state variables can be measured (measurement from body fluid) or estimated. Hence, in the following, we only investigate the following modified equations:

$$\begin{aligned} \Delta\dot{Q}_1(t) = {} & \frac{\Delta D_2(t)}{\tau_D V_G} - \frac{\Delta F(Q_1)}{\Delta Q_1(t)}\Delta Q_1(t) + k_{12}\Delta Q_2(t) \\ & -EGP_0\Delta x_3(t) - x_{1d}\Delta Q_1(t) - Q_1(t)\Delta x_1(t) \end{aligned} \tag{4.48a}$$

$$\begin{aligned} \Delta\dot{Q}_2(t) = {} & -k_{12}\Delta Q_2(t) + x_{1d}\Delta Q_1(t) + \\ & Q_1(t)\Delta x_1(t) - x_{2d}\Delta Q_2(t) - Q_2(t)\Delta x_2(t) \end{aligned} . \tag{4.48b}$$

Since, each modified state equation is available, the unified state space equation can be described by (4.20). The derived equations (4.38)-(4.47) and (4.48a)-(4.48b), if the state variables are $\Delta x = [\Delta D_1, \Delta D_2, \Delta Q_1, \Delta Q_2, \Delta S_1, \Delta S_2, \Delta I, \Delta x_1, \Delta x_2, \Delta x_3]^\top$:

$$\begin{pmatrix} \Delta\dot{x}(t) \\ \Delta y(t) \end{pmatrix} = \mathbf{S} \begin{pmatrix} \Delta x(t) \\ \Delta u(t) \\ \Delta d(t) \end{pmatrix} = \begin{bmatrix} \frac{-1}{\tau_D} & 0 & 0 & 0 & 0 \\ \frac{1}{\tau_D} & \frac{-1}{\tau_D} & 0 & 0 & 0 \\ 0 & \frac{1}{\tau_D V_G} & -\left(x_{1d} + \frac{\Delta F(Q_1)}{\Delta Q_1(t)}\right) & k_{12} & 0 \\ 0 & 0 & x_{1d} & -(k_{12} + x_{2d}) & 0 \\ 0 & 0 & 0 & 0 & \frac{-1}{\tau_S} \\ 0 & 0 & 0 & 0 & \frac{1}{\tau_S} \\ 0 & 0 & 0 & 0 & 0 \\ 0 & 0 & 0 & 0 & 0 \\ 0 & 0 & 0 & 0 & 0 \\ 0 & 0 & 0 & 0 & 0 \\ 0 & 0 & \frac{1}{V_G} & 0 & 0 \end{bmatrix}$$

$$\begin{bmatrix} 0 & 0 & 0 & 0 & 0 & 0 & \frac{1000 A_G}{MwG} \\ 0 & 0 & 0 & 0 & 0 & 0 & 0 \\ 0 & 0 & -Q_1(t) & 0 & -EGP_0 & 0 & 0 \\ 0 & 0 & Q_1(t) & -Q_2(t) & 0 & 0 & 0 \\ 0 & 0 & 0 & 0 & 0 & 1 & 0 \\ \frac{-1}{\tau_S} & 0 & 0 & 0 & 0 & 0 & 0 \\ \frac{1}{\tau_S V_I} & -k_e & 0 & 0 & 0 & 0 & 0 \\ 0 & k_{b1} & -k_{a1} & 0 & 0 & 0 & 0 \\ 0 & k_{b2} & 0 & -k_{a2} & 0 & 0 & 0 \\ 0 & k_{b3} & 0 & 0 & -k_{a3} & 0 & 0 \\ 0 & 0 & 0 & 0 & 0 & 0 & 0 \end{bmatrix} \begin{pmatrix} \Delta x(t) \\ \Delta u(t) \\ \Delta d(t) \end{pmatrix} \tag{4.49}$$

4.5.3. TP model form

After the derivation of the appropriate qLPV model in convenient state space form (4.49), TP model transformation can be executed on it. Broadly, the $\mathbf{p}(t)$ dependent qLPV model of 4.49 were sampled over the domains of $Q_1(t) = 34 \dots 185$ mmol and $Q_2(t) = 34 \dots 185$ mmol with 151 grid points at each dimensions. The application of the compact HOSVD algorithm [92] provided the compact $\mathbb{S}$ core tensor and the MVS-type weighting functions – which can be seen on Fig. 4.9 – were used to realize the TP model in the form of (4.7). In this way, the obtained TP model was the following:

$$\begin{aligned} \mathbf{S}(Q_1(t), Q_2(t)) &= \mathcal{S} \overset{2}{\underset{n=1}{\boxtimes}} \mathbf{w}^{(n)}(p_n) = \\ &= \mathcal{S} \times_1 \mathbf{w}_1(Q_1(t)) \times_2 \mathbf{w}_2(Q_2(t)) \end{aligned} . \tag{4.50}$$

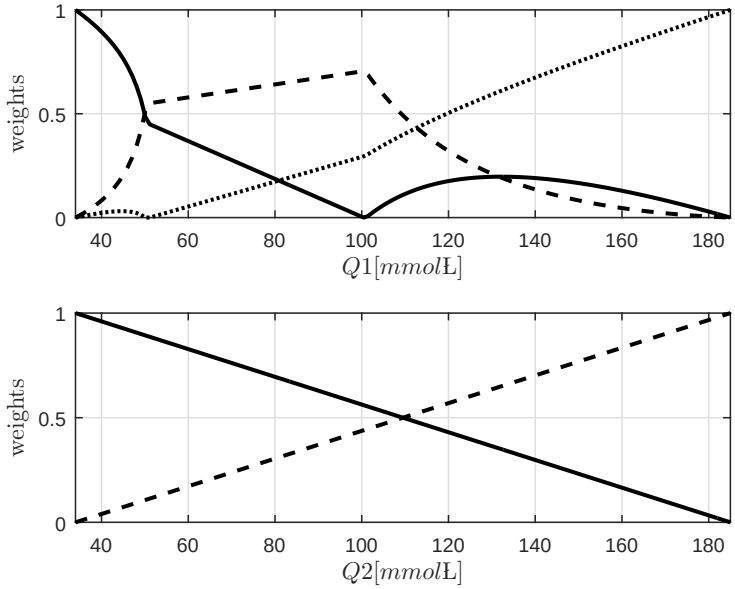

Figure 4.9.: Weighting functions regarding the Hovorka TP model

4.5.4. Validation

I compared the "performance" of the new TP model to the original nonlinear model. The applied CHO and insulin intakes were dense impulse functions. The physiological validity of these are not relevant at this point since I aimed as worse (impulse kind and with high frequency) external excitations as possible to demonstrate that the realized TP model can approximate the original model even under these circumstances. This

comparison is based on simple subtractions, namely, we subtracted each TP state from the corresponding original state. Since my goal was to realize such a TP model which can appropriately mimic the original model, the results are satisfying.

The simple error based comparison can be seen on Fig. 4.10. On the figure, each block represents the subtraction of the time vectors or the corresponding states, except the last two, which are the external CHO and insulin excitations. As it can be seen, the $e_{Q1}(t)$ and $e_{Q2}(t)$ produces the highest errors, however, the order of this error is around 10^{-4}. In other cases, only numerical error occurred. The reason for these "higher" errors are the saturation, the high nonlinearities and the multiple coupling between the states. Base on the results it can be stated that the TP model is able to approximate the original nonlinear model with very low approximation error – despite the applied high external excitation signals.

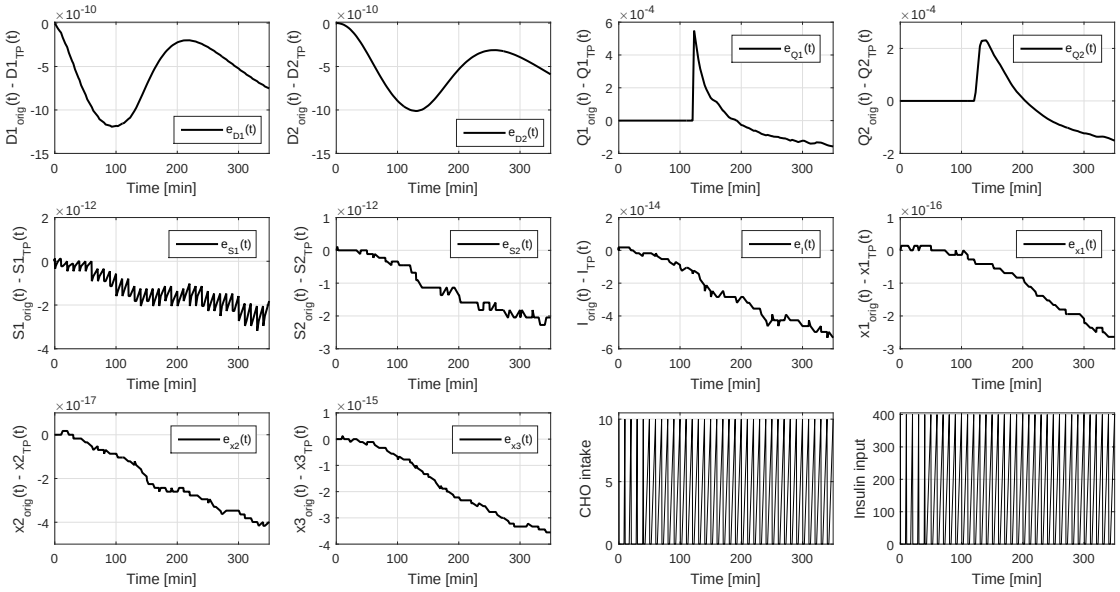

Figure 4.10.: Validation of the TP model

4.5.5. Summary

The Section summarized the realization of a TP kind convex polytopic T1DM model via the utilization of the recently developed TP model transformation tool. The main considered steps were the transformation of the original nonlinear complex Hovorka model into a control oriented, deviation based qLPV model. The main challenges were the handling of the nonlinearity causing parts of the "core patient submodel" of the selected Hovorka model. This part is loaded with unfavorable saturations, coupled states

and other nonlinearities. However, more than one mathematically precise qLPV model can be derived from the original model, and we developed such a model, where the scheduling parameters (the elements of the parameter vector of the qLPV model) were the blood glucose related state variables, since only these can be measured or estimated in real life. The TP model transformation was executed on this specific qLPV model. The resulting TP model were compared with the original numerical model. In most of the states only numerical errors appeared. However, the "core patient model" part contains higher error, which refers rougher approximation. Nevertheless, the order of these errors is 10^{-4}. Hence, the developed TP model appropriately mimics the original model.

Thesis Group 3

Thesis group 3: Usability of the TP model transformation for DM

Thesis 3.1
I have realized a TP-based ICU model with small approximation error. I proved that in case of the given nonlinear ICU model better approximation error can be reached, if the operating equilibrium of glycemia (G_d) of the model was not equal to the model equilibrium of glycemia (G_E).

Thesis 3.2
I have investigated the robustization possibility of the blood glucose Minimal Model via TP framework. I have realized robust T1DM and T2DM TP-models, robust from parameter variation point of view. Regarding the LMI-based controller design, this property can be useful in guaranteeing the controller's robustness by the created robust TP models.

Thesis 3.3
I have proven the usability of TP-model transformation in case of highly complex T1DM model. I have demonstrated that several control oriented qLPV models can be derived from the original model approximating it with high accuracy.

Relevant own publications pertaining to this thesis group: [114, 115, 116].

5. Conclusion

This dissertation presented three control engineering solutions which can be applied in case of physiological controls. Each of them can be divided smaller developments which are strengthen by case studies.

The first thesis group investigated the usability of RFPT theorems in conjunction with T1DM control. I have examined three cases, which were different from the applied T1DM model, absorption submodel point of view, however, I used almost the same control strategies in each cases, namely, PID-kind control laws in the control block. I followed the general RFPT controller design steps, what I summarized at the beginning of the given chapter. The results showed that the RFPT-based controllers can be used in case of T1DM models with low and high complexity beside unfavorable disturbances (glucose loads). The developed controller were able to keep the BG level in the normal glycemic range; totally avoid hypoglycemia; however, short hyperglycemic periods occurred during the simulations. With this research I have proven that the RFPT-based controller design method can be used for controller design in case of T1DM models with high nonlinearities.

Although, the reached results were appropriate, I have found several opportunities for further improvements which are beyond this research. First, the velocity of convergence of the Cauchy-series – which is the key point of the RFPT method – depends on the measurements update. The currently used technology is capable to provide BG measurements at every 5 min, which makes the convergence slower and through the reaching of the desired BG levels become later. This can be faster, if an interim Kalman estimator or equivalent is used and the measurements can be completed by estimation. Since the estimation horizon is small (5 min) precise estimations can be done and via the convergence can be faster. Investigation of usability of pure input-output models based on real measurements can be done, as well. In this work, I have used the model equations to realize approximating inverse models. However, I used rough approximations this can be the next step, since the patient data reflects the glucose-insulin dynamics of the patient and more robust solutions can be reached by using this fact.

The second thesis group introduces a two novel achievements in the field of LPV-based control. I have developed a norm based tool in which the norm (2-norm) is defined on

the abstract parameter space of LPV systems and can be used as a metric between LTI systems. This tool can be used as error or difference metric and via quality requirements can be defined with it. The second achievement can be divided into two parts: I have developed a novel LPV completed controller scheme which can be used for control of LPV (and trough nonlinear) systems with given properties; moreover, I have developed a completed LPV controller-observer scheme in order to control given LPV systems. The novel controller design tools are a mixture of linear state-feedback theorem and the matrix similarity theorems. I have proven the usability of the methods via nonlinear physiological examples including DM control. I provided deep analysis of the methods.

This novel development has several further improvement possibilities. The first is the generalization - in order to use it in case of arbitrary nonlinear systems further research is needed. Moreover, it should be investigated how can be decreased the conservatism regarding the structures of the input/output matrices, which is currently a strict restriction. Furthermore, an interesting question can be the extension of the method for those cases, where the elements of the parameter vector cannot be directly measured and the only possibility is the model-based estimation. The examination of these questions are beyond this dissertation.

The third thesis group investigates the TP modeling possibilities of different DM models – due to I want to use the developed TP models as subjects for TP-based controller design in the future. The first step of this direction was made during my research, namely, I have introduced control oriented LPV models via mathematical transformation from the existing DM models and I successfully developed the TP model form of them. I showed three possible direction during this part: it is possible to use TP model transformation and realize TP model in case of simple ICU kind DM model with high nonlinearities; it is possible to use TP model transformation and realize TP model in case of highly complex T1DM model with high nonlinearities and coupling; and I showed that how is it possible to increase the robustness of the TP model (from parameter point of view).

Further step regarding this thesis will be the usage of the developed TP models for TP-based controller design. Moreover, I would like to investigate the opportunity of robustization possibilities not just from model but controller design point of views, as well.

Bibliography

References

[1] J.D. Bronzino and D.R. Peterson, eds. *The Biomedical Engineering Handbook*. 4th. Boca Raton, USA: CRC Press, 2015.

[2] L.A. Segel and L. Edelstein-Keshet. *A Primer on Mathematical Models in Biology*. 1st. Philadelphia, USA: Society for Industrial and Applied Mathematics, 2013.

[3] International Diabetes Federation. *IDF Diabetes Atlas*. 7th. London, United Kongdom: International Diabetes Federation, 2015.

[4] World Health Organization. *Global Report on Diabetes*. Geneva, Switzerland: WHO Press, 2016.

[5] A. Fonyó and E. Ligeti. *Physiology (in Hungarian)*. 3rd. Budapest, Hungary: Medicina, 2008.

[6] V. Adam. *Medical Biochemistry (in Hungarian)*. 4th. Budapest, Hungary: Medicina Press, 2006.

[7] R. Bilous and R. Donnelly. *Handbook of Diabetes*. 4th. Chichester, UK: Wiley-Blackwell, 2010.

[8] S.A. Billings. *Nonlinear System Identification*. 1st. Chichester, UK: John Wiley & Sons, 2013.

[9] M. Pisano. "Overview of Insulin and Non-Insulin Delivery Devices In the Treatment of Diabetes". In: *Pharmacy and Therapeutics* 39.12 (2014), pp. 866–873.

[10] J.L. Selam. "Evolution of Diabetes Insulin Delivery Devices". In: *J Diabetes Sci Technol* 4.3 (2010), pp. 505–513.

[11] D.M. Maahs, L.A. Horton, and H.P. Chase. "The Use of Insulin Pumps in Youth with Type 1 Diabetes". In: *Diabetes Technol Ther* Suppl1 (2010), S59–S65.

[12] Y. Reznik and O. Cohen. "Insulin Pump for Type 2 Diabetes". In: *Diabetes Care* 36.Suppl2 (2013), S219–S225.

[13] B.H. McAdams and A. Ali. “An Overview of Insulin Pumps and Glucose Sensors for the Generalist”. In: *J Clin Med* 5.1 (2016), p. 5.

[15] F. Chee and T. Fernando. *Closed-Loop Control of Blood Glucose*. Heidelberg, Germany: Springer, 2007.

[16] C. Cobelli, E. Renard, and B. Kovatchev. “Artificial Pancreas: Past, present and future”. In: *Diabetes* 60.11 (2011), pp. 2672–2682.

[17] V.N. Shah, A. Shoskes, B. Tawfik, and S.K. Garg. “Closed-Loop System in the Management of Diabetes: Past, Present, and Future”. In: *Diabetes Technol The* 16.8 (2014), pp. 477–490.

[18] S. Trevitt, S. Simpson, and A. Wood. “Artificial Pancreas Device Systems for the Closed-Loop Control of Type 1 Diabetes: What Systems Are in Development?” In: *J Diabetes Sci Technol* Preprint version, 2015 (2015), pp. 1–10.

[19] T. Peyser, E. Dassau, and J.S. Skyler. “The artificial pancreas: current status and future prospects in the management of diabetes”. In: *Ann N Y Acad Sci* 1311 (2014), pp. 102–123.

[20] F.J. Doyle, L.M. Huyett, J.B. Lee, H.C. Zisser, and E. Dassau. “Closed-Loop Artificial Pancreas Systems: Engineering the Algorithms”. In: *Diab Care* 37.5 (2014), pp. 1191–1197.

[24] H. Thabit and R. Hovorka. “Coming of age: the artificial pancreas for type 1 diabetes”. In: *Diabetologia* 59.9 (2016), pp. 1795–1805.

[25] S. Kamath. “Model based simulation for Type 1 Diabetes Patients”. In: *Asian Am J Chem* 1.1 (2013), pp. 11–19.

[26] G. Marchetti, M. Barolo, L. Jovanovic, H. Zisser, and D.E. Seborg. “An Improved PID Switching Control Strategy for Type 1 Diabetes”. In: *IEEE T Bio-Mde Eng* 55 (3 2004), pp. 857–865.

[27] Y. Ramprasad, G.P. Rangaiah, and S. Lakshminarayanan. “Robust PID Controller for Blood Glucose Regulation in Type I Diabetics”. In: *Ind Eng Chem Res* 43 (26 2004), pp. 8257–8268.

[28] C. Ionescu, Y. Zhou, and J.A.T. Machado. “Special Issue: Advances in Fractional Dynamics and Control”. In: *J Vib Control* 22.8 (2016), pp. 1969–1971.

[29] M. Goharimanesh, A. Lashkaripour, and A. Abouei Mehrizi. “Fractional Order PID Controller for Diabetes Patients”. In: *J Comp Appl Mech* 46.1 (2015), pp. 69–76.

[30] C. E. Garcia, D. M. Prett, and M. Morari. “Model Predictive Control: Theory and Practice&Mdash;a Survey”. In: *Automatica* 25.3 (1989), pp. 335–348.

[31] M. Morari and J.H. Lee. “Model Predictive Control: Past, Present and Future”. In: *Comp Chem Eng* 23 (1997), pp. 667–682.

[32] J.H. Lee. “Model predictive control: Review of the three decades of development”. In: *International Journal of Control, Automation and Systems* 9.3 (2011), p. 415.

[33] M. E. Villanueva, R. Quirynen, M. Diehl, B. Chachuat, and B. Houska. “Robust MPC via min-max differential inequalities”. In: *Automatica* 77 (Mar. 2017), pp. 311–321.

[34] A. Gentilini, C. Frei, A.H. Glattfelder, M. Morari, T.J. Sieber, R. Wymann, T. Schnider, and A.M. Zbinden. *Closed loop control in Anesthesia*. Tech. rep. July 2000.

[35] N. Cardoso and J. M. Lemos. “Model Predictive control of Depth of Anaesthesia: Guidelines for controller configuration”. In: *2008 30th Annual International Conference of the IEEE Engineering in Medicine and Biology Society*. (Vancouver, Aug. 20–25, 2008). Vancouver, BC, Canada: ACM, 2008, pp. 5822–5825.

[36] I. Nascu, A. Krieger, C.M. Ionescu, and E.N. Pistikopoulos. “Advanced model-based control studies for the induction and maintenance of intravenous anaesthesia”. In: *IEEE Tran Biomed Eng* 62.3 (2015), pp. 832–841.

[37] P. Maxime, H. Gueguen, and A. Belmiloudi. “A Robust Receding Horizon Control Approach to Artificial Glucose Control for Type 1 Diabetes”. In: *Nonlin Contr Sys* 9.1 (2013), pp. 833–838.

[38] G. Schlotthauer, L.G. Gamero, M.E. Torres, and G.A. Nicolini. “Modeling, identification and nonlinear model predictive control of type I diabetic patient”. In: *Med Eng Phys* 28 (3 2006), pp. 240–250.

[39] H. Kirchsteiger and L. del Re. “Nonlinear model predictive control with moving horizon state and disturbance estimation - Application to the normalization of blood glucose in the critically ill”. In: *Proceedings of the 17th World Congress The International Federation of Automatic Control*. (Seoul, Korea, July 6–11, 2013). Seoul: IFAC, 2013, pp. 9069–9074.

[40] R. Hovorka, V. Canonico, L.J. Chassin, U. Haueter, M. Massi-Benedetti, M. Orsini-Federici, T.R. Pieber, H.C. Schaller, L. Schaupp, T. Vering, and Wilinska M.E. “Nonlinear model predictive control of glucose concentration in subjects with type 1 diabetes”. In: *Physiol Meas* 25.4 (2004), pp. 905–920.

[41] Y. Ho, B.P. Nguyen, and C-K. Chui. “Ant Colony Optimization for Model Predictive Control for Blood Glucose Regulation”. In: *Proceedings of the Third Symposium on Information and Communication Technology*. (Ha Long). SoICT ’12. Ha Long, Vietnam: ACM, 2012, pp. 214–217.

[42] C-K. Chui, B.P. Nguyen, Y. Ho, Z. Wu, M. Nguyen, G-S. Hong, D. Mok, S. Sun, and S. Chang. “Embedded Real-Time Model Predictive Control for Glucose Regulation”. In: *World Congress on Medical Physics and Biomedical Engineering May 26-31, 2012, Beijing, China*. Ed. by M. Long. Berlin, Heidelberg: Springer Berlin Heidelberg, 2013, pp. 1437–1440.

[43] E. Atlas, R. Nimri, S. Miller, E.A. Grunberg, and M. Phillip. “MD-Logic Anrtificial Pancreas System. A pilot study in adults with type 1 diabetes”. In: *Diab Care* 33 (2010), pp. 1072–1076.

[44] P. Herrero, P. Georgiou, N. Oliver, D.G. Johnston, and C. Toumazou. “A Bio-Inspired Glucose Controller Based on Pancreatic β-Cell Physiology”. In: *J Diabetes Scien Technol* 6.3 (2012), pp. 606–616.

[45] K.G. Osgouie and A. Azizi. “Optimizing fuzzy logic controller for diabetes type I by genetic algorithm”. In: *2010 The 2nd International Conference on Computer and Automation Engineering (ICCAE)*. (Singapore, Singapore, Feb. 26–28, 2010). Singapore: ICCAE, 2010, pp. 4–8.

[46] L. Kovács, P. Szalay, Zs. AlmKovácsssy, and L. Barkai. “Applicability Results of a Nonlinear Model-Based Robust Blood Glucose Control Algorithm”. In: *J Diabetes Scien Technol* 7.3 (2013), pp. 708–716.

[47] L. Kovács, P. Szalay, B. Benyó, and G.J. Chase. “Applicability Results of a Nonlinear Model-Based Robust Blood Glucose Control Algorithm”. In: *IFAC WC - 18th World Congress of the International Federation of Automatic Control*. (Milano, Italy, Aug. 29–Sept. 2, 2011). Milano: 2011, pp. 4995–5000.

[48] L. Kovács, B. Benyó, J. Bokor, and Z. Benyó. “Induced L_2-norm Minimization of Glucose-Insulin System for Type I Diabetic Patients”. In: *Comp Meth Prog Biomed* 102.2 (2011), pp. 105–118.

[51] P. Latafat, P. Palumbo, P. Pepe, L. Kovács, S. Panunzi, and A. De Gaetano. “An LMI-based Controller for the Glucose-Insulin System”. In: *2015 European Control Conference (ECC)*. (Linz, Austria, July 15–17, 2015). Linz: IFAC, 2015, pp. 7–12.

[52] V. Bátora, M. Tŕnik, J. Murgas, S. Schmidt, K. Nogaard, N.K. Poulsen, H. Madsen, and J.B. Jorgensen. “Bihormonal Control of Blood Glucose in People with Type 1 Diabetes”. In: *2015 European Control Conference (ECC)*. (Linz, Austria, July 15–17, 2015). Linz: IFAC, 2015, pp. 25–30.

[53] V. Gingras, R. Rabasa-Lhoret, V. Messier, M. Ladouceur, L. Legault, and A. Haidar. “Efficacy of dual-hormone artificial pancreas to alleviate the carbohydrate-counting burden of type 1 diabetes: A randomized crossover trial”. In: *Diabetes Metab* (2015), p. 3636.

[54] A.M. Lyapunov. “A General Task About the Stability of Motion (in Russian)”. PhD thesis. Kharokov, Russia: University of Kharkov, 1892.

[55] A.M. Lyapunov. *Stability of Motion*. New York, USA: Academic Press, 1966.

[56] B. Lantos. *Theory and design of control systems [in Hungarian]*. 2nd. Budapest, Hungary: Akademia Press, 2005.

[57] T. Várkonyi. “New adaptive methods for Robust Fixed Point Transformations-based control of nonlinear systems”. PhD thesis. Budapest, Hungary: Applied Informatics Doctoral School, Óbuda University, 2013.

[58] J.Y. Tjalling. “Historical development of the Newton-Raphson method”. In: *SIAM Review* 37.4 (1995), pp. 531–551.

[59] C.T. Kelley. *Solving Nonlinear Equations with Newton’s Method, no 1 in Fundamentals of Algorithms*. SIAM, 2003.

[60] P. Deuflhard. *Newton Methods for Nonlinear Problems. Affine Invariance and Adaptive Algorithms, Springer Series in Computational Mathematics, Vol. 35*. Berlin, Germany: Springer, 2004.

[61] M. Abedini, M.A. Nojoumian, H. Salarieh, and A. Meghdari. “Model reference adaptive control in fractional order systems using discrete-time approximation methods”. In: *Commun Nonlinear Sci* 25 (1-3 2015), pp. 27–40.

[62] Q. Shen and T. Zhang. “A novel adaptive synchronization control of a class of master–slave large-scale systems with unknown channel time-delay”. In: *Commun Nonlinear Sci* 22 (1-3 2015), pp. 83–91.

[63] S. Banach. “Sur les opérations dans les ensembles abstraits et leur application aux équations intégrales (About the Operations in the Abstract Sets and Their Application to Integral Equations)”. In: *Fund Math* 3 (1922), pp. 133–181.

[64] J.K. Tar, L. Nádai, and I.J. Rudas. *System and Control Theory with Especial Emphasis on Nonlinear Systems*. 1st. Budapest, Hungary: Typotex, 2012.

[65] J.K. Tar, J.F. Bitó, L. Nádai, and J.A.T. Machado. “Robust Fixed Point Transformations in Adaptive Control Using Local Basin of Attraction”. In: *ACTA Pol Hung* 6.1 (2009), pp. 21–37.

[66] D. Kondepudi and I. Prigogine. *Modern Thermodynamics: From Heat Engines to Dissipative Structures*. 2nd. Chichester, UK: John Wiley & Sons, 2014.

[67] P. Palumbo, S. Ditlevsen, A. Bertuzzi, and A. de Gaetano. “Mathematical modeling of the glucose-insulin system A review”. In: *Math Biosci* 244.2 (2013), pp. 69–81.

[68] K.P. Sucher, M. Nelms, S. Long-Roth, and K. Lacey. *Nutrition Therapy and Pathophysiology*. Cengage Learning, 2011.

[69] L. Magni, D.M. Raimondo, C. Dalla Man, M. Breton, S. Patek, G. De Nicolao, C. Cobelli, and B.P. Kovatchev. “Evaluating the Efficacy of Closed-Loop Glucose Regulation via Control-Variability Grid Analysis”. In: *J Diab Scien Techn* 2.4 (2008), pp. 630–635.

[70] R. Hovorka, F. Shojaee-Moradie, P.V Carroll, L.J Chassin, I.J Gowrie, N.C Jackson, R.S Tudor, M. Umpleby, and D.H Jones. “Partitioning glucose distribution/transport, disposal, and endogenous production during IVGTT”. In: *Am J Physiol Endocrinol Metab* 282.5 (2002), E992–1007.

[71] M. Naerum. *Model Predictive Control for Insulin Administration in People with Type 1 Diabetes*. Tech. rep. Technical University of Denmark, 2010.

[76] J.W. Haefner. *Modeling biological systems: Principles and applications*. 2nd. New York: Springer, 2005.

[77] B. Hannon and M. Ruth. *Modeling Dynamic Biological Systems*. 2nd ed. Modeling Dynamic Systems. New York: Springer International Publishing, 2014.

[78] J. Sájevicsé Sápi. “Controller-managed automated therapy and tumor growth model identification in the case of antiangiogenic therapy for most effective, individualized treatment”. PhD thesis. Budapest, Hungary: Applied Informatics and Applied Mathemathics Doctoral School, Óbuda University, 2015.

[79] L. Kovács, P. Szalay, Zs. Almássy, and L. Barkai. “Applicability Results of a Nonlinear Model-Based Robust Blood Glucose Control Algorithm”. In: *J Diabetes Scien Technol* 7.3 (2013), pp. 708–716.

[80] W.S. Levine. *The Control Engineering Handbook*. 2nd. Boca Raton: CRC Press, Taylor and Francis Group, 2011.

[81] O. Sename, P. Gáspár, and J. Bokor. “Robust Control and Linear Parameter Varying Approaches, Application to Vehicle Dynamics”. In: vol. 437. Lecture Notes in Control and Information Sciences. Berlin: Springer-Verlag, 2013.

[82] A.P. White, G. Zhu, and J. Choi. *Linear Parameter Varying Control for Engineering Applicaitons*. 1st. London: Springer, 2013.

[83] C. Scherer and S. Weiland. *Lecture Notes DISC Course on Linear Matrix Inequalities in Control*. 2nd. Delft University, The Netherlands: Delft University, 1999.

[84] S. Boyd, L. El Ghaoui, E. Feron, and V. Balakrishnan. *Linear Matrix Inequalities in System and Control Theory*. 1st. SIAM Studies in Applied Mathematics. Philadelphia: SIAM, 1994.

[85] X.W. Wong, J.G. Chase, G.M. Shaw, C.E. Hann, J. Lin, and T. Lotz. “Comparison of adaptive and sliding-scale glycaemic control in critical care and the impact of nutritional inputs”. In: *12th International Conference On Biomedical Engineering*. (Singapore,Singapore, Dec. 7–10, 2005). Singapore: 2005, pp. 1–4.

[86] X.W. Wong, J.G. Chase, G.M. Shaw, C.E. Hanna, T. Lotz, J. Lin, I. Singh-Levett, L.J. Hollingsworth, and O.S.W. Wong. “Model predictive glycaemic regulation in critical illness using insulin and nutrition input: A pilot study”. In: *Med Eng Phys* 28 (2006), pp. 665–681.

[87] L. Kovács, A. György, B. Kulcsar, P. Szalay, B. Benyó, and Z. Benyó. “Robust control of type 1 diabetes using μ-synthesis”. In: *UKACC International Conference on Control 2010*. (Coventry, UK, Sept. 7–10, 2010). Coventry: 2010, pp. 1–6.

[88] R.S. Burns. *Advanced Control Engineering*. 1st. Oxford, UK: Butterworth – Heinemann, 2001.

[89] D.J. Leith and W.E. Leithead. “Survey of Gain-Scheduling Analysis Design”. In: *International Journal of Control* 73 (1999), pp. 1001–1025.

[90] D.W. Gu, P.H. Petkov, and M.M. Konstantinov. *Robust Control Design with Matlab*. 2nd. London: Springer, 2013.

[92] P. Baranyi, Y. Yam, and P. Várlaki. *Tensor Product Model Transformation in Polytopic Model-Based Control*. 1st. Series: Automation and Control Engineering. Boca Raton, USA: CRC Press, 2013.

[93] J. Kuti, P. Galambos, and P. Baranyi. “Minimal volume simplex (MVS) convex hull generation and manipulation methodology for TP model transformation”. In: *Asian J Control* (2015). submitted.

[94] F. Wettl. *Linear Algebra [in Hungarian]*. 1nd. Budapest, Hungary: Budapest University of Technology and Economy, Faculty of Natural Sciences, 2011.

[95] R.A. Beezer. *A First Course in Linear Algebra*. Version 3.40. Washington, USA: Congruent Press, 2014.

[96] K. Tanaka and H.O. Wang. *Fuzzy Control Systems Design and Analysis: A Linear Matrix Inequality Approach*. 1st. Chichester, UK: John Wiley and Sons, 2001.

[97] J.K. Tar, L. Nádai, I. Felde, and I.J. Rudas. In: *Advances in Robot Design and Intelligent Control: Proceedings of the 24th International Conference on Robotics in Alpe-Adria-Danube Region (RAAD)*. Ed. by T. Borangiu. Springer International Publishing, 2016. Chap. Cost Function-Free Optimization in Inverse Kinematics of Open Kinematic Chains, pp. 137–145.

[98] L. Kovács, B. Benyó, J. Bokor, and Z. Benyó. "Induced L_2-norm minimization of glucose–insulin system for Type I diabetic patients". In: *Comput Meth Prog Bio* 102.2 (2011), pp. 105–118.

[99] MATLAB. *Control System Toolbox Getting Started Guide*. English. Version Version 2016a. The MathWorks, Inc. 196 pp. March 2016.

[100] M.S. Grewal and A.P. Andrews. *Kalman Filtering: Theory and Practice Using MATLAB*. 3rd. Chichester, UK: John Wiley and Sons, 2008.

[101] J. Hartikainen, A. Solin, and S. Särkkä. *Optimal Filtering with Kalman Filters and Smoothers a Manual for the Matlab toolbox EKF/UKF*. English. Version Version 1.3. Aalto University. 2011. 131 pp. August 16, 2011.

[106] P. Baranyi, D. Tikk, Y. Yam, and R. Patton. "TP model transformation as a way to LMI-based controller design". In: *Comput Ind* 51.3 (2003), pp. 281–297.

[107] P. Baranyi. "TP model transformation as a way to LMI-based controller design". In: *IEEE T Ind Electron* 51.2 (2004), pp. 387–400.

[108] P. Galambos and P. Baranyi. "TP Model Transformation: A Systematic Modelling Framework to handle Internal Time Delays in Control Systems". In: *Asian J Control* 17.2 (2015), pp. 1–11.

[109] J. Kuti, P. Galambos, and P. Baranyi. "Minimal Volume Simplex (MVS) approach for convex hull generation in TP Model Transformation". In: *2014 18th International Conference on Intelligent Engineering Systems (INES 2014)*. (Tihany, Hungary). IEEE Hungary Section, 2014, pp. 187–192.

[110] P. Galambos, J. Kuti, P. Baranyi, G. Szögi, and I.J Rudas. “Tensor Product based Convex Polytopic Modeling of Nonlinear Insulin-Glucose Dynamics”. In: *Proceedings of the 2015 IEEE International Conference on Systems, Man, and Cybernetics*. (Hong Kong, China, Oct. 9–12, 2015). IEEE SMC, 2015, pp. 2597–2602.

[111] B. Takarics and P. Baranyi. “TP Model-based Robust Stabilization of the 3 Degrees-of-Freedom Aeroelastic Wing Section”. In: *ACTA Polytech Hung* 12.1 (2015), pp. 209–228.

[112] B. Takarics and P. Baranyi. “Friction Compensation in TP Model Form - Aeroelastic Wing as an Example System”. In: *ACTA Polytech Hung* 12.4 (2015), pp. 127–145.

[113] MTA SZTAKI. *TPtool - Tensor Product MATLAB Toolbox*. 2016. URL: http://tptool.sztaki.hu (visited on 03/01/2016).

[132] R.N. Bergman and J. Urquhart. “The pilot gland approach to the study of insulin secretory dynamics”. In: *Recent Prog Horm Res* 27 (1971), pp. 583–605.

[133] R.N. Bergman, L.S. Phillips, and C. Cobelli. “Physiological evaluation of factors controlling glucose tolerance in man”. In: *J Clin Invest* 68 (1981), pp. 1456–1467.

[134] L. Magni, D.M. Raimondo, C. Dalla Man, G. De Nicolao, B. Kovatchev, and C. Cobelli. “Model Predictive Control of glucose concentration in subjects with type 1 diabetes: an in silico trial”. In: *Proceedings of the 17th World Congress The International Federation of Automatic Control*. (Seoul, Korea, July 6–11, 2008). Ed. by M.J Chung and P Misra. International Federation of Automatic Control, 2008, pp. 4246–4251.

[135] C. Dalla Man, R.A. Rizza, and C. Cobelli. “Mixed Meal Simulation Model of Glucose-Insulin System”. In: *Proceedings of the 28th IEEE EMBS Annual International Conference*. (New York City, USA, Aug. 30–Sept. 3, 2006). IEEE EMBS, 2006, pp. 307–310.

[136] C. Dalla Man, G. Toffolo, R. Basu, R.A. Rizza, and C. Cobelli. “A Model of Glucose Production During a Meal”. In: *Proceedings of the 28th IEEE EMBS Annual International Conference*. (New York City, USA, Aug. 30–Sept. 3, 2006). IEEE EMBS, 2006, pp. 5647–5652.

[137] C. Dalla Man, F. Micheletto, D. Lv, M. Breton, B. Kovatchev, and C. Cobelli. “The UVA/PADOVA Type 1 Diabetes Simulator: New Features.” In: *J Diab Scien Techn* 8.8 (2014), pp. 26–34.

[138] Ferrier D.R. *Biochemistry*. 6th. Amsterdam, The Netherlands: Lippincott Williams and Wilkins, 2014.

[144] W.F. Boron and E.L. Boulpaep. *Medical Physiology*. 3rd. Heidelberg, Germany: Elsevier, 2016.

[146] B. Hellman, E. Gylfe, E. Grapengiesser, H. Dansk, and A. Salehi. "Insulin oscillations – clinically important rhythm. Antidiabetics should increase the pulsative component of the insulin release". In: *Lakartidningen* 104 (2007), pp. 32–33.

[147] B. Hellman. "Pulsatility of insulin release - a clinically important phenomenon". In: *Upsala J Med Sci* 114.4 (2009), pp. 193–205.

[149] F.G. Banting, C.H. Best, J.B. Collip, W.R. Campbell, and A.A. Fletcher. "Pancreatic extracts in the treatment of diabetes mellitus". In: *Can Med Assoc J* 12.3 (1922), pp. 141–146.

[150] A.M. Ahmed. "History of diabetes mellitus". In: *Saudi Med J* 23.4 (2002), pp. 373–378.

[156] B. Takarics and P. Baranyi. "TP Model-based Robust Stabilization of the 3 Degrees-of-Freedom Aeroelastic Wing Section". In: *ACTA Polytech Hung* 12.1 (2015), pp. 209–228.

[157] B. Takarics and P. Baranyi. "Friction Compensation in TP Model Form - Aeroelastic Wing as an Example System". In: *ACTA Polytech Hung* 12.4 (2015), pp. 127–145.

[158] F.A. Möbius. *The Barycentric Calculus (in German)*. 1st. Leipzig: Verlag von Johann Ambrosius Barth, 1827.

[159] J. Fauvel, F. Raymond, and R. Wilson, eds. *Möbius and his Band*. 1st. Oxford: Oxford University Press, 1993.

[160] J. Warren, S. Schaefer, A.N. Hirani, and M. Desbrun. "Barycentric coordinates for convex sets". In: *Advances in Computational Mathematics* 27 (2007), pp. 319–338.

Online sources

[14] G. Scheiner. *Product Guide - Insulin Pumps*. 2016. URL: http://www.diabetesforecast.org/2016/mar-apr/product-guide-insulin-pumps.html (visited on 08/08/2016).

[23] S. Glynn. *Artificial Pancreas Set To Transform Treatment Of Diabetes*. 2016. URL: http://www.medicalnewstoday.com/articles/262354.php (visited on 08/08/2016).

[139] dream10f. *Digestion of glucose*. 2016. URL: http://www.slideshare.net/dream10f/4-digestion-pdf (visited on 08/14/2016).

[140] Austin Community College. *Glucose Regulation*. 2016. URL: http://www.austincc.edu/apreview/EmphasisItems/Glucose_regulation.html (visited on 08/14/2016).

[141] Darekk2. *Stoichiometry of aerobic respiration and most known fermentation types in eucaryotic cell*. 2016. URL: https://en.wikipedia.org/wiki/Cellular_respiration#/media/File:Cellular_respiration.gif (visited on 08/15/2016).

[142] Narayanese. *Cytric Acid Cycle*. 2008. URL: https://commons.wikimedia.org/wiki/File:Citric_acid_cycle_with_aconitate_2.svg (visited on 08/15/2016).

[143] Benjamin Cummings. *Regulation of the utilization of glucose*. 2001. URL: http://weightlossfrogs.blogspot.hu/2010/11/glucose-glucagon-and-insulin.html (visited on 08/15/2016).

[145] Stephanie Schaefer. *Insulin secreation mechanism*. 2011. URL: http://stephanieschaefer.ca%20/2011/03/longtime-mystery-solved-the-mechanism-of-insulin-secretion/ (visited on 08/15/2016).

[148] M. Häggström. *Insulin oscillations, Medical gallery of Mikael Häggström 2014*. 2014. URL: https://en.wikiversity.org/wiki/Wikiversity_Journal_of_Medicine/Medical_gallery_of_Mikael_H%C3%A4ggstr%C3%B6m_2014#/media/File:Insulin_oscillations.svg (visited on 08/19/2016).

[151] Diabetes Health Center. *Types of Insulin for Diabetes Treatment*. 2016. URL: http://www.webmd.com/diabetes/guide/diabetes-types-insulin (visited on 08/19/2016).

[152] XcepticZP. *Insulin oscillations, Medical gallery of Mikael Häggström 2014*. 2014. URL: https://upload.wikimedia.org/wikipedia/en/thumb/4/45/Citric_acid_cycle_noi.JPG/754px-Citric_acid_cycle_noi.JPG (visited on 08/19/2016).

[153] K. Cherney and S.J. Bliss. *A Complete List of Diabetes Medications*. 2016. URL: http://www.healthline.com/health/diabetes/medications-list#Overview1 (visited on 08/19/2016).

[154] UPMC Life Changing Medicine. *Insulin Pens: How to Give a Shot*. 2013. URL: http://www.upmc.com/patients-visitors/education/diabetes/Pages/insulin-pens-how-to-give-a-shot.aspx (visited on 08/19/2016).

[155] Mayo Clinic. *Artificial Pancreasa*. 2016. URL: http://www.mayo.edu/research/labs/artificial-pancreas/overview (visited on 08/19/2016).

Own Publications Pertaining to Theses

[22] Gy. Eigner and L. Kovács. "Realization methods of continuous glucose monitoring systems". In: *Scientific Bulletin of Politechnica University of Timisoara Transactions on Automatic Control and Computer Science* 59.2 (2014), pp. 175–183.

[72] Gy. Eigner, J.K. Tar, and L. Kovács. "Adaptive Control Solution for T1DM Control". In: *Proceedings of the 10th Jubilee IEEE International Symposium on Applied Computational Intelligence and Informatics (SACI 2015)*. (Timisoara, Romania, Jan. 22–24, 2015). Ed. by A. Szakál. IEEE Hungary Section, 2015, pp. 215–220.

[73] Gy. Eigner, P. Horváth, J.K. Tar, I. Rudas, and L. Kovács. "Application of Robust Fixed Point control in case of T1DM". In: *IEEE International Conference on Systems, Man, and Cybernetics 2015: IEEE SMC 2015*. (Hong Kong, China, Oct. 9–12, 2015). Ed. by S. Kwong and D. Yeung. IEEE SMC, 2015, pp. 2459–2464.

[74] Gy. Eigner, Tar J.K., and L. Kovács. "Fixed Point Transformation-based Adaptive Control for Type 1 Diabetes Mellitus". In: *Scientific Bulletin of Politechnica University of Timisoara Transactions on Automatic Control and Computer Science* 60.1 (74 2015), pp. 1–9.

[75] L. Kovács and Gy. Eigner. "Opportunities of using Robust Fixed Point Transformation-based controller design in case of Type 1 Diabetes Mellitus". Manuscript in preparation. 2016.

[91] Gy. Eigner, J.K. Tar, I. Rudas, and L. Kovács. "LPV-based quality interpretations on modeling and control of diabetes". In: *ACTA Pol Hung* 13.1 (2016), pp. 171–190.

[103] Gy. Eigner, J.K. Tar, and L. Kovács. "Novel Error Interpretation in case of Linear Parameter Varying Systems". In: *16th IEEE International Symposium on Computational Intelligence and Informatics, CINTI 2015*. (Budapest, Hungary, Nov. 19–19, 2015). Ed. by A. Szakál. IEEE Hungary Section, 2015, pp. 243–248.

[104] Gy. Eigner. "Novel LPV-based control approach for nonlinear physiological systems". In: *ACTA Pol Hung* 14.1 (2017), pp. 45–61.

[105] Gy. Eigner, P. Pausits, and L. Kovács. “A novel completed LPV controller and observer scheme in order to control nonlinear compartmental systems”. In: *14th IEEE International Symposium on Intelligent Systems and Informatics, CINTI 2015*. (Subotica, Serbia, Aug. 29–31, 2016). Ed. by A. Szakál. IEEE Hungary Section, 2016, pp. 85–92.

[114] L. Kovács and Gy. Eigner. “Usability of the Tensor Product based modeling in the modeling of Diabetes Mellitus”. Manuscript in preparation. 2016.

[115] Gy. Eigner, I. Rudas, and L. Kovács. “Investigation of the TP-based modeling possibility of a nonlinear ICU diabetes model”. In: *IEEE International Conference on Systems, Man, and Cybernetics 2016: IEEE SMC 2016*. (Budapest, Hungary, Oct. 9–12, 2016). IEEE SMC, 2016, pp. 3405–3410.

[116] L. Kovács and Gy. Eigner. “Convex Polytopic Modeling of Diabetes Mellitus: A Tensor Product based approach”. In: *IEEE International Conference on Systems, Man, and Cybernetics 2016: IEEE SMC 2016*. (Budapest, Hungary, Oct. 9–12, 2016). IEEE SMC, 2016, pp. 3393–3398.

Own Publications Not Pertaining to Theses

[21] L. Kovács and Gy. Eigner. “System Engineering Approach of Diabetes Treatment”. In: *Int J Diabetes Clin Diagn* 3.116 (1 2016), pp. 1–6.

[49] P. Szalay, Gy. Eigner, and L. Kovács. “Linear Matrix Inequality-based Robust Controller design for Type-1 Diabetes Model”. In: *Proceedings of the 19th IFAC World Congress, 2014*. (Cape Town, South Africa, Aug. 24–29, 2014). Ed. by E. Boje and X. Xia. IFAC, 2014, pp. 9247–9252.

[50] P. Szalay, Gy. Eigner, M. Kozlovszky, I. Rudas, and L. Kovács. “The significance of LPV modeling of a widely used T1DM model”. In: *EMBC 2013 – 35th Annual International Conference of the IEEE Engineering in Medicine and Biology Society*. (Osaka, Japan, July 3–7, 2013). Ed. by K. Sunagawa. IEEE Engineering in Medicine and Biology Society, 2013, pp. 3531–3534.

[102] P. Szalay, Gy. Eigner, Z. Benyó, I. Rudas, and L. Kovács. “Comparison of sigma-point filters for state estimation of diabetes models”. In: *2014 IEEE International Conference on Systems, Man and Cybernetics (SMC)*. (San Diego, USA, Oct. 5–8, 2014). Ed. by W.A Gruver. IEEE SMC, 2014, pp. 2476–2481.

[117] M. Kozlovszky, K. Hegedűs, S. Szénási, G. Kiszler, B. Wichmann, I. Bándi, Gy. Eigner, P.I Sas, L. Kovács, Z. Garaguly, V. Jónás, G. Kiss, G. Valcz, and B. Molnár. "Parameter assisted HE colored tissue image classification". In: *IEEE 17th International Conference on Intelligent Engineering Systems (INES)*. (San Jose, Costa Rica, June 19–21, 2013). Ed. by IEEE. IEEE Hungary Section, 2013, pp. 203–207.

[118] M. Kozlovszky, L. Kovács, M. Törőcsik, G. Windisch, S. Ács, D. Prém, Gy. Eigner, P.I. Sas, T. Schubert, and V. Póserné. "Cloud security monitoring and vulnerability management". In: *IEEE 17th International Conference on Intelligent Engineering Systems (INES)*. (San Jose, Costa Rica, June 19–21, 2013). Ed. by IEEE. IEEE Hungary Section, 2013, pp. 265–269.

[119] L. Kovács, J. Sápi, T. Ferenci, P. Szalay, D. Drexler, Gy. Eigner, P.I. Sas, I. Harmati, M. Kozlovszky, and Z. Sápi. "Model-based optimal therapy for high-impact diseases". In: *IEEE 17th International Conference on Intelligent Engineering Systems (INES)*. (San Jose, Costa Rica, June 19–21, 2013). Ed. by IEEE. IEEE Hungary Section, 2013, pp. 209–214.

[120] L. Kovács, P. Szalay, P.I. Sas, Gy. Eigner, Zs. Almássy, E. Felszeghy, Gy. Kocsis, J. Fövényi, A. Körner, L. Kautzky, H. Soós, A. Orbán, T. Niederland, A. Juhászné Tuifel, T. Tóthné Sebestyén, A. Soós, A. Török, and L. Barkai. "Preliminary model-free results of a Hungarian robust artificial pancreas algorithm: Abstracts of 6th International Conference on Advanced Technologies & Treatment for Diabetes, Paris, France". In: *Diabetes Technol The* 15.Suppl1 (2013), A-96 –A-97.

[121] Gy. Eigner, P.I. Sas, and L. Kovács. "Insulin pump testing platform for robust control framework". In: *Proceedings of IEEE 9th International Conference on Computational Cybernetics*. (Tihany, Hungary, July 8–10, 2013). Ed. by A. Szakál. IEEE Hungary Section, 2013, pp. 201–205.

[122] L. Kovács, J. Sápi, Gy. Eigner, T. Ferenci, P. Szalay, J. Klespitz, B. Kurtán, M. Kozlovszky, D. Drexler, P. Pausits, I. Harmati, Z. Sápi, and I. Rudas. "Model-based healthcare applications at Obuda University". In: *9th IEEE International Symposium on Applied Computational Intelligence and Informatics*. (Timisoara, Romania, May 15–17, 2014). Ed. by A. Szakál. IEEE Hungary Section, 2014, pp. 183–187.

[123] L. Kovács, M. Kozlovszky, P. Szalay, Gy. Eigner, P. Sas, T. Ferenci, Zs. Almássy, E. Felszeghy, G. Kocsis, J. Fövényi, K. Wudi, A. Körner, L. Kautzky, H. Soós, A. Orbán, T. Niederland, A. Juhászné Tuifel, M. Tóthné Sebestyén Hocsi, A.

Soós, A. Török, and L. Barkai. “ relax Magyar mesterséges hasnyálmirigy projekt. Eredmények és távlatok - in Hungarian”. In: *Diabetologia Hungarica XXII.* (Szeged, Hungary, Apr. 24–27, 2014). Hungarian Diabetes Associasion, 2014, pp. 73–76.

[124] L. Kovács, M. Kozlovszky, P. Szalay, Gy. Eigner, P. Sas, Zs. Almássy, E. Felszeghy, G. Kocsis, J. Fövényi, A. Körner, L. Kautzky, H. Soós, A. Orbán, T. Niederland, A. Juhászné Tuifel, M. Tóthné Sebestyén Hocsi, A. Soós, A. Török, and L. Barkai. “ relax Newest results of the Hungarian artificial pancreas project”. In: *7th International Conference on Advanced Technologies & Treatment for Diabetes.* (Wien, Austria, Feb. 5–8, 2014). Ed. by M. Phillip and T. Battelino. Mary Ann Liebert, 2014, A-149 –A-150.

[125] Gy. Eigner, P.I. Sas, and L. Kovács. “Continuous glucose monitoring systems in the service of artificial pancreas”. In: *9th IEEE International Symposium on Applied Computational Intelligence and Informatics.* (Timisoara, Romania, May 15–17, 2014). Ed. by A. Szakál. IEEE Hungary Section, 2014, pp. 117–122.

[126] L. Kovács, P. Szalay, Gy. Eigner, P. Sas, Zs. Almássy, and L. Barkai. “LPV-based robust control for Artificial Pancreas”. In: (2014). Online Abstract.

[127] L. Kovács, T. Ferenci, J. Sápi, Gy. Eigner, J. Klespitz, P. Szalay, M. Kozlovszky, and I. Rudas. “Physiological Modeling and Control at Obuda University”. In: *Proceedings of the 10th Jubilee IEEE International Symposium on Applied Computational Intelligence and Informatics (SACI 2015).* (Timisoara, Romania, Jan. 22–24, 2015). Ed. by A. Szakál. IEEE Hungary Section, 2015, pp. 21–25.

[128] P. Balla, P. Kocsis, Gy. Eigner, and Á. Antal. “Surface reconstruction with Wavelet transformation”. In: *20th Jubilee IEEE International Conference on Intelligent Engineering Systems 2016.* (Budapest, Hungary, June 30–July 1, 2016). Ed. by A. Szakál. IEEE Hungary Section, 2016, pp. 201–206.

[129] L. Kovács and Gy. Eigner. “Clinical decision support systems for personalized healthcare”. In: *International Conference on Automation, Quality and Testing, Robotics, AQTR 2016.* (Cluj-Napoca, Romania, May 19–21, 2016). IEEE Hungary Section, 2016, pp. 1–6.

[130] Á. Takács, Gy. Eigner, L. Kovács, I. Rudas, and T. Haidegger. “Teachers Kit: Development, Usability and Communities of Modular Robotic Kits for Classroom Education”. In: *The IEEE Robotics and Automation Magazine* (2016), pp. 2–11.

[131] I. Rudas, Gy. Eigner, and L. Kovács. “SMC 2016 and SMC Junior 2016”. In: *IEEE Systems, Man, and Cybernetics Magazine* 2 (1 2016), pp. 41–44.

A. Summary of the new scientific results

In this Chapter, I have collected to one place the new scientific results what I achieved during my research by Thesis points.

Thesis Group 1

Thesis group 1: T1DM control via RFPT framework

Thesis 1
I have developed an RFPT-based controller design framework for physiological systems. The provided solutions allows the using of highly approximating (rough) model of the physiological system to be controlled.

Thesis 1.1
I have proven the usability of the developed framework in case of the low complexity T1DM model, the Minimal Model. The designed controller keeps the BG level in a narrow range and it is able to suppress high glucose variability as well.

Thesis 1.2
I have proven the usability of the RFPT-based controller design framework in case of highly complex T1DM models: the Cambridge model (so called Hovorva-model) and the Pavia-Padova model (so called Magni-model). The developed RFPT-based controllers provide fast adaptivity and they are able to keep the blood glucose level of the complex T1DM models inside a given selected range even under unfavorable glucose loads or soft blood sugar variability.

Relevant own publications pertaining to this thesis group: [22, 72, 73, 74, 75].

Thesis Group 2

Thesis group 2: Completed LPV controller and observer scheme for LPV systems.

Thesis 2

I have introduced mathematical tools for LPV related control tasks which successfully exploit the possibilities lied in the specific properties of the parameter space of LPV systems. By using these tools different quality markers can be defined and specific complementary LPV controller and observer structures can be designed.

Thesis 2.1

I have introduced a norm based "difference" interpretation regarding the LPV systems, based on the properties of the LPV parameter space. I have defined how to use these interpretations as error and quality criteria during modeling and control and demonstrated my theoretical findings on a concrete example in diabetes modeling.

Thesis 2.2

I have developed an LPV based complementary controller structure in order to control nonlinear systems. The developed method requires the knowledge of classical state feedback theorems and less complex than the LMI-based methods, moreover it requires less computational capacity than the LMI-based techniques. I have demonstrated the usability of the developed tool in case of different nonlinear systems, with unfavorable circumstances demonstrating that the developed method provides stability and appropriate control action.

Thesis 2.3

I have developed an LPV based complementary observer structure which can estimate the actual values of the states in case of directly not measurable ones. I demonstrated the usability of the developed tools in case of a nonlinear system. I have proven that the complementary observer can accurately estimate the states of the given specific LPV systems.

Relevant own publications pertaining to this thesis group: [91, 103, 104, 105].

Thesis Group 3

Thesis group 3: Usability of the TP model transformation for DM

Thesis 3.1

I have realized a TP-based ICU model with small approximation error. I proved that in case of the given nonlinear ICU model better approximation error can be reached, if the operating equilibrium of glycemia (G_d) of the model was not equal to the model equilibrium of glycemia (G_E).

Thesis 3.2

I have investigated the robustization possibility of the blood glucose Minimal Model via TP framework. I have realized robust T1DM and T2DM TP-models, robust from parameter variation point of view. Regarding the LMI-based controller design, this property can be useful in guaranteeing the controller's robustness by the created robust TP models.

Thesis 3.3

I have proven the usability of TP-model transformation in case of highly complex T1DM model. I have demonstrated that several control oriented qLPV models can be derived from the original model approximating it with high accuracy.

Relevant own publications pertaining to this thesis group: [114, 115, 116].

B. Detailed description of the used DM models

In this Chapter I have summarized the descriptions and used parameters sets of each applied DM models during my research.

B.1. Minimal Model

The Minimal Model was originally developed by Bergman et al [132, 133]. Over years, several form of it appears [16]. In this Theses I used a modified version of it which can be found in [15]. This Minimal Model is appropriate to describe the T1DM and T2DM cases, respectively [15]. The model equations are the following:

$$\dot{G}(t) = -(p_1 + X(t))G(t) + p_1 G_B + d(t) \tag{B.1a}$$

$$\dot{X}(t) = -p_2 X(t)) + p_3(I(t) - I_B) \tag{B.1b}$$

$$\dot{I}_{T2DM}(t) = \begin{cases} \gamma(G(t) - h)t - n(I(t) - I_B) + u(t) & \text{for } G(t) - h > 0 \\ -n(I(t) - I_B) + u(t) & \text{for } G(t) - h \leq 0 \end{cases} \tag{B.1c}$$

$$\dot{I}_{T1DM}(t) = -n(I(t) - I_B) + u(t) \tag{B.1d}$$

The model has three states: $G(t)$ [mg/dL] the blood glucose concentration, which represents at the same time the output of the model; $X(t)$ [1/min] the insulin-excitable tissue glucose uptake activity, and $I(t)$ [μU/mL] the blood insulin concentration. The model has two inputs: the external insulin intake $u(t)$ [μU/mL/min] and the glucose intake $d(t)$ [mg/dL/min].

The T2DM state is described by (B.1c), where the internal insulin production is only possible when the $G(t)$ is higher than a threshold h. The simplified T1DM case is represented by (B.1d), where is no internal insulin production.

The symbols p_1, p_2, p_3, G_B, I_B, and n denote model parameters.

Table B.1.: States, inputs and output of the used Minimal-model

Notation	Unit	Description
p	mg/dL/min	Amount of absorbed glucose
u	μU/mL/min	External insulin injection
G	mg/dL	Plasma glucose concentration
X	min^{-1}	Glucose uptake activity of the insulin-dependent tissues
I	μU/mL	Plasma insulin concentration

Table B.2.: Parameters and their details in the used Minimal-model

Notation	Unit	Description	Value
BW	kg	Body weight	70
M_{wG}	g/mol	Molecular weight of glucose	180.15588
p_1	min^{-1}	Transfer rate	0.028
p_2	min^{-1}	Transfer rate	0.025
p_3	min^{-1}	Transfer rate	0.00013
n	min^{-1}	Time constant for insulin disappearance	0.23
G_B	mg/dL	Basal glucose level	85
I_B	μU/mL	Basal insulin level	15
A_G	-	CHO to glucose utilization	0.8

B.2. Model for Intensive Care Unit

B.2.1. The Wong model

The Wong-model consist of the following equations [85, 86]:

$$\begin{aligned}\dot{G}(t) &= -p_G G(t) - S_I(G(t)+G_E)\frac{Q(t)}{1+\alpha_G Q(t)} + P(t)\\ \dot{X}(t) &= -kI(t) - kQ(t)\\ \dot{I}(t) &= -\frac{nI(t)}{1+\alpha_I I(t)} + \frac{u_{ex}(t)}{V}\end{aligned} \tag{B.2}$$

The main aspect of the model is to describe the glucose-insulin dynamics of an inpatient who suffers from T1DM and is nurtured on ICU [85, 86]. It is expected that this simple model -after preliminary identification-, can provide the current and the future Blood Glucose (BG) level of the patient with a precision that is good enough for the realization of the tight glycemic control.

The following table contains the parameters, their descriptions and their values which were used in this thesis regarding to the Wong-model [85, 86].

B.3. Complex DM models

B.3.1. The Hovorka model

The equations of the model are the following [70, 71]:

$$\dot{D}_1(t) = A_G D(t) - \frac{D_1(t)}{\tau_D}\ , \tag{B.3a}$$

$$\dot{D}_2(t) = \frac{D_1(t)}{\tau_D} - \frac{D_2(t)}{\tau_D}\ , \tag{B.3b}$$

$$\dot{S}_1(t) = u(t) - \frac{S_1(t)}{\tau_S}\ , \tag{B.3c}$$

$$\dot{S}_2(t) = \frac{S_1(t)}{\tau_S} - \frac{S_2(t)}{\tau_S}\ , \tag{B.3d}$$

Table B.3.: Detailed desriptions and values of the parameters of the Wong-model

Notation	Unit	Description	Value
G	mmol/L	Plasma glucose above equilibrium level	-
Q	mU/L	Concentration of insulin bounded to interstitial sites	-
I	mU/L	Plasma insulin resulting from external input	-
P	mmol/L/min	Total plasma glucose input	-
u_{ex}	mU/min	External insulin input	-
G_E	mmol/L	Plasma equilibrium level	10.5
p_G	1/min	Endogenous glucose clearance	0.01
S_I	L/mU/min	Insulin sensitivity	0.001
V	L	Insulin distribution volume	12
k	1/min	Effective life of insulin in the compartment	0.0198
n	1/min	First order decay rate from plasma	0.16
α_I	L/mU	Plasma insulin disappearance	0.0017
α_G	L/mU	Insulin effect	0.0154

$$\dot{Q}_1(t) = \frac{D_2(t)}{\tau_D} - F_{01,c} - F_R(t) - x_1(t)Q_1(t) + k_{12}Q_2(t) + EGP_0(1 - x_3(t)) \ , \quad \text{(B.3e)}$$

$$\dot{Q}_2(t) = x_1(t)Q_1(t) - (k_{12} + x_2(t))Q_2(t) \ , \quad \text{(B.3f)}$$

$$\dot{I}(t) = \frac{S_2(t)}{\tau_S V_I} - k_e I(t) \ , \quad \text{(B.3g)}$$

$$\dot{x}_1(t) = -k_{a1}x_1(t) + k_{b1}I(t) \ , \quad \text{(B.3h)}$$

$$\dot{x}_2(t) = -k_{a2}x_2(t) + k_{b2}I(t) \ , \quad \text{(B.3i)}$$

$$\dot{x}_3(t) = -k_{a3}x_3(t) + k_{b3}I(t) \ . \tag{B.3j}$$

The model consist of four main submodel assigned to the state variables. The CHO absorption submodel (D_1, D_2 states) represent the glucose absorption; the nonlinear glucose-insulin core model (Q_1, Q_2 states) describes the glucose-insulin dynamics and cross effects; the insulin absorption (S_1, S_2 states) realizes the subcutaneous insulin absorption and the insulin kinematic submodel (I, x_{1-3} states) represents the insulinaemia and insulin effects and $d(t)$ g/min and $u(t)$ mU/min are the CHO and insulin intakes, respectively. The equations are completed with other functions, as well:

$$D(t) = \frac{1000 \cdot d(t)}{M_{wG}} \ , \tag{B.4a}$$

$$G(t) = \frac{Q_1(t)}{V_G} \ , \tag{B.4b}$$

$$F_R = \begin{cases} 0.003(G(t) - 9)V_G & G(t) \geq 9mmol/L \\ 0 & otherwise \end{cases} \ , \tag{B.4c}$$

$$F_{01,c} = \begin{cases} F_{01} & G(t) \geq 4.5mmol/L \\ \dfrac{F_{01}G(t)}{4.5} & otherwise \end{cases} \ , \tag{B.4d}$$

where $D(t)$ is the CHO input in mmol/min, $G(t)$ is the output of the model and $F_{01,c}, F_R$ are the output related saturations (nonlinearities). Table B.4-B.5 contains the detailed descriptions of the state variables and the used parameters of the model in this study based on [70, 71].

Table B.4.: States, inputs and output of the used Hovorka-model

Notation	Unit	Description
d	g/min	CHO input in g/min
D	mmol/min	CHO input in mmol/min
D_1	mmol	Glucose masses in the accessible compartment
D_2	mmol	Glucose masses in the non-accessible compartment
u	mU/min	External insulin input
S_1	mU	Masses of insulin in accessible compartment
S_2	mU	Masses of insulin in non-accessible compartment
Q_1	mmol/min	Masses of glucose in the accessible (where measurements are made) compartments
Q_2	mmol/min	Masses of glucose in the non-accessible compartments
G	mmol/min/L	Glucose concentration in the blood
x_1	-	Remote effect of insulin on glucose distribution
x_2	-	Remote effect of insulin on glucose disposal
x_3	-	Remote effect of insulin on endogenous glucose production
I	mU/L	Insulin concentration in the blood
$F_{01,c}$	mmol/min	Glucose consumption of the central nervous system
F_R	mmol/min	Production of glucose in the kidneys

Table B.5.: Parameters and their details in the used Hovorka-model

Notation	Unit	Description	Value
BW	kg	Body weight	70
M_{wG}	g/mol	Molecular weight of glucose	180.15588
k_{12}	min^{-1}	Transfer rate	0.066
k_{a1}	min^{-1}	Deactivation rate	0.006
k_{a2}	min^{-1}	Deactivation rate	0.06
k_{a3}	min^{-1}	Deactivation rate	0.03
k_e	min^{-1}	Insulin elimination rate	0.138
τ_D	min	CHO absorption constant	40
τ_S	min	Insulin absorption constant	55
A_G	-	CHO to glucose utilization	0.8
V_I/BW	$\text{L}\cdot\text{kg}^{-1}$	Insulin distribution volume	0.12
V_G/BW	$\text{L}\cdot\text{kg}^{-1}$	Glucose distribution volume	0.16
EGP_0/BW	$\text{L}\cdot\text{kg}^{-1}\ \text{min}^{-1}$	Liver glucose production at zero insulin	0.0161
F_{01}/BW	$\text{L}\cdot\ \text{kg}^{-1}\ \text{min}^{-1}$	Insulin independent CNS consumption	0.00097
S_{IT}	L/mU	Insulin sensitivity of transport / distribution	$51.2\cdot10^{-4}$
S_{ID}	L/mU	Insulin sensitivity of disposal	$8.2\cdot10^{-4}$
S_{IE}	L/mU	Insulin sensitivity of EGP	$520\cdot10^{-4}$

B.3.2. The Magni model

During the investigations, we used a well-known, high order digestion (B.5) and T1DM (B.6) models, presented by [134–136]. Also, these models are the base of the UVA/Padova

simulator [137].

$$
\begin{aligned}
\dot{Q}_{sto}(t) &= Q_{sto1}(t) + Q_{sto2}(t) \\
\dot{Q}_{sto1}(t) &= -k_{gri}Q_{sto1}(t) + d(t) \\
\dot{Q}_{sto2}(t) &= -k_{gut}(t, Q_{sto})Q_{sto2}(t) + k_{gri}Q_{sto1}(t) \\
\dot{Q}_{gut}(t) &= -k_{abs}Q_{gut}(t) + k_{gut}(t, Q_{sto})Q_{sto2}(t) \\
Ra(t) &= \frac{f k_{abs} Q_{gut}(t)}{BW} \ .
\end{aligned}
\tag{B.5}
$$

$$
\begin{aligned}
\dot{G}_M(t) &= -k_{sc}G_M(t) + \frac{k_{sc}}{V_G}G_p(t) \\
\dot{G}_p(t) &= EGP(t) + Ra(t) - U_{ii} - E(t) - k_1 G_p(t) + k_2 G_t(t) \\
\dot{G}_t(t) &= -U_{id} + k_1 G_p(t) - k_2 G_t(t) \\
\dot{X}_t(t) &= -p_{2U}X(t) + p_{2U}[I(t) - I_b] \\
\dot{I}_d(t) &= -k_i I_d(t) + k_i I_1(t) \\
\dot{I}_1(t) &= -k_i I_1(t) + k_i I(t) \\
\dot{I}_p(t) &= -(m_2 + m_4)I_p(t) + m_1 I_l(t) + k_{a2}S_2(t) + k_{a1}S_1(t) \\
\dot{I}_l(t) &= m_2 I_p(t) - (m_1 + m_3)I_l(t) \\
\dot{S}_2(t) &= -k_{a2}S_2(t) + k_d S_1(t) \\
\dot{S}_1(t) &= -(k_{a1} + k_d)S_1(t) + u(t)
\end{aligned}
\quad . \tag{B.6}
$$

The unified complex model has two inputs and one output, namely, $u(t)$ is the injected insulin, d is the amount of ingested glucose and the output $G_M(t)$ represents the subcutaneous glucose level.

The model contains several additional equations:

$$
k_{gut}(t, Q_{sto}) = k_{min} + \frac{k_{max} - k_{min}}{2}\Big(tanh[\alpha(Q_{sto} - b\bar{D}(t))] - tanh[\beta(Q_{sto} - d\bar{D}(t))] + 2\Big) \ , \tag{B.7a}
$$

$$
\alpha = \frac{5}{2\bar{D}(t)(1-b)} \ , \tag{B.7b}
$$

$$
\beta = \frac{5}{2\bar{D}(t)d} \ , \tag{B.7c}
$$

$$\bar{D}(t) = Q_{sto}(t) + \int_{\bar{t}}^{\bar{t}_f} d(\bar{\tau})d\tau \ , \tag{B.7d}$$

$$E(t) = \begin{cases} k_{e1}(G(t) - k_{e2}) & \mathrm{if} G_p(t) > k_{e2} \\ 0 & \mathrm{if} G_p(t) \leq k_{e2} \end{cases} \ , \tag{B.7e}$$

Table B.6.: States, inputs and output of the used Magni-model

Notation	Unit	Description
$Q_{sto}(t)$	mg	Amount of glucose in the stomach
$Q_{sto1}(t)$	mg	Solid phase of the amount of glucose in the stomach
$Q_{sto2}(t)$	mg	Liquid phase of the amount of glucose in the stomach
$Q_{gut}(t)$	mg	Glucose mass in the intestine
$R_a(t)$	mg/kg/min	Glucose rate of appearance in plasma
$d(t)$	mg/min	Rate of ingested glucose
G_p	mg/kg	Glucose masses in plasma and rapidly equilibrating tissues
G_t	mg/kg	Glucose masses in slowly equilibrating tissues
$G_M(t)$	mg/dL	Subcutaneous glucose level
$I_1(t)$	pmol/L	Insulin transfer
$I_d(t)$	pmol/L	Delayed insulin signal
$X_t(t)$	pmol/L	Remote insulin signal
$S_1(t)$	pmol/kg/min	Amount of the monomeric insulin in the subcutaneous space
$S_2(t)$	pmol/kg/min	Amount of the nonmonomeric insulin in the subcutaneous space
$I_l(t)$	pmol/kg	Insulin masses in liver
$I_p(t)$	pmol/kg	Insulin Masses in plasma
$I(t)$	pmol/L	Palsma insulin concentration
$u(t)$	pmol/kg/min	External insulin intake
$E(t)$	mg/kg/min	Renal excretion
$EGP(t)$	mg/kg/min	Endogenous glucose production
$U_{id}(t)$	mg/kg/min	Insulin-dependent glucose utilizations
$V_m(t)$	mg/kg/min	Insulin affected volume

Table B.7.: Parameters and their details in the used Magni-model

Notation	Unit	Description	Value
V_G	dL/kg	Body weight normalized glucose volume	1.49
$k1$	min^{-1}	Rate parameter	0.042
$k2$	min^{-1}	Rate parameter	0.071
V_I	L/kg	Body weight normalized insulin volume	0.04
m_1	min^{-1}	Model parameter	0.379
m_2	min^{-1}	Model parameter	0.673
m_3	min^{-1}	Model parameter	0.5685
m_4	min^{-1}	Model parameter	0.269
k_{max}	min^{-1}	Model parameter	x
k_{min}	min^{-1}	Model parameter	x
k_{abs}	min^{-1}	Rate constant of intestinal absorption	x
k_{gri}	min^{-1}	Rate of grinding	x
f		Fraction of intestinal absorption which actually appears in plasma	x
b		Model parameter	x
d		Model parameter	x
k_1	min^{-1}	Rate parameter	x
k_2	min^{-1}	Rate parameter	x
k_{a1}	min^{-1}	Rate constant of insulin absorption	0.1
k_{a2}	min^{-1}	Rate constant of monomeric insulin	0.2
k_d	mg/kg/min	Rate constant of insulin absorption	0.3
k_{p1}	mg/kg/min	Extrapolated EGP at zero glucose and insulin	3.09
k_{p2}	min^{-1}	Liver glucose effectiveness	$7e-4$
k_{p3}	$\frac{\text{mg/kg/min}}{\text{pmol/L}}$	Parameter governing amplitude of insulin action on the liver	0.005

Table B.8.: Parameters and their details in the used Magni-model

Notation	Unit	Description	Value
k_i	min^{-1}	Rate parameter accounting for delay between insulin signal and insulin action	0.0066
V_{m0}	mg/kg/min	Model parameter for insulin-dependent glucose utilization	4.65
V_{mx}	$\frac{\text{mg/kg/min}}{\text{pmol/L}}$	Model parameter for insulin-dependent glucose utilization	0.034
K_{m0}	mg/kg	Model parameter for insulin-dependent glucose utilization	466.21
p_{2U}	min^{-1}	Rate constant of insulin action on the peripheral glucose utilization	0.084
α	min^{-1}	Model function	x
β	$\frac{\text{pmol/kg/min}}{\text{mg/dL}}$	Model function	x
k_{e1}	min^{-1}	Glomerular filtration rate	$7e-4$
k_{e2}	mg/kg	Renal threshold of glucose	269
k_{sc}	mg/kg	Rate constant	0.1
I_b	pmol/L	Basal state plasma insulin concentration	102.3516
GM_{basal}	mg/dL	Basal state plasma insulin concentration	90
BW	kg	Body weight	78
U_{ii}	mg/kg/min	Insulin-independent glucose utilizations	1

C. Physiological background and treatment

C.1. Utilization of glucose

The human body can utilize the CHOs with $\alpha - D$ structure (the cellulose (with $\beta - D$ structure cannot be utilized). The primary source of energy for the human body is the glucose which is known as dextrose, monosaccharide, simple sugar, simple CHO, etc. The chemical formula of it is $C_6H_{12}O_6$. Other simple CHOs can be used by the body (eg. fructose), but the amount of them compared to the glucose can be neglected.

The complex CHO entering the human body via nutrition. The food enters into the gastrointestinal system which through the nutrients – including CHO – are absorbed. First, the ingested polisaccharides (complex sugar) are broken down into smaller mono- and di-saccharides (simple sugar) by the digestive enzymes, after the monosaccharides are absorbed in the small intestine via sodium-dependent glucose cotransporters (SGLT1 protein channels; same proteins, the SGLT2 provide the renal reabsorbtion in the proximal tubule of the nephron), which are driven by sodium gradient (created by Na-K energy consumer primer pumps on the basolateral membrane of the enterocytes). Finally, the monosaccharides (glucose, galactose, fructose) enter to the blood stream on the other sides of the enterocytes via glucose transporters (GLUT) membrane proteins; the glucose becomes absorbed via GLUT2 gate (the whole path can be seen on Fig. C.1). The absorbed nutrients will be transported by the blood stream to the liver through the portal vein [5, 6, 138].

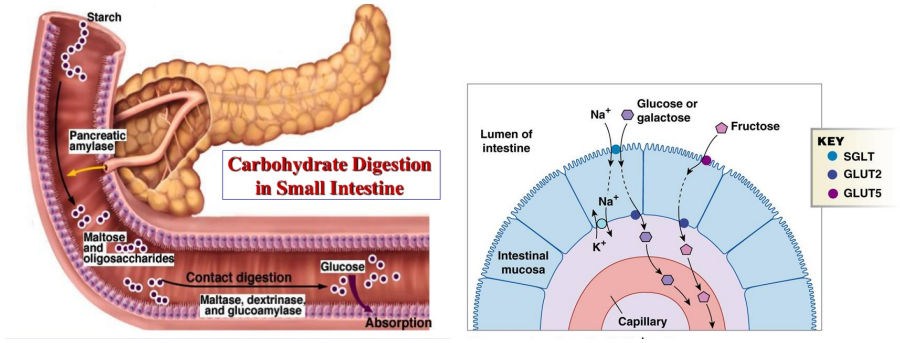

Figure C.1.: Process of digestion and absorption of glucose, Credit: dream10f (left), Austin Community College (right) [139, 140]

The glucose is consumed by glucose consumer body cells – like muscle-, fatty-, brain-cells and others –, these cells uptake the glucose via GLUT gates (this process will be detailed later).

In the cells the energy stored by glucose will be freed via anaerobic and aerobic chemical reactions. Also, this energy is used to restore the adenosine diphosphate (ADP) with a phosphor atom (ATP); drive the different protein pumps; drive the electron transport chain; etc. Figure C.2. shows these processes in case of eukaryotic cells (like the human cells).

The first step of the catabolism of the glucose is the glycolisis. Through glycolisis one molecule glucose is oxidised to two molecules of pyruvate ($C_6H_{12}O_6 + 2\,NAD^+ 2\,ADP + 2\,Pi \rightarrow 2\,C_3H_4O_3 + 2\,NADH + 2\,H^+ + 2\,ATP + 2\,H_2O$) and energy (ATP) released [138].

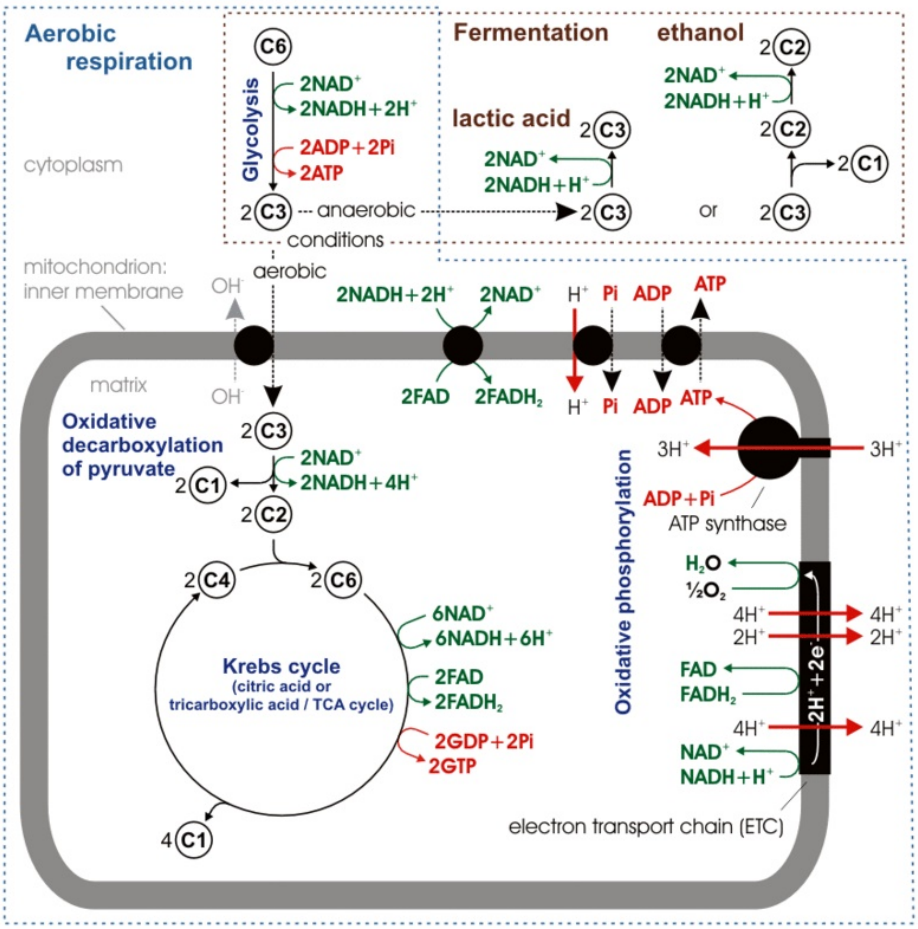

Figure C.2.: Stoichiometry of aerobic respiration and most known fermentation types in eucaryotic cell, Credit: Darekk2 [141]

The main energy producing cycle of the cells located in the mitochondria. The aerobic respiration in the presence of oxygen is become here. The pyruvate enters into the mitochondria and through the Szentgyörgyi-Krebs is oxidised – finally – to carbon dioxide (CO_2) and water (H_2O) (Fig. C.3).

The simplified aerobic route is: $C_6H_{12}O_6 + 6O_2 \rightarrow 6CO_2 + H_2O + energy$.

There is an other way for the usage of the energy of glucose. Via anaerobic (without oxygen) reactions the pyruvate can be reduced to lactate (fermentation); or via enzymatic reactions the pyruvate could become ethanol as well.

The lactate can be directly oxidised again to pyruvate and this can be used in the citric acid cycle or can be used in gluconeogenesis in order to realize glucose.

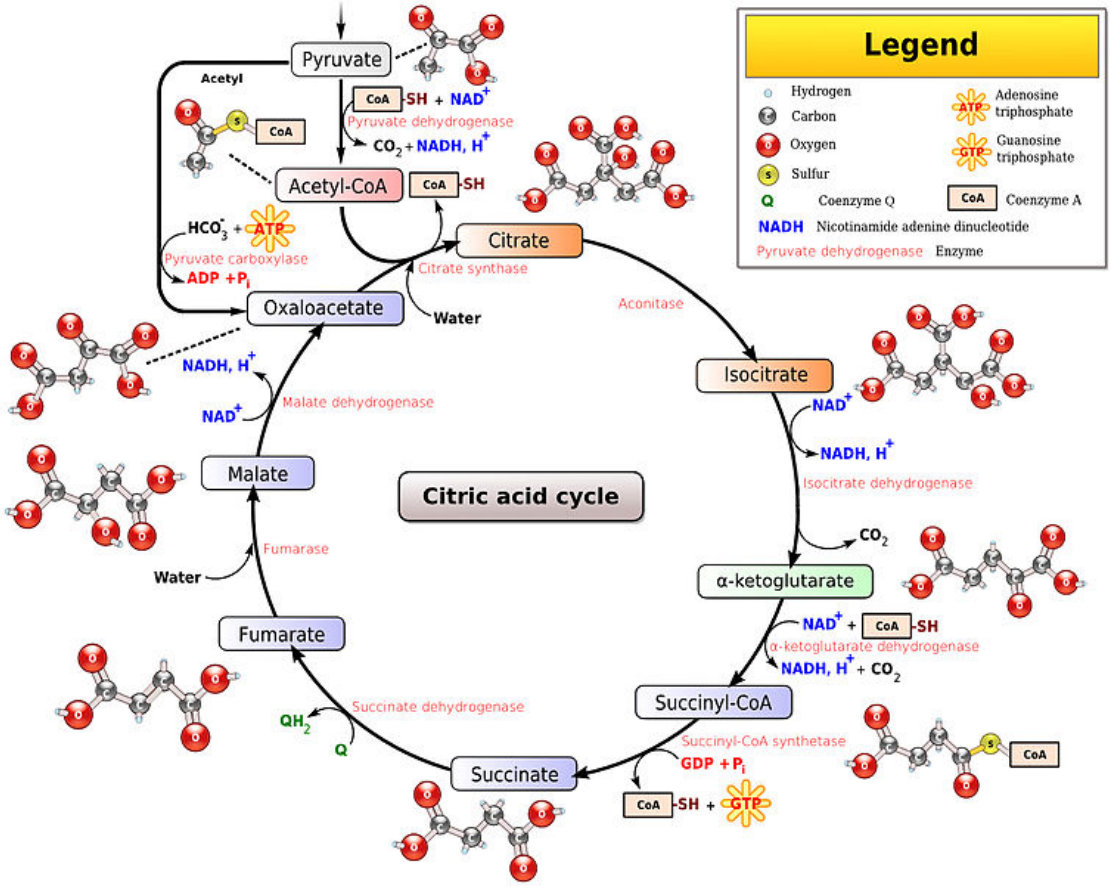

Figure C.3.: The citric acid (Szentgyörgyi-Krebs) cycle, Credit: Narayenese [142]

The main energy storing part of the body is the liver and the triglycerides (adipose or fatty cells). The liver storing the energy in a special compressed polysaccharide known as glycogen ($(C_6H_{12}O_6)_2$), which consists of glucose molecules and the compression is made by weak bonds. The glycogen is mainly realized by the liver cells via an endergonic chemical process. Adipose cells storing the energy as fatty acids. Through estherification of fatty acids and glycerol, the adipose cells can storing the energy as adipose tissue and reach high energy density. If the body needs energy, the glycogen (via glycogenolysis) and glycerol (via oxygen bond) can be transformed into glucose again and can be used in the citric acid cycle.

The physiological processes regarding the glucose, including utilization, clearance, storage are mostly controlled by two pancreatic hormones – insulin and glucagon. The regulation process can be seen on Fig. C.4.

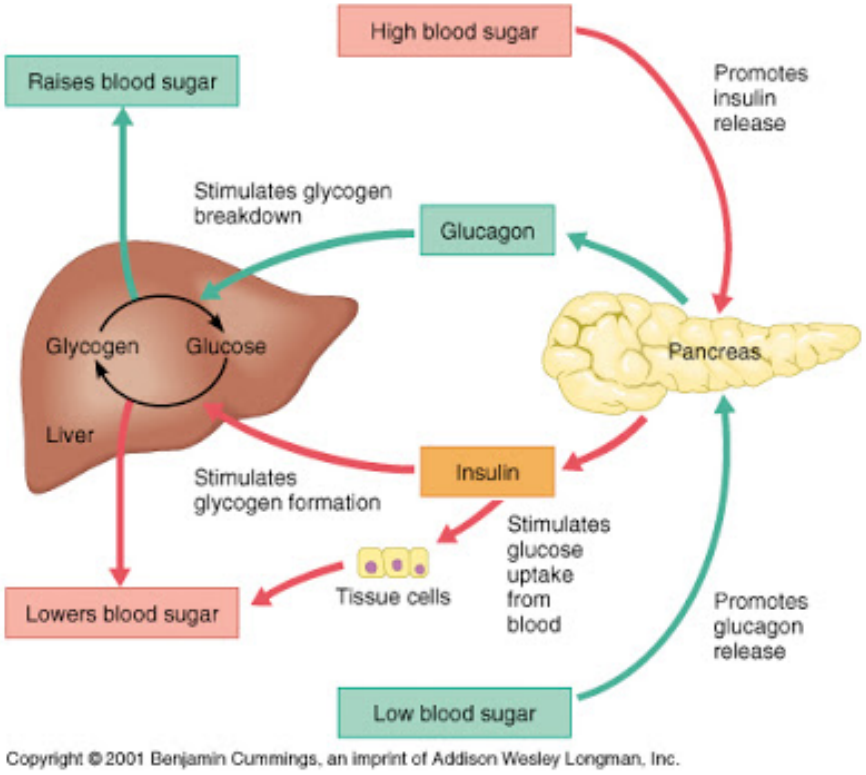

Figure C.4.: Regulation of the utilization of glucose, Credit: Benjamin Cummings [143]

In case of high blood sugar the pancreas releases insulin and the insulin level (insulinemia) in blood is increasing, which stimulates: the glycogen synthesis (the liver cells utilizes the glucose and storing it as glycogen); the estherification (convert glucose to glycerol); decrease the production of glucagon; and many influences many other processes. In this way, the blood glucose level becomes low. Low blood glucose level increases the production of glucagon. The increasing glucagon level stimulates: the glycogenolysis (glycogen convert to glucose; glucose secretion by the liver cells); decrease the insulin production (this connection is much weaker than the revers); and influences on other processes [5, 144].

Glycogen is produced not just the liver cells, but the muscle cells as well. However, the amount of glycogen in muscles is much lower than in the liver – muscles are using this low amount of local glycogen as fast and immediate supply of glucose till the metabolic processes reach the optimal energy producing state. The liver stores the glycogen in fully mobilizable form. During the daily routine depends on the hormone control, the liver producing and secretes even 500 g of glucose per day [138]. The liver is the central organ

in the glucose homeostasis.

It should be noted that the adrenaline (epinephrine) can trigger the glucose secretion of the liver as well – in case of stress reactions the adrenal glands secretes adrenalin which increase the amount of secreted glucose by the liver in order to perform the requirements of the body (eg. flight-or-fight reaction).

The primary energy source of the brain is the glucose – it requires continuous supply of it in order to keep its normal functioning. The brain consumes significant part from the daily glucose (around 25 %). The glycogen storing capacity of the brain is very limited – this small amount can be used during hypoglycemic periods. However, the persistent low blood sugar level causes several negative effect, such as poor decision making, dizziness, fainting, metabolic collapse and finally coma or even death [144].

The kidney play massive role in the glucose homeostasis, since the the kidneys reabsorb the nutrients and minerals from the primer filtrate. The kidneys consuming glucose as energy source to keep up the cellular filtration. The tubular cells contain the similar GLUT gates as the intestine's cells. Through these the tubular cells reabsorb the glucose (and avoid the excretion of it) and via the peritubular capillaries the reabsorbed glucose enters the renal veins (as other nutrients). In that case, if the blood glucose level persistently high, the tubular transporters can be saturated (over longer period they can be even damaged due to the continuous load) and the glucose is excreted out in the urine. The name of the disease came from this fact ("diabetes" "pass trough" and "mellitus" "sweet as honey"), since it is an indicator of the malady – the ancient doctors can diagnose it from the sweet urine [7, 144].

The usually used units for blood glucose concentration measurement is mg/dL and mmol/L (1 mmol/L $\approx$ 18.018 mg/dL). I have used both units in this dissertation.

C.2. The Insulin

Insulin is a peptide hormone produced by the β-cells in the Langerhans islets of the pancreas. The production and secretion of insulin is catalyzed by the amount of glucose in the blood stream, nervous affections and the actual state of the hormone household – however, the most significant effect is the blood sugar level [5, 8].

The secretion of insulin in the β-cells can be seen on Fig. C.5. Due to the increasing blood glucose level in the blood, the glucose uptake of the GLUT2 gate increases. The increased glucose level inside the cell via glycolytic phosphorylation of glucose causes rises the ATP/ADP ratio – namely, the energetic level of the cells increasing. The higher level of ATP blocking the the $Na-K$ channel proteins which causes the increasing level

of K. This rise indicates depolarization, which affects on the the Ca channels – via these gates the Ca ions inflow the cells. The increasing calcium level causes exocytotic release of insulin (the storage granule merged with the membrane of the cell) [6].

The production and secretion of insulin mostly depends on the blood glucose level, however, other physiological signals, like nervous activity and adrenaline can increase them. Basically, a negative feedback loop connects the frequency of the secretion and the actual BG level. In that case of the BG level is low, the production and secretion frequency is lower, but with increasing BG level this frequency increases too [7].

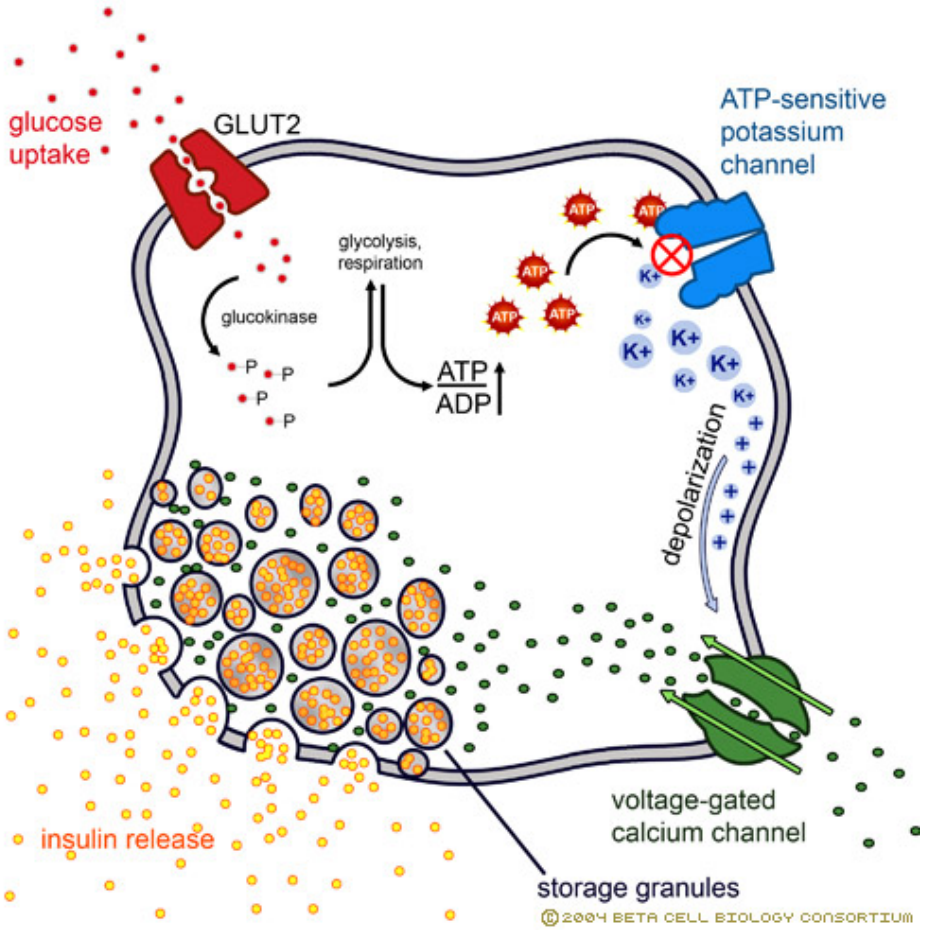

Figure C.5.: Insulin production and secretion, Credit: Beta Cell Biology Consortium [145]

The secretion of insulin have impulse nature (Fig. C.6.) and oscillating with a period of 3 – 6 minutes [146, 147]. The hormone enters the blood stream through the portal vein.

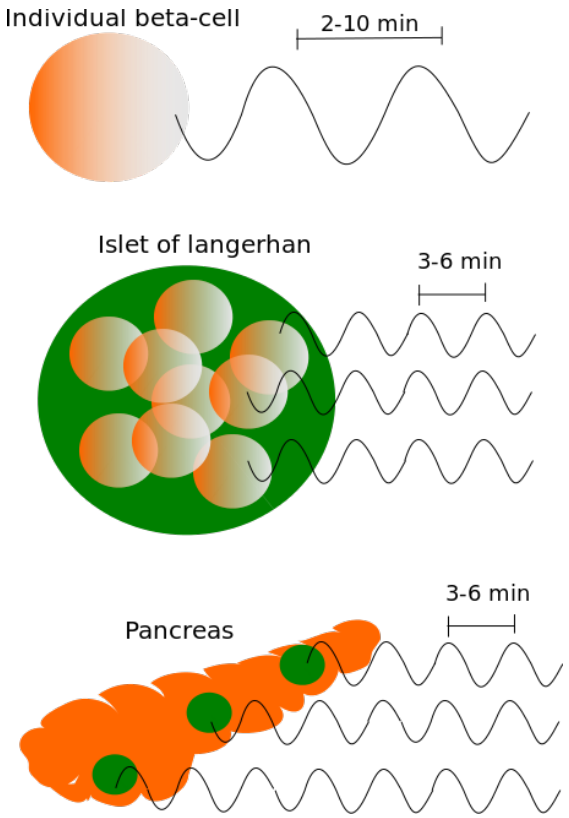

Figure C.6.: Pulsating nature of insulin secretion [148]

The insulin was discovered by Banting et al in 1922 [149, 150]. They firstly synthetized the hormone from dogs, later they could extract it from ox-calf. Until the early 1960s the available insulins were zoogenic. In the mid 1960s opens the road to realize human insulin in quantities thankfully the recombinant DNA technology. This technique allows to embed human DNA into bacterial DNA – in this way safe human insulin is produced by bacteria. Today, most of the insulin come from this source, however, zoogenic insulins are available for those elderly people, who have started their therapy before the invention of recombinant insulins and their body adapted to zoogenic insulins. Famous recombinant insulin are the Humulin, Novolin and Apidra. In the early 1990s the first insulin analogues (insulin receptor ligands) were introduced. These medications mimic the effects of insulin, however, the effect of them take longer time. The type of requested insulins depends on the expected effect. Before and shortly after the meals, the rapid acting insulins have to be used. In order to maintain the basal insulin level, mid and long acting insulin is the general solution. It should be noted that during the treatment with insulin pump, the rapid acting insulins are the usually used. Figure C.7 shows the available insulin types

on the market, their effects and durations.

Type of Insulin & Brand Names	Onset	Peak	Duration	Role in Blood Sugar Management
Rapid-Acting				
Lispro (Humalog)	15-30 min.	30-90 min	3-5 hours	Rapid-acting insulin covers insulin needs for meals eaten at the same time as the injection. This type of insulin is often used with longer-acting insulin.
Aspart (Novolog)	10-20 min.	40-50 min.	3-5 hours	
Glulisine (Apidra)	20-30 min.	30-90 min.	1-2½ hours	
Short-Acting				
Regular (R) humulin or novolin	30 min. -1 hour	2-5 hours	5-8 hours	Short-acting insulin covers insulin needs for meals eaten within 30-60 minutes.
Velosulin (for use in the insulin pump)	30 min.-1 hour	1-2 hours	2-3 hours	
Intermediate-Acting				
NPH (N)	1-2 hours	4-12 hours	18-24 hours	Intermediate-acting insulin covers insulin needs for about half the day or overnight. This type of insulin is often combined with a rapid- or short-acting type.
Long-Acting				
Insulin glargine (Basaglar, Lantus)	1-1½ hour	No peak time. Insulin is delivered at a steady level.	20-24 hours	Long-acting insulin covers insulin needs for about one full day. This type is often combined, when needed, with rapid- or short-acting insulin.
Insulin detemir (Levemir)	1-2 hours	6-8 hours	Up to 24 hours	
Ultra-Long-Acting				
Insulin degludec (Tresiba) 30-90 min.		No Peak onset.	42 hours	Ultra-Long-Acting insulin provides steady insulin levels for over 24 hours. Injected once daily to provide base insulin levels. May be combined with short-acting insulin to cover meals.
Pre-Mixed*				
Humulin 70/30	30 min.	2-4 hours	14-24 hours	These products are generally taken two or three times a day before mealtime.
Novolin 70/30	30 min.	2-12 hours	Up to 24 hours	
Novolog 70/30	10-20 min.	1-4 hours	Up to 24 hours	
Humulin 50/50	30 min.	2-5 hours	18-24 hours	
Humalog mix 75/25	15 min.	30 min.-2½ hours	16-20 hours	
*Premixed insulins combine specific amounts of intermediate-acting and short-acting insulin in one bottle or insulin pen. (The numbers following the brand name indicate the percentage of each type of insulin.)				

Figure C.7.: Different types of insulin and their effect [151]

The last part what should be highlighted regarding the insulin is the actual effect of them. Figure C.8 illuminate how the insulin works on cell size in case of a liver cell (but the insulin works similarly in case of fatty acid and muscle cells as well). The insulin binds to the receptor, which suffers spatial shape changes. Through chemical messenger molecules different physiological processes become: the insulin dependent GLUT gates let through the glucose, in the presence of glucose the glycogen production starts, the glucose is burned via the cytric acid cycle, or in case of adipose tissues the production of fatty acids begins.

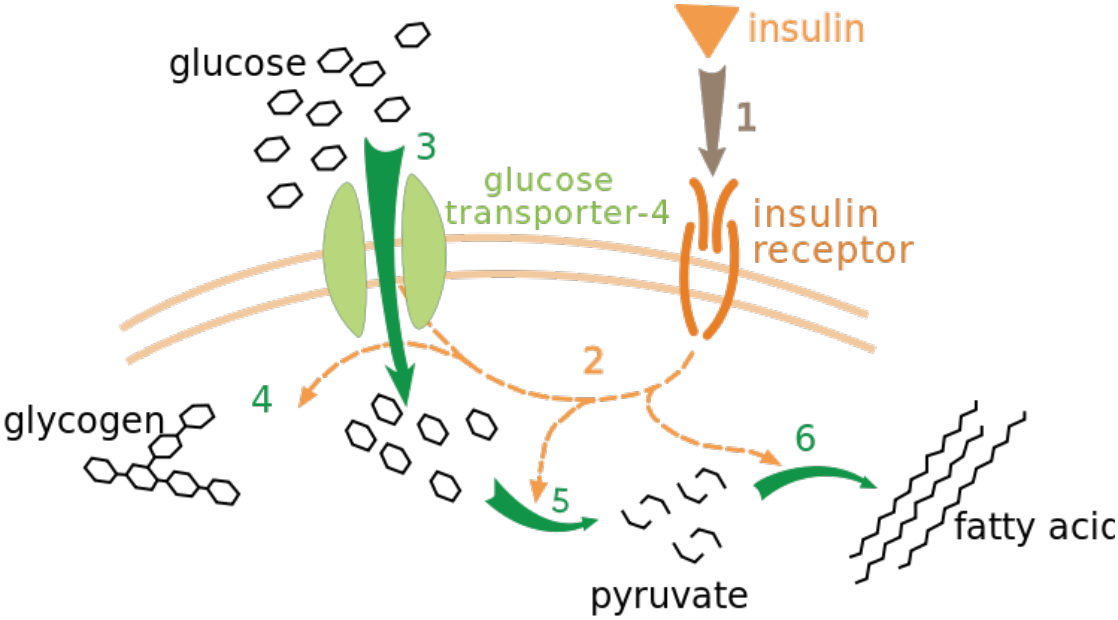

Figure C.8.: Effect of insulin on hepatic cells. Insulin binds to its receptor (1), which starts many protein activation cascades (2). These include translocation of Glut-4 transporter to the plasma membrane and influx of glucose (3), glycogen synthesis (4), glycolysis (5) and triglyceride synthesis (6)., Credit: XcepticZP [152]

C.3. Types of the disease

C.3.1. Type 1 DM

The Type 1 DM is caused by an autoimmune reaction, in which the body's own immune system destroys the insulin producer β-cells in the pancreas. As a result, the internal insulin production is ceased and the patients need external insulin intake in order to being alive. Without insulin, the blood glucose will be high, however, the body cells are

starving. The reasons are not fully understood yet. T1DM can occur in any age, but the most affected age group is the older children and young adults. Most of the syndrome appears suddenly, without any foreshadow. The usual symptoms are the following: thirst and dry mouth, frequent urination, lack of energy, tiredness, constant hunger, sudden weight loss, blurred vision, dizziness, confusion, blurred vision. If the current symptoms appears the disease can be diagnosed based on blood test. Occurrence of T1DM is much lower than T2DM, however, it's around 10% in the global diabetic population. With well controlled daily insulin administration and healthy lifestyle people with T1DM can be expected to the long and healthy life [3].

C.3.2. Type 2 DM

Type 2 DM is the most common type of DMs. It usually occurs in mid-aged adults, but the occurrence is dramatically increasing in case of children and adolescents as well. The emergence of the disease is related to predisposing factors (eg. genetic susceptibility, age, weight, gender, etc.) and life style. This type is also known as *civilizational disease*. In T2DM the body can produce insulin, but because of the persistently high blood glucose level over years the body cells become resistant to the hormone and insulin becomes ineffective. Because of the insulin resistance, the blood glucose will be high, because the cells cannot intake the glucose from the blood. The emergence if T2DM can be divided into periods. In the first period, the high glucose level demands high insulin level in blood. In order to keep the BG level in a normal range, the β-cells secrets increased amount of insulin. Because of the high insulin level the cells intake lot of glucose from the blood – over time, the cells saturates and cannot use the lot of glucose. In this case, the cells begins chemical reactions in order to decrease this extreme glucose load and the insulin receptors will be changed on molecular levels. Over time, more and more insulin is needed to reach the same effect as in younger age. At the last stage, because of the persistent load the β-cells are burning out and the T2DM become T1DM. The most specific symptoms are the followings: frequent urination, excessive thirst, weight loss, blurred vision. Many people with T2DM do not faces about their diabetic conditions until the side effects of DM cause serious problems (eg. longer healing, diabetic foot, damaging nervous system, etc.). As a result, many people already have evidence of complications when they are diagnosed with T2DM. Although the exact causes for the emergence of T2DM are still not known, there are well characterized risk factors which predispose for the disease. The most important are excess body weight, lack of physical activity and poor nutrition. Other occasional factors are the gender, ethnicity, genetics, family history of diabetes, past history of gestational diabetes and advancing age. In contrast to

people with T1DM, most people with T2DM do not require daily insulin intake in order to survive. In the early stage the changed life-style, namely healthy diet and increased physical activity can be enough to manage the diabetic state. Later, oral medications help to decrease the internal glucose production (eg. Metformin), or increase insulin sensitivity. The last solution – similarly to T1DM – is the external insulin administration [3, 6, 7].

C.3.3. Gestational DM

This category includes the occurrence of hyperglycemia at any stage of pregnancy. Two main categories can be distinguished into gestational DM and DM in pregnancy based on slightly of substantially elevated BG level. Most of the cases, GDM disappears after the pregnancy, however, in the rest of the cases the diabetic state become persistent and transforms to T2DM [3].

C.3.4. Double DM

This type of DM is heavily increasing. Its characterized by increasing insulin resistance and decreasing insulin production [4].

C.3.5. Rare types

These types affect infinitesimal slice of the diabetic population. Mostly caused by genetic disorders. Frequent types are the monogenic diabetes and secondary diabetes [3].

C.4. General side-effects of DM

Diabetic people are at higher risk of developing several disabling and life-threatening health problems. Persistently high BG level may causes heart-, brain-, nerve-, kidney- and eye-diseases and damaging blood vessels. Moreover, diabetic patient have increased risk of developing infections. Most of the developing countries DM is the leading cause of cardiovascular disease, blindness, kidney failure and lower-limb amputation. The life-style and civilizational behaviors is closing to the high income countries in the mi- and low-income lands as well. However, the health care systems are much underdeveloped. In this countries diabetic patients are in higher danger from the side effects of the disease.

Here I listed the most usual side effects of DM [3, 5]:

- Retinopathy (eye disease): the network of the blood vessels which supplies the retina with nutrients and oxygen become damaged which leads to partial or full blindness.
- Cardiovascular disease: several cardiovascular problems can occur beside DM as side effect, for example angina, myocardial infarction, stroke, arterial diseases, heart failure.
- Pregnancy complications: hyperglycemia during pregnancy may cause problems regarding the development of the fetus and long-term negative effects of the adolescents and children; the birth size of the fetus could be high or extreme high which leads to birth complications; there is higher risk that the fetus birth with such kind of DM
- Diabetic foot: because of damaging blood vessels there will be poor circulation in the feet which increase the possibility for ulceration, infections and amputation. Moreover, because of the damaging nervous system diabetic people do not sense the problems in time.
- Periodontitis (oral health problems): increased risk of inflammation of the tissue surrounding the tooth which leads to inflammations, loss of tooth, etc.
- Nephropathy (kidney disease): chronic kidney disease which is caused by the damage of the small blood vessels – due to this effect the kidney's performance will become lower.
- Neuropathy (nerve damage): includes the center and peripheral nerve damage, however, the latter is more frequent. Peripheral nerve damage leads to pain, tingling, loss of sensation, loss of motoric functions. Neuropathy may cause erectile dysfunctions, problems with digestion, urination and other sympatic and parasympatic functions.

C.5. Treatment possibilities

There are regular and rare therapies regarding the DM. Here, I only report from the regular therapies, the rare ones (eg. Langerhans-islets transplantation, DNA techniques, etc.) are beyond the topic of this Theses.

C.5.1. Prevention

It's a cliche, but the best way in order to avoid side effects is the prevention of them. In general, non of the complications of DM are inevitable – all of them can be prevented by tight (good) control of glycemia, blood pressure, cholesterol level, avoid the high blood glucose variability, hold an appropriate physical activity and diet. However, this requires a high educational level regarding the DM, adherence of the medical prescriptions and appropriate medical equipments.

C.5.2. Medication by drugs

Luckily, several type of drugs are available for medication purposes. Frequently used tool by the doctors is the well-known *Biguanides*, like Metformin, which is effectively inhibits the internal glucose production of the liver. An other popular drug is *α-glucosidase inhibitors*, like Acarbose, which help to the body to break down the starch and complex sugars. *Dopamin agonists* help to prevent insulin resistance. *DPP-4 inhibitors*, like Linagliptin, increasing the amount and frequency of insulin production. *Incretin mimetics (glucagon analogues)*, like Albiglutide, are slowing down the emptying of the stomach, decrease the usage of natural glucagon in the body. *Meglitinides*, like Nateglinide, helps the body to release insulin. *Sodium glucose transporter (SGLT) 2 inhibitors*, like Dapaglifozin, prevents the kidneys and help the excretion of glucose to urine. The oldest type of DM drugs are the *Sulfonylureas*, like Glimepirid, which increase the activity of β-cells. *Thiazolidinediones*, like Rosiglitazone, decrease the glucose level in the liver and help the effecty usage of insulin by the adipose tissue, however, they cause increased risk for heart failures.

Beside the DM drugs other medication are frequently used: Aspirin, for the cardiovascular system protection; drugs in order to decrease cholesterol level; and drugs to maintain the high blood pressure. [153]

C.5.3. Life-style therapies and diet

The physical activity is crucial part of the treatment, since, the muscle cells contain such kind of GLUT gates, trough which the glucose can enter the muscle cells without insulin – in this way the required amount of insulin can be lower. Moreover, active muscle cells consumes more glucose which realize a demand against the body and decrease the possibility of insulin resistance [5]. In general, the required activity (depends on the gender, age and general health status of the patient) is: for beginners, the recommended is a short intensive sport activity with total duration of 20 minutes 2-3 times on a week

with 90 pulse (HRT) until sweating; for trained persons, the recommended is a longer intensive sport activity with duration between 40 and 90 minutes 5-7 times on a week with 120 pulse (HRT). The increased metabolic state after physical activities have to be monitoring and the insulin therapy should follow the actual needs.

A corner stone of treatment is the diet. Usually, the diabetic patients are overweighted so the goal is to reduce the total weight and reach a healthy level. In other cases, the target is the steady glucose intake in order to avoid the high variability and keep the BG level in normal ranges. Generally, the diet has to be individual, meets with the needs and follow the prescriptions.

C.5.4. Intensive Conservative Therapy (ICT)

The most used type of treatment is the ICT. The main goal of it to keep the blood glucose level in a narrow healthy range and avoid the variability. In order to reach these goals it uses external insulin (more than one type) intake, intensive medication (combined drug therapy), intensive physical activity and high education. The patients use different mid- and long-term insulins to keep the appropriate basal insulin level and rapid- and short-acting insulins before and/or after meals. ICT needs conscious meal schedule and strong collaboration of the medical staff and the patient – its not recommended for uncooperative patients.

C.5.5. Insulin intake by insulin pen

Most usual way for insulin intake is the injecting to the subcutaneous level by insulin pen. Figure C.9. shows the general construction of a modern insulin pen which includes the insulin reservoir, the thin needle and the dispenser as main units. The dispenser allows the precise dosage. The best places for insulin injection on the body are the thigh-abdomen-arm regions; however, usually the abdomen is used. It should be noted that the best way to avoid inflammations and infections is the sequential toggling of the area of injection [9, 10, 12].

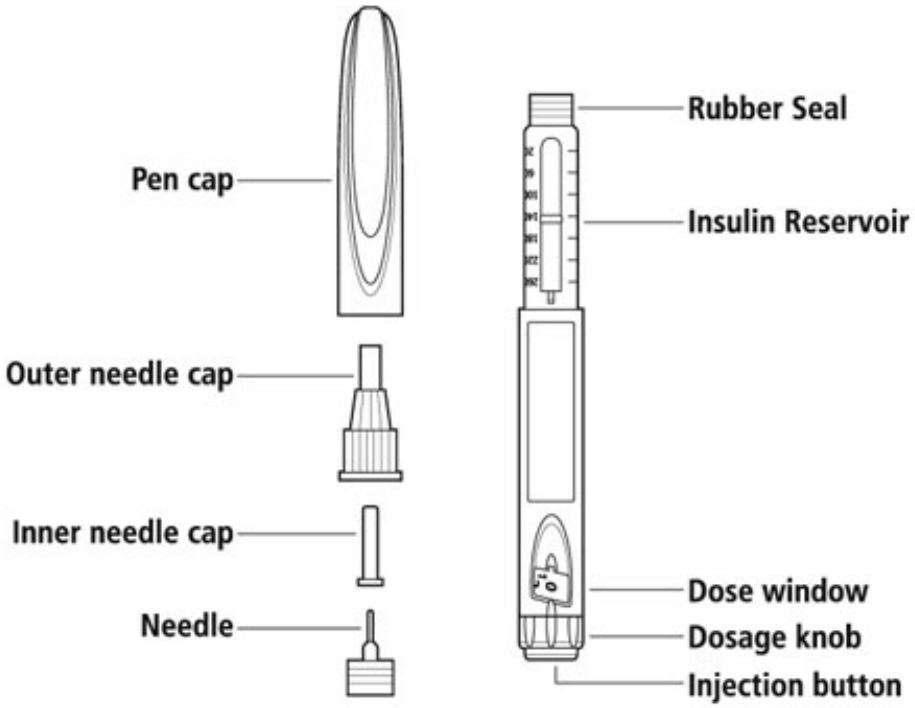

Figure C.9.: Insulin pen, Credit: UPMC [154]

C.5.6. Insulin intake by insulin pump

A relatively new option for insulin administration – which play the key role in the AP concept as well – is the insulin pump. The main parts of the device were introduced in the introduction.

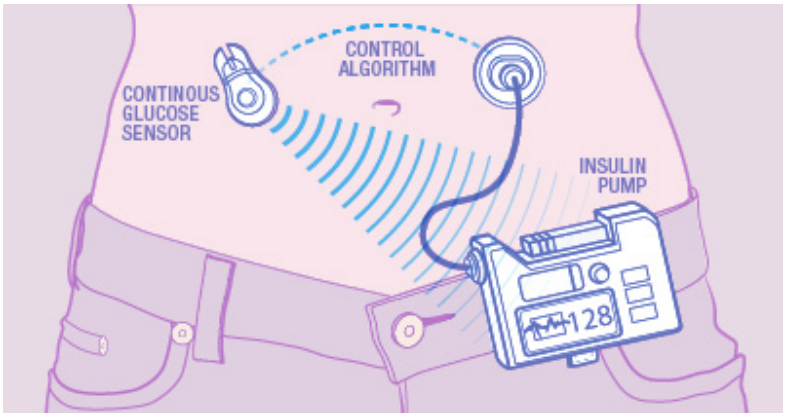

Figure C.10.: Insulin pump, Credit: Mayo Clinic [155]

D. Linear Parameter Varying Systems

D.1. Dynamical and LPV systems

D.1.1. State space representation of dynamic systems

A general NLTV system can be represented with the following functions [81, 82, 90]:

$$\begin{aligned} \dot{\mathbf{x}}(t) &= f(\mathbf{x}(t), \mathbf{u}(t), \mathbf{d}(t)) \\ \mathbf{y}(t) &= h(\mathbf{x}(t), \mathbf{u}(t), \mathbf{d}(t)) \end{aligned}, \tag{D.1}$$

where $\mathbf{x}(t) \in \mathbb{R}^n$ is the state vector, $\mathbf{y}(t) \in \mathbb{R}^k$ is the output vector, $\mathbf{u}(t) \in \mathbb{R}^m$ is the output vector, $\mathbf{d}(t) \in \mathbb{R}^p$ is the disturbance vector, $f(\mathbf{x}(t), \mathbf{u}(t), \mathbf{d}(t))$ is a nonlinear state function and $h(\mathbf{x}(t), \mathbf{u}(t), \mathbf{d}(t))$ is the nonlinear output function. With reformulation this can be described in SS form:

$$\begin{aligned} \dot{\mathbf{x}}(t) &= \mathbf{A}(t)\mathbf{x}(t) + \mathbf{B}(t)\mathbf{u}(t) + \mathbf{E}(t)\mathbf{d}(t) \\ \mathbf{y}(t) &= \mathbf{C}(t)\mathbf{x}(t) + \mathbf{D}(t)\mathbf{u}(t) + \mathbf{D_2}(t)\mathbf{d}(t) \end{aligned}, \tag{D.2}$$

where $\mathbf{A}(t) \in \mathbb{R}^{n \times n}$ is the state matrix, $\mathbf{B}(t) \in \mathbb{R}^{n \times m}$ is the control input matrix, $\mathbf{E}(t) \in \mathbb{R}^{n \times p}$ is the disturbance input matrix, $\mathbf{C}(t) \in \mathbb{R}^{k \times n}$ is the output matrix, $\mathbf{D}(t) \in \mathbb{R}^{k \times m}$ is the control feed-forward matrix and $\mathbf{D_2}(t) \in \mathbb{R}^{k \times p}$ is the disturbance feed-forward matrix. In this case, the elements that give rise to the nonlinearity are included in the given matrices. However, this is the general notation for such LTV systems, even where the matrices do not contain nonlinearity causing elements. The state matrices in (D.2) can be united into a single system matrix (or system function) $\mathbf{S}(t)$:

$$\mathbf{S}(t) = \begin{pmatrix} \mathbf{A}(t) & \mathbf{B}(t) & \mathbf{E}(t) \\ \mathbf{C}(t) & \mathbf{D}(t) & \mathbf{D_2}(t) \end{pmatrix}, \tag{D.3}$$

where $\mathbf{S}(t) \in \mathbb{R}^{(n+k)\times(n+m+p)}$.

Thereby (D.2) in simpler form via (D.3) is:

$$\begin{pmatrix} \dot{\mathbf{x}}(t) \\ \mathbf{y}(t) \end{pmatrix} = \mathbf{S}(t) \begin{pmatrix} \mathbf{x}(t) \\ \mathbf{u}(t) \\ \mathbf{d}(t) \end{pmatrix} . \tag{D.4}$$

If the state matrices do not depend on time, LTI system occurs, described by the following SS equation:

$$\begin{aligned} \dot{\mathbf{x}}(t) &= \mathbf{A}\mathbf{x}(t) + \mathbf{B}\mathbf{u}(t) + \mathbf{E}\mathbf{d}(t) \\ \mathbf{y}(t) &= \mathbf{C}\mathbf{x}(t) + \mathbf{D}\mathbf{u}(t) + \mathbf{D_2}\mathbf{d}(t) \end{aligned} \tag{D.5}$$

and can be written in the previous compact form as in (D.4), however, here $\mathbf{S}$ does not depend on time:

$$\begin{pmatrix} \dot{\mathbf{x}}(t) \\ \mathbf{y}(t) \end{pmatrix} = \mathbf{S} \begin{pmatrix} \mathbf{x}(t) \\ \mathbf{u}(t) \\ \mathbf{d}(t) \end{pmatrix} . \tag{D.6}$$

In that case, where external disturbance does not not occur or can be neglected, the SS description and compact form of a LTV system can be simplified:

$$\begin{aligned} \dot{\mathbf{x}}(t) &= \mathbf{A}(t)\mathbf{x}(t) + \mathbf{B}(t)\mathbf{u}(t) \\ \mathbf{y}(t) &= \mathbf{C}(t)\mathbf{x}(t) + \mathbf{D}(t)\mathbf{u}(t) \end{aligned} \tag{D.7}$$

and

$$\begin{pmatrix} \dot{\mathbf{x}}(t) \\ \mathbf{y}(t) \end{pmatrix} = \mathbf{S}(t) \begin{pmatrix} \mathbf{x}(t) \\ \mathbf{u}(t) \end{pmatrix} , \tag{D.8}$$

where $\mathbf{S}(t) \in \mathbb{R}^{(n+k)\times(n+m)}$. Hence, the disturbance free LTI systems can be described with the same equations as in (D.7-D.8), where the matrices do not depend on time ($\mathbf{A}, \mathbf{B}, \mathbf{C}$ and $\mathbf{D}$) and $\mathbf{S} \in \mathbb{R}^{(n+k)\times(n+m)}$. Basically, every LTV system can be described with infinite number of LTI systems in continuous time domain and finite number of LTI systems in discrete time domain, if only the elements of the state matrices vary over time, but the structure of the SS representation is invariant. This concept appears behind the gain scheduling theorem too. In other words, the LTV systems run through a "trajectory" during operation over time – where the trajectory consists of infinite number

of LTI systems. Fixing the elements of the SS representation of a LTV system at a given moment means that the LTV system is simplified to a LTI structure. For example, $\mathbf{S}(t)$ exactly at 10 minutes is equal to $S(t_{10}) = S_{10}$.

D.1.2. State space representation of LPV systems

The most important definitions regarding LPV theorem is the scheduling variable, the parameter vector and the parameter space and box.

Definition D.1.1. Scheduling variable or parameter: real valued scalar or function, which is a multiplied out term of a mathematical model and determines a particular property of the model. Notations: scalar case: $p = \{p \in \mathbb{R}, p_{min} \leq p \leq p_{max}\}$; function case: $p(x) = \{p(x) \in \mathbb{R}, p_{min} \leq p(x) \leq p_{max}\}$. ■

Remark D.1.1.1. *In this Theses, I only discuss those cases, when the scheduling parameter is a function of time:* $p(t) = \{p(t) \in \mathbb{R}, p_{min} \leq p(t) \leq p_{max}\}$

Remark D.1.1.2. *The scheduling variables can be complex valued scalars or functions and they may depend on the properties of the mathematical models too. This Theses does not discuss this possibility, since the investigated systems do not have such properties.*

The purpose of the selection of the scheduling variables are manyfold. If, the scheduling variables are simple parameters, the LPV model becomes appropriate to describe multiple model cases via the varying of the parameters. A more sophisticated reason is to select those functions (mostly time functions) as scheduling variables which cause nonlinearities in order to avoid this unfavorable property that I will present later on.

Definition D.1.2. Parameter vector: a real valued, bounded, permanent or time varying vector, which consist of scheduling variables. The dimension of the parameter vector is equal to the number of selected scheduling variables, q, Notations: permanent case: $\mathbf{p} \in \mathbb{R}^q$; time varying case: $\mathbf{p}(t) \in \mathbb{R}^q$. ■

The literature distinguishes between the LPV models according to the fact when the selected scheduling variables are not state variables (LPV) and when state variables are also selected as scheduling parameters (qLPV). Nevertheless, there is no difference between them from notation point of view. However, the eligible interpretation of the cases is important to be noticed.

Definition D.1.3. Parameter Space (PS): a q dimensional real vector space $\mathbb{R}^q$, where each dimension represents the possible values of a given scheduling variable. ■

Definition D.1.4. Parameter box (PB): a q dimensional simplex inside the $\mathbb{R}^q$ space, which is determined by the minimum $p_{i,min}$ and maximum $p_{i,max}$ values of the scheduling variables $p_i(t)$. Usually, the PB represents those space which is the meaningful region of the parameters from the physical or physiological point of view. The size of the PB (the minimum $p_{i,min}$ and maximum $p_{i,max}$ values of the scheduling variables) can be tighter as that allowed by the reality – in this case the PB means the "region of interest". ■

The general SS representation of LPV systems, where disturbance is not considered can be described as follows:

$$\begin{aligned} \dot{\mathbf{x}}(t) &= \mathbf{A}(\mathbf{p}(t))\mathbf{x}(t) + \mathbf{B}(\mathbf{p}(t))\mathbf{u}(t) \\ \mathbf{y}(t) &= \mathbf{C}(\mathbf{p}(t))\mathbf{x}(t) + \mathbf{D}(\mathbf{p}(t))\mathbf{u}(t) \end{aligned} . \tag{D.9}$$

Unification can be made similarly as in (D.3) and from (D.7):

$$\mathbf{S}(\mathbf{p}(t)) = \begin{pmatrix} \mathbf{A}(\mathbf{p}(t)) & \mathbf{B}(\mathbf{p}(t)) \\ \mathbf{C}(\mathbf{p}(t)) & \mathbf{D}(\mathbf{p}(t)) \end{pmatrix} . \tag{D.10}$$

The compact form of general LPV system from (D.8) becomes:

$$\begin{pmatrix} \dot{\mathbf{x}}(t) \\ \mathbf{y}(t) \end{pmatrix} = \mathbf{S}(\mathbf{p}(t)) \begin{pmatrix} \mathbf{x}(t) \\ \mathbf{u}(t) \end{pmatrix} . \tag{D.11}$$

The classical approaches that use LPV form in modeling apply general, affine and polytopic LPV system models [81–83]. However, in the recent years a soft-computing based LPV modeling approach gave rise to the TP transformation-based LPV modeling possibility [156, 157]. Because the developed quality interpretation can be used beside general, affine and polytopic configurations, as well, I shortly summarized these representations below.

General LPV configuration

A general, parameter dependent, nonlinear model represented by its SS form (D.9) can be handled as an LPV model, if each nonlinearity causing element is selected as scheduling parameter and it is assumed that these terms only vary between strict limits $p_i(t) \in [p_{i,min}, .., p_{i,max}]$.

For example, a simple nonlinear system (with two states $x_1(t)$ and $x_2(t)$, one input

$u(t)$ and one output $y(t) = x_1(t)$) can be described with the following equations:

$$\begin{aligned} \dot{x_1}(t) &= \sqrt{x_1(t)}x_2(t) + u(t) \\ \dot{x_2}(t) &= -k_1 x_2(t) \\ y(t) &= x_1(t) \end{aligned} \quad . \tag{D.12}$$

We can select $p_1(t) = \sqrt{x_1(t)}$ as scheduling parameter, in this way the parameter vector will be one dimensional: $\mathbf{p}(t) = p_1(t) \in \mathbb{R}^1$. If it is assumed that the scheduling parameter can only vary between a minimum and maximum level ($p_1(t) \in [p_{1,min}, .., p_{1,max}]$), the general LPV description similar to (D.8) is the following:

$$\begin{pmatrix} \dot{\mathbf{x}}(t) \\ \mathbf{y}(t) \end{pmatrix} = \begin{bmatrix} 0 & p_1(t) & 1 \\ 0 & -k_1 & 0 \\ 1 & 0 & 0 \end{bmatrix} \begin{pmatrix} \mathbf{x}(t) \\ \mathbf{u}(t) \end{pmatrix}. \tag{D.13}$$

It is clear that in this case the LPV means a unique approach and does not change the basic SS structure of the system. Naturally, if the occurrence of disturbances is considered to be known too, then the SS description of the system has to be completed with the disturbance related matrices $\mathbf{E}(\mathbf{p})(t)$ and $\mathbf{D_2}(\mathbf{p})(t)$ as follows:

$$\begin{aligned} \dot{\mathbf{x}}(t) &= \mathbf{A}(\mathbf{p}(t))\mathbf{x}(t) + \mathbf{B}(\mathbf{p}(t))\mathbf{u}(t) + \mathbf{E}(\mathbf{p}(t))\mathbf{d}(t) \\ \mathbf{y}(t) &= \mathbf{C}(\mathbf{p}(t))\mathbf{x}(t) + \mathbf{D}(\mathbf{p}(t))\mathbf{u}(t) + \mathbf{D}_2(\mathbf{p}(t))\mathbf{d}(t) \end{aligned} \quad . \tag{D.14}$$

Affine LPV configuration

In this type, the LPV systems are affine functions of the parameter vector. If the system is given with its SS representation, then it consists of two main parts: a permanent, which is independent from the parameter vector $\mathbf{p}(t)$ and a varying, where the dependency appears. If we have preliminary information about the disturbance, it can be a part of

the affine model description:

$$\begin{aligned}
\mathbf{A}(\mathbf{p}(t)) &= \mathbf{A}_0 + \sum_{i=1}^{q} p_i(t)\mathbf{A}_i \\
\mathbf{B}(\mathbf{p}(t)) &= \mathbf{B}_0 + \sum_{i=1}^{q} p_i(t)\mathbf{B}_i \\
\mathbf{E}(\mathbf{p}(t)) &= \mathbf{E}_0 + \sum_{i=1}^{q} p_i(t)\mathbf{E}_i \\
\mathbf{C}(\mathbf{p}(t)) &= \mathbf{C}_0 + \sum_{i=1}^{q} p_i(t)\mathbf{C}_i \\
\mathbf{D}(\mathbf{p}(t)) &= \mathbf{D}_0 + \sum_{i=1}^{q} p_i(t)\mathbf{D}_i \\
\mathbf{D_2}(\mathbf{p}(t)) &= \mathbf{D_2}_0 + \sum_{i=1}^{q} p_i(t)\mathbf{D_2}_i
\end{aligned} \quad . \tag{D.15}$$

The permanent matrices are the $\mathbf{A}_0, \mathbf{B}_0, \mathbf{E}_0, \mathbf{C}_0, \mathbf{D}_0$ and $\mathbf{D}_{2,0}$ which represent the independent parts from the parameter vector. The permanent and varying parts can be written in short form similar to (D.10):

$$\mathbf{S}(\mathbf{p}(t)) = \begin{pmatrix} \mathbf{A}_0 + \sum_{i=1}^{q} p_i(t)\mathbf{A}_i & \mathbf{B}_0 + \sum_{i=1}^{q} p_i(t)\mathbf{B}_i & \mathbf{E}_0 + \sum_{i=1}^{q} p_i(t)\mathbf{E}_i \\ \mathbf{C}_0 + \sum_{i=1}^{q} p_i(t)\mathbf{C}_i & \mathbf{D}_0 + \sum_{i=1}^{q} p_i(t)\mathbf{D}_i & \mathbf{D}_{2,0} + \sum_{i=1}^{q} p_i(t)\mathbf{D}_{2,i} \end{pmatrix} . \tag{D.16}$$

If the disturbance is not assumed to be known, or it is not modeled, the affine description becomes:

$$\mathbf{S}(\mathbf{p}(t)) = \begin{pmatrix} \mathbf{A}_0 + \sum_{i=1}^{q} p_i(t)\mathbf{A}_i & \mathbf{B}_0 + \sum_{i=1}^{q} p_i(t)\mathbf{B}_i \\ \mathbf{C}_0 + \sum_{i=1}^{q} p_i(t)\mathbf{C}_i & \mathbf{D}_0 + \sum_{i=1}^{q} p_i(t)\mathbf{D}_i \end{pmatrix} \tag{D.17}$$

and in this way the complex system matrix can be simplified as:

$$\mathbf{S}(\mathbf{p}(t)) = \mathbf{S}_0 + \sum_{i=1}^{q} p_i(t)\mathbf{S}_i \ . \tag{D.18}$$

The affine LPV system can be written in compact form similar to (D.11).

The affine LPV models keep their validity only in inside the PB during operation. This

configuration is very advantageous from control engineering points of view, since

- The PB represents the workspace where the LTV system can be found during operation and each of the points can also represent an LTI system at a given moment;
- The control design tasks may be easier, because these regions are usually small;
- In case of robust control, the borders of the PB can be the borders of parameter uncertainties;
- With affine LPV representation, nonlinearities can be hidden. Moreover, a given time stamp represents an LTI system, which can be selected as "operating or reference system", if its properties are appropriate from control design point of view.

In Fig. D.1, I highlighted a 3D PS, where $\mathbf{p}(t) \in \mathbb{R}^3$ and the values of the scheduling parameter are varying among the range which is determined by the minimum and maximum values of the parameters. Mathematically, this can be obtained if the parameter vector is:

$$\mathbf{p}(t) = \begin{pmatrix} p_1(t) \\ p_2(t) \\ p_3(t) \end{pmatrix} = \begin{pmatrix} [p_1^- .. p_1^+] \\ [p_2^- .. p_2^+] \\ [p_3^- .. p_3^+] \end{pmatrix} . \tag{D.19}$$

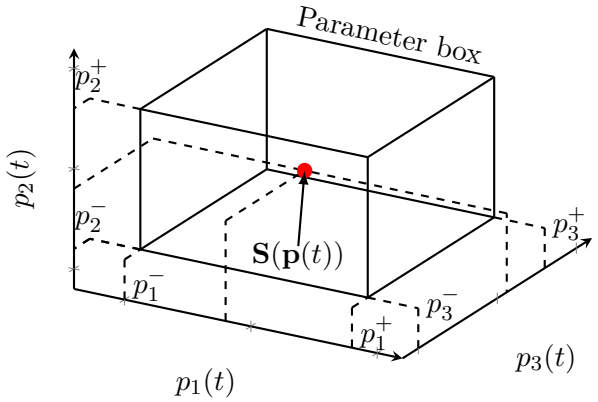

Figure D.1.: Affine LPV model example in the $3D$ parameter space

Polytopic LPV configuration

Affine LPV configuration means a natural way to describe or highlight different properties of a system, however, usually not directly used in controller design [80].

Nevertheless, the polytopic LPV configuration, which is directly derivable from affine configuration (and gives a basis for the TP-transformation based design as well) is directly usable in such design methods. Practically, the polytopic LPV theory is based on the barycentric theorem of Möbius, describing the position of a point in a triangle with using the vertices of the triangle as reference points [158, 159]. Further, Warren and his colleagues have proved the possibility that in case of arbitrary convex sets it is also true that by using the vertices of a convex set as reference points, the position of an arbitrary internal point can be described [160]. This is the key property which can be used in control engineering approaches [82].

As the affine LPV system is only operating inside the parameter box, the vertices of the parameter box can be used as reference points to describe each system that can occur during operation, namely, each such internal system will be the convex combination of the vertices of the polytope, if the convexity criteria is satisfied. In the case of a control system, the convexity depends on the following considerations. An internal system $\mathbf{S}$ can be described with polytopic coordinates α_i, if the system representation belonging to α_i, i.e. $\mathbf{S}_i$ satisfies the following restrictions:

- The polytopic coordinates should be non-negative real values, $\alpha_i \geq 0$;
- The sum of the polytopic coordinates should be equal to one, $\sum_{i=1}^{j} \alpha_i = 1$;
- The internal system is the convex combination of the vertices of the polytope, $\mathbf{S} = \sum_{i=1}^{j} \alpha_i \mathbf{S}_i$.

or shortly [90]:

$$\left\{ \mathbf{S} = \sum_{i=1}^{j} \alpha_i \mathbf{S}_i : \alpha_i \geq 0, \sum_{i=1}^{j} \alpha_i = 1 \right\} . \tag{D.20}$$

Normally, when $j > q$ we have a redundant representation that generally allows the satisfaction of the restrictions. The barycentric coordinate function can be given in the following way [82].

The barycentric coordinate function belonging to a given a point inside the convex polytope can be calculated as follows, where the Υ_i is the weight function belonging to

the ith vertex of the given a point:

$$\alpha_i(a) = \frac{\Upsilon_i(a)}{\sum_i \Upsilon_i(a)} \tag{D.21}$$

The $\Upsilon_i(a)$ weight function can be described with:

$$\Upsilon_i(a) = \frac{\mathrm{vol}(\Pi_i)}{\prod_{b \in \mathrm{ind}(\Pi_i)} (n_b \cdot (\Pi_i - a))} \tag{D.22}$$

where $\mathrm{vol}(\Pi_i)$ is the volume of the parallelepiped spanned by the normals to the facets incident on vertex i, i.e., Π_i, $\{n_b\}$ is the collection of normal vectors to the facets incident on vertex i, and $\mathrm{ind}(\Pi_i)$ denotes the set of indices j such that the facet normal to n_b contains the vertex Π_i [82]. The volume of the given parallelepiped can be calculated as:

$$\mathrm{vol}(\Pi_i) = |det(n_{ind})| \tag{D.23}$$

where n_{ind} is a matrix whose rows are the vectors n_b where $b \in \mathrm{ind}(V_i)$ [82].

Fig. D.2. shows an example where the aforementioned theories were taken into account in case of 3 scheduling variables. In this case, the parameter space is 3 dimensional and it is visible that the parameter box is determined by the minimum and maximum values of the parameter vector. Furthermore, the vertices of this box, $\mathbf{S}_i$ serve as reference points and α_i are the convex coordinates at the same time. The actual system inside can be calculated with the barycentric calculus, namely, the actual system $\mathbf{S}(\mathbf{p}(t))$ will be the convex combination of the vertices, i.e.:

$$\mathbf{S}(\mathbf{p}(t)) = \sum_{i=1}^{8} \alpha_i(p(t))\mathbf{S}_i \quad . \tag{D.24}$$

Obviously, if the actual system reaches a vertex that means the convex coordinate of the particular vertex will be equal to one, however, the others will be equal to zero. For example, if the system reaches the vertex $\mathbf{S}_1$, then $\alpha_1 = 1$, furthermore $\sum_{i=2}^{8} \alpha_i(p(t))\mathbf{S}_i = 0$ and the actual system is:

$$\mathbf{S}(\mathbf{p}(t)) = \alpha_1(p(t))\mathbf{S}_1 + \sum_{i=2}^{8} \alpha_i(p(t))\mathbf{S}_i = \alpha_1(p(t))\mathbf{S}_1 \ . \tag{D.25}$$

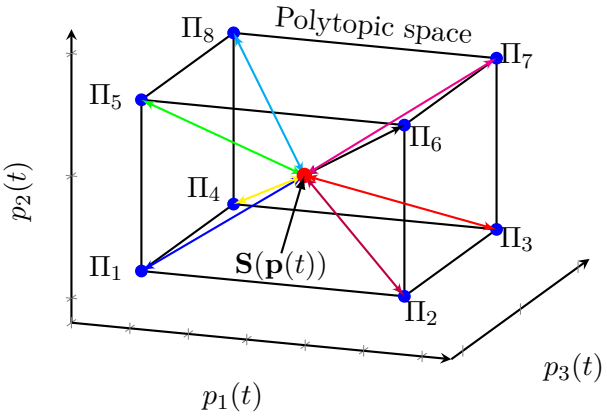

Figure D.2.: Polytopic LPV model examples in the $3D$ parameter space